MONTHLY NOTICES

OF THE

ROYAL ASTRONOMICAL SOCIETY

Vol. 96 No. 5

MEETING OF 1936 MARCH 13

Dr. H. Knox-Shaw, Vice-President, in the Chair.

The election by the Council of the following Fellows was duly confirmed :—

Max Krook, Gonville and Caius College, Cambridge ; and
Arthur Mulligan, M.Sc., 6 Keswick Road, St. Helens, Lancs.

The following candidates were proposed for election as Fellows of the Society, the names of the proposers from personal knowledge being appended :—

Stanley Philip Benge, 84 Muswell Hill Road, London, N. 10 (proposed by C. C. L. Gregory) ;
Ralph Judson, Lyndhurst, Lion Road, Bexley Heath, Kent (proposed by H. Spencer Jones) ;
Samuel Keir, F.C.I.S., Rossmore, Scotforth, Lancaster (proposed by C. L. Brook) ; and
Arnold Petrie Watson, M.A., 61 Netherhall Gardens, Hampstead, London, N.W. 3 (proposed by A. R. Wesley).

One hundred and forty-one presents were announced as having been received since the last ordinary meeting, including :—

Belgrade, Observatoire Astronomique de l'Université : Nouvelles tables de précession, par V. V. Michkovitch ;
Fox (Philip), "Edwin Brant Frost, 1866–1935" ;
Hale (George E.), "The Astrophysical Observatory of the California Institute of Technology : The 200-inch Reflector" ;

Kendall (Phebe Mitchell), "Maria Mitchell, Life, Letters and Journals" (presented by Miss M. Harwood);
Mills (Charles E.) and C. F. Brooke, "Sir William Huggins";
The Physical Society, "Reports on Progress in Physics," Vol. II;
Skellett (A. M.), "On the Correlation of Radio Transmission with Solar Phenomena" (Bell Telephone System Technical Publications—Radio: Monograph B—895);
Stalinabad, Tadjik Astronomical Observatory, "Catalogue and Ephemeris of Short-period Cepheids for 1935–1936," by W. Zessewitsch.

SOLAR GRANULATION.

H. H. Plaskett.

Introduction.—If the thermal and mechanical equilibrium of the solar atmosphere were determined solely by radiation and gravitation, a smoothly varying and structureless atmosphere would result. The existence of granulation, sunspots and prominences shows, as Schwarzschild pointed out in his classical paper on radiative equilibrium, that superposed on and probably disturbing this equilibrium are turbulent variations. To pass beyond the first approximation given by radiative equilibrium to something more nearly resembling the actual structure of the solar atmosphere, the nature and origin of each of these phenomena will have to be studied in detail. It is clear, however, that granulation, unvarying with time and uniform in distribution, must be regarded as a permanent characteristic of the atmosphere, and it is probable that a detailed study of its nature will be more revealing than a study of the widely variable sunspots and prominences.

Though observable with difficulty, the early visual * and photographic † studies have led to a well-established description of granulation. It consists of luminous patches, or granules, circular or elliptical in outline and some 2″ of arc, or 1500 km. in diameter. These granules are distributed more or less uniformly on a less luminous background, with a ratio of granular to intergranular area of between one-half and unity (Chevalier). The life of an individual granule lies between one and three minutes (Hansky and Chevalier). Random displacements of individual granules of the order of 4 km. per second have been observed by both Hansky and Chevalier; according to the latter these are to be interpreted as motions of the luminous centroid of the granule, due to brightness variations over its surface rather than to bodily movements. Granulation is observed over the whole solar disc, including the equator and poles (Janssen), but there is some difference

* The visual work of Herschel, Dawes and others is well summarized by S. P. Langley, *Am. Jour. Science*, **7**, 87, 1874.

† J. Janssen, *Ann. de l'Obs. Ast. Phys. de Paris*, **1**, 103, 1896; A. Hansky, *Mitt. der Nik.-Hauptsternwarte Pulkowa*, **3**, 1, 1908; S. Chevalier, *Ann. de l'Obs. de Zô-Sè*, **8**, C 1, 1912.

of opinion on whether it is as distinctly visible at the extreme limb. From a long series of plates, 1905 to 1912, Chevalier has definitely established that granulation preserves these various characteristics unchanged over at least half a sunspot cycle.

Further observational data are furnished by the recent work of Strebel and Thüring.* Their quantitative results are based on an uncalibrated photograph taken in the ultra-violet ($\lambda\lambda$ 3300–4000) on 1928 October 6 with a reflector giving a solar image 86·8 mm. in diameter. From measures of plate density made every 0·1 mm. along four diameters, in part with a Koch and in part with a Hartmann microphotometer, transformed to incident fluxes by means of a characteristic curve supplied by the plate manufacturers, these writers reach four conclusions. (1) Measured down to a "granulation base," they find the diameter of a granule to be $9''{\cdot}8$, and the ratio of granular to intergranular area approximately 3 : 2. (2) The maximum measured intensity ratio of granular maximum to intergranular minimum is 0·11 magnitudes. (3) The brightness difference of granule to "base" is a linear function of the measured diameter of the granule. (4) For a given granular diameter the intensity ratio of granule to "base" is greater the closer the granule is to the limb. The relation of this pioneer work on surface brightness variation to the earlier observations is somewhat obscure ; apart from the fact that the photographic photometry is unsatisfactory, so that a much too pronounced darkening towards the limb is obtained, it seems probable that these observations refer to low-lying minute flocculi, seen in spectroheliograms, rather than to the photospheric granules seen visually and photographically.†

It is the purpose of the present paper to present in the first section an independent determination of the surface brightness differences due to granulation, and in the second section to discuss the origin of granulation and its effect on atmospheric structure in the light of these measures and the other available information.

Section 1.—Observational Determination of Granular Surface Brightness

1.1. *Observational Data.*—In order to find the surface brightness of granules as a function of wave-length in spectral regions relatively free from absorption lines observation has been spectroscopic throughout. After some preliminary experiments in 1930 September, the spectra on which the present investigation is based were obtained in part at Victoria during 1931 July and August, and in part at Oxford during 1935 September and October.

The 72-inch Victoria reflector gives at its Cassegrain focus a strictly

* H. Strebel and B. Thüring, *Zs. f. Ap.*, 5, 348, 1932 ; *A.N.*, 258, Nr. 6170, 1936.

† H. Strebel (*Zs. f. Ap.*, 5, 36, 1932) states that ultra-violet photographs taken under identical circumstances with the plate concerned show faculæ over the whole surface of the Sun, not just at the limb. This is the characteristic of a low-level spectroheliogram, and is what would be expected of a photograph taken in a region riddled with numerous and strong absorption lines.

achromatic solar image 306 mm. (12·1 inches) in diameter. A small part of this image, after passing through a Bausch and Lomb shutter of 50 mm. aperture fell on the slit (16 mm. in length) of the Cassegrain spectrograph. The maximum shutter speed was $\frac{1}{75}$th of a second, and with this exposure it was necessary to diaphragm the collimator with a central rectangular aperture of 14·8 mm. by 15 mm. If the granules are 2″ in diameter, their size on the slit will be 0·32 mm., and their angular size, as seen from the collimator, exceeds by a factor of seven the resolving power limit of the thus diaphragmed spectroscope. The telescope was focussed by examining the image of a bright star, Capella or Arcturus, by means of the slit guiding telescope; this procedure was adopted in part because it was difficult to focus with the small part of the solar image which reached the slit, and in part because the focus necessarily changed on exposure of the mirrors to the Sun. After the focussing had been completed a spring roller blind was drawn across the open top of the telescope tube, the telescope pointed at the centre of the disc by means of a guiding telescope, the shutter set and the plate-holder slide withdrawn; the spring blind was then opened, the exposure made, the blind drawn again and the plate-holder slide replaced. The total exposure of the mirrors to the Sun during this operation was of the order of 15 seconds. The neutral tint wedge, W. iv, was then placed on the slit, the jaws opened from 0·025 mm. to 1·5 mm., and a ground-glass screen placed on the shutter to diffuse the light. The rectangular collimator diaphragm was removed, and, following the same procedure as described above, a wedge spectrum of the same exposure time as the granulation spectrum was made on another part of the same photographic plate. In order to correct for possible non-uniformity of illumination over the height of the wedge, a third exposure, the illumination test, was made through a magnification diaphragm, instead of the wedge, but with otherwise identical exposure conditions except that the incident flux was reduced by some constant factor. A Victoria plate carried, therefore, three spectra, each with an exposure of $\frac{1}{75}$th of a second; the first was a spectrum of the centre of the disc which, if the "seeing" were sufficiently good for granulation to be visible, would show dark streaks along the length of the spectrum corresponding to the granular images on the slit, and the second and third were the calibration spectra.

The solar telescope at Oxford is of the vertical Cassegrain type, and gives a strictly achromatic image 208 mm. (8·2 inches) in diameter. A part of this image fell on the 18-mm. long slit of a Hilger Medium Glass Spectrograph, placed in the optical axis of the telescope. A Compur shutter of over 30 mm. clear aperture, with a maximum speed of $\frac{1}{200}$th of a second, was mounted inside the spectroscope in front of the collimating lens. Since the aperture ratio of the solar telescope is $f/70$ and the focal length of the collimator is 62 cm., the diameter of the extra focal patch on the collimator is 8·9 mm.; at this effective aperture the diameter of a granular image on the slit of 0·22 mm. exceeds by a factor of five the resolving power limit of the spectrograph. The telescope was focussed by means of the solar image itself seen on a bristol board diaphragm in the plane of the slit; because

of the fused silica mirrors the telescope remained in focus indefinitely, so that it was possible, by watching the definition of the image itself, to choose the instant of best "seeing" for making an exposure. Five spectra, each of $\frac{1}{25}$th second exposure, were made on the one plate; two of these were calibration exposures, wedge and illumination test, made with a slit width of 0·175 mm., while the remaining three were direct exposures of the centre of the disc made with a slit width of 0·005 mm.

At Victoria 49 spectra of the Sun were secured on 49 plates in 25 days, and at Oxford 60 spectra on 20 plates in 7 days. Of these 109 spectra 18 were selected as showing the most marked granulation, and observational details for these plates are given in Table I. The first column gives the plate number, the second the number of granulation spectra measured on the plate, the third the time when the granulation exposures were made, the fourth the exposure time, the fifth the slit width for the granulation exposures, the sixth the dispersion in A.U. per mm. at *Hγ*, and the last the emulsion. All plates except the Eastman 33 were backed, and all plates were developed with Parkhurst developer—the Oxford plates by the brush method.

1.2. *Measurement.*—By means of a needle pivoted to a Hilger Measuring Micrometer * the plates listed in Table I were marked with an accuracy

TABLE I

Observational Data

Plate	No.	Date U.T.	Exp.	Slit	Disp.	Emulsion
Victoria		1931	secs.	mm.		
W. 601	1	July 22.94	0·013	0·025	9·3 A.	Eastman 33
637	1	Aug. 19.99	·013	·025	29·3 A.	Royal Lantern Slide
639	1	Aug. 20.97	·013	·025	29·3 A.	Royal Lantern Slide
641	1	Aug. 21.95	·013	·025	29·3 A.	Royal Lantern Slide
645	1	Aug. 22.87	·013	·025	29·3 A.	Royal Lantern Slide
Oxford		1935				
W. 733	3	Sept. 25.39	0·04	0·005	16·8 A.	Ilford Empress
741	3	Oct. 3.42	·04	·005	16·8 A.	Ilford Empress
742	1	Oct. 3.44	·04	·005	16·8 A.	Ilford Empress
746	3	Oct. 7.46	·04	·005	16·8 A.	Ilford Rap. Process Pan.
747	3	Oct. 7.48	·04	·005	16·8 A.	Ilford Rap. Process Pan.

of about four microns at one or more of four wave-lengths. These wave-lengths were selected from a study of microphotometer records and of Rowland's Map as those least affected by absorption lines. Details of the regions selected are given in Table II, where the first column contains the wave-length of the centre of the region, the second its width in A.U., the third the width in mm. for the smallest dispersion (29·3 A. per mm.), and the columns headed Rowland contain the number of lines of listed intensity

* Loaned by the Government Grant Committee of the Royal Society.

TABLE II

Wave-length Regions

λ	$\Delta\lambda$	Δx	Rowland								Fraction Continuous
			−3	−2	−1	0	1	2	3	4	5	
		mm.										
4012·2	8·4 A.	0·34	...	14	20	10	6	4	6	1	2	0·80
4365·4	11·5	·38	3	13	30	13	11	3	...	1	1	·87
4811·2	25·1	·45	42	23	10	8	6	4	2	...	...	·95
5836·9	41·1	·91*	37	45	20	9	4	1	2	...	1	·98

* This is the linear width on the 16·8 A. at $H\gamma$ dispersion.

in the region. From the equivalent breadths given by Mulders * we can find the fraction of each region which is due to pure continuous spectrum, and this fraction is given in the last column of the table.

Microphotometer records † with a magnification of 6·89 were obtained perpendicular to the direction of dispersion at each of the marked wave-length regions. The length of the illuminated area on the plate was always less than 0·34 mm., and its width sufficiently small to give no error due to finite resolving power. Once secured, these records were measured for deflection from the zero line to a smooth line drawn through the mean of the fluctuations due to plate grain. The result of the record measurement was thus to give y/y_0 as a function of distance across the recorded spectrum, distance on the record itself being converted directly into x, measured in seconds of arc on the disc, by means of the magnification of the spectroscope and the focal length of the telescope. To convert the deflections y/y_0 into the flux incident on the photographic plate, the characteristic curve of the plate for the wave-length concerned is required.

To find the characteristic curve from the wedge spectrum, where the flux, $I_0(h)$, incident on the wedge is not constant over its height, as it rarely is,‡ the following procedure is adopted. On the microphotometer record the galvanometer deflections y/y_0 are measured for both the wedge and the illumination spectra, and these deflections are plotted, as in fig. 1, against h, the height in mm. on the slit. Let the two curves cross at height H. Then if $\phi(h)$ is the known transmission of the wedge at the height h, the ratio of fluxes transmitted by the wedge at heights h and H is

$$\frac{I(h)}{I(H)} = \frac{\phi(h)}{\phi H} \cdot \frac{I_0(h)}{I_0(H)}. \qquad (1)$$

Our required characteristic curve is then found by plotting galvanometer deflections y/y_0, occurring at height h in the wedge spectrum, against

* *Zs. f. Ap.*, **10**, 297, 1935.

† Cf. *M.N.*, **95**, 160, 1934, for a description of the Oxford microphotometer, and the method of measuring records.

‡ *M.N.*, **91**, 878, 1931.

the flux ratio given by equation (1). In this equation we know $\phi(h)/\phi(H)$, but not the ratio of incident fluxes $I_0(h)/I_0(H)$. From the illumination spectrum, however, we can find in fig. 1 the galvanometer deflection y'/y_0 at any

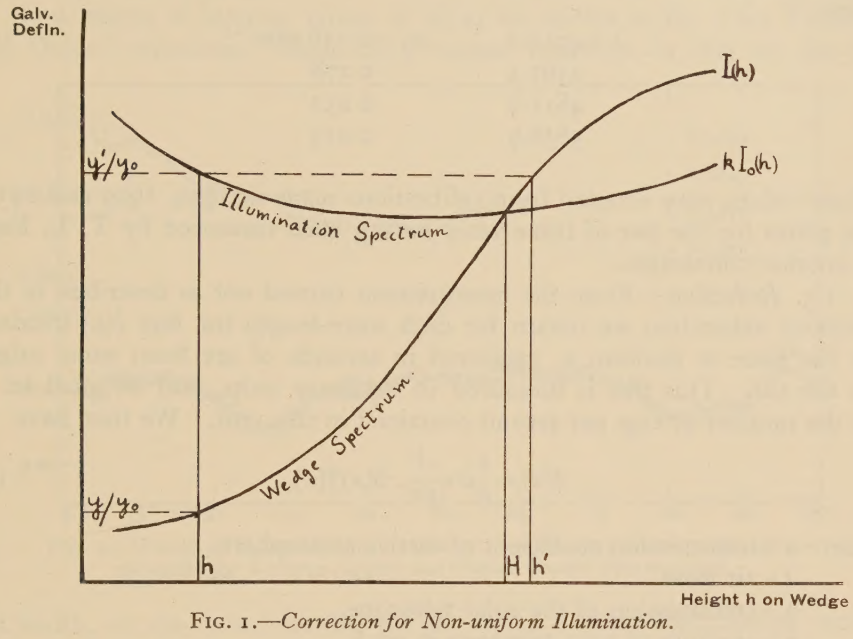

FIG. 1.—*Correction for Non-uniform Illumination.*

height h, corresponding to the incident flux $kI_0(h)$, where k is unknown, but constant over the height of the slit. This same galvanometer deflection occurs at height h' on the wedge spectrum, so that $kI_0(h) = I(h') = \phi(h') \,.\, I_0(h')$, or

$$\frac{I_0(h)}{I_0(H)} = \frac{\phi(h')}{\phi(H)} \cdot \frac{I_0(h')}{I_0(H)}. \tag{2}$$

In equation (2) we have the unknown $I_0(h)/I_0(H)$ of equation (1), expressed in terms of the known $\phi(h')/\phi(H)$, and the ratio of incident fluxes at h' and H, very close together on the slit. Unless the incident flux changes very rapidly $I_0(h')/I_0(H) = 1$; if not, and this can be seen from the illumination test, the above process may be repeated. For the present plates one stage sufficed, and the characteristic curve was found by plotting the deflection y/y_0 occurring at height h in the wedge spectrum against the logarithm of the flux ratio obtained from equations (1) and (2), namely,

$$\log I(h)/I(H) = \log \phi(h)/\phi(H) + \log \phi(h')/\phi(H). \tag{3}$$

Since the wedge, W. iv., used in the present investigation is linear,*

$$\log \phi(h) = \log b_\lambda - h\sigma_\lambda, \tag{4}$$

it follows that the correcting term on the right-hand side of equation (3)

* *M.N.*, **91**, 878, 1931.

is simply $(h' - H)\sigma_\lambda$. The characteristic curve is, therefore, found directly by displacing each point h of the wedge curve horizontally by $(h' - H)$.

The values of σ_λ, the wedge constant, used in the present investigation were

$\lambda = 4012{\cdot}2$	$\sigma_\lambda = 0{\cdot}336$ mm.$^{-1}$
4365·4	0·278
4811·2	0·232
5836·9	0·215

These values were adopted from calibrations made in 1922, 1929 and 1931, the plates for the last of these years having been measured by T. L. Page in another connection.

1·3. *Reduction.*—From the measurement carried out as described in the previous subsection we obtain for each wave-length the flux $I(x)$ incident on the plate at position x, measured in seconds of arc from some origin on the slit. This flux is measured in arbitrary units, and we shall let E be the number of ergs per second contained in this unit. We then have

$$I(x) = \frac{1}{E} a^t \alpha \frac{A}{F^2} \cdot \beta(x) \mathcal{J}(x), \tag{5}$$

where a = transmission coefficient of earth's atmosphere,
t = air mass,
α = transmission of the solar telescope,
A = aperture of solar telescope in cm.^{2},
F = focal length of solar telescope in cm.,
$\beta(x)$ = transmission of spectroscope, as determined by variable slit width, magnification and spectroscope absorption,
$\mathcal{J}(x)$ = surface brightness on the solar disc at point corresponding to x.

The first four factors on the right-hand side of equation (5) are independent of x, so that if G_1 is the mean of $I(x)$ for all x's for a single exposure, then

$$\frac{I(x)}{G_1} = \frac{\beta(x)\mathcal{J}(x)}{\overline{\beta(x) \cdot \mathcal{J}(x)}}, \tag{6}$$

where $\overline{\beta(x) \cdot \mathcal{J}(x)}$ is the mean of $\beta(x) \cdot \mathcal{J}(x)$ for all x's for the given exposure. If, further, we have a number of exposures taken with identical slit conditions, the mean at a given x of $I(x)/G_1$ for all the exposures may be designated by $G_2(x)$. Then

$$G_2(x) = \beta(x) \cdot \left[\Pi \frac{\mathcal{J}_i(x)}{\overline{\beta(x) \cdot \mathcal{J}(x)_i}} \right]^{\frac{1}{n}}, \tag{7}$$

since by hypothesis $\beta(x)$ at a given x is a constant for all exposures. The expression in square brackets, or the corresponding expression if the arithmetic mean is taken in place of the geometric mean, is the same for all values of x. Thus by its definition the denominator of a typical factor in equation (7) is independent of x, while the numerator, $\mathcal{J}(x)$, oscillates for the different exposures with small amplitude about some mean value, and this mean

value is the same for all x's in the centre of the disc. Hence we may write

$$G_2(x) = K_1 \cdot \beta(x), \tag{7a}$$

where K_1 is a constant.

As a matter of interest values of $G_2(x)$ are shown in fig. 2 for Victoria and Oxford exposures. Since the principal variations in $\beta(x)$ are due to

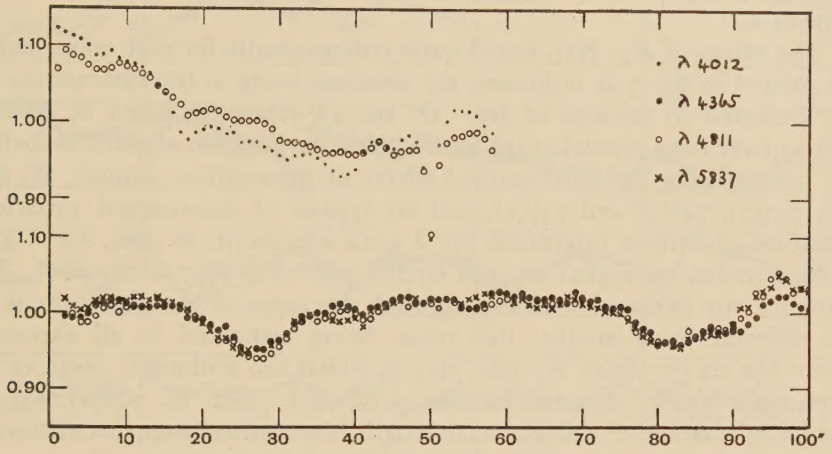

FIG. 2.—*Values of* $G_2(x) = K$, $\beta(x)$. *Curves represent very closely variation of slit width for Victoria (upper) and Oxford (lower) Spectroscopes.*

slit width, we may conclude that the slit of the Victoria spectroscope varies by 10 per cent. of its width, or 2·5 μ, from one end to the other, while the slit of the Hilger spectroscope varies by about 6 per cent. of its width, or 0·3 μ.

If now we divide equation (6) by $G_2(x)$ from equation (7*a*), we find

$$I(x)/G_1 \cdot G_2(x) = K_2 \cdot \mathcal{J}(x), \tag{8}$$

where $K_2 = [K_1 \cdot \overline{\beta(x) \cdot \mathcal{J}(x)}]^{-1}$ is also independent of x. The procedure indicated in equation (8) is that which has been followed in reducing the measured plate flux, $I(x)$, to solar surface brightness $\mathcal{J}(x)$.

1.4. *Granular Surface Brightness.*—Measures of the deflection y/y_0 were made on the average at intervals of 1″·3 along the microphotometer record for each wave-length of each of the exposures listed in Table I. These deflections were converted into the quantities $I(x)$, the flux incident on the plate, by means of the characteristic curve for that wave-length, found as indicated in § 1.2 ; in all some 400 such determinations of flux were made from the Victoria exposures, and some 2250 from the Oxford exposures. The reduction of these incident fluxes then followed in accordance with § 1.3. For each wave-length of each exposure the geometric mean, G_1, of $I(x)$ over all values of x was formed, and the quantity $I(x)/G_1$ for that wave-length and exposure plotted. A curve was run through the observed points, and the value of $I(x)/G_1$ was read off at intervals of 1″ from some fixed origin on the slit and the values entered in a table for the wave-length and plate group concerned. Exposures with identical slit conditions,

that is identical $\beta(x)$, were grouped together as follows: Group I, the four Victoria exposures W. 637, 639, 641, 645; Group II, five Oxford exposures on W. 733, 741; and Group III, six Oxford exposures on W. 746, 747. The geometric mean, $G_2(x)$, was then formed for all exposures of a group at each value of x, and finally for each exposure of this group the value of $I(x)/G_1 \,.\, G_2(x)$, that is $K_2 \,.\, \mathcal{J}(x)$, was determined for each tabulated value of x.

The values of $K_2 \,.\, \mathcal{J}(x)$, found quite independently for each wave-length, are plotted in fig. 3 as ordinates, the abscissæ being x, the distance on the slit measured in seconds of arc. Of the 18 exposures listed in Table I only 11 have been plotted in the figure, these having been selected to include the five showing the most marked effects of granulation, namely, W. 637, 639, 733(3), 746(3) and 747(1), and six typical of less-marked variations. Measures of surface brightness for λ 4012 are shown as dots, for λ 4365 as filled circles, for λ 4811 as open circles, and for λ 5837 as crosses.* The curve for any exposure is drawn through the mean of the observations for the different wave-lengths, this mean being estimated in all exposures except the six on plates W. 746, 747, in which the arithmetic mean of the three wave-length observations was computed. For W. 746(2), (3) the standard deviation of a single wave-length observation from this arithmetic mean was also determined for the 200 values of x in these two exposures. The mean of these standard deviations of a single wave-length observation is $\pm$ 0·011, or $\pm$ 1·1 per cent., an exceedingly small accidental error for photographic spectrophotometry. The systematic error, arising only from possible errors in the determination of the wedge constant, is given by

$$\frac{\Delta R}{R} = \frac{\Delta \sigma_\lambda}{\sigma_\lambda} \log_e R, \tag{9}$$

where R is the ratio of maximum to minimum flux measured. If R is taken to be 1·10, and the percentage error of the wedge constant as much as $\pm$ 5 per cent., the resulting systematic error in the observed surface brightness ratios is only $\pm$ 0·4 per cent. In view of these small accidental and systematic errors there can be no doubt of the reality of the variation in surface brightness as a function of x, shown in fig. 3, small though that variation is; nor any doubt that this observed variation is due to granulation on the solar surface, the maxima of brightness arising from granules, the minima from the intergranular regions.

1.41. An inspection of fig. 3 shows that the amplitude (maximum – minimum) of variation changes from some 2 per cent. in W. 746(2) through intermediate stages to some 8 per cent. in W. 733(3), 746(3), and 747(1). This is an effect of "seeing"; and indeed if the "seeing" is bad, a straight line parallel to the x axis will be obtained, as is nearly the case for W. 746(2). It is legitimate to enquire what the amplitude of variation would become in perfect "seeing."

* In fig. 3 the designation 733(2) should read 733(3); further, in this exposure alone filled circles are measures of surface brightness for λ 4811, and open circles for λ 4365.

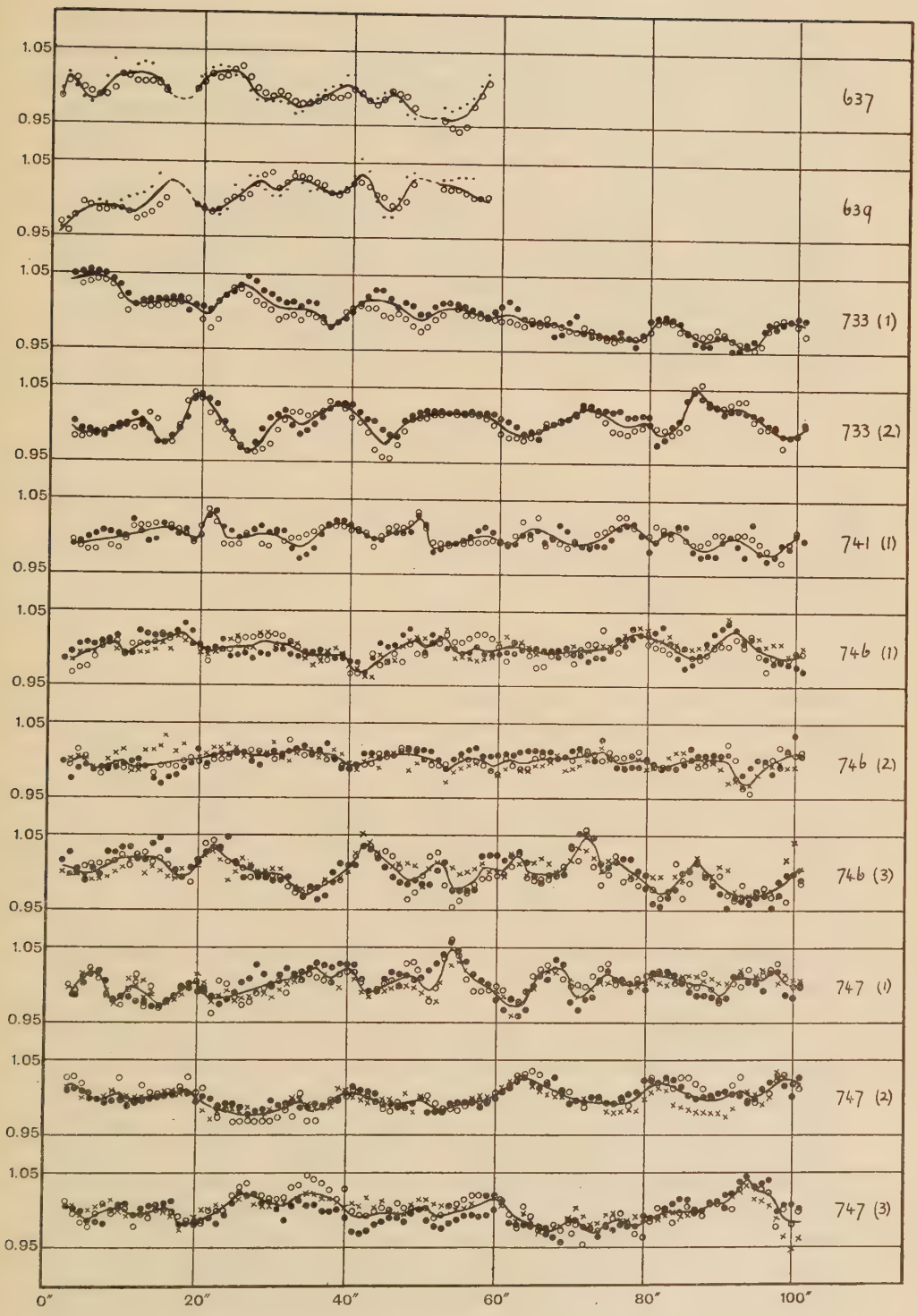

FIG. 3.—*Surface Brightness of Granulation.*

As pointed out by Wanders,* the sum total of the effects due to bad "seeing," scattering in the earth's atmosphere, and optical aberration is that a point in the object plane gives rise in the image plane to an intensity distribution $S(x, y)$, the so-called scattering function. If we may assume, as is not unreasonable, that $S(x, y) = \frac{a}{\pi} e^{-a(x^2+y^2)}$, then the value of a can be found, as Wanders has shown, from the observed intensity distribution in the vicinity of the solar limb. Using a rather under-exposed spectrum of the solar limb, W. 742(2), which showed almost no effect due to granulation, the measured intensity distribution was found to be best fitted by $a = 0{\cdot}09$ sec.$^{-2}$. Adopting this value, which according to Wanders corresponds to good "seeing" at Utrecht, it can be seen that the observed surface brightness, $j(x)$, due to granulation will be given by the integral equation

$$j(x) = \frac{a}{\pi}\int_{-\infty}^{\infty}\int_{-\infty}^{\infty} \mathcal{J}(\xi) e^{-a\{(x-\xi)^2+\eta^2\}} d\xi d\eta = \sqrt{\frac{a}{\pi}}\int_{-\infty}^{\infty} \mathcal{J}(\xi) e^{-a(x-\xi)^2} d\xi, \qquad (10)$$

where $\mathcal{J}(\xi)$ is the true surface brightness, assumed a linear function of ξ, and a takes the above observed value. Using a second approximation to the solution of this integral equation, given by Burger and van Cittert,† we find

$$\mathcal{J}_2(x) = 2j(x) - \sqrt{\frac{a}{\pi}}\int_{-\infty}^{\infty} j(\xi) e^{-a(x-\xi)^2} d\xi. \qquad (11)$$

Taking as a typical case of well-marked granulation the central part of the exposure W. 746(3), the mean observed surface brightness, $j(x)$, being shown again in fig. 4 as a continuous line, the integral in equation (11) was evaluated by Simpson's one-third rule for 13 values of x. The resulting values of $\mathcal{J}_2(x)$, the second approximation to the true surface brightness, are shown in fig. 4 as open circles, connected by a dotted line. It is probable that these represent an over-correction, since W. 746(2), showing well-marked granulation, must have a larger value of a than W. 742(2) showing almost none. Nevertheless the effect of this over-correction is only to increase the surface brightness ratio of granule to intergranular region from $1{\cdot}04/0{\cdot}97 = 1{\cdot}072$ to $1{\cdot}06/0{\cdot}96 = 1{\cdot}103$. It may therefore be concluded that the maximum amplitude due to granulation does not exceed 10 per cent.

1.42. It may now be asked whether the amplitude of variation due to granulation is a function of wave-length. In order to test for such an effect the maxima and minima on the five exposures already noted as showing the most marked granulation were picked out, and the amplitude (maximum – minimum) for each wave-length relative to λ 4811 measured. In the mean it was found that λ 4012 had an amplitude 0·010 unit greater, while λ 4365 and λ 5837 had amplitudes 0·002 and 0·010 units respectively smaller than λ 4811. Since the mean amplitude on these five exposures is 0·029, it follows that the observed amplitudes are 0·039 for λ 4012, 0·027 for λ 4365, 0·029 for λ 4811 and 0·019 for λ 5837. While these measured

* *Zs. f. Ap.*, **8**, 108, 1934. † *Zs. f. Phys.*, **79**, 722, 1932.

differences are not much larger than the accidental errors, it is probable that the surface brightness ratio increases with decreasing wave-length.

1.43. The surface brightness variations in fig. 3 are due to granulation observed at the centre of the disc. A limb spectrum, somewhat under-exposed so that it could only be measured at λ 4365, was secured with good definition on W. 741(2), and the resulting values of $K_2 . \mathcal{J}(x)$ are plotted in fig. 5. It will be noted that the variation in surface brightness due to granulation is very well marked, even at a distance of 12″ from the limb ($\cos\theta = 0{\cdot}12$), and indeed is more conspicuous than on any of the numerous exposures of the centre of the disc. This may be only the result of exceptionally good "seeing," though from the discussion in § 1.41 this does not seem

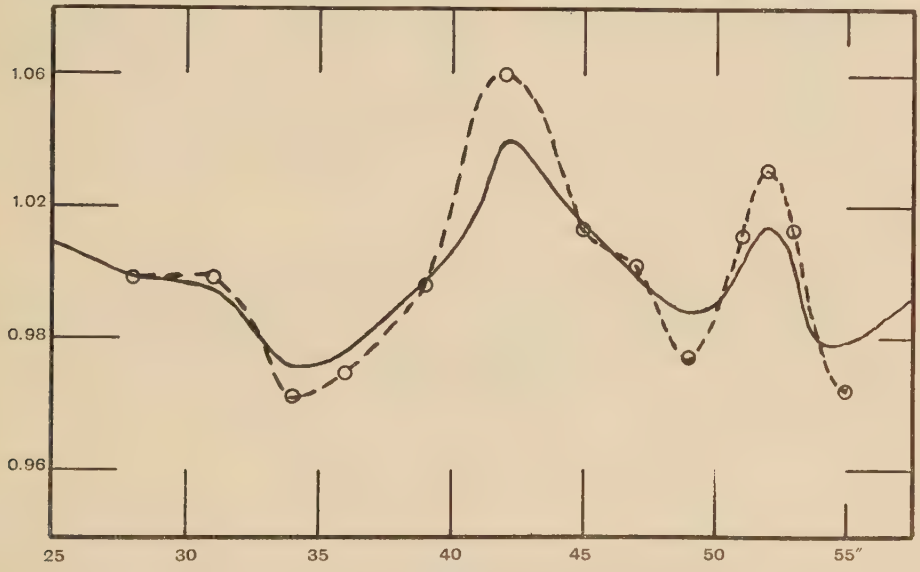

FIG. 4.—*Surface Brightness Corrected for Seeing.*
Full Line—Observed; Circles and Dotted Line—Corrected.

likely, or it may be due to spectrophotometric errors, since the surface brightness measurement is made at only one wave-length. For what it is worth, however, fig. 5 suggests that the surface brightness variations due to granulation are at least as fully marked at the limb as at the centre of the disc.

1.44. Assuming for the present purpose, what an inspection of fig. 3 makes not unlikely, that granules and intergranular regions occupy an equal area, then the length of the slit, divided by the number of maxima and minima occurring within its length, gives the diameter of an average granule. The results of this determination from the five good exposures are shown in Table III, and they lead to a mean diameter for a granule, measured at the mean surface brightness of the disc, of 4″·8. This is considerably larger than the diameters found by Janssen, Hansky and Chevalier, which averaged under 2″. It should, however, be recalled that these diameters were measured on plates obtained after repeated copyings from the original in order to increase the contrast, and consequently that the measured diameters

would tend to refer to the width of the peaks of the maxima. In view of the size of the direct solar images used in the present work, and the consistency

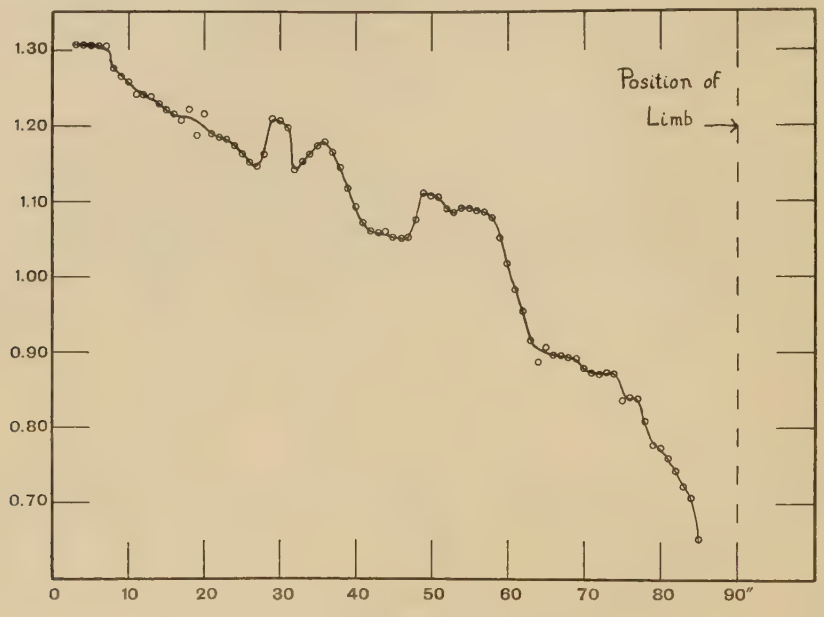

FIG. 5.—*Granular Surface Brightness at Limb. Measured at λ 4365 on W. 741(2).*

TABLE III

Granule Diameter

Exposure	N_{max}	N_{min}	Slit Length	Diameter
			″	″
W. 637	6	6	55	4·6
639	6	5	56	5·1
733(3)	8	9	98	5·8
746(3)	11	11	98	4·5
747(1)	12	12	98	4·1
			Mean	4·8

of the results from the Victoria and Oxford exposures, there can be little doubt that the diameter of a granule, measured at the mean surface brightness of the disc, is of the order of 5″ of arc, or 3700 km.

1.45. Summarizing the results of the present observational investigation it has been shown that—

(1) The maximum value of the surface brightness ratio of granule to intergranular region is 1·10.

(2) This surface brightness ratio increases with decreasing wave-length.
(3) The surface brightness ratio, if it does not increase towards the limb, at least remains constant over the disc.
(4) The average diameter of a granule, measured at the mean surface brightness of the disc, is of the order of 5″.

Section 2.—The Origin of Granulation and the Structure of the Solar Atmosphere

2.1. The existence of granulation with a flux variable both in position and time is a departure from the consequences of a purely radiative transfer of energy through the solar atmosphere. This departure may arise from the omission, in the equation of equilibrium, of a term due to energy generation, or to energy transport by convection. Now if we suppose that granulation is produced by some process of energy generation, the amount of energy generated in the mass of gas composing the granule can be calculated from the total emission of the granule during its lifetime. This is roughly given by

$$E = 4\pi r^2 \sigma t [T_2^4 - T_1^4], \tag{12}$$

where r, the radius of the granule, is taken to be $1{\cdot}9 \times 10^8$ cm., and t, its duration, as two minutes. T_2 is the temperature of the granule, T_1 is the temperature of its surroundings and σ is Stefan's constant. From Wien's law the temperatures T_2 and T_1 can be found from the surface brightness ratio $\mathcal{J}_2/\mathcal{J}_1$ of granular maximum to intergranular minimum, in accordance with the relation

$$\log \frac{\mathcal{J}_2}{\mathcal{J}_1} = 0{\cdot}4343 \frac{hc}{k\lambda}\left(\frac{1}{T_1} - \frac{1}{T_2}\right). \tag{13}$$

From § 1.4 $\mathcal{J}_2/\mathcal{J}_1 = 1{\cdot}10$, and assuming $T_1 = 6000°$, then $T_2 = 6100°$; inserting the various numerical values in equation (12) we thus find $E = 2{\cdot}7 \times 10^{29}$ ergs. Neglecting the ionization energy, the heat capacity of the monochromatic gas at pressure P, of which the granule is composed, is given by

$$\tfrac{4}{3}\pi r^3 \frac{P}{RT} \times \tfrac{3}{2} R \,.\, \Delta T = 2\pi r^3 P \frac{\Delta T}{T}, \tag{14}$$

where R is the gas constant. If we suppose the energy E to have been supplied by spontaneous generation in a time short in comparison with the life of a granule, a not unreasonable assumption, and put $P = 10^2$ dynes cm.$^{-2}$, $T = 6000°$, we find that ΔT must be $3{\cdot}8 \times 10^5$ degrees. In short, the heat capacity of the granule is so small that it could not handle an energy generation of $2{\cdot}7 \times 10^{29}$ ergs unless that energy were doled out uniformly over the life of the granule.

Under these circumstances it seems more reasonable to suppose that convection of warm matter from below is responsible for the production of granulation, rather than energy generation. This suggestion is not contradicted by the tentative observational conclusion of § 1.4 that the surface brightness contrast may increase towards the limb, a result which from

the integrations of Minnaert and Wanders * is a property of a region in convective equilibrium adjacent to one in radiative equilibrium.

2.2. *Convection in the Solar Atmosphere.*—The mechanical stability of an atmosphere in radiative equilibrium was first discussed by Schwarzschild.† An atmosphere is described as stable when a mass of gas, hypothetically displaced upwards, whose density and temperature have changed adiabatically, finds itself in a region of smaller density, or higher temperature, and is consequently forced back to its original position. To such displacements an adiabatic atmosphere will be in neutral equilibrium ; the stability of any atmosphere can therefore be determined by comparing its temperature gradient dT/dh with that of the adiabatic atmosphere, namely $(dT/dh)_{ad}$. Clearly the atmosphere in question will be stable, neutral or unstable according as

$$\frac{dT}{dh} \lessgtr \left(\frac{dT}{dh}\right)_{ad}.$$

Consider an atmosphere of perfect gas stratified in plane parallel layers, the depth h being measured in the same direction as the gravitational field. Then we have

$$\frac{dp}{p} = \frac{\mu g}{RT} dh. \tag{15}$$

Since for a gas in radiative equilibrium, whose absorption coefficient is independent of the pressure $dp/p = \{4T^3/(T^4 - T_0^4)\}dT$, and for a gas in adiabatic equilibrium $dp/p = \frac{\gamma}{\gamma - 1}\frac{dT}{T}$, it follows that

$$\left(\frac{dT}{dh}\right)_{rad} = \frac{\mu g}{4R}\left(1 - \frac{T_0^4}{T^4}\right); \qquad \left(\frac{dT}{dh}\right)_{ad} = \frac{\mu g}{R} \cdot \frac{\gamma - 1}{\gamma}. \tag{16}$$

Consequently an atmosphere in radiative equilibrium will be stable if

$$\left(\frac{dT}{dh}\right)_{rad} < \left(\frac{dT}{dh}\right)_{ad}, \quad \text{that is, if} \quad \gamma > \frac{4}{3 + \left(\frac{T_0}{T}\right)^4}. \tag{17}$$

Since for a monatomic gas $\gamma = 5/3$, Schwarzschild concluded that such an atmosphere would be stable provided it was not composed of polyatomic molecules.

In an important paper Unsöld,‡ however, has pointed out that if ionization as well as translational energy is taken into account, the ratio of specific heats may well fall below Schwarzschild's critical value. Following Fowler and Guggenheim,§ Unsöld finds for a one-constituent atmosphere that

$$\gamma = (\tfrac{5}{2} + X)/(\tfrac{3}{2} + X) \quad \text{where} \quad X = \frac{I_1}{kT} \Big/ \left[1 + \frac{2}{x(1-x)(I_1/kT + 5/2)}\right], \tag{18}$$

---

* *Zs. f. Ap.*, 5, 297, 1933.
† *Gott. Nachr.*, 41, 1906.
‡ *Zs. f. Ap.*, 1, 138, 1930.
§ *M.N.*, 85, 961, 1925.

so that when x, the fraction of ionized atoms, is greater than zero and less than one, $X > 0$ and $\gamma < 5/3$. Thus for $x = 0{\cdot}009$, $T = 6080°$, and hydrogen with $I_1 = 13{\cdot}54$ volts, $\gamma = 1{\cdot}23$. If hydrogen is the dominant constituent of the solar atmosphere, Unsöld finds that between $\tau = 3$ and $\tau = 20$, a depth of some 650 km., there should be a zone of instability where $\gamma < 4/\{3 + (T_0/T^4)\}$. A more refined calculation with similar results has recently been given by Cowling.*

2.21. Granted that granulation is probably due to convection, and granted that there exists a zone of instability, it has still to be shown, first, that convection does take place in the zone of instability, and secondly, that the observed granulation is the result of this convection. That instability is not in itself sufficient to produce motion, is shown by the frequent occurrence of super-adiabatic temperature gradients in the Earth's atmosphere. The theoretical investigations of Rayleigh † and Jeffreys,‡ following the experimental work of Bénard § on vertical instability, have shown that no motion will take place in a zone of instability until the temperature gradient exceeds the adiabatic by an amount

$$\beta = \lambda \frac{\kappa \nu}{g \alpha c \rho h^4}. \qquad (19)$$

This relation, in which λ (of the order of 1000) is a constant dependent upon the boundary conditions, g is the acceleration due to gravity, h is the depth of the layer, and κ, ν, α, c, ρ are respectively the thermal conductivity, the kinematic viscosity, the coefficient of expansion, the specific heat and the density of the fluid, has been experimentally verified by Schmidt and Milverton.‖ It may therefore be applied to the Unsöld zone of instability, and adopting the numerical values, $g = 2{\cdot}7 \times 10^4$ cm. sec.$^{-1}$, $\kappa/c\rho = \nu = 2$ cm.^{2} sec.$^{-1}$ (an over-estimate), $\alpha = 3{\cdot}7\ 10^{-3}$ per degree, and $h = 6{\cdot}5 \times 10^7$ cm., we find that the adiabatic gradient must be exceeded by $2{\cdot}2 \times 10^{-30}$ degrees per cm. before motion can take place. Since from equation (16)

$$\left(\frac{dT}{dh}\right)_{\text{rad}} - \left(\frac{dT}{dh}\right)_{\text{ad}} \doteq \frac{\mu g}{R}\left[\frac{1}{4} - \frac{\gamma - 1}{\gamma}\right] = 2{\cdot}7 \times 10^{-5} \text{ degrees cm.}^{-1} \qquad (20)$$

for $\gamma = 1{\cdot}2$, it is evident that there will be convection in the zone of instability.

From the work of Bénard,§ to which Deslandres ¶ has already drawn attention in the interpretation of spectroheliograms, it is probable that the motion in the zone of instability will be steady and in "convection cells." In the laboratory these convection cells cover the whole surface of the unstable layer, each cell ordinarily showing up-flow in the centre and down-flow at the edges, with a separation between the two oppositely directed streams of 1·5 times the depth of the layer. Brunt ** has pointed out that these cells may be readily seen in volatile gold paint, which is rendered vertically unstable by surface evaporation. In addition, these cells have been

* *M.N.*, **96**, 15, 1935.
† *Phil. Mag.*, **32**, 529, 1916.
‡ *Phil. Mag.*, **2**, 833, 1926.
§ *Ann. Phys. Chem.*, **23**, 62, 1901.
‖ *Proc. Roy. Soc.*, A, **152**, 586, 1935.
¶ *Ann. Obs. d'Ast. Phys.* (*Meudon*), **4**, 119, 1910.
** *Met. Mag.*, **60**, 1, 1925.

studied when formed under laboratory conditions in gases, and have also been observed in the Earth's atmosphere.* The similarity in distribution and appearance of granulation and convection cells is striking, particularly if the gold-paint experiment is repeated for one's self, and in view of the probability that granules are due to convection streams, it is reasonable to identify the granule and the surrounding intergranular region as a Bénard cell in the zone of instability. It should be noted, however, that the convection cells observed in the laboratory, unlike the granules, are relatively permanent affairs. The more temporary nature of the granule is presumably the result of the disturbance in the temperature gradient, at the best very little greater than the adiabatic, produced by the radiation from the upstream itself on its surroundings.

2.3. *Temperature Distribution in the Solar Atmosphere.*—The foregoing discussion has made it probable that granulation is the result of a partially successful attempt to set up Bénard convection cells in the Unsöld zone of instability. If this hypothesis is correct, these convection streams should warm their immediate surroundings in the zone of instability by radiation, so that, while at any one point in the zone the temperature will vary from that of radiative equilibrium to something higher, taking either a space or time average the zone of instability should be warmer than if there were no convection streams.

This is a prediction which may be tested by the observed darkening towards the limb. In its most general form the equation of transfer may be written

$$\cos\theta\frac{dI_\lambda}{\rho dx}=(k_\lambda+s_\lambda)I_\lambda-k_\lambda B_\lambda-s_\lambda\mathfrak{J}_\lambda. \tag{21}$$

In a spectral region free from absorption lines $s_\lambda=0$, and k_λ becomes the continuous absorption coefficient appropriate to the wave-length. Introducing the optical depth $\tau=\int k_\lambda\rho d_x$ where τ is a function of λ if k_λ is, the equation becomes

$$\cos\theta\frac{dI_\lambda(\tau,\theta)}{d\tau}=I_\lambda(\tau,\theta)-B_\lambda(\tau), \tag{21a}$$

or

$$I_\lambda(0,\theta)=\int_0^\infty B_\lambda(\tau)e^{-\tau\sec\theta}\sec\theta\,.\,d\tau. \tag{22}$$

This last is an integral equation giving the temperature distribution, $B_\lambda(\tau)$, which we require, in terms of $I_\lambda(0,\theta)$, the observed surface brightness as a function of θ. This equation may be thrown into a form suitable for numerical integration by the substitution

$$y=e^{-\tau\sec\theta}, \tag{23}$$

from which

$$I_\lambda(0,\theta)=\int_0^1 B_\lambda(\tau)\,.\,dy. \tag{24}$$

* G. T. Walker and S. Mal, *Quart. Journ. Roy. Met. Soc.*, 57, 413, 1931 ; A. C. Phillips and G. T. Walker, *ibid.*, 58, 23, 1932 ; A. Graham, *Phil. Trans.*, A, 232, 285, 1933.

Equation (24), which in this form is due to Eddington,* has been used by him to predict $I_\lambda(0, \theta)$ for an atmosphere in radiative equilibrium. Varying his treatment slightly it is possible to invert the problem, and to solve the equation for $B_\lambda(\tau)$; the method used will be made clear by reference to Table IV, a selection from the much larger table used in making the solution. The solar atmosphere is divided according to τ into 17 layers, the limits of these layers being given in the first column, and the mean τ for the layer in the second column. Down to $\tau = 2$, the portion of the atmosphere responsible for the greater part of the contribution to $I_\lambda(0, \theta)$, the division has been at intervals of 0·2 in optical depth, but for greater depths a much coarser division has been used. To each value of τ in the first column we may compute from equation (23) the corresponding value of y for any desired value of sec θ, and the difference of these y's gives Δy for the layer in question. These values of Δy are given in the first columns of the sections of Table IV headed sec $\theta = 1{\cdot}00$, 2·00, etc. The integral in equation (24) may be now replaced by a summation

$$\sum_1^n B_\lambda(\bar{\tau}_i) \,.\, \Delta y_i(\theta) = I_\lambda(0, \theta), \qquad (25)$$

TABLE IV

Temperature Distribution

$\tau_1 - \tau_2$	$\bar{\tau}$	Radiative		Observed		Sec $\theta = 1{\cdot}00$		
		T	$B_\lambda(T)$	T	$B_\lambda(T)$	Δy	Rad.	Obs.
0·0– 0·2	0·1	5750	0·254	5500	0·206	0·1813	0·0461	0·0374
0·2– 0·4	0·3	6090	·326	5885	·280	·1484	·0484	·0416
0·4– 0·6	0·5	6385	·401	6950	·561	·1215	·0488	·0682
0·6– 0·8	0·7	6640	·472	7285	·671	·0995	·0470	·0668
0·8– 1·0	0·9	6870	·540	7285	·671	·0814	·0439	·0546
1·0– 1·2	1·1	7080	·604	7285	·671	·0667	·0403	·0448
1·2– 1·4	1·3	7285	·671	7285	·671	·0546	·0366	·0366
1·4– 1·6	1·5	7455	·734	7455	·734	·0447	·0328	·0328
1·6– 1·8	1·7	7625	·792	7625	·792	·0366	·0290	·0290
1·8– 2·0	1·9	7785	·851	7785	·851	·0300	·0255	·0255
2·0– 2·4	2·2	7995	·934	7995	·934	·0446	·0416	·0416
2·4– 2·8	2·6	8250	1·038	8250	1·038	·0299	·0310	·0310
2·8– 3·2	3·0	8505	1·148	8505	1·148	·0200	·0230	·0230
3·2– 4·0	3·6	8835	1·289	8835	1·289	·0225	·0290	·0290
4·0– 4·8	4·4	9215	1·473	9215	1·473	·0101	·0149	·0149
4·8– 8·0	6·4	10010	1·877	10010	1·877	·0079	·0148	·0148
8·0–12·0	10·0	11100	2·478	11100	2·478	·0003	·0007	·0007
						1·000	0·5534	0·5923
							1·000	1·000

* *Internal Constitution*, 326, 1926.

TABLE IV—*continued*

$\bar{\tau}$	Sec $\theta = 2{\cdot}00$			Sec $\theta = 3{\cdot}00$			Sec $\theta = 4{\cdot}00$		
	Δy	Rad.	Obs.	Δy	Rad.	Obs.	Δy	Rad.	Obs.
0·1	0·3297	0·0837	0·0679	0·4512	0·1147	0·0931	0·5507	0·1399	0·1134
0·3	·2210	·0720	·0619	·2476	·0807	·0693	·2474	·0806	·0693
0·5	·1481	·0594	·0831	·1359	·0545	·0763	·1112	·0446	·0625
0·7	·0993	·0469	·0666	·0746	·0352	·0501	·0499	·0236	·0335
0·9	·0666	·0360	·0447	·0409	·0221	·0274	·0225	·0121	·0151
1·1	·0446	·0270	·0300	·0225	·0136	·0151	·0101	·0061	·0068
1·3	·0299	·0201	·0201	·0123	·0083	·0083	·0045	·0030	·0030
1·5	·0200	·0147	·0147	·0068	·0050	·0050	·0021	·0015	·0015
1·7	·0135	·0107	·0107	·0037	·0029	·0029	·0009	·0007	·0007
1·9	·0090	·0077	·0077	·0020	·0017	·0017	·0004	·0003	·0003
2·2	·0101	·0094	·0094	·0018	·0017	·0017	·0002	·0002	·0002
2·6	·0045	·0047	·0047	·0005	·0005	·0005	·0001	·0001	·0001
3·0	·0020	·0023	·0023	·0001	·0001	·0001			
3·6	·0014	·0018	·0018	·0001	·0001	·0001			
4·4	·0002	·0003	·0003						
6·4	·0001	·0002	·0002						
10·0									
	1·000	0·3969	0·4261	1·000	0·3411	0·3516	1·000	0·3127	0·3064
		0·717	0·719		0·616	0·594		0·565	0·517

where clearly equation (25) is one of the n linear equations which, if we know $I_\lambda(0, \theta)$, may be solved for $B_\lambda(\bar{\tau}_i)$. In the present case $n = 17$, and correspondingly we need $I_\lambda(0, \theta)$ at 17 values of θ.

The most accurate determination of $I_\lambda(0, \theta)$ is probably that of Moll, Burger and van der Bilt.* Their values of $I_\lambda(0, \theta)/I_\lambda(0, 0)$ for λ 5500, the wave-length region which is probably most free of absorption lines, are shown, plotted against cos θ, as a continuous line in fig. 6. The solution of the linear equations (25) has been effected by trial and error, the result of two preliminary trials being shown by dotted lines in the figure. Both are the predicted darkenings towards the limb for a radiative temperature distribution of $T^4 = T_0^4(1 + \frac{3}{2}\bar{\tau})$, in the one case for $T_0 = 4830°$, and in the other for $T_0 = 5800°$; in neither case is the observed darkening reproduced within anything like the estimated 1 per cent. accuracy of the observations. Referring now to Table IV, the third column gives $T = 5550°(1 + \frac{3}{2}\bar{\tau})^{1/4}$, another radiative temperature distribution, the fourth column gives the values of $B_\lambda(\bar{\tau})$, calculated from Planck's law in watts cm.$^{-2}$ per A.U., and the second columns of the various sec θ sections of the table give the corre-

* *B.A.N.*, 3, 83, 1925.

sponding values of $B_\lambda(\bar{\tau}) \cdot \Delta y$. Their sums are shown in the first line at the foot of the columns, and these sums are the absolute values of the surface brightness at these various θ's for this particular wave-length in watts cm.$^{-2}$ per A.U. For the present application we need only the relative values $I_\lambda(0, \theta)/I_\lambda(0, 0)$, and these are given in the second line at the foot of the table. Though these predicted ratios are not plotted in fig. 6, a

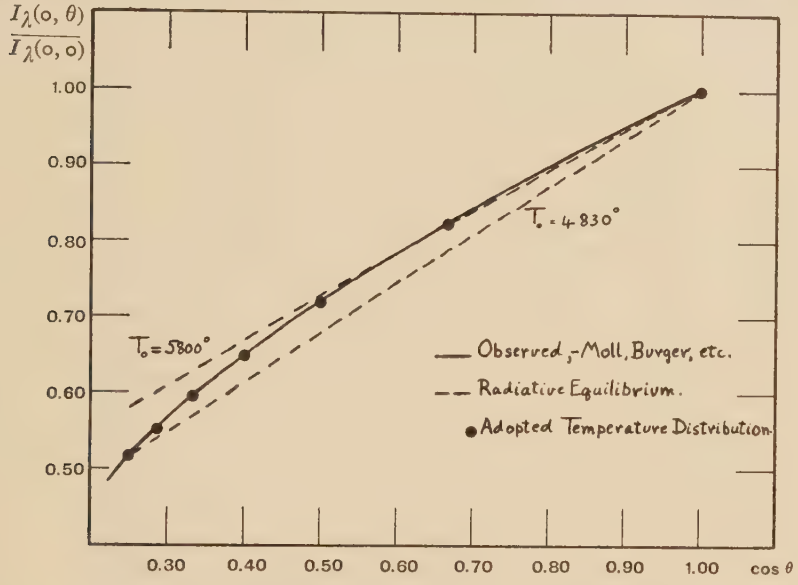

FIG. 6.—*Observed and Predicted Darkening at λ 5500.*

comparison between the table and the figure shows another failure of radiative equilibrium to reproduce the observed darkening.

Generally speaking, it can be seen that the radiative temperature distributions lead to a nearly linear change of $I_\lambda(0, \theta)/I_\lambda(0, 0)$ with cos θ, while the observed change is convex upwards. Some curvature, though not enough, can be introduced into the predicted darkening by increasing the temperature in the median layers around $\bar{\tau} = 1{\cdot}5$, and agreement with observation can be reached by increasing the median and decreasing the boundary values of $B_\lambda(\bar{\tau})$. The values of $B_\lambda(\bar{\tau})$ which meet these requirements are given in the sixth column, and the corresponding values of $B_\lambda(\bar{\tau}) \cdot \Delta y$ in the third columns of the sec θ sections ; the thus predicted values of $I_\lambda(0, \theta)/I_\lambda(0, 0)$ are shown in fig. 6 as filled circles, and it will be noted that they fall well on the observed curve. The temperatures corresponding to the adopted values of $B_\lambda(\tau)$ are found from Planck's law, and are given in the fifth column of the table ; these temperatures are shown as open circles, joined by a continuous line, in fig. 7, a figure in which optical depths are plotted as ordinates and temperatures as abscissæ. Where the radiative temperature distribution $T = 5550°(1 + \frac{3}{2}\bar{\tau})^{1/4}$ differs from the adopted temperature, the former is shown as a dotted line.

Inspection of fig. 7 shows that the observed temperature distribution

differs from the radiative, in much the way anticipated if granulation were due to convection streams. In this diagram it seems reasonable to identify the top of the zone of instability with the temperature bump occurring at $\tau = 1$; the bottom of the zone is presumably in deeper layers which affect but little the observed darkening. A noteworthy and unexpected feature of the temperature distribution is the large temperature gradient between $\tau = 0{\cdot}6$ and 0; it suggests that the atmosphere is trying to reach, in spite of the disturbance lower down, the radiative boundary temperature appro-

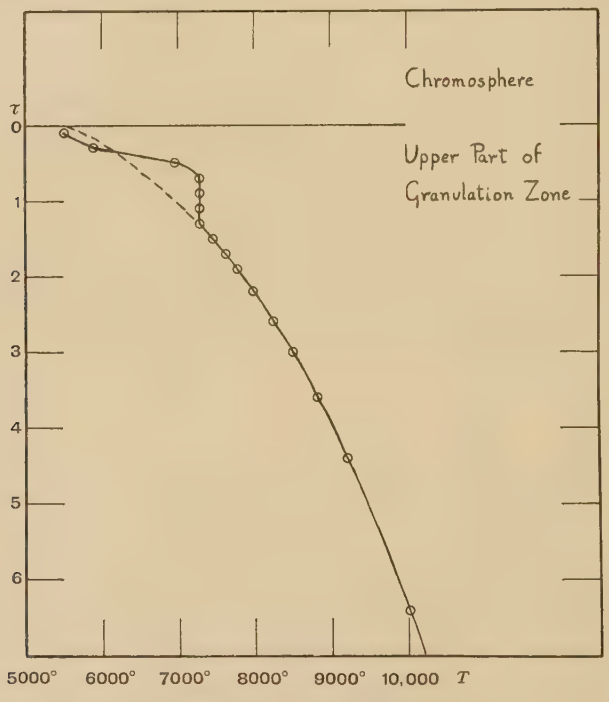

FIG. 7.—*Observed Temperature Distribution as Function of* τ *at* λ 5500.
Full Line and Circles—Observed.
Dotted Line—Radiative Equilibrium $T_0 = 5550°$.

priate to the net flux. The consequence of this large temperature gradient is that the convection streams will probably not die out at the top of the zone of instability, but will persist to the boundary $\tau = 0$.

This view can be tested in two ways, namely, from the observed contrast ratio of granulation at the limb, and from the diameter of a granule. Assume that the top of the convection stream terminates at optical depth τ_1, and that its surface brightness there is $I_1(\tau_1, \theta)$; let the surface brightness in the adjacent region at the same depth be $I(\tau_1, \theta)$. Then by an integration of the equation of transfer (21*a*) from τ_1 to 0 in these two regions, and by subtraction, we find

$$I_1(0, \theta) - I(0, \theta) = [I_1(\tau_1, \theta) - I(\tau_1, \theta)]e^{-\tau_1 \sec\theta} + \int_0^{\tau_1} [B_1(\tau) - B(\tau)]e^{-\tau_1 \sec\theta} \sec\theta d\tau. \quad (26)$$

Consequently the observed surface brightness difference will decrease towards the limb if the granulation terminates at optical depth $\tau_1 > 0$. The tentative conclusion from § 1.4 that the observed difference remains unaffected, or increases towards the limb, indicates that $\tau_1 = 0$. If, however, τ_1 is 0, then the depth of granulation must be greater than the 650 km. which Unsöld estimates as the thickness of the zone of instability. Such an increase of depth is just what the granulation diameter of 3700 km. requires ; for from the 1·5 ratio between diameter and depth it follows that the granular convection cells must take their origin in a layer 2500 km. thick. In short, the observed temperature distribution not only confirms the view that granulation is due to convection, but makes it highly probable that the granules extend above the zone of instability to $\tau = 0$.

Before leaving this temperature distribution attention may be drawn to the wealth of information on physical conditions in the solar atmosphere, which will be made available by numerical integrations of equation (24), when observation has yielded accurate values of $I_\lambda(0, \theta)$ in ergs cm.$^{-2}$ for spectral regions free from absorption lines. Not only will there result temperature distribution more accurate than that in fig. 7, but also relative values of the absorption coefficient as a function of wave-length and optical depth. Observations towards this end have been in progress in Oxford for several years, and an account of them will shortly be published. It is greatly to be desired, however, that other and more powerful attacks should be made on this fundamental problem of observational astrophysics.

2.4. *Granulation and Related Solar Phenomena.*—In concluding this discussion of the origin of solar granulation there are three related solar phenomena to which reference should be made. The first of these are the filaments observed in the penumbra of sunspots, and beautifully shown in the drawings of Langley.* It is tempting to suppose that these are granular convection cells under a shear. From the work of Idrac,† and of Walker and his pupils (*loc. cit.*), it is known that convection cells arrange themselves in lines parallel to a shear when one is applied. In the penumbra such a shear would be produced by the radial outward flow from the spot, and it is significant that where this flow stops—that is, at the boundary of penumbra and photosphere—there the filaments stop and ordinary granulation is observed. More observational work is badly needed here, however, for while Evershed ‡ finds the flow stopping abruptly at the photosphere, St. John § believes that it continues into the ordinary granulation region. If St. John is correct, the present view of the origin of filaments would have to be abandoned.

The second of these phenomena is the absence of granulation on faculæ.‖ If the faculæ lie above the granules, as Chevalier believed, this observation is readily explained, but from § 2.3 this requires that the faculæ must lie above $\tau = 0$. In spite of an earlier suggestion of mine to the contrary,¶ it follows from equation (26) that if the faculæ occurred at some optical

* *Am. Journ. Science*, **7**, 87, 1874.
† *Comptes Rendus*, **171**, 42, 1920.
‡ *Kodaikanal Obs. Bull.*, **15**, 1909 ; **51**, 1916.
§ *Ap. J.*, **37**, 322, 1913.
‖ *Ann. de l'Obs. de Zô-Sè*, **8**, C 18, 1912.
¶ *M.N.*, **91**, 927, 1931.

depth τ_1 greater than zero, they would be *less*, not more, conspicuous at the limb. Consequently faculæ must occur above $\tau = 0$, and the absence of granulation is understood.

The third of these phenomena are the minute bright flocculi observed in spectroheliograms and discussed by Hale and Ellerman.* In the wings of the *K* line these flocculi are comparable in dimensions with the granules, but as the core of the line is approached, and more particularly the core of *Hα*, the bright minute flocculi increase in size. Considering that part of the absorption line which arises from scattering, then it is clear from equation (26), applied to scattering, that as the core of the line is approached the observed appearance of a vertical luminous column will refer more and more to its upper part. It is reasonable, therefore, to follow Hale and Ellerman in regarding the flocculi as expanding columns standing on the granules, columns which, seen edgewise in the chromosphere outside the solar limb, give the appearance of "blades of grass." The origin of these columns is more difficult to understand. Chandrasekhar's interesting theory † implies a greater surface brightness difference between granule and intergranular region than found in § 1.4, and in any event is only applicable to Ca^+ atoms. Another possibility is that some of the atoms in the up-going stream may actually overshoot $\tau = 0$ and pass into the chromosphere. While there is evidence from McCrea and Mitra's discussion of the limb effect ‡ that the upward motion in the upstream must be greater than 0·7 km. per second, definite spectroscopic evidence of the velocity in the granules themselves is badly needed.

Summary.

From spectrophotometric investigations of solar granulation at Victoria and Oxford it has been shown that—

1. The maximum value of the surface brightness ratio of granule to intergranular region, after correction to perfect seeing, is 1·10.
2. The surface brightness ratio increases slowly with decreasing wavelength.
3. The surface brightness ratio, if it does not increase at the limb, at least remains constant over the disc.
4. The diameter of a granule, measured at the mean surface brightness of the disc, is of the order of 5″, or 3700 km.
5. From the total emission during its lifetime, and from its heat capacity, it is concluded that granules probably arise from convection rather than spontaneous energy generation.
6. From the Rayleigh-Jeffreys' theory of vertical instability it is shown that the temperature gradient in the Unsöld zone of instability is sufficient to set up motion, and it is suggested that the granules are the upstreams in the Bénard convection cells to be expected in such motion.

* *Proc. Nat. Acad.*, **2**, 102, 1916.
† *M.N.*, **94**, 14, 1933.
‡ *The Observatory*, **57**, 379, 1934.

7. The integral equation of radiative transfer is solved numerically, and the temperature distribution in the solar atmosphere is found from the observed darkening towards the limb. An isothermal layer is found near the top of the zone of instability, and this is attributed to heat conveyed by the granular convection streams.
8. The relation of granulation to some other solar phenomena is briefly discussed.

In conclusion I wish to express my thanks to the Milton Fund of Harvard and to the Dominion Government for grants which made the Victoria part of this work possible, and to my father, Dr. J. S. Plaskett, for the use of the telescope there. In addition I should like to acknowledge the value of helpful discussions of these problems with Professor Milne and Mr T. L. Page.

University Observatory,
Oxford :
1936 *March* 6.

SPECTROPHOTOMETRIC MEASURES OF NOVA HERCULIS 1934.

W. M. H. Greaves and E. Martin.

(Communicated by the Astronomer Royal)

1. Nova Herculis 1934 was discovered by Mr. J. P. M. Prentice on the morning of 1934 December 13. Its spectrum was photographed at Greenwich on the same morning and on twenty-five subsequent occasions, the last plate being taken on 1935 April 6. From December 16 onwards, on the seventeen occasions when the sky was judged to be uniformly transparent, the spectrum of a comparison star was photographed on the Nova plates, the Nova and comparison star being approximately at equal altitudes above the horizon. The plates were obtained with the 36-inch Yapp reflector used in conjunction with a slitless spectrograph. The spectrograph is of the same general design as that previously used with the 30-inch reflector, and described in a Greenwich publication.* The most important modification consists of the method employed for broadening the spectra. In the spectrograph attached to the 36-inch, this is effected by an electric motor, a cam being utilised for the production of an oscillatory motion of the metal plate on which the photographic plate carrier is mounted. A set of cams provide different breadths of spectra. The breadth used is 0·5 mm. and the period of the complete double stroke is five seconds. The dispersion is 237 A. per mm. at $H\alpha$ and 48 A. per mm. at $H\delta$.

The plates used were Ilford "Hydrogen-Alpha" plates. They were

* *Observations of Colour Temperatures of Stars*, 1932.

calibrated with a multiple slit spectrograph, used in conjunction with a set of filters, and employing a standard exposure time of 20s. All magnitude differences obtained from the measures were multiplied by the factors given in *The Observatory*, 59, 11, 1936, these factors depending on the exposure time with the telescope. For measurements of line intensities, which consisted of comparing a line contour with the neighbouring continuous spectrum, the calibration was of course adjusted to the actual exposure time for the Nova spectrum. For continuous spectrum work where a spectrum of the Nova with exposure time t_1 was being compared with a spectrum of the comparison star with exposure time t_2, the calibration was adjusted to an exposure time t, where $\log t = \frac{1}{2}(\log t_1 + \log t_2)$. Apart from this adjustment differences of exposure time were ignored, it being known that when the relative distribution of energy in the continuous spectrum of a star is being measured, the error produced by such treatment is inappreciable.*

Nine of the plates taken were selected for measurement, the details being given in Table I. The dates were selected as being representative of various typical stages in the development of the Nova. On each plate there were, as a rule, several spectra of the Nova, with varying exposure times. The times t_1 given in the table refer to the spectra on which measures of the continuous spectrum were taken.

TABLE I

U.T.	Comparison Star	Exposure Times	
		t_1 Nova (continuous)	t_2 Comparison Star
		s	s
1934 Dec. 18.74	ζ Lyræ	60	255
Dec. 23.76	ζ Lyræ	90	300
Dec. 27.27	ρ Herculis	90	270
Dec. 31.74	ζ Lyræ	120	390
1935 Jan. 13.26	ρ Herculis	60	300
Feb. 9.24	ρ Herculis	30	360
Mar. 8.20	ρ Herculis	120	360
Mar. 26.10	ρ Herculis	720	360
Apr. 6.12	ρ Herculis	...	420

The measures were taken in spectral regions surrounding the Balmer lines *Hα*, *Hβ*, *Hγ* and *Hδ*, and (for the later plates) surrounding the "forbidden" lines of neutral oxygen at λ 5577, λ 6300 and λ 6364. The measures were made with the visual microphotometer which has been described in the Greenwich Colour Temperature Volume.† The breadth of the image of the lamp filament on the plate was approximately 12 microns. This corresponds to the breadth of the analysing slit in other forms of microphotometer. It would be too large for the measurement of slit spectra, but for the slitless spectra here considered, in which one second of arc corresponds to 27 microns, no object would be served by improving the resolution.

* *Loc. cit.*, pp. 7–9 and 17.

† *Loc. cit.*, p. 15.

The measurements were made with a view to obtaining the following information :—

(1) The relative distribution of energy in the continuous spectrum of the Nova for the spectral regions considered.

(2) The intensities of the lines measured in terms of the neighbouring continuous spectrum.

By combining these results the relative intensities of the lines in terms of $H\alpha$ as unit were deduced. Further, the absolute intensities of $H\alpha$ were obtained. For the last purpose, however, the differences of exposure time had to be taken into account. It will be seen that the uncertainty introduced thereby is not serious.

2. *Measurement of the Continuous Spectrum.*—For each spectral region considered the spectrum of the Nova was measured at a number of selected points, including the points of maximum and minimum density discernible. The comparison star was also measured over the same regions, the densities plotted and the continuous spectrum drawn in. As both of the comparison stars used were of early type, this presented no difficulty. The magnitude differences between Nova and comparison star were then derived for each wave-length at which the Nova was measured, and the results plotted on a diagram against reciprocal of wave-length. The continuous spectrum of the Nova was then drawn in. The fixation of the "continuous spectrum" of a complicated spectrum like that of a nova, involving both absorption and emission lines, must necessarily depend to some extent on individual judgment. It does not appear to us that the uncertainty thereby introduced into the results can exceed a tenth of a magnitude.

The two comparison stars were compared in the ordinary way with members of the Greenwich Standard System and their colour temperatures deduced. The values of ϕ and T obtained for them are

	Magnitude Spectral Type	ϕ	T
ζ Lyræ (Br.)	4·3 A_3	1·42	10900°
ρ Herculis (sum of components)	4·1 Ao	1·04	16800°

The values of T are based on the adopted value $\phi_0 = 1{\cdot}0$ ($T = 18000°$) for the zero point of the Greenwich Standard System.*

With the aid of these colour temperatures the results given in Table II for the Nova were obtained. The quantity tabulated is I_λ, the energy in 1 A. of continuous spectrum. The unit in each case is the energy in 1 A. at $H\alpha$.

No continuous spectrum is visible on the plate taken on April 6. With a 30-minute exposure on the Nova, the only features visible on this plate are the lines $H\alpha$, λ 6300 and λ 6364.

If the values in Table II be plotted against λ, the resulting curves are

* *M.N.*, **94**, 6, 507, 1934.

TABLE II

Energy Distribution in Continuous Spectrum of Nova Herculis

Values of I_λ

U.T.	$H\alpha$	λ 6364	λ 6300	λ 5577	$H\beta$	$H\gamma$	$H\delta$
1934 Dec. 18.74	1				1·94	2·75	2·90
Dec. 23.76	1				1·72	2·13	2·36
Dec. 27.27	1				1·35	1·86	1·79
Dec. 31.74	1				1·69	2·27	2·67
1935 Jan. 13.26	1	1·09	1·12	1·41	1·80	2·10	2·36
Feb. 9.24	1	1·06	1·07	1·36	1·80	2·46	2·75
Mar. 8.20	1	1·06	1·08	1·35	1·84	2·44	2·49
Mar. 26.10	1	1·07	1·09	1·27	2·04	2·70	3·03

not Planck curves. For each plate a Planck curve was fitted to the values at $H\alpha$, $H\beta$, $H\gamma$ and $H\delta$, and the residuals from this curve derived. These residuals are given in Table III. They are expressed in magnitudes, a positive sign denoting that at the wave-length in question I_λ is in excess of the value given by the Planck curve. The last column of the table gives the value of T corresponding to the Planck curve in question. It is hardly necessary to emphasise the circumstance that these "temperatures" have little physical significance, as the atmosphere of the Nova is certainly not in an equilibrium condition.

TABLE III

Residuals from Planck Curves

U.T.	$H\alpha$	$H\beta$	$H\gamma$	$H\delta$	λ 6364	λ 6300	λ 5577	T
	m	m	m	m				°
1934 Dec. 18.74	+0·02	−0·07	+0·05	0·00				11200
Dec. 23.76	+0·02	−0·05	−0·01	+0·04				9100
Dec. 27.27	+0·04	−0·14	+0·09	+0·01				7800
Dec. 31.74	+0·05	−0·12	−0·01	+0·08	m	m	m	10000
1935 Jan. 13.26	+0·01	−0·01	−0·03	+0·03	+0·03	+0·03	−0·01	9100
Feb. 9.24	+0·03	−0·09	+0·02	+0·04	0·00	−0·02	−0·07	10500
Mar. 8.20	+0·01	−0·05	+0·05	−0·01	−0·01	−0·02	−0·09	9900
Mar. 26.10	+0·01	−0·04	+0·01	+0·02	−0·01	−0·02	−0·20	11500

The really surprising feature is that the departures from the Planck curves are as small as they are. It seems that this is partly an accident depending on the range of wave-length considered. From the results of Beileke and Hachenberg,* it appears that the continuous spectrum of the Nova can be fitted to within 10 per cent. to a Planck curve from λ 4000 to λ 6200, but that for wave-lengths below λ 4000 the spectrum rises considerably above these Planck curves, the excess at λ 3700 amounting to as much as three-quarters of a magnitude.

3. *Measurement of Line Intensities.*—In utilising the Greenwich slitless spectrograms for the measurement of line intensities, we are really applying the instrument to a purpose for which it was never intended. The slitless spectrograph was designed for the photometry of the continuous spectra

* *Zs. f. Ap.*, **10**, 5, 366, 1935.

of early-type stars, and its comparatively small dispersion, together with the circumstance that, being slitless, the lines are affected by atmospheric tremor, make it unsuitable for line contour work. But although the contours are necessarily distorted, there seems no valid argument against the application of the instrument to the measurement of *total* intensities, and it was accordingly decided to measure the Balmer lines $H\alpha$, $H\beta$, $H\delta$, and the neutral oxygen lines at λ 5577, λ 6300 and λ 6364. $H\gamma$ was not measured for the reason given below.

The measurement was made in the usual way. Each line was contoured by a large number of successive settings with the photometer, and the magnitude differences against the neighbouring continuous spectrum formed. These were then converted into light ratios, and the resulting contour of the line plotted. Since the violet sides of the emission lines are affected by the accompanying absorption lines, only the redward halves of the contours, *i.e.* the portions of the areas to the long wave-length side of the maximum, were measured. To make this clear the results will be referred to as "half-intensities." For each emission line the area bounded by the contour, the interpolated continuous and the maximum ordinate was measured by means of a planimeter, and it is to these areas that the results below refer.

In the case of $H\gamma$, the redward wing of the emission line was badly affected by blending with λ 4351 and this line was accordingly not measured.

On 1934 December 23.76, the usual emission spectrum of the Nova was replaced by an absorption spectrum. $H\alpha$ appears as a (relatively weak) emission line, but $H\beta$ and $H\delta$ are shown only in absorption. In this case also only the redward halves of the lines were measured.

On the last plate, taken on April 6.12, there was no continuous spectrum visible, and the three lines measured were compared with the continuous spectrum of ρ Herculis.

Table IV gives the exposure times. As stated above, the appropriate factor was applied in each case to the magnitude differences deduced from the calibration exposures.

TABLE IV

Exposure Times for Line Intensities

U.T.	$H\alpha$	$H\beta$	$H\delta$	λ 6300 / λ 6364	λ 5577
	s	s	s		
1934 Dec. 18.74	60	60	60		
Dec. 23.76	40	90	90		
Dec. 27.27	20	90	90		
Dec. 31.74	20	120	120		s
1935 Jan. 13.26	25	60	60	s	60
Feb. 9.24	10	30	60	30	60
Mar. 8.20	30	120	300	120	300
Mar. 26.10	90	720	720	720	720
Apr. 6.12	1800	...	...	1800	...

The results are given in Table V, the half-intensities being expressed in terms of a unit of 10 A. of the neighbouring continuous spectrum. For the

line λ 6364 the unit is 10 A. of the continuous at λ 6300. In the case of the last plate the unit is 10 A. of the comparison spectrum (ρ Herculis). The redward wing of λ 6300 was always blended with the violet wing of λ 6364, and some allowance had to be made for this.

TABLE V

Half-Intensities of Lines

Unit = 10 A. of neighbouring continuous spectrum

U.T.	*Hα*	*Hβ*	*Hδ*	λ 6300	λ 6364	λ 5577
1934 Dec. 18.74	1·71	0·56	0·14			
Dec. 23.76	0·12	0·15 *a**	0·10 *a**			
Dec. 27.27	3·72	2·01	0·23			
Dec. 31.74	12·2	3·23	1·01			
1935 Jan. 13.26	11·8	3·06	0·72			0·27
Feb. 9.24	19·8	4·52	0·85	0·84	0·44	0·49
Mar. 8.20	34·0	3·91	1·27	3·09	1·25	0·67
Mar. 26.10	17·3	2·40	1·49†	2·23	1·76	(0·6)‡
Unit = 10 A. of comparison spectrum						
Apr. 6.12	4·74	...	...	1·64	0·79	

* Absorption line.

† Blended with 4128. The value given represents the half-intensity of *Hδ plus* the whole intensity of 4128. The lines on this plate are broad with extensive wings.

‡ Difficult. Result uncertain.

On multiplying the quantities in Table V by the corresponding values of I_λ given in Table II (by the values of I_λ for ρ Herculis, corresponding to $T = 16800°$, in the case of the April 6 plate), and dividing the results by the result for *Hα*, we obtain the relative intensities of the lines considered in terms of *Hα* as unit. The results are given in Table VI.

TABLE VI

Relative Line Intensities (*Hα* = 1)

U.T.	*Hα*	*Hβ*	*Hδ*	λ 6300	λ 6364	λ 5577
1934 Dec. 18.74	1	0·64	0·24			
Dec. 23.76	1	(2·2 *a**)	(2·0 *a**)			
Dec. 27.27	1	0·73	0·11			
Dec. 31.74	1	0·45	0·22			
1935 Jan. 13.26	1	0·47	0·14			0·03
Feb. 9.24	1	0·41	0·12	0·05	0·02	0·03
Mar. 8.20	1	0·21	0·09	0·10	0·04	0·03
Mar. 26.10	1	0·28	0·26†	0·14	0·11	(0·05‡)
Apr. 6.12	1	...	...	0·40	0·19	

* Absorption line. The figure given is the energy absorbed, the unit being the energy emitted in *Hα*.

† Blended with 4128. See previous note.

‡ Difficult. Result uncertain.

The most striking feature of this table is the decrease, as the Nova develops, of the value for $H\beta$. The strengthening, in March and April, of the neutral oxygen lines λ 6300 and λ 6364 is also clearly marked. The values for $H\delta$ are probably affected throughout by blending.

4. *Absolute Intensities of Hα.*—Table V gives the intensities of the lines referred in each case to the neighbouring continuous spectrum. To derive absolute values it is necessary to have monochromatic magnitudes for the continuous spectrum. Since the exposure times for Nova (continuous) and comparison star are different, the monochromatic magnitudes in question can only be derived by making some assumption concerning the way in which the exposure time enters into the density-intensity relationship.

It is well known that for moderate ranges in exposure time, such as are used here, the law propounded by Schwarzschild is a very good approximation. According to Schwarzschild's formula the density is a function of It^p, where for a given plate p is a constant. If, then, t_1 and t_2 be the respective exposure times for Nova (continuous) and comparison star, and if for a given wave-length $\Delta m'$ be the measured magnitude difference, ignoring the difference of exposure time, then the true magnitude difference Δm is given by

$$\Delta m = \Delta m' + c,$$

where

$$c = 5/2p \log (t_2/t_1).$$

The magnitude differences are reckoned positively in the sense bright *minus* faint.

To determine p we must compare a star with itself using different exposure times. (In this case $\Delta m = 0$ and so $c = -\Delta m'$.) The varying exposure times given to the Nova on the majority of the plates were utilised for this purpose, the comparison being made at selected wave-lengths. The values of p obtained in this way from six plates ranged from 0·92 to 0·65 with a mean of 0·81. The value 0·80 was adopted.

From the values of t_1 and t_2 given in Table I the quantities c were computed. The results are given in the following table. The last column

TABLE VII

Values of c

U.T.	c	δc ($\pm$ ·05 in p)
	m	m
1934 Dec. 18.74	+1·26	± 0·07
Dec. 23.76	+1·04	± 0·07
Dec. 27.27	+0·95	± 0·06
Dec. 31.74	+1·02	± 0·07
1935 Jan. 13.26	+1·40	± 0·09
Feb. 9.24	+2·16	± 0·14
Mar. 8.20	+0·95	± 0·06
Mar. 26.10	−0·60	± 0·04
Apr. 6.12*	−1·27	± 0·08

* Here $t_1 = 1800^s$, $t_2 = 420^s$. See subsequent remark.

gives the errors in c corresponding to an error of $\pm$ 0·05 in p, and these may be taken as a fair estimate of the uncertainties introduced by the employment of the Schwarzschild formula.

The subsequent reductions proceeded as follows. A set of comparisons, using equal exposure times, between ζ Lyræ and ρ Herculis was utilised for the purpose of reducing all the Nova comparisons to ρ Herculis as comparison star. The values of Δm for Nova (continuous) *minus* ρ Herculis were then derived by the use of the values of c tabulated above. The resulting values were subtracted from $4^{m}\cdot14$. This is the visual magnitude of ρ Herculis (sum of components) and, the star being an Ao, was taken as representing the monochromatic magnitude at any wave-length. The monochromatic magnitudes thus obtained for the continuous spectrum of the Nova in the wave-length of $H\alpha$ are given in Table VIII.

TABLE VIII

Monochromatic Magnitudes at Hα for Nova Herculis (continuous)

U.T.	m
1934 Dec. 18.74	2·54
Dec. 23.76	1·63
Dec. 27.27	1·98
Dec. 31.74	2·44
1935 Jan. 13.26	2·62
Feb. 9.24	2·50
Mar. 8.20	3·43
Mar. 26.10	3·95

As a check, monochromatic magnitudes were also obtained for $H\beta$ and then, by interpolation, for λ 5300 which, according to Brill, may be taken as the effective wave-length for the Harvard scale of visual magnitudes. The resulting monochromatic magnitudes can be compared with visual magnitudes, it being remembered that the visual magnitudes include the effect of the lines. On December 23.76, when the lines were mostly absorption, the monochromatic magnitude would be brighter than the visual, and for the remaining dates it would be fainter. From the diagrams of Δm (Nova *minus* comparison) plotted against $1/\lambda$, which were referred to above, it is estimated that the difference would vary from rather less than $0^{m}\cdot05$ for the earlier plates, to rather more than $0^{m}\cdot10$ for the later plates. The comparison is given in Table IX, the visual magnitudes being those given by H. Krumpholtz * and by W. H. Steavenson.† Only magnitudes corresponding to epochs within $0^{d}\cdot1$ of the U.T. of the Greenwich plates are included.

The comparisons are as satisfactory as can be expected. They confirm the conclusion that no gross errors result from the use of the Schwarzschild coefficient.

With the aid of the $H\alpha$ continuous spectrum magnitudes given in Table VIII, the half-intensities of the $H\alpha$ line given in Table V can be

* *Wien Obs. Publ.*, No. 4, 1935. The magnitudes are compiled from various sources.

† *M.N.*, 95, 8, 639.

TABLE IX

Values of m

U.T.	Continuous Spectrum λ 5300	Krumpholtz	Steavenson
1934 Dec. 18.74	2·72	2·68	2·64
Dec. 23.76	1·92	2·05	2·12
Dec. 27.27	2·44		
Dec. 31.74	2·75	2·60	2·42
1935 Jan. 13.26	2·87		
Feb. 9.24	2·75	2·69	
Mar. 8.20	3·67	3·56	
Mar. 26.10	4·11	4·01	3·90

converted to an absolute basis. The results are given in Table X, the quantities tabulated being the values of $5/2 \log I\alpha$, where $I\alpha$ is the half-intensity of $H\alpha$ in terms of a unit, which is 10 A. of the continuous spectrum, at $H\alpha$, of an Ao star of magnitude 5·0. The value for the last date (April 6) was obtained by a direct comparison between the line and the continuous spectrum of ρ Herculis, using the appropriate value of c. The visual magnitude for April 5.96 is given by Steavenson as 8·3.

TABLE X

Nova Herculis. Absolute Half-Intensities of Hα

Unit = 10 A. at $H\alpha$ for continuous spectrum of an Ao star of magnitude 5·0

U.T.	$5/2 \log Ia$	$5{\cdot}0 - m$ (m = visual magnitude)
1934 Dec. 18.74	3·04	2·3
Dec. 23.76	1·07	3·0
Dec. 27.27	4·45	2·6
Dec. 31.74	5·28	2·3
1935 Jan. 13.26	5·06	2·2
Feb. 9.24	5·74	2·3
Mar. 8.20	5·40	1·4
Mar. 26.10	4·15	1·0
Apr. 6.12	2·55	−3·3

In Table X the logarithms of $I\alpha$ have been multiplied by 5/2 so as to give the familiar magnitude scale. It is to be noted, however, that increasing values correspond to increasing brightness. The values of the visual magnitude of the Nova, subtracted from 5·0, are given for comparison. The absolute line intensities do not appear to bear any relation to the visual magnitudes. The output of $H\alpha$ energy seems to have been greatest in February, more than a month after the visual maximum. In default of a comprehensive quantitative theory of the formation of the $H\alpha$ line any suggestion must be very tentative. If the line is formed in the process of recombination following ionisation, it is possible that the values of $I\alpha$ reflect the output of energy from the star in the extreme ultra-violet.

Royal Observatory,
Greenwich:
1936 *March* 6.

NOTE ON THE COLOUR-TEMPERATURE OF NOVA HERCULIS 1934.

E. G. Williams, M.A., and H. E. Green, M.A.

(Communicated by the Director, Cambridge Observatory)

The energy distribution in the spectrum of Nova Herculis has been the subject of three published papers.*

In view of differences between the results of the various observers it has been thought worth while to reduce the only plate, taken 1935 March 5.15 at the Cambridge Observatory, on which the spectrum of a comparison star was also photographed.

The 2-inch calcite prismatic camera mounted on the Thorrowgood telescope was used.† The dispersion is 60 A. per mm. at λ 3800, and the spectra are measurable from $H\alpha$ to λ 3100.

The comparison star, ι Herculis, was photographed immediately after the Nova, the interval between mid-exposures being 35^m, whilst the respective zenith distances were $25^\circ{\cdot}6$ and $35^\circ{\cdot}4$. No corrections for differential extinction have been applied.

In the auxiliary spectrograph used for plate calibration a continuous wedge-spectrum is produced by a 100-watt lamp. The intensity in this spectrum below λ 3900 is too weak to be of any use. Consequently it was necessary to use the calibration at λ 4100 for all shorter wave-lengths of measurement. A test-plate with two spectra of β Cephei, in a known intensity ratio produced by a perforated screen, showed that the difference between the characteristic curve in the violet and in the observed ultra-violet range is inappreciable for the emulsion used. Any such differences which may exist will have negligible effect, as the density differences to be measured between nova and comparison star are small. For the longer wave-length region the appropriate wedge calibration was, of course, used in each case.

In common with all other B3 stars, ι Herculis shows fairly strongly the continuous hydrogen absorption below the Balmer limit. Quantitative measures of this absorption in a number of early-type stars have been published by Barbier, Chalonge and Vassy.‡ They express by D_0 the logarithmic ratio of the hypothetical black body and observed intensities at the Balmer limit, and find that in B-type stars this continuous absorption either remains constant or decreases slightly from the limit towards shorter wave-lengths. Full results are not yet published for ι Herculis, but M. Chalonge very

* Petrie, *Ap. J.*, **81**, 482, 1935 ; Beileke and Hachenberg, *Zs. f. Ap.*, **10**, 366, 1935 ; Barbier, Chalonge and Vassy, *C.R.*, **201**, 128, 1935.

† See H. E. Green, *M.N.*, **95**, 694, 1935.

‡ *Journal de Physique*, série VII, **6**, 137, 1935.

kindly informs us that $D_0 = 0{\cdot}17$ for this star. We have assumed that this figure gives the absorption to the lower wave-length limit of the plate. The requisite correction to the values of $\Delta \log$ (Intensity) below the Balmer limit has been introduced in our reductions (Table I). Petrie, and Beileke

TABLE I

Values of $log_{10} I_{\text{Nova}}$ minus $log_{10} I_{\iota\,\text{Her.}}$

λ	3133	3180	3235	3292	3387	3433	3540	3610	3690
Corrected $\Delta \log I$	·220	·180	·179	·176	·150	·150	·110	·114	·095
λ	3940	4040	4210	4380	4780	5100	5510	5870	6150
Corrected $\Delta \log I$	·159	·114	·134	·186	·190	·334	·326	·310	·350

and Hachenberg, expressed their results in terms of colour-temperature, whilst Barbier, Chalonge and Vassy gave curves of absolute intensity plotted against wave-length. For the sake of uniformity we here consider all observations in terms of "relative gradient" in conformity with the practice adopted by the Greenwich observers.* As is well known, when the measured energy difference between two spectra at different temperatures is plotted against the reciprocal of the wave-length, a straight line results, to a close approximation, if the energy distribution in both spectra is of black-body type. The slope of this line (ϕ, the gradient) is correlated with the colour-temperature, T, through the relation

$$\phi = \frac{c_2}{T} \Big/ \left(1 - e^{\frac{-2c_2}{T}}\right),$$

where c_2 is a constant.

In fig. 1 the logarithmic intensities are all plotted relative to a black body at 10,000 degrees, so that a horizontal line on the diagram would correspond to this colour-temperature. The slope of the dotted line running up diagonally to the left corresponds to infinite temperature.

The dots in fig. 1 represent our plate, and are derived through the assumption of a colour-temperature for ι Herculis of 31,000°, which is the smoothed mean value for B3 stars as observed at Greenwich.

The curve drawn through these points suggests that the intensity distribution in the spectrum of the Nova is far from being of black-body type. The gradient as drawn down to λ 3800 corresponds to a temperature of 12,000°, whilst that in the ultra-violet, when interpreted in the usual manner, is indicative of $T > \infty$.

Although no correction was applied to our measures to allow for the 10° difference in zenith-distance, it is worth noting that, provided the sky remained clear over the period of observation, such corrections would act in the direction of raising still further the colour-temperature of the Nova, since the comparison star was observed at the greater altitude.

The two other curves in the figure are derived from plates of the French

* *Observations of Colour Temperatures of Stars*, Greenwich, 1932.

and German workers, both taken within one day of our plate. Petrie's published observations have not been entered, as they do not extend beyond

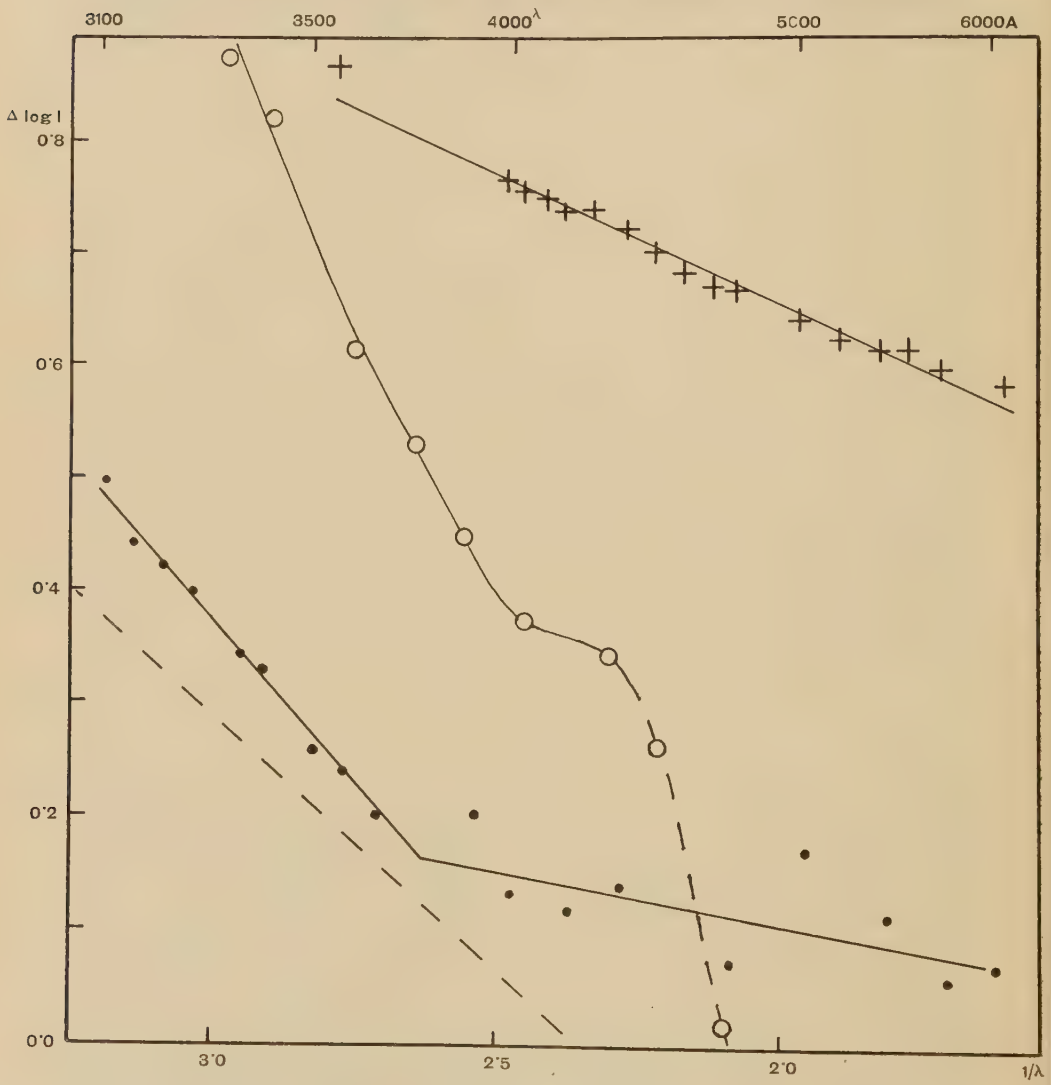

FIG. 1.—*The relation between* $\log_{10} I_{Nova}/I_{10,000°}$ *and* $1/\lambda$. *Dots represent the Cambridge plate of March 5; crosses, that of Beileke and Hachenberg for March 4; circles, Barbier, Chalonge and Vassy's measurements for March 6. The broken line on the left represents the gradient corresponding to infinite temperature.*

February 27. His temperatures are lower by about 20 per cent. when compared with those of Beileke and Hachenberg extending over the same period of time and reduced to the Greenwich scale.

The latter observers in their discussion gave temperatures for Nova Herculis which were based on $T = 20{,}730°$ for ι Herculis. In order to bring their results into line with the others discussed here, we have re-reduced

the points for their March 4 plate, represented by crosses in fig. 1, on the assumption of $T = 31{,}000°$ for ι Herculis.

Their original curves for the intensity ratio between the Nova and standard star all show a sudden increase below $\lambda 3900$. This is due to the hydrogen absorption in the comparison star, since the Balmer lines begin to overlap one another at this wave-length. When the correction of 0·17 in $\Delta \log I$ appropriate for ι Herculis is applied to their March 4 curve, the last measured point at $\lambda 3600$ is brought, as here shown, closely into line with the other points for the region free from this absorption effect.* The slope of the line corresponds to $T = 17{,}600°$.

The curve joining the circles represents the data from a plate taken on March 6.01 by Barbier, Chalonge and Vassy. They remark that the broken portion of the curve is of rather low weight.

The figure shows that the rate of energy increase toward shorter wave-lengths found by them in the ultra-violet is much more rapid than would be shown by a perfect radiation at any finite temperature. This is true of all their plates.†

In spite of the manifest difficulty of reconciling the various observations two conclusions can be drawn. One is that the energy distribution is not Planckian; the other, that the intensity in the ultra-violet is extremely high.

The marked change of gradient, occurring as it does in the vicinity of the Balmer limit, suggests that continuous hydrogen absorption or emission may be in some way responsible. If this is the case, the trouble may lie either in the Nova or in the comparison spectra.

As the French observers compared the Nova with three stars for which they had previously made absolute energy measurements in the ultra-violet, and as one of these, γ Cassiopeiæ, has continuous hydrogen *emission*, a systematic error due to the comparison stars seems unlikely.

The observed ultra-violet spectrum in the Nova is, of course, the resultant of a continuous spectrum suffering continuous hydrogen absorption on which is superimposed the continuous hydrogen emission arising in the expanding nebular shell. This combination of emission and absorption is incapable of producing a sufficiently large change of gradient to meet the observed change, unless the intensity of the continuous Balmer emission increases rapidly with decreasing wave-length below the limit.

All the results reviewed here have been obtained from small dispersion spectra, and it is inevitable that the crowded absorption and emission lines which were such a conspicuous feature of the spectrum should have an

* Brill (*Potsdam Astrophysical Observations*, **23**, No. 70, 1914) in discussing the energy distribution in the continuous spectrum of N. Geminorum 1912, made his measurements with reference to a B9-type star in the same field. He found intensity maxima in both red-yellow and ultra-violet. He did not, however, correct for the continuous hydrogen absorption in the comparison star. When the mean value of this correction for a B9-type star, as found by Barbier, Chalonge and Vassy, is applied to his measures, the ultra-violet maximum in the Nova is removed.

† M. Chalonge informs us that re-examination of their records precludes the possibility of decreasing the slope of their curves to that for infinite temperature.

influence on the measured energy distribution. The combined effect of these must await photometric work on plates of higher dispersion.

As the general tendency is for the emission lines to be stronger in the longer wave-length region and for the absorption lines to be at least relatively stronger in the ultra-violet, it does not seem possible to explain the relatively high ultra-violet intensity as an effect of blended emission bands. The smooth run of the values of $\Delta \log I$ in this region also suggests that these minor irregularities due to emission and absorption lines have tended to cancel out.

Cohn * has recently suggested that the energy hump in the blue part of the spectrum observed by Barbier, Chalonge and Vassy may be explicable as continuous electron radiation superimposed on a normal black-body distribution, and that this additional radiation dies out as the Nova fades. It seems, however, that the radiation outside the hump itself obeys no ordinary black-body law, and therefore, if the explanation of the observed distribution is to be found through a continuous electron-radiation hump, the best place to have it is with its maximum in the unobservable ultra-violet.

Observatory, Cambridge :
1936 *March* 7.

ON REFLECTION COMPENSATORS FOR TESTING PARABOLOIDS.

C. R. Burch, B.A.

Summary.—Methods are described for testing paraboloids null-fashion at the centre of curvature, as if spherical, compensating the spherical aberration with a reflecting compensator which is four times smaller than the paraboloid. For apertures up to $F/5$ the two compensating surfaces may be spherical. The use of this method in refiguring a 36-inch mirror is discussed.

1. *Introduction.*—The nicest way of testing a paraboloid—from the point of view of the optician who has to figure it—is by autocollimation, with the aid of an optical flat as big as the mirror under test. One has then only to look at the surface of the mirror, with an artificial star and knife-edge, to see the differential of the error, or with a Zernike disk † to see a coloured contour map of the hills and hollows. In the simpler method of testing at the centre of curvature, on the other hand, it is necessary to deduce the error by integrating measurements of focal position, taken over a large number of zones—a lengthy and less accurate process. So highly does G. W. Ritchey ‡ assess the advantage of the "null" autocollimative

* *Nature*, **137**, 150, 1936.

† Zernike, *M.N.*, **94**, 377, 1934, and *Physica*, **1**, No. 8, 689. Burch, *M.N.*, **94**, 384, 1934.

‡ *Smithsonian Contributions to Knowledge*, **34**, 1904.

method that he actually advises making the necessary flat, just to test one paraboloid during manufacture, unless the diameter of the paraboloid exceeds 2 feet.

In 1935 I was given permission by the Board of Education to refigure the 36-inch paraboloid made in 1890 by Dr. A. A. Common, and now in use at the Solar Physics Observatory, Cambridge. This mirror was not a surface of revolution; it had about two wave-lengths error, composed of astigmatism of the second and fourth orders, together with irregular coma. To test it at the centre of curvature I should therefore have had to make a double graphical integration of a series of sets of zonal measurements—a process which, from experience on a similar smaller mirror, I regard as quite impracticable. I could not test it autocollimatively for I had no 36-inch flat. I was therefore led to devise a method of testing it null-fashion, at its centre of curvature—as if it were a sphere—by compensating its spherical aberration with the aid of a "reflecting compensator" consisting of one concave spherical mirror $9\frac{1}{2}$ inches diameter, one very nearly spherical convex mirror 1·05 inches diameter, and one 1-inch diameter flat. I shall describe in §§ 2–7 the analysis which led me, *via* two simpler compensators, to the design of this type. In §§ 8–10 I shall discuss practical considerations and working instructions, giving formulæ to cover the needs of the practical optician wishing to use these compensators, who might otherwise justly resent having to disinter his working instructions from a mass of algebraic camouflage. In § 11 I shall discuss the first stage of the refiguring of the 36-inch mirror.

2. *Derivation of Formulæ used in Compensator Design.* — We require formulæ for the longitudinal spherical aberration (L.S.A.) of the image produced by a spherical mirror from an object which may itself have a given L.S.A. These formulæ will now be derived.

Let the spherical mirror have radius ρ. Let object and image rays intersect the optic axis at distances u and v respectively from the pole, measured positively on the concave side of the pole. Let object and image rays make angles θ and ϕ respectively with the optic axis, the sign of ϕ being that of $\theta u/v$. Let the angle of incidence on the mirror be i, taken with that sign which makes $\phi = \theta + 2i$. Then (see fig. 1)

$$\left.\begin{aligned} \sin\phi &= \frac{OQ}{OV}\sin i, \qquad = \frac{\rho}{\rho - v}\sin i \ . \ . \ . \\ \sin\theta &= \frac{OQ}{OU}\sin i, \qquad = \frac{\rho}{u - \rho}\sin i \ . \ . \ . \end{aligned}\right\}. \tag{1}$$

Set $(u-\rho)/\rho = k$, then

$$\begin{aligned} \sin\phi, \qquad &= \sin\theta\cos 2i + \cos\theta\sin 2i \\ &= \sin\theta[1 - 2k^2\sin^2\theta + 2k\sqrt{1 - k^2\sin^2\theta}\sqrt{1 - \sin^2\theta}]. \end{aligned} \tag{2}$$

Set $\sin\phi = y$, $\sin\theta = x$, and let also

$$\Delta = 1 - 2k^2x^2 + 2k\sqrt{1 - k^2x^2}\sqrt{1 - x^2}. \tag{3}$$

Then we have

$$y = x\Delta, \qquad = \rho kx/[\rho - v], \tag{4}$$

so that

$$\frac{v}{\rho} = 1 - \frac{kx}{y}. \tag{5}$$

The problem we now have to solve is: Given the L.S.A. of the object—

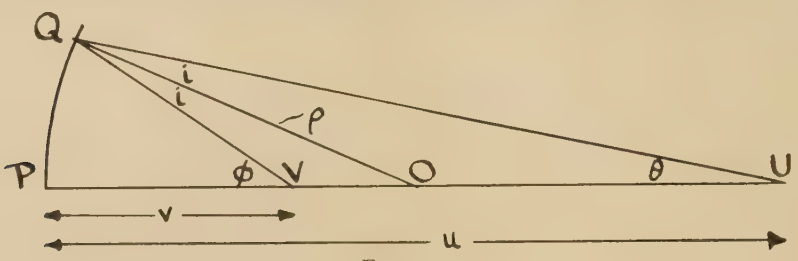

FIG. 1.

that is, given k as a function of $x^2(=\sin^2\theta)$—to find v/ρ, *i.e.* the L.A.S. of the image, as a function of $y^2(=\sin^2\phi)$. We assume, then,

$$k = k_0 + k_2x^2 + k_4x^4 + k_6x^6 + \text{ etc.} \tag{6}$$

First, expand Δ as a power series in x:

$$\Delta = 1 + 2k - x^2[k(k+1)^2] - x^4 \cdot \frac{k}{4}[k^2-1]^2$$
$$- x^6 \cdot \frac{k}{8}[k^2-1]^2[k^2+1] - x^8 \cdot \frac{k}{64}[k^2-1]^2[5k^4+6k^2+5] - \text{etc.} \tag{7}$$

Replace k by its series expansion, (6), giving

$$\Delta = A_0 + A_2x^2 + A_4x^4 + A_6x^6 + A_8x^8 + \text{ etc.}, \tag{8}$$

where

$$A_0 = [1 + 2k_0]$$
$$A_2 = [2k_2 - k_0(k_0+1)^2]$$
$$A_4 = \left[2k_4 - k_2(1+k_0)(1+3k_0) - \frac{k_0}{4}(k_0^2-1)^2\right]$$
$$A_6 = \left[2k_6 - k_4(1+k_0)(1+3k_0) - k_2^2(2+3k_0) - \frac{k_2}{4}(k_0^2-1)(5k_0^2-1) - \frac{k_0}{8}(k_0^2-1)^2(k_0^2+1)\right]$$
$$A_8 = \left[2k_8 - k_6(1+k_0)(1+3k_0) - 2k_4k_2(2+3k_0) - k_2^3 - \frac{k_4}{4}\{5k_0^4 - 6k_0^2 + 4\}\right.$$
$$\left. - \frac{k_2^2k_0}{2}(5k_0^2-3) - \frac{k_2}{8}(k_0^2-1)\{7k_0^4+2k_0^2-1\} - \frac{k_0}{64}\{k_0^2-1\}^2(5k_0^4+6k_0^2+5)\right]. \tag{9}$$

Now

$$y = x\Delta, \qquad = A_0x + A_2x^3 + A_4x^5 + A_6x^7 + A_8x^9 + \text{ etc.} \tag{10}$$

Revert expression (10) to obtain

$$x = B_1y + B_3y^3 + B_5y^5 + B_7y^7 + \ + \text{ etc.} \tag{11}$$

This gives

$$B_1 = A_0^{-1}; \qquad B_3 = A_2 \,.\, A_0^{-4}; \qquad B_5 = [A_0A_4 - 3A_2^2]A_0^{-7};$$
$$B_7 = [12A_2^3 - 8A_0A_2A_4 + A_6A_0^2] \,.\, A_0^{-10};$$
$$B_9 = [55A_2^4 - 55A_0A_2^2A_4 + 10A_0^2A_2A_6 + 5A_0^2A_4^2 + A_0^3A_8] \,.\, A_0^{-13}. \quad (12)$$

Then since by (5), $v/\rho = 1 - kx/y$, we have that

$$\frac{v}{\rho} = 1 - [k_0 + k_2x^2 + k_4x^4 + \text{etc.}] \,.\, [B_1 + B_3y^2 + B_5y^4 + \text{etc.}]. \quad (13)$$

Replace x by means of (11) and the B's by means of (12), obtaining

$$\frac{v}{\rho} = [1 + k_0] \,.\, A_0^{-1} + y^2[k_0A_2 - k_2A_0] \,.\, A_0^{-4}$$
$$+ y^4[(k_0A_4 - k_4A_0)A_0 - 3A_2(k_0A_2 - k_2A_0)] \,.\, A_0^{-7}$$
$$+ y^6[(k_0A_6 - k_6A_0)A_0^2 - 5A_2A_0(k_0A_4 - k_4A_0)$$
$$+ 3(4A_2^2 - A_0A_4)(k_0A_2 - k_2A_0)] \,.\, A_0^{-10}, \text{ etc.} \quad (14)$$

Replacing the A's by means of (9) we obtain

$$\frac{v}{\rho} = \left[\frac{1 + k_0}{1 + 2k_0}\right] + y^2 \,.\, \left[\frac{-k_0^2(k_0+1)^2 - k_2}{(1+2k_0)^2}\right]$$
$$+ y^4\left[\frac{-k_4}{(1+2k_0)^6} - k_2 \,.\, \frac{2k_0(1+k_0)(2+k_0)}{(1+2k_0)^7} + \frac{6k_2^2}{(1+2k_0)^7} - \frac{k_0^2(k_0+1)^2}{(1+2k_0)^4}\right.$$
$$\left.\left\{\frac{(k_0-1)^2}{4(1+2k_0)^2} + \frac{3k_0(k_0+1)^2}{(1+2k_0)^3}\right\}\right]$$
$$+ y^6\left[\frac{-k_6}{(1+2k_0)^8} + \frac{16k_4k_2}{(1+2k_0)^9} - k_4 \,.\, \frac{2k_0(1+k_0)(3+2k_0)}{(1+2k_0)^9} - \frac{48k_2^3}{(1+2k_0)^{10}}\right.$$
$$+ k_2^2\left\{\frac{24k_0^3 + 64k_0^2 + 38k_0 - 3}{(1+2k_0)^{10}}\right\} + k_2k_0(k_0^2 - 1)\left\{\frac{4k_0^3 + 10k_0^2 + 8k_0 + 1}{(1+2k_0)^{10}}\right\}$$
$$\left.- \frac{k_0^2(1+k_0)^2}{(1+2k_0)^4}\left\{\frac{(k_0-1)^2(k_0^2+1)}{8(1+2k_0)^4} + \frac{2k_0(k_0^2-1)^2}{(1+2k_0)^5} + \frac{12k_0^2(k_0+1)}{(1+2k_0)^6}\right\}\right] + \text{etc.}$$
$$= C_0 + C_2y^2 + C_4y^4 + C_6y^6 + \text{etc.} \quad (15)$$

This is the required formula for the L.S.A. of the image, in terms of y^2, ($=\sin^2\phi$), and of the L.S.A. of the object expressed as a power series in terms of object-ray angle $\sin\theta$:

$$\frac{u - \rho}{\rho} = k_0 + k_2\sin^2\theta + k_4\sin^4\theta + k_6\sin^6\theta + \text{etc.}$$

We shall also require an expression for the image at u which would produce, or be produced by, a stigmatic image at v. We can obtain this by equating all the terms in (15) depending on y^2 to zero. This gives, for the L.S.A. of the object at u producing a stigmatic image at v,

$$k_0 = [u_0 - \rho]/\rho; \qquad k_2 = -k_0^2(k_0+1)^2;$$
$$k_4 = k_0^2(k_0+1)^2[3k_0^3 + \tfrac{15}{4}k_0^2 + \tfrac{3}{2}k_0 - \tfrac{1}{4}]. \quad (16)$$

3. *Properties of the Single-mirror Compensator* (*Type* 1).—If a point-source is placed at the centre of apical curvature of a paraboloid of focal length F, the image-ray making angle θ with the optic axis cuts it at a point outside the centre of curvature by the amount

$$2F[\sin^2\theta+\tfrac{5}{2}\sin^4\theta+\tfrac{29}{4}\sin^6\theta+\text{etc.}]. \qquad (17)$$

If, then, we place at the centre of curvature the paraxial image from a compensator which focusses the ray at angle θ short with respect to paraxial focus by the amount given by expression (17), the final image formed by the paraboloid will be free from spherical aberration.

I consider first a compensator consisting of a single concave spherical mirror, radius ρ, with the star placed at a distance v, $=v_0$, $=\rho[1+k_0]/[1+2k_0]$ from its pole, so that the paraxial image is formed at a distance u_0, $=\rho[1+k_0]$ from its pole. The marginal image-ray making angle θ with the axis is then focussed short with respect to paraxial focus by the amount

$$-\rho k_2\sin^2\theta-\rho k_4\sin^4\theta-\text{etc.},$$

where k_2, k_4, etc., are given by expression (16).

That is, the marginal rays focus short by the amount

$$\rho k_0^2(k_0+1)^2[\sin^2\theta-[3k_0^3+\tfrac{15}{4}k_0^2+\tfrac{3}{2}k_0-\tfrac{1}{4}]\,.\,\sin^4\theta-\text{etc.}]. \qquad (18)$$

If, then, we set $\rho k_0^2(k_0+1)^2=2F$, the primary L.S.A. (*i.e.* the part proportional to $\sin^2\theta$) of the paraboloid will be correctly compensated.

The $\sin^4\theta$ term will be under-compensated by the amount

$$2F\,.\,3[k_0^3+\tfrac{5}{4}k_0^2+\tfrac{1}{2}k_0+\tfrac{3}{4}]\sin^4\theta, \qquad (19)$$

so that the "pseudoparaboloid," for which the test is null, will differ from a true paraboloid by having its edge turned up. The amount of the turn-up is given (to a first approximation) by multiplying the L.S.A. by $\frac{1}{2}\sin\theta$ and integrating with respect to $\sin\theta$. Thus the error of height of the pseudo-paraboloid is

$$\delta h=F\,.\left[\frac{k_0^3}{2}+\frac{5k_0^2}{8}+\frac{k_0}{4}+\frac{3}{8}\right].\sin^6\theta. \qquad (20)$$

Now, we are interested in values of k_0 for which the necessary diameter of the compensator, d, say, is less than D, the diameter of the paraboloid which it will feed fully with light. We have that

$$\frac{d}{\rho(1+k_0)}\geqslant\frac{D}{2F},\quad\text{so that}\quad\frac{d}{D}\geqslant\frac{1}{k_0^2(k_0+1)}. \qquad (21)$$

Let us consider $k=1$, for which $\frac{d}{D}\geqslant\frac{1}{2}$ and $k=3/2$, for which $\frac{d}{D}\geqslant\frac{8}{45}$, $=0{\cdot}0177$.

Set $F=$ say, 4 m., and δh, the error of the pseudoparaboloid, not greater than one-fortieth of a wave-length (*i.e.* $1{\cdot}25\times10^{-6}$ cm.). Then (20) gives that if $k_0=1$, $\sin\theta\leqslant0{\cdot}03483$, while if $k=3/2$, $\sin\theta\leqslant0{\cdot}03055$. The reciprocal of

$\sin\theta$ is four times the $F/$ number of the paraboloid. Thus, this compensator is usable, when $F \leqslant 4$ m. for a paraboloid of aperture not exceeding $F/7{\cdot}2$ if $k_0 = 1$, or $F/8{\cdot}2$ if $k_0 = 3/2$. Practical points are discussed in § 8.

4. *The "Pseudoautostigmatic" Compensator, with "Roof-reflector" (Type 2).*—A drawback of Type 1 compensator is that the artificial star must be placed in the middle of the compensated beam, so that it is necessary to make a special star which will not obstruct much of the light.

It occurred to me that one could avoid this difficulty if, instead of placing the star of Type 1 at $v_0 (v_0 < \rho)$ to produce an image at u $(u > \rho)$, one placed the star at u_0, and reflected the image formed at v back on to the concave mirror by means of a "roof-reflector" (*i.e.* two small perpendicular flats) with its ridge on the axis at v_0, an image with twice as much primary L.S.A. would be formed at u (*i.e.* at the star). By displacing the star slightly from the optic axis the final image could be formed slightly to one side of the star, and an ordinary artificial star could then be used. (The set-up is shown in fig. 3 and discussed practically in § 9.)

To calculate the secondary spherical aberration, evaluate by means of (15) the L.S.A. of the image at v of the star at $u = u_0 = 1 + k_0$ (setting $k_2 = k_4 = 0$, since the star has no L.S.A.). Let this image be given by

$$v_1/\rho = C_0' + C_2' y^2 + C_4' y^4 + \text{etc.} \qquad (22)$$

Evaluate also the L.S.A. of that image (v_2, say) which would be created by reversing the rays of the compensator's final image,

$$u = \rho[1 + k_0 + k_2 x^2 + k_4 x^4, \ + \ \text{etc.}].$$

Expression (15) gives for this image

$$v_2/\rho = C_0 + C_2 y^2 + C_4 y^4 + \text{etc.} \qquad (23)$$

We have $C_0' = [1 + k_0]/[1 + 2k_0]$. Since the ridge of the roof-reflector is placed at $\rho[1 + k_0]/[1 + 2k_0]$, it will convert the image v_1 into the image v_2 if

$$C_0' = C_0 ; \qquad C_2' = -C_2 ; \qquad C_4' = -C_4, \text{ etc.}$$

Thus, when the paraxial final image is formed level with the star (so that $C_0' = C_0$) it must have such values of k_2, k_4, etc., that their presence in expression (15) reverses the sign of the y^2, y^4, etc., terms. And, therefore, the L.S.A. of the final image of this compensator, $-\rho[k_2 \sin^2\theta + k_4 \sin^4\theta]$, etc., is given by

$$-\rho \,.\, 2k_0^2(k_0+1)^2\left[\sin^2\theta - \sin^4\theta\left\{6k_0^3 + \frac{33}{4}k_0^2 + \frac{9k_0}{4} - \frac{5}{8} + \frac{3}{8(1+2k_0)}\right\}\right], \qquad (24)$$

this being the distance by which marginal rays focus long with respect to paraxial rays.

If we set $\rho k_0^2(k_0+1)^2 = F$, the primary L.S.A. of the paraboloid of focal length F will be correctly compensated, and the $\sin^4\theta$ term in L.S.A. will be under-compensated by the amount

$$2F\left[6k_0^3 + \frac{33}{4}k_0^2 + \frac{9k_0}{4} + \frac{15}{8} + \frac{3}{8(1+2k_0)}\right]\sin^4\theta. \qquad (25)$$

Multiplying by $\frac{1}{2}\sin\theta$ and integrating with respect to $\sin\theta$, we obtain the error of height, δh, by which the surface of the psuedoparaboloid lies above that of a true paraboloid :

$$\delta h = F\,.\left[k_0^3+\frac{11k_0^2}{8}+\frac{3}{8}k_0+\frac{5}{16}+\frac{1}{16(1+2k_0)}\right]\sin^6\theta. \qquad (26)$$

If d be the diameter of the concave compensating mirror and D that of the paraboloid, we must have

$$\frac{d}{\rho(1+k_0)} \geqslant \frac{D}{2F}, \quad \text{so that} \quad \frac{d}{D} \geqslant \frac{1}{2k_0^2(k_0+1)}. \qquad (27)$$

Let us take $k=1$, so that $d/D \geqslant 1/4$. Let as before $F \leqslant 4$ m. and $\delta h \leqslant \lambda/40$. Then from (26) $\sin\theta \leqslant 0{\cdot}0317$, and so this compensator is suitable (when $F \leqslant 4$ m.) for an aperture not greater than $F/8$.

5. *The Pseudoautostigmatic Two-Mirror Compensator* (*Type* 3).—I next realised that if for the roof-reflector of Type 2 compensator we substitute a small spherical mirror, to return the light of the intermediate image to the main compensating mirror, it is possible by a suitable choice of the radius of this new mirror to correct the $\sin^4\theta$ term in the compensation, and so to obtain a compensator suitable for greater apertures than $F/8$. The radius of this new mirror is determined as follows. Start with a point-source at distance $u=u_0=\rho(1+k_0)$ from the concave mirror of radius ρ. Then expression (15) gives for the image at v :

$$\frac{v}{\rho}=\left[\frac{1+k_0}{1+2k_0}\right]-y^2\left[\frac{k_0^2(k_0+1)^2}{(1+2k_0)^4}\right]-y^4\left[\frac{k_0^2(k_0+1)^2}{(1+2k_0)^4}\left\{\frac{(k_0-1)^2}{4(1+2k_0)^2}+\frac{3k_0(1+k_0)^2}{(1+2k_0)^3}\right\}\right]-\text{etc.} \qquad (28)$$

Use this image as object, with the paraxial image point at the centre of a spherical mirror of radius ρ/q, the concavity of which faces the same way as that of the mirror of radius ρ (physically, a convex mirror). With regard to this ρ/q mirror, the image (28), used as an object, has

$$k_0'=0-x^2q\left[\frac{k_0^2(1+k_0)^2}{(1+2k_0)^4}\right]-x^4q\left[\frac{k_0^2(1+k_0)^2}{(1+2k_0)^4}\left\{\frac{(k_0-1)^2}{4(1+2k_0)^2}+\frac{3k_0(1+k_0)^2}{(1+2k_0)^3}\right\}\right]-\text{etc.} \qquad (29)$$

Substituting k' for k in expression (15), we find that the image v_1, say, produced by the convex mirror has

$$qv_1/\rho=1+y^2q\left[\frac{k_0^2(1+k_0)^2}{(1+2k_0)^4}\right]$$
$$+y^4q\left[\frac{k_0^2(1+k_0)^2}{(1+2k_0)^4}\left\{\frac{(k_0-1)^2}{4(1+2k_0)^2}+\frac{3k_0(1+k_0)^2}{(1+2k_0)^3}\right\}+6\left\{\frac{k_0^2(1+k_0)^2}{(1+2k_0)^2}\right\}^2q\right],\ \text{etc.} \qquad (30)$$

Now begin at the other end of the compensating system and take as object the final image we wish to get, which must have

$$(u-\rho)/\rho=k=k_0-x^2\,.\,2k_0^2(k_0+1)^2-x^4\,.\,5k_0^2(k_0+1)^2-\text{etc.} \qquad (31)$$

in order that the $\sin^4\theta$ term in the compensation shall be correct. Sub-

stituting this value of k in expression (15) we find that this object would produce in the concave mirror an image v_2, say, having

$$\frac{v_2}{\rho}=\left[\frac{1+k_0}{1+2k_0}\right]+y^2\left[\frac{k_0^2(1+k_0)^2}{(1+2k_0)^2}\right]+y^4\left[\frac{5k_0^2(k_0+1)^2}{(1+2k_0)^6}\right.$$
$$+\frac{2k_0^2(k_0+1)^2\,.\,2k_0(1+k_0)(2+k_0)}{(1+2k_0)^7}+6\,.\,4\,.\,\frac{[k_0^2(k_0+1)^2]^2}{(1+2k_0)^7}$$
$$\left.-\frac{k_0^2(k_0+1)^2}{(1+2k_0)^4}\left\{\frac{(k_0-1)^2}{4(1+2k_0)^2}+\frac{3k_0(1+k_0)^2}{(1+2k_0)^3}\right\}\right]+\text{etc.} \tag{32}$$

The paraxial part of v_2 coincides in space with that of v_1, the image produced by the convex mirror, and the y^2 terms are the same. We have therefore only to equate the y^4 terms in order to secure that our final image will have (neglecting y^6) the k postulated in (31). This gives

$$6\left[\frac{k_0^2(1+k_0)^2}{(1+2k_0)^4}\right]^2 q=\left[\frac{5k_0^2(1+k_0)^2}{(1+2k_0)^6}+\frac{2k_0^2(1+k_0)^2\,.\,2k_0(1+k_0)(2+k_0)}{(1+2k_0)^7}\right.$$
$$\left.+6\,.\,4\,.\,\frac{[k_0^2(1+k_0)^2]^2}{(1+2k_0)^7}-\frac{2k_0^2(1+k_0)^2}{(1+2k_0)^4}\left\{\frac{(k_0-1)^2}{4(1+2k_0)^2}+\frac{3k_0(1+k_0)^2}{(1+2k_0)^3}\right\}\right], \tag{33}$$

which is satisfied if

$$q=8k_0+3+\frac{2}{k_0}+\frac{5}{4k_0^2}-\frac{(1+2k_0)}{2k_0^2(1+k_0)^2}. \tag{34}$$

We must next ask what fraction of the diameter of the concave mirror will be in the shadow of the convex mirror. The ratio diameter of convex/diameter of concave mirror will be

$$\frac{\rho}{qv_0}, \qquad =\frac{1+2k_0}{q(1+k_0)}, \tag{35}$$

and the ratio diameter of shadow of convex/diameter of convex mirror will be

$$\frac{u_0}{u_0-v_0+\rho/q}, \qquad =\frac{1+2k_0}{2k_0+\dfrac{1+2k_0}{q(1+k_0)}}. \tag{36}$$

Thus the fraction of the diameter of the concave compensating mirror which will be shadowed is

$$\frac{[1+2k_0]^2}{2k_0(1+k_0)q+(1+2k_0)}. \tag{37}$$

From (31) we have to set

$$\rho k_0^2(k_0+1)^2=F, \tag{38}$$

so that

$$\frac{d}{D}\geqslant\frac{\rho(1+k_0)}{2F}, \qquad >\frac{1}{2k_0^2(1+k_0)}. \tag{39}$$

Let us choose $k_0 = 1$, so that $\frac{d}{D} \geqslant \frac{1}{4}$. Then (34) gives

$$q = 111/8, \tag{40}$$

and from (37) the shadowed fraction of the diameter of the concave mirror is 2/13—a reasonably small fraction.

We have now to determine up to what aperture the compensation may be regarded as perfect. The explicit expression for the sixth-power term of L.S.A. is unduly long, so that it is better to apply (15) numerically to find the L.S.A. first of the two intermediate images in turn, and then of the final image. Setting $\rho k_0^2(k_0+1)^2 = F$; $k_0 = 1$; $q = 111/8$, I obtain in this way that the marginal rays of the final image focus short with respect to paraxial rays by the amount

$$2F[\sin^2\theta + \tfrac{5}{2}\sin^4\theta + 697{\cdot}4\sin^6\theta + \text{etc.}] \tag{41}$$

—the $\sin^2$ and $\sin^4\theta$ terms being correct, and the $\sin^6\theta$ term in excess of the desired value by

$$2F \,.\, 690{\cdot}1\sin^6\theta. \tag{42}$$

Multiplying by $\frac{1}{2}\sin\theta$ and integrating with respect to $\sin\theta$, we obtain δh, the height *deficit* of the pseudoparaboloid for which the test is null, below the surface of a true paraboloid :

$$\delta h = F \,.\, 86{\cdot}3\sin^8\theta. \tag{43}$$

Setting as before $F \leqslant 4$ m., and $\delta h \leqslant \lambda/40$, we find that

$$\sin\theta \leqslant 0{\cdot}04953. \tag{44}$$

So for $F \leqslant 4$ m., we can regard the compensation as "perfect" for apertures not greater than $F/5$.

The 36-inch mirror which I wished to test has $F = 3{\cdot}42$ m. and aperture $F/3{\cdot}75$. For this mirror, then, the pseudoparaboloid for which the compensator gives a null test will have a height deficit at the edge of

$$\frac{3{\cdot}42}{4} \times \left(\frac{5}{3{\cdot}75}\right)^8 \times \frac{\lambda}{40}, \qquad = 0{\cdot}214\,\lambda \tag{45}$$

—an error of nearly twice the "Rayleigh limit."

To remove this error of compensation it will be necessary to figure the convex compensating mirror aspherical, giving it a height deficit proportional to the eighth power of the zonal radius, and reaching $0{\cdot}214\,\lambda$ below sphere at the edge. As this mirror is only about 1 inch diameter it can be tested by contact interference with a spherical test-plate : I think it should be possible thus to measure its asphericity correct to $\lambda/20$, though probably not to $\lambda/40$. It is indeed fortunate that the desired asphericity should consist of a steeply turned-*down* and not a steeply turned-up edge.

As a check on the analysis, I have traced trigonometrically a ray starting at $3^\circ - 30' - 0''$ to the axis of such a compensator, with $\rho = 100$ cm. ; $k = 1$, using 7-figure tables. This ray emerges at $3^\circ - 24' - 15{\cdot}2''$, with an L.S.A.

of 2·86423 cm. The analysis (neglecting $\sin^8\theta$) gives for this ray an L.S.A. of 2·8634 cm. The difference, 0·0008 cm., corresponds to less than a $\lambda/40$ change in height of the pseudoparaboloid.

Let us rough out a design for a compensator of this type for the 200-inch mirror of the California Institute of Technology. This mirror is to have $F = 666''$, so if we set $k_0 = 1$, the compensator would require a concave spherical mirror of radius $\rho = 166{\cdot}67''$, and diameter 52 inches (the 2 inches over and above 200/4 being partly an allowance for lateral displacement of the rays, at their second incidence on it, due to the decentring of the star so that it shall not obstruct the final image, and partly an allowance for turned-down edge). The convex mirror would have radius $\rho/q = 12''$ and diameter

$$d(1+2k_0)/q(1+k_0) = \frac{8}{111} \times \frac{3}{2} \times 50'', \qquad = 5{\cdot}41''.$$

A small flat 1 or 2 inches diameter would also be required to send the compensated beam to the paraboloid. Since $666'' = 16{\cdot}92$ m., the error of the pseudoparaboloid at the edge would be

$$\frac{16{\cdot}92}{4} \times \left(\frac{5}{3{\cdot}33}\right)^8 \times \frac{\lambda}{40}, \qquad = 2{\cdot}732\ \lambda, \tag{46}$$

so that it would be necessary to turn down the edge of the convex mirror by approximately $2{\cdot}8\ \lambda$. The exact asphericity would have to be determined either by ray-tracing or by the inclusion of several more terms in the analysis, as the $\sin^8\theta$ term of L.S.A. will probably not be negligible for this great focal length and aperture.

The convex mirror would undoubtedly be difficult and expensive to make. But its cost would be negligible compared with that of the 200-inch mirror.

6. *The Astigmatism due to Decentring in Compensators of Type* 3.—It is necessary to calculate the astigmatism due to the slight lateral displacement of the star from the optic axis of the compensator required to form the final image a little to one side of the star. Before this can be done, we have first to find which ray from the star constitutes the *principal ray* of the displaced cone—*i.e.* the ray which must be made to hit the centre of figure of the paraboloid under test. That is, we have to find which ray emerges from the compensator *coma-free*. Professor L. C. Martin pointed out to me that that ray from the star which, after reflection in the concave mirror, hits the pole of the convex mirror passes symmetrically through the system, and is therefore free from coma when regarded as a principal ray.

To calculate the astigmatism of this ray, due to a displacement δ of the star from the revolution axis of the compensator, we must first find the corresponding displacement, δ_1 of the star, from the normal at the incidence point of the principal ray on the concave mirror, and the displacement δ_2 of its intermediate image (formed by the principal ray and infinitesimally adjacent rays) from the normal at the incidence point of the principal ray on the convex mirror (*i.e.* at the pole of the convex mirror). We have that the principal ray cuts the revolution axis at the image of the pole of the

convex mirror in the concave one—*i.e.* at the image of the point distant $v_0 - \rho/q$ from the surface of the concave mirror. This image lies at a distance

$$u_p, \qquad = \rho(qv_0 - \rho)/[2(qv_0 - \rho) - q\rho] \tag{47}$$

from the pole of the concave mirror. Since the star is distant u_0, $=(1 + k_0)\rho$ from the concave mirror, the incidence height of the principal ray on the concave mirror is

$$\frac{\delta \,.\, u_p}{u_0 - u_p}, \tag{48}$$

and the distance of the star from the normal at this height is

$$\delta\left[\left(\frac{u_p}{u_0 - u_p}\right)\left(\frac{u_0 - \rho}{\rho}\right) + 1\right], \qquad = \delta_1, \qquad = \left[\frac{1 + k_0}{1 + 2k_0}\right]\left[\frac{k_0 q}{1 + 2k_0} + 1\right], \tag{49}$$

while the distance at which the principal ray, after reflection in the concave mirror, passes the centre of the convex mirror is

$$\delta_2, \qquad = \delta\left[\frac{u_p}{u_0 - u_p} \,.\, \left(\frac{\rho/q}{v_0 - \rho/q}\right)\right], \tag{50}$$

so that

$$\delta_2 = \frac{v_0}{u_0} \,.\, \delta, \qquad = \delta(1 + 2k_0). \tag{51}$$

Now the longitudinal astigmatism (L.A.) (= distance between focal lines) due to the decentring of the intermediate image from the centre of the convex mirror, radius ρ/q, is

$$2\delta_2{}^2 q/\rho, \tag{52}$$

the focal line in the decentring direction being further from the pole by this amount. The corresponding L.A. due to the imaging of (52) in the concave mirror is obtained by multiplying (52) by $-[u_0/v_0]^2$, so that the convex mirror's contribution to the L.A. of the final image will be

$$-2\delta_2{}^2[1 + 2k_0]^2 \,.\, q/\rho. \tag{53}$$

The contribution to the L.A. of the final image due to its two reflections in the concave mirror, with decentring δ_1, from the normal at object-distance u_0 from the pole, will be

$$4\delta_1{}^2/\rho. \tag{54}$$

Thus the total L.A. of the final image, measured from the focal line in the direction of the displacement to the other focal line, and taken positively towards the concave mirror, will be

$$\frac{4\delta_1{}^2}{\rho} - \frac{2\delta_2{}^2 q}{\rho}[1 + 2k_0]^2,$$

$$= \frac{2}{(1 + 2k_0)^2} \,.\, \frac{\delta^2}{\rho}\left[2(1 + k_0)^2\left\{\frac{k_0 q}{1 + 2k_0} + 1\right\}^2 - (1 + 2k_0)^2 q\right]. \tag{55}$$

For $k_0 = 1$, implying $q = 111/8$, this becomes

$$\text{L.A.} = \frac{57}{2}\frac{\delta^2}{\rho}. \tag{56}$$

Now the L.A. introduced by the decentring, δ_p say, of the compensated image from the axis of the paraboloid is

$$\delta_p{}^2/F, \tag{57}$$

and when $k_0 = 1$, $\rho = F/4$. Thus if we arrange that

$$\delta_p = \sqrt{114}\,.\,\delta, \qquad = 10{\cdot}68\delta, \tag{58}$$

but make the two displacements δ and δ_p perpendicular, these two astigmatisms will cancel. If it is inconvenient to do this, we must cancel these astigmatisms either by a pair of plane-parallel plates of suitable thickness set with equal and opposite obliquities to the principal ray, or better by an astigmatic lens, placed in front of the final image formed by the paraboloid.

It is desirable to keep δ as small as possible, because although the principal ray is coma-free, and its astigmatism has been annulled, the marginal rays of the compensated cone will contain longitudinal comatic aberrations proportional to δ^3 and L.A. proportional to δ^4. There is little doubt that if the primary aberrations can be kept as low as $\lambda/4$ (and this value can be realised for the L.A. given by (56) in testing the 36-inch mirror) the third-order coma and fourth-order astigmatism will be quite negligible.

We can reduce the value of δ necessary to prevent obstruction of light by changing the position of the star, so that the circle of least confusion of the image shall form level with the star. (The design-condition we have considered forms the *paraxial* image level with the star, so that δ would have to be at least as great as the marginal confusion-radius in the paraxial image-plane.)

We have therefore to consider the effect of moving the star towards the concave mirror by a distance equal to half the distance between the paraxial image and the circle of least confusion. For a given $\theta_{\max}$ the confusion radius is minimal at a distance from paraxial focus equal approximately to 3/4 of the marginal L.S.A. Thus we consider moving the star towards the concave compensating mirror by an amount

$$\tfrac{3}{8}\rho\,.\,2k_0(1+k_0)^2\,.\,\sin^2\theta_{\max} = 3\rho\sin^2\theta_{\max}, \qquad \text{setting } k_0 = 1. \tag{59}$$

Neglecting $[3\sin^2\theta_{\max}]^4$ compared with unity, the primary L.S.A. of the compensator can then be shown to be multiplied by

$$1 + \tfrac{873}{64}\sin^4\theta_{\max}, \tag{60}$$

so that even for a paraboloid of $F/3$ ($\sin\theta_{\max} = 1/12$) this change only increases the L.S.A. by 0·66 part per thousand. Accordingly we can safely correct for the effect of moving the star by $3\rho\sin^2\theta$, by decreasing ρ in the ratio of expression (60) to unity, or alternatively by reducing k_0 from unity to

$$1 - \tfrac{291}{64}\sin^2\theta_{\max}, \tag{61}$$

which effects a corresponding reduction of $\rho k_0{}^2(k_0+1)^2$.

7. *The Astigmatism Due to Decentring in Type 2 Compensator.*—The compensator should be decentred (to make the image clear the star) in a direction perpendicular to the ridge of the roof-reflector, for then one can arrange that all the light traverses the two flats of the roof-reflector in the same order. No line, due to the junction of the flats, then appears on the mirror, and the exact angle between the flats is unimportant, except in so far as it influences the astigmatism consequent on a given decentring of the star. Since the paths of the rays, outside the roof-reflector, are not influenced by rotating it about its ridge, we may assume that it is symmetrically placed with respect to the perpendicular from the centre of the mirror to its ridge. This perpendicular will be called the symmetry axis of the compensator.

The ray traversing the system symmetrically will emerge coma-free ; this ray will be the principal ray of the displaced cone. It is the only ray which cuts the symmetry axis in four points coinciding in pairs—one before entering (or after leaving) the compensator, and one before (or after) reflection in the roof-reflector. We shall assume that the distance from the concave mirror of the former intersection (measured positively if on the concave side of the mirror) has been determined experimentally for the given decentring δ of the star. Let this distance be denoted by Z. Then the distance of the star from the normal at the point of first incidence of the principal ray on the compensator will be

$$\delta_1, \qquad = \frac{\delta(1+k_0)(\rho - Z)}{\rho(1+k_0) - Z}, \tag{62}$$

and, since the concave mirror is used twice, the focal line, perpendicular to the decentring direction, will be formed nearer to the concave mirror than the other focal line by the amount

$$\frac{4(1+k_0)^2(\rho - Z)^2 \,.\, \delta^2}{\rho[\rho(1+k_0) - Z]^2}. \tag{63}$$

This can be made zero by adjusting either δ or the angle between the roof-reflector's flats, until $Z = \rho$. The other case of special interest is when the flats are exactly perpendicular, when $Z = \rho/2$, independent of δ, and the longitudinal astigmatism is then

$$\frac{16\delta^2}{9\rho}. \tag{64}$$

As in the case of the Type 3 compensator discussed in § 6, it is permissible to move the star from the position $\rho(1+k_0)$ to the position

$$\rho(1+k_0) - \tfrac{3}{4}\rho(1+k_0)^2 \,.\, k_0^2 \,.\, \sin^2\theta_{\max},$$

so that the least confusion circle may image level with the star, when a smaller value of δ is practicable.

8. *Practical Considerations and Design Instructions (Type 1 Compensator).*—The set-up is shown diagrammatically in fig. 2. S is the star, placed at a distance v from the pole of the concave spherical mirror C of radius ρ and diameter d. A small plane mirror M (which need not be more than 1 cm. diameter) is placed either just inside or just outside the image of S formed by

C, so as to direct the light on to the paraboloid (diameter D, focal length F)—not shown—whence it returns to form the final image I, close to the centre of curvature of the paraboloid. The paraboloid is tested by means of this image with a Zernike disk or knife-edge, as if it were a sphere.

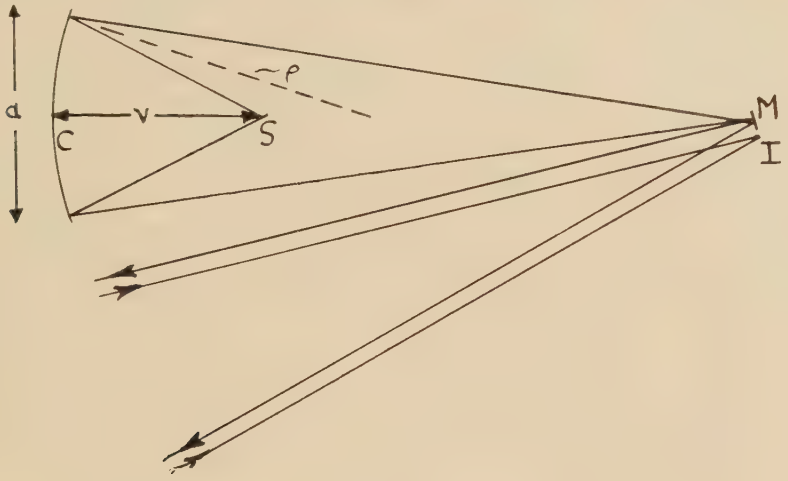

FIG. 2.

Choice of the dimensions d, ρ, v. Let k be a number lying between 1 and $1\frac{1}{2}$. Then the following conditions are to be satisfied :—

$$\rho k^2(k+1) = 2F\,; \qquad v = \frac{1+k}{1+2k}\cdot\rho\,; \qquad d \geqslant \frac{D}{k^2(k+1)} \tag{65}$$

—the excess of d over $D/k^2(k+1)$ being, say, $\frac{1}{2}-1$ cm., so that the extreme edge of the mirror C need not be used.

The ratio F/D must be not less than 7·2 if $k=1$, or 8·2 if $k=1\frac{1}{2}$. Then if C is spherical, the compensation will be accurate to $\lambda/40$ if $F \leqslant 4$ m.

To centre the compensated beam on the paraboloid, place a pair of crossed threads approximately midway between S and C and adjust them laterally until each shows two coincident shadows on C: they then intersect the optic axis of the compensator. Orient the plane mirror M so that their shadows are centred on the paraboloid. If the paraboloid is known to be a surface of revolution, the threads are unnecessary, for if the compensated cone is off centre on the paraboloid to the observer's left, the left-hand edge of the paraboloid will appear turned down and the right-hand edge turned up. Accordingly one can simply reorient M so that this error—coma—vanishes.

The Plane Mirror, M.—Since this mirror is used very near to a focus, narrow scratches on it will show as quite broad depressions on the surface of the paraboloid. I found it extremely difficult to polish a speculum-metal mirror for this purpose so well that no trace of pattern, due to its crystal structure, could be seen on the paraboloid. I find aluminised glass entirely satisfactory.

The Star.—The compensator magnifies the pinhole $1+2k$ times, so that the pinhole should be made $1+2k$ times smaller than would be used to test a sphere of the same $F/$ number as the paraboloid. That is, the pinhole diameter should be of the order of smallness of $\frac{0{\cdot}001}{(1+2k)}\frac{F}{D}$ mm. diameter.

The principal difficulty I found in making pinholes ·0025 mm. diameter, by piercing tinfoil with a needle, lay in making the needle really sharp. But Dr. J. M. Dodds, of the Metropolitan-Vickers Co., solved this difficulty by the following honing technique. The needle, mounted on a rod, is first honed on a fine stone until the diameter of its "point" does not exceed 0·01 mm. This is not difficult, provided one inspects the point frequently during honing with a microscope. The final honing is done on glass. Lay the needle on a glass plate, and press heavily with one finger behind its point. Lift the rod in which it is mounted slightly so that the needle is bent through several degrees. Then, still pressing with the finger, simultaneously twist and withdraw the slightly lifted rod, so drawing out the needle under the pressing finger. This process is repeated until on inspection under 500 diameters magnification the needle looks quite "sharp"—that is, its "point" is of the order of 0·001 mm. diameter or even less. Fifteen minutes honing on glass usually suffices.

The "tinfoil" in which cigarettes are wrapped forms an excellent material for the pinhole. The foil is tacked (at its edges only) to a glass plate; the needle-point is then placed very gently on it, and the needle rotated without pressure through at least one revolution and then lifted off. Some practice is necessary to avoid dragging the point sideways in lifting it off. If the needle is not rotated the hole will not be reasonably circular. The needle requires rehoning after a few piercings. Not every pierce is successful, but one can in this way make reasonably circular pinholes 0·002 mm. diameter, and occasionally even smaller.

The part of the star lying in the compensated beam must be kept small to avoid the obstruction of the light. There are thus two possible star designs. (*a*) One can use a very small ("pea") lamp as source, imaging its filament on the pinhole with a small lens, and so make the whole star only 1 cm. or so diameter. But, on the one hand, the intrinsic brilliancy obtainable with reasonable life from tungsten *in vacuo* is not as high as one could wish, and, on the other hand, the bulbs of most "pea" lamps are optically very irregular—they are in fact visibly wrinkled—so that the image of the pinhole on the filament cannot be made to lie wholly within the filament—that is, the filament is not wide enough to feed the pinhole fully through the irregular bulb. One can, it is true, increase the effective width of the filament by frosting the bulb, but only at the cost of reducing greatly the effective filament brilliance. (*b*) One can place the source outside the compensated cone and feed the pinhole *via* a small prism placed close behind it, from a condensing system outside the cone. A source of higher intrinsic brilliance may then be used. I have used a gas-filled (railway signalling) lamp having a very close helical filament. I found it essential, in order to cut down stray light, to use a double-condensing system, in which the filament is

first imaged (with unit magnification) on a hole a few millimetres wide in a diaphragm, so as to form a "new source," the angular aperture of which is not greater than that required by the second condensing lens, which images it *via* the prism on the pinhole. I worked the first face of the prism convex so as to make it a combined prism and Amici lens. This reduces the diameter necessary for the second condensing lens, incidentally reducing its aberrations, and so permitting a smaller hole in the diaphragm, and reducing still further the stray light.

The necessity for a pinhole $(1+2k)$ times—say 3 times—smaller than usual is not, *per se*, an objection. On account of the compensator's magnification of $1+2k$, the amount of light available for the test is the same as usual. But the necessity for a special star is certainly rather inconvenient.

9. *Type 2 Compensator.*—The arrangement is shown in fig. 3. S is the star, placed at a distance u from the concave spherical mirror C of radius

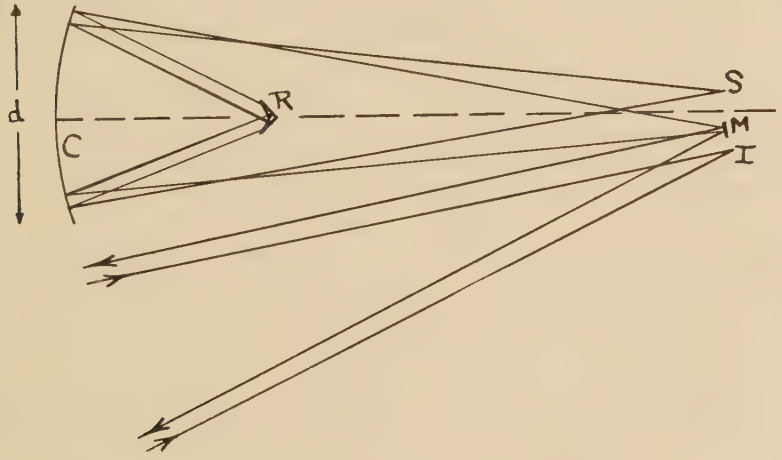

Fig. 3.

ρ and diameter d. R is a "roof-reflector" consisting of two small flats approximately but not necessarily exactly perpendicular. Its ridge is placed at a distance v from C. It returns to C the light from the image in C of S, so as to form the final compensated image slightly to one side of S, so that the light may pass to the small plane mirror M, and thence to the paraboloid, whence it returns to form the final image at I.

Choice of the dimensions d, ρ, u, v. Let k be a number nearly equal to unity (0·9–1·1). Then the following conditions are to be satisfied :—

$$\rho k^2(k+1)=F\,; \qquad v=\frac{1+k}{1+2k}\cdot\rho\,; \qquad u\doteqdot(1+k)\rho\,;$$

$$d>D/2k^2(k+1)\,; \qquad F>8D \tag{66}$$

—d being made in excess of the above minimum value by, say, 1 cm., to allow for the slight lateral displacement of the light (due to the decentring of the star) at its second reflection in C.

If $F \leqq 4$ m., and if C is spherical, the compensation of spherical

aberration will be accurate to $\lambda/40$. It is permissible to place S nearer to C than $u=(1+k)\rho$ by the amount necessary to make the least-confusion circle (instead of the paraxial image) form level with S.

To centre the compensated cone on the paraboloid, and also to determine the astigmatism of the compensator due to the decentring of S, crossed threads are stretched between R and C, one parallel to the decentring direction and the other perpendicular to it.

In general, each thread intercepts four rays, so that four shadows will be seen on the surface of C. By adjusting the decentring direction to be perpendicular to the ridge of R, and by adjusting the orientation and lateral position of the thread parallel to the decentring direction, all its four shadows may be made coincident, wherever it is placed between R and C. It then passes through the "principal" (*i.e.* central) ray of the compensated cone. The perpendicular thread will also show four shadows (unless the angle of R is not nearly 90°). Two of these shadows, due to its intercepting rays from R to C and C to R, will be thicker than the other two, which are due to its intercepting rays from S to C and C to M.

There is one, and only one, position for this thread at which the two thin shadows coincide, and simultaneously lie midway between the two thick shadows. This is the position at which the principal ray cuts the symmetry axis of the compensator. Its distance from C is to be measured and denoted by Z. Z depends on the decentring of S, unless R has exactly 90°, when $Z=\frac{1}{2}\rho$. If Z lies outside v, and the image Z' of Z in C lies inside v, it will be possible to make the thick shadows coincide and lie midway between the thin shadows, by placing the thread at Z'. Z may then be calculated from the formula $Z=\rho Z'/(2Z'-\rho)$.

If Z and Z' both lie outside v, Z is determined as the only place at which the two thread-shadows coincide, and simultaneously lie midway between the two shadows due to a thread stretched across the main cone, at the ridge of the roof-reflector.

After setting the two threads in this way, measure the distance 2δ from S to the centre of the confusion-circle of the compensator's image: this is conveniently done by moving a thread across just in front of S from the one to the other position at which its shadow is central on C.

The plane mirror M may now be placed in position and oriented so as to centre the thread-shadows on the paraboloid. If the paraboloid is a nearly centred surface of revolution, one may of course orient M to secure zero coma on the paraboloid. If also the roof-reflector is known to have exactly 90°, so that Z is known, the crossed threads may be dispensed with.

The astigmatism of the compensator's image may now be calculated: the focal line perpendicular to the decentring direction is formed nearer to C than the other by the amount

$$\frac{4\delta^2(\rho-Z)^2(1+k)^2}{\rho[(1+k)\rho-Z]^2}. \qquad (67)$$

The corresponding longitudinal astigmatism due to the decentring 2Δ of the compensator's image from the paraboloid's final image is

$$\frac{\Delta^2}{F'} = \frac{\Delta^2}{\rho k^2(k+1)^2}. \qquad (68)$$

These two astigmatisms add if the decentrings are in the same direction, so that by making δ perpendicular to Δ, and suitably adjusting δ/Δ, they can be made to cancel. If, alternatively, the decentrings are made in the same direction and are cancelled by an astigmatic lens, the lens should be placed last of all in the optical train. I have tried both an astigmatic lens and an "astigmatism compensator" consisting of a pair of plane-parallel plates of equal thickness, placed with equal and opposite obliquities to the principal ray. (Although one plate will introduce astigmatism, it will also introduce chromatic dispersion of lateral displacement of the image, and slight coma. The second plate is necessary to cancel these effects.) I prefer the lens because (1) it loses less light by reflection at its surfaces; (2) it can be thinner, so that non-homogeneity of refractive index will be less serious; (3) I think it likely that the error of its astigmatic surface is less than that of the three flat surfaces which it replaces. I made the lens by astigmatising a rectangular plane parallel plate $2{\cdot}7 \times 2{\cdot}2$ cm. on a rectangular pitch-polisher $3{\cdot}3 \times 3{\cdot}5$ cm., testing frequently with an optical flat, and inverting the lens end-for-end at intervals so as to prevent the development of conical error (coma). I use only the middle third of the lens, which suffices to annul one wave-length of astigmatism in the final image. As a check on its performance I have tested a certain spherical mirror, (1) with a large decentring, annulling the resulting one wave-length astigmatism with the lens; (2) with a negligible decentring, without the lens. Using the Zernike test, I could see no difference in the apparent shape of this mirror, the error of which is of the order of $\lambda/40$.

What has been said in § 8 about the necessity for freedom from scratches on the plane mirror M applies even more forcibly to the roof-reflector. I found chemically silvered glass flats unsatisfactory, because of scratches made in polishing after silvering. Aluminised glass, however, was entirely satisfactory.

10. *Type* 3 *Compensator.*—The set-up, shown in fig. 4, is the same as for the Type 2 compensator, except that a convex spherical mirror Q is substituted for the roof-reflector. The centre of curvature of this mirror (radius ρ/q) is placed at a distance v from the concave spherical mirror C: the star is placed at distance u from C.

The dimensions u, v, d, ρ, q are determined by the following conditions:—

$$\rho k^2(k+1)^2 = F; \qquad v = \frac{1+k}{1+2k}\cdot\rho; \qquad u \doteqdot (1+k)\rho;$$

$$d > D/2k^2(k+1); \qquad q = 8k+3+\frac{2}{k}+\frac{5}{4k^2}-\frac{2k+1}{2k^2(k+1)^2}; \qquad (69)$$

$$d_Q \geqslant \frac{(1+2k)}{q(1+k)}; \qquad F \geqslant 5D.$$

d_Q is the diameter of the convex mirror; k, as before, is to be nominally unity. If $k=1$, $q=111/8$.

As with the Type 2 compensator, if the star is placed at $u=(1+k)$, the paraxial image is formed level with it. It is permissible to move the star towards C so that the least-confusion circle is formed level with the star.

To centre the compensated beam on the paraboloid, stretch threads across the main cone, at surface of the convex mirror, along and perpendicular to the direction of decentring of S. An orientation and position can be found for the thread along the decentring direction, in which it shows

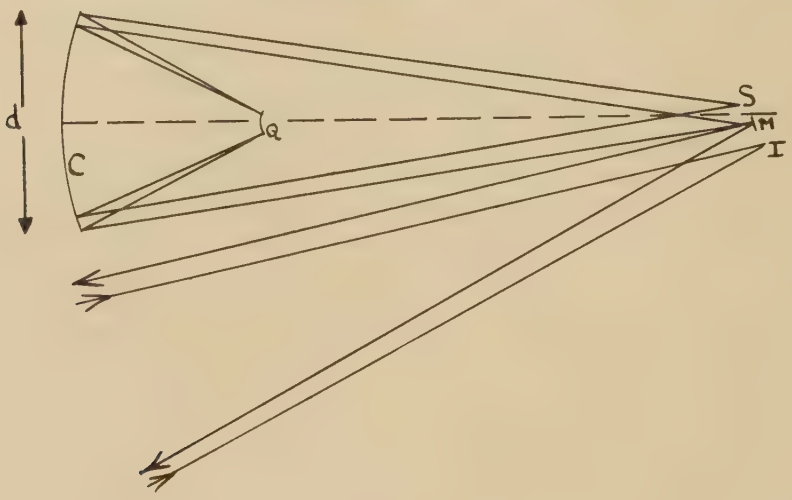

FIG. 4.

only one shadow, instead of three, on C. A lateral position can be found for the other thread at which the thickest of the shadows bisects the distance between the centres of the thinner two. In these positions both threads intersect the "principal" ("central") ray of the compensated cone, which passes through the pole of the convex mirror.

I find that a more precise setting of the threads is possible if one views the shadows through an $\times 4$ telescope so focussed that the two thinner shadows appear of equal width.

The plane mirror M is then oriented so as to centre the thread-shadows on the paraboloid, or alternatively, to give zero coma.

The decentring 2δ of S from the compensator's final image is measured, and the astigmatism may be calculated from the expression

$$\frac{2}{(1+2k)^2}\cdot\frac{\delta^2}{\rho}\left[2(1+k)^2\left\{\frac{kq}{1+2k}+1\right\}^2-(1+2k)^2q\right], \qquad (70)$$

this being the amount by which the focal line perpendicular to the decentring direction is nearer to C than the other focal line.

The astigmatism may be compensated either by an astigmatic lens placed a suitable distance in front of the final image I formed by the paraboloid, or by an appropriate adjustment of the decentring of the compensator's image from the paraboloid's image of S. I do not recommend using a very much larger value of δ than suffices to make the compensator's

image miss the star: this may make the compensation of astigmatism by "crossed decentring" more convenient, but it introduces the possibility of appreciable error depending on δ^3.

It will be appreciated that in this and in the Type 2 compensator any error on the spherical mirror C appears doubled on the paraboloid, while error on Q appears with unit magnification. One should therefore make C and Q three times as accurate as one hopes to make the paraboloid.

(Error on the plane mirror M should be negligible, as only a small part of its surface is used. One can, moreover, change the part used.)

11. *Testing the 36-inch Mirror during Refiguring.*—I used the Type 3 compensator and the Zernike test on the 36-inch Common mirror of the Cambridge Solar Physics Observatory, while removing the very large departure from revolution-symmetry which it was known to possess. As was pointed out in § 5, since this mirror has $F=3{\cdot}42$ m. and aperture $F/3{\cdot}75$, the convex compensating mirror must have its edge turned down by $0{\cdot}22\ \lambda$ if the test is to be null for a paraboloid. But as this amount is only about a tenth of the initial revolution-asymmetry of the Common mirror, I decided to begin with both compensating mirrors spherical for simplicity.

The mirror was handled on a machine consisting of a steel table 37 inches diameter, which could be rotated by a variable-speed motor, for hand figuring, or tilted into a vertical position for testing. Before tilting the table, the mirror was raised about 1 inch from the thick felt pad on which it rested, by three lead-shod screws passing through the table and the felt. Brackets carrying lead-shod kinematic supports for the mirror's edge were then bolted on to the table, so that the mirror could be arranged, when vertical, to be *balanced* on edge, pressing extremely lightly against one screw at the top of its back, and not touching the felt pad at all. It was sometimes tested exactly balanced, with nothing touching its front or back, to check that the very light pressure usually applied by one screw to its back (to steady it) was not astigmatising it appreciably.

The compensating system had $\rho=85{\cdot}32$ cm.; $d=24{\cdot}3$ cm.; $k=1{\cdot}000$ (for $F=341{\cdot}3$ cm., $D=91{\cdot}5$ cm.); $v=56{\cdot}88$ cm.; $u=169{\cdot}5$ cm. (so that the least-confusion circle imaged level with the star); $d_Q=2{\cdot}62$ cm.; $q=111/8$. It was assembled, together with the 0·007-mm. diameter star, on a steel joist, which also carried the focussing carriage, holding the Zernike disk, on which the image formed by the 36-inch mirror was centred. This joist, and the whole line of sight, was boxed in by a cloth-lined framework to exclude draughts.

So large was the initial revolution-asymmetry of the mirror, and so queer its shape, that it was necessary, in order to see the Zernike fringes at all, to use a Z-disk very much larger than the Airy disk associable with the focal ratio ($F/7{\cdot}5$) of the image. The use of an over-size Z-disk has the consequence that the Zernike fringes are then not simple contours of the mirror's error, but tend to show local errors more strongly than slow variations of curvature (*e.g.* astigmatism), and to give bad visibility on those parts of the mirror which have large errors of tilt. Thus when I set the Z-disk near the vertical focal line I could see broad patches of primary

"high" Zernike colour on the (horizontal) "high" astigmatic axis, surrounded above and below by about four successive "low" orders of fringe, of rather bad visibility. The distribution of patches of primary "high" colour showed that the high astigmatic axis was prolate, but the pattern was lop-sided, wherever the principal ray of the compensated beam was placed on the mirror. Thus the high astigmatic axis was also irregularly comatic.

When I set the Z-disk near the horizontal focal line I could see only two very small patches of primary "low" colour, near but not at the ends of the (vertical) low astigmatic axis. These were surrounded on either side by many orders of "high" fringe of even worse visibility. These fringes were strongly curved, so that while the high axis was straight and prolate, the low axis was curved and oblate, the total error of the surface being of the order of 4 fringes ($=2\lambda$).

I verified, by rotating the mirror and retesting at intervals in different azimuths, that these asymmetries belonged to it and not to the compensating system, and that they were not thermal transients.

A preliminary refiguring operation, lasting about eight weeks, sufficed to remove the greater part of the error, and incidentally to set at rest my fears regarding possible traps in the method of testing. I figured the mirror by hand, working locally on the areas shown by the Zernike test to be high, with pitch-polishers from 1 inch to 10 inches diameter. The interpretation of the Zernike fringes became progressively easier as the worst of the irregularity was reduced, and a smaller Z-disk could be used. I tried cancelling most of the astigmatism with a lens and the coma by decentring the test, but it was the large irregular errors, rather than the primary error, which produced the principal spread of the image, and consequent loss of fringe visibility.

Vibration proved a very serious trouble, the fringe system frequently dancing about, and often fading right out, due to high-speed vibration. It was often impossible to test while a motor-car remained within earshot. As the experiment was carried out in London (during my tenure of a Leverhulme Fellowship at the Imperial College of Science and Technology) the trouble from cars was considerable. Even when no car could be heard the fringes lacked contrast, compared with Zernike fringes on smaller mirrors. This also was due to vibration; I found that from 1.30 a.m. to 5 a.m. the fringes were quite steady, except when an occasional car passed, and their contrast was as good as that on smaller mirrors. I was finally forced to work only at night.

It thus became important to test as soon after each figuring operation as the relaxation of thermal transients due to the figuring and washing permitted. I washed the disk after tilting it into the vertical position. I found it very important to wash the whole front surface of the disk uniformly, even though only a part of it had been rouged for figuring. (I usually moistened the parts which were not to be figured, to secure a more uniform chilling by evaporation.) When this was done, the transient coma and astigmatism were quite small, so that one could often tell whether the figuring had done what was expected within 10 minutes of centring the

Z-disk on the image. Tilting, washing and drying took 20 minutes, and it usually required a further 5–10 minutes to adjust the mirror so that when it was very nearly balanced the image came in the desired place. On the other hand, if one either washed the rouged parts only, or washed them more intensively than the rest of the mirror's surface, transient coma would usually appear, and remain perceptible for an hour or so.

The aspherical transients always equilibrated more quickly than the focal length, which did not become constant for many hours. One of the advantages of any kind of null test over zonal tests is in fact that the mirror's error can be seen, and the next figuring operation started before complete thermal equilibrium has been reached.

At first I marked the high areas on the mirror by outlining them with rouge, sketching in the outline in stages, testing in between, to check that I was sketching it in correctly. As the figure became more accurate two difficulties arose. First, that the act of standing in front of the mirror warmed the air in front of it and so introduced anything up to $\lambda/2$ of temporary irregularity into the test. During the first minute or two, of course, the fringes would move irregularly: the important point, which I had not expected, but which I verified repeatedly, is that even though the fringes have become apparently quite steady, there may still be as much as $\lambda/2$ of transient coma or astigmatism, due to the hot air, which can persist for 5 or 10 minutes, sometimes changing its orientation very slowly the while. Thus the first rule in null-testing a large mirror is: Go on looking at it for at least 15 minutes.

Second, the act of outlining the high areas in (wet) rouge would slowly chill them, as the water evaporated, so that by the time the transient "atmospheric" coma had disappeared the high areas were high no longer. I then tried outlining the high areas by sticking rubber "suction hooks" on to the mirror: these have to be moistened to stick on, but since most of the moisture is enclosed they do not chill the mirror appreciably. After retesting at leisure, I then sketched in the high areas, with the hooks as guiding points.

I usually figured for 20–30 minutes between tests, reducing this time to 10 minutes as the error decreased. I figured 4–5 times per night, the last two operations being generally restricted to dealing with highly localised bumps, for I was afraid the total transient coma and astigmatism from the three preceding washings might not be negligible; moreover, the arrival of the first milk cart rendered delicate testing impossible. Now that the residual irregularity of the surface is of the order of $\pm \lambda/8$, and the residual astigmatism is of the order of $\lambda/4$, it will be necessary to proceed more slowly.

There are two difficulties in this kind of figuring. It is difficult to remove a high area extending to the edge of the mirror without either turning the edge down or leaving it strongly turned up. The best procedure seems to be to have the polisher slightly overhanging the edge, and then move it so that its inner edge rolls along the inner edge of the high area; when it has reached one end of the high area roll it back again. The

second point is that one tends to divide each bump into two, so that the number of bumps requiring individual attention tends to become prohibitive. The only cure for this is to proceed more slowly, giving more careful attention to the individual bumps.

I found one difficulty with the test. The method of centring the compensated cone by means of crossed threads, described in § 10, is not as accurate as I could wish, for, using the finest thread which gives a reasonably visible shadow (No. 200 cotton, 0·15 mm. diameter), one cannot, even with great care, be certain of centring the 5-mm. diameter shadow which this thread casts on the 36-inch mirror, with an error of less than 1 mm. This amount of decentring produces about $\lambda/4$ of coma at the edge of the mirror—an amount five if not ten times larger than the smallest coma that would be detectable in the absence of other errors, and quite easily seen even in the presence of the irregular error which the mirror now has. Thus I could not hope with this test to figure the mirror so as to bring its centre of figure closer to the centre of the disk than about 1 mm., nor could I expect when I rotated the disk and tested in several azimuths that the coma seen would rotate with the disk with greater accuracy than $\lambda/4$. When I had reached the stage of figuring where successive re-alignments of the threads sometimes reversed the apparent coma, I tested the disk in several azimuths and found that the apparent coma axis remained in the same octant of the disk, and that the variation of magnitude of the coma was of the same order as the probable error of alignment. I did not, however, feel certain that alignment error was wholly responsible for the comatic variation. It is possible that the disk may sag comatic, under gravity, when on edge: this effect has been shown by Couder * to be negligible for a 36-inch flat, but his analysis does not apply to a concave mirror.

In the further figuring I therefore did not attempt to improve the accuracy of centring of the mirror's figure, but tried simply to remove irregular error, using the crossed threads from time to time to verify that the centring of figure was still comparable with the thread-alignment accuracy.

The removal of the original astigmatism and irregular coma has reduced considerably the size of the final image, in spite of the $\pm \lambda/8$ "cobbled pavement" figure which the rather hurried local polishing has produced.

This preliminary refiguring operation, then, has served its purpose, which was to show that the atmospheric and seismic conditions, even of a laboratory in London, permit the application of the Zernike test to large paraboloids, and that quasi-null tests, less expensive than autocollimation, can be devised which enable one to see directly revolution-asymmetry in a large mirror, and so to reduce it without "regrinding and starting again."

It remains to fit a mechanical traverse to the polishing machine, and to continue the figuring with a half-size polisher, to remove the $\pm \lambda/8$ "cobbles," at the same time making the convex compensating mirror aspherical by $0{\cdot}22\ \lambda$, as explained in § 5, to make the test null for a true and not a pseudo-

* *Bulletin Astronomique*, **7**, 6, p. 201, and **7**, 7, p. 283.

paraboloid. This I propose to do in the H. H. Wills Physical Laboratory of Bristol University in 1937.

Meanwhile, the 36-inch mirror has been replaced in the telescope. Dr. R. O. Redman then reported that the image was two or three wave-lengths astigmatic. Obviously, the diagonal mirror was to blame. But I must admit a certain sensation of relief when Dr. Redman wrote that a knife-edge test at the primary focus did not show this astigmatism, nor did it appear when another diagonal mirror was used, which was thought to be flat to a wave-length or so.

I have spoken of the 2λ error of the 36-inch mirror, measured forty-six years after Dr. Common made it. In justice to Dr. Common I must add that the diagonal mirror which Dr. Redman has had to discard was made in 1926. I have examined it with polarised light and it is not unduly strained. I have knife-edge tested it, with the concave spherical compensating mirror, and it is *five wave-lengths concave.*

Imperial College of Science and Technology : London, 1935.
H. H. Wills Physical Laboratory : Bristol, 1936.

ON THE DETERMINATION OF THE SOLAR MOTION.

W. M. Smart, M.A., D.Sc.

(Communicated by the Director, Cambridge Observatory)

1. In investigations of the solar motion which are based either on proper motions or on radial velocities, it is the practice to divide the sky into areas of several hundred square degrees and to form the equations of condition for the centres of the several areas. For instance, if we are dealing with radial velocities and if $(-X, -Y, -Z)$ denote the linear components of the solar motion with respect to the assembly of stars for which we have the required observational material, the equation of condition for a particular star in a given area is (including the K term)

$$lX+mY+nZ+K=\rho, \qquad (1)$$

where (l, m, n) are the direction-cosines for the star with reference to one of the usual systems of co-ordinate axes—equatorial or galactic—and ρ is the observed radial velocity. In a strict calculation we should require to form an equation of the form of (1) for each star ; but for the sake of economy in calculation when the data refer to several thousands of stars, the usual procedure is to form equations of condition of the type

$$LX+MY+NZ+K=\bar{\rho}, \qquad (2)$$

where (L, M, N) are the direction-cosines for the centre of the area and $\bar{\rho}$ is the mean algebraic radial velocity of the stars in the area, and to attach

the weight N to the equation, N being the number of stars in the area. This is tantamount to the assumption that all the N stars are situated at the centre of the area and that their radial velocities, if so situated, are the same as the observed values. A similar argument applies to the determination of the solar motion from the observed proper motions. So far as I am aware it has not been noticed hitherto that this procedure is likely to introduce a systematic error into one or more of the quantities to be found.

If we consider the proper motion equations in greater detail we have, in addition to the terms in X, Y and Z, certain terms involving Δk and Δn which may be briefly described as corrections to the precessional and allied constants. It will be shown later that if the areas into which the stars are grouped are about four or five hundred square degrees, a systematic correction of the order of half a kilometre per second can result in one component of the solar motion; relatively, this is about one-quarter * of the magnitude of the corrections Δk and Δn. With somewhat larger areas the correction to the solar motion would be, relatively, of the same order of magnitude as the quantities Δk and Δn. It seems, therefore, important to investigate the effects of the corrections due to the grouping of the stars.

As regards the determination of the solar motion from radial velocities it is easily seen that the practical procedure leads to a value of the motion that is systematically too small.

Clearly, the ideal way to deal with the problem is to subdivide the celestial sphere into areas not exceeding a hundred square degrees, for in this case the systematic corrections can be neglected. But this entails a vast expenditure of labour and time which many astronomers might not consider commensurate with the subsequent gain in precision. The alternative is to continue to deal with large areas, thereby keeping the equations of condition comparatively small in number, and to correct the observed quantities—or rather their means over the areas—in accordance with the systematic effects which can be easily calculated in normal circumstances.

2. Let (x, y, z) denote the components of the linear motion of a star, corresponding to the annual proper motion components $\mu_\alpha \cos\delta$, μ_δ, and to the radial velocity ρ. Then for a star with co-ordinates (α, δ) in a particular region of the sky we have

$$x = \frac{\kappa}{p}\mu_\alpha \cos\delta, \qquad y = \frac{\kappa}{p}\mu_\delta, \qquad z = \rho, \tag{3}$$

where κ is 4·74 and p is the star's parallax; the components x, y and z are then expressed in km./sec. If (U, V, W) are the components of the star's motion with respect to the usual equatorial system, we have the following well-known equations connecting (x, y, z) and (U, V, W):—

$$x = -U\sin\alpha + V\cos\alpha \tag{4}$$

* The solutions given by L. Boss (*A.J.*, **26**, 112, 1910) show that Δk and Δn are each numerically one-tenth of the centennial parallactic drift, compared with which the correction of $\frac{1}{2}$ km./sec. is about $\frac{1}{40}$ of the total solar motion.

$$y = -U\cos\alpha\sin\delta - V\sin\alpha\sin\delta + W\cos\delta, \quad (5)$$

$$z = \quad U\cos\alpha\cos\delta + V\sin\alpha\cos\delta + W\sin\delta, \quad (6)$$

or, in the alternative form,

$$U = -x\sin\alpha - y\cos\alpha\sin\delta + z\cos\alpha\cos\delta, \quad (7)$$

$$V = \quad x\cos\alpha - y\sin\alpha\sin\delta + z\sin\alpha\cos\delta, \quad (8)$$

$$W = \quad y\cos\delta + z\sin\delta. \quad (9)$$

Let (A, D) be the co-ordinates of the centre, R, of the region. Let (x', y', z') denote the values of (x, y, z) if the star were observed at R with the components (U, V, W) unaltered. Then

$$x' = -U\sin A + V\cos A, \quad (10)$$

$$y' = -U\cos A\sin D - V\sin A\sin D + W\cos D, \quad (11)$$

$$z' = \quad U\cos A\cos D + V\sin A\cos D + W\sin D. \quad (12)$$

From (4) and (10) we obtain

$$x' - x = U(\sin\alpha - \sin A) - V(\cos\alpha - \cos A),$$

whence, using (7) and (8),

$$x' - x = -x[1 - \cos(\alpha - A)] - y\sin(\alpha - A)\sin\delta + z\sin(\alpha - A)\cos\delta. \quad (13)$$

Similarly we derive

$$y' - y = x\sin(\alpha - A)\sin D + y[\cos D\cos\delta + \cos(\alpha - A)\sin D\sin\delta - 1] + z[\cos D\sin\delta - \cos(\alpha - A)\sin D\cos\delta] \quad (14)$$

and

$$z' - z = -x\sin(\alpha - A)\cos D + y[\sin D\cos\delta - \cos(\alpha - A)\cos D\sin\delta] + z[\sin D\sin\delta + \cos(\alpha - A)\cos D\cos\delta - 1]. \quad (15)$$

The three formulæ (13), (14) and (15) are accurate formulæ, and the values $x' - x$, $y' - y$ and $z' - z$ can be found if all the observational data are completely known for the star.

The formulæ are also accurate if we are dealing with parallactic motion alone. In this case, writing X, Y and Z for U, V and W in (4), (5) and (6), we have that (4) and (5) are Airy's formulæ for determining the solar motion from the proper motions, and (6) is Campbell's equation for the radial velocities (we omit here the consideration of the Δk, Δn and the K terms). Also, the values of x, y and z on the right of (13), (14) and (15) are the corresponding components of the parallactic motion.

We shall suppose that a given region is defined by the meridians $A - \phi$ and $A + \phi$ and by parallels of declination $D - \theta$ and $D + \theta$. For parallactic motion it is seen that, if the stars are uniformly distributed over the region, the values of $\Sigma x' - \Sigma x$, $\Sigma y' - \Sigma y$, and $\Sigma z' - \Sigma z$ are of order θ^2 and ϕ^2, the angles θ, ϕ being expressed in circular measure and the summations being taken over the whole area. It follows that, in the general case, when using

the formulæ for $\Sigma x' - \Sigma x$, etc. it will be adequate to replace x, y and z on the right of (13), (14) and (15) by the corresponding parallactic values.

Let N be the number of stars in the region. We write

$$\Sigma x' - \Sigma x = NC_x, \tag{16}$$

$$\Sigma y' - \Sigma y = NC_y, \tag{17}$$

$$\Sigma z' - \Sigma z = NC_z, \tag{18}$$

in which C_x, C_y and C_z can be found from the expressions on the right of (13), (14) and (15) with x, y and z referring to parallactic motion.

For example, if we introduce the terms * in Δk and Δn in the first of Airy's formulæ, the correct equation of condition for the region as a whole is

$$-X \sin A + Y \cos A + \frac{\kappa}{p}\Delta k \cos D + \frac{\kappa}{p}\Delta n \sin A \sin D = \frac{1}{N}\Sigma x + C_x, \tag{19}$$

its weight being N.

As already stated, the value of C_x for large areas is comparable in magnitude with the values of Δk and Δn.

We now consider the evaluations of the corrections, C, assuming that the stars are uniformly distributed over the particular region concerned. A further refinement would be to take account of the varying distribution according to galactic latitude, but unless the regions were of considerable extent in latitude it would appear that little would be gained in the way of precision.

It may be noted here that the equations so far derived hold for galactic co-ordinates on the understanding that α, A and δ, D refer in this case to galactic longitude and latitude respectively.

3. *Evaluation of* C_x.—In the figure let R denote the centre (A, D) of the region and X the position of a star (α, δ) in the region. Let M be the

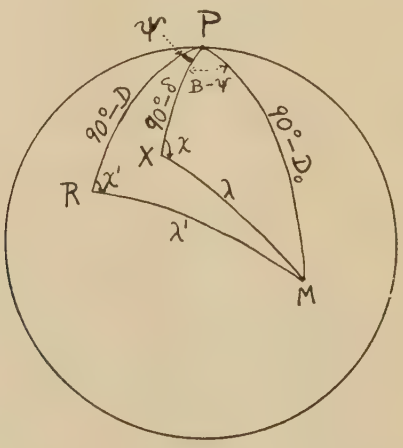

position of the solar antapex (A_0, D_0) and let the solar motion be U. We denote by λ and χ the angular distance of X from M and the position angle

* L. Boss, *A.J.*, **26**, 95, 1910.

of M with reference to X, respectively; λ' and χ' refer similarly to R. Also write

$$A_0 - A = B; \qquad \alpha - A = \psi.$$

We consider the region to be defined by the meridians $A - \phi$ and $A + \phi$ and by the parallels of declination δ_1 and δ_2, where

$$\delta_1 = D - \theta; \qquad \delta_2 = D + \theta. \tag{20}$$

The area of an element of the region is $\cos\delta\, d\delta\, d\psi$, and the total area, Δ, of the region is given by

$$\Delta = \int_{\delta_1}^{\delta_2} \cos\delta\, d\delta \int_{-\phi}^{\phi} d\psi$$
$$= 2\phi\,(\sin\delta_2 - \sin\delta_1),$$

whence, by (20),

$$\Delta = 4\phi \sin\theta \cos D. \tag{21}$$

Equating $x' - x$ to the difference of the parallactic components at R and X, we have

$$x' - x = U \sin\lambda' \sin\chi' - U \sin\lambda \sin\chi,$$

and hence

$$x' - x = U \cos D_0 \{\sin B - \sin(B - \psi)\}.$$

Let n denote the number of stars per unit area so that the number in the elementary area is $n \cos\delta\, d\delta\, d\psi$. Also

$$N = n\Delta. \tag{22}$$

Hence we obtain

$$\frac{\Sigma x' - \Sigma x}{U \cos D_0} = n\Delta \sin B - n\int_{\delta_1}^{\delta_2}\int_{-\phi}^{\phi} \cos\delta \sin(B - \psi) d\delta\, d\psi,$$

so that, by (16) and (22),

$$\frac{1}{U \cos D_0} C_x = \sin B - \frac{1}{\Delta}\{\sin\delta_2 - \sin\delta_1\}\{\cos(B - \phi) - \cos(B + \phi)\}.$$

Hence, using (20), we have

$$C_x = U \cos D_0 \sin B\left(1 - \frac{\sin\phi}{\phi}\right). \tag{23}$$

With the assumption as to the uniformity of distribution of the stars over the area this is an accurate formula. If ϕ is no greater than 20°, say, it will be sufficient to write (23) in the form

$$C_x = \tfrac{1}{6}\phi^2 U \cos D_0 \sin(A_0 - A), \tag{24}$$

where ϕ is in circular measure.

4. *Evaluation of C_y.*—At X, the parallactic component in declination is $U \sin\lambda \cos\chi$. We then have

$$y' - y = U \sin\lambda' \cos\chi' - U \sin\lambda \cos\chi$$
$$= U(\sin D_0 \cos D - \cos D_0 \sin D \cos B)$$
$$- U\{\sin D_0 \cos\delta - \cos D_0 \sin\delta \cos(B - \psi)\}.$$

Hence

$$\frac{\Sigma y' - \Sigma y}{U} = \sin D_0 \left\{ N \cos D - n \int_{\delta_1}^{\delta_2} \cos^2 \delta \, d\delta \int_{-\phi}^{\phi} d\psi \right\}$$

$$- \cos D_0 \left\{ N \sin D \cos B - n \int_{\delta_1}^{\delta_2} \sin \delta \cos \delta \, d\delta \int_{-\phi}^{\phi} \cos (B - \psi) d\psi \right\},$$

from which

$$C_y = U \sin D_0 \left\{ \cos D - \frac{\phi}{\Delta} (\sin 2\theta \cos 2D + 2\theta) \right\}$$

$$- U \cos D_0 \left\{ \sin D \cos B - \frac{1}{\Delta} \sin \phi \cos B \sin 2\theta \sin 2D \right\}$$

or

$$C_y = U \sin D_0 \cos D \left\{ 1 - \frac{1}{2 \cos^2 D} \left(\frac{\theta}{\sin \theta} + \cos \theta \cos 2D \right) \right\}$$

$$- U \cos D_0 \sin D \cos B \left\{ 1 - \frac{\sin \phi \cos \theta}{\phi} \right\}. \qquad (25)$$

Approximating as before, we obtain

$$C_y = \frac{U}{12} \theta^2 (3 \cos 2D - 1) \sin D_0 \sec D$$

$$- \frac{U}{6} (3\theta^2 + \phi^2) \cos D_0 \sin D \cos (A_0 - A). \qquad (26)$$

With the assumption as to the distribution of the stars over the area, (25) is an accurate formula.

5. *Evaluation of* C_z.—At X, the parallactic radial component is $U \cos \lambda$. Hence

$$z' - z = U \cos \lambda' - U \cos \lambda,$$

from which

$$\frac{z' - z}{U} = \sin D_0 \sin D + \cos D_0 \cos D \cos B$$

$$- \{ \sin D_0 \sin \delta + \cos D_0 \cos \delta \cos (B - \psi) \}.$$

Hence

$$\Sigma z' - \Sigma z = U \sin D_0 \left\{ N \sin D - n \int_{\delta_1}^{\delta_2} \sin \delta \cos \delta \, d\delta \int_{-\phi}^{\phi} d\psi \right\}$$

$$+ U \cos D_0 \left\{ N \cos D \cos B - n \int_{\delta_1}^{\delta_2} \cos^2 \delta \, d\delta \int_{-\phi}^{\phi} \cos (B - \psi) d\psi \right\},$$

from which

$$C_z = U \sin D_0 \left\{ \sin D - \frac{\phi}{2\Delta} (\cos 2\delta_2 - \cos 2\delta_1) \right\}$$

$$+ U \cos D_0 \left\{ \cos D \cos B - \frac{1}{\Delta} \sin \phi \cos B (2\theta + \sin 2\theta \cos 2D) \right\},$$

or

$$C_z = U \sin D_0 \sin D(1 - \cos\theta) + U \cos D_0 \cos D \cos B\left\{1 - \frac{\sin\phi}{\phi}\left(\frac{2\theta + \sin 2\theta \cos 2D}{4 \sin\theta \cos^2 D}\right)\right\}. \quad (27)$$

Approximately as before we obtain

$$C_z = \frac{U}{2}\theta^2 \sin D_0 \sin D + \frac{U}{6} \cos D_0 \cos D \cos(A_0 - A)\{\phi^2 + \theta^2(3 - 2\sec^2 D)\}. \quad (28)$$

Again, (27) is an accurate formula, assuming that the distribution of the stars is uniform over the area.

6. *The Effect of* C_x.—For the sake of arriving at numerical estimates of the effects of the various corrections, we shall suppose that the sky is divided into regions by meridians $22\frac{1}{2}^\circ$ apart with their centres at 0°, $\pm 20^\circ$, $\pm 40^\circ$, $\pm 60^\circ$, the declination boundaries being 20° apart; we ignore the polar caps bounded by small circles of declination $\pm 70^\circ$. There will thus be 112 areas. If we exclude the areas centred at declination $\pm 80^\circ$ in L. Boss's division * of the sky in his well-known determination of the solar motion by means of the proper motions of the *P.G.C.*, there are 100 areas left. Similarly, by excluding the polar areas beyond $\pm 64^\circ$ in the division of the sky by Campbell and Moore in their determination of the solar motion † from radial velocities, there are 84 areas left. Thus our regions, although they decrease in area towards the poles, are of much the same average extent as in these well-known investigations.

Solving in equatorial co-ordinates, we can take advantage of the fact that the right ascension, A_0, of the antapex is approximately 90°, and we shall write

$$A_0 = 90^\circ \quad \text{and} \quad D_0 = -30^\circ.$$

Thus our correction C_x becomes

$$C_x = a \cos A, \quad (29)$$

where

$$a = \frac{U}{6}\phi^2 \cos D_0. \quad (30)$$

Thus, with $U = 19{\cdot}5$ km./sec., the value of a is $\frac{1}{9}$ km./sec.

The equation of condition depending on the μ_α component of proper motion, assuming that each star of the region is at the centre of the region and applying the correction C_x to each star, is

$$-X \sin A + Y \cos A + \frac{\kappa}{p}\Delta k \cos D + \frac{\kappa}{p}\Delta n \sin A \sin D = \bar{x} + a \cos A$$

with weight N (the number of stars in the region), where $\bar{x}$ is the mean of

* *A.J.*, **26**, 97, 1910. † *Lick Publications*, **16** (Introduction, 35), 1928.

the quantities $\frac{\kappa}{p}\mu_a \cos\delta$. The equation can be written

$$-X\sin A+(Y-a)\cos A+\frac{\kappa}{p}\Delta k\cos D+\frac{\kappa}{p}\Delta n\sin A\sin D=\bar{x}. \qquad (31)$$

It is clear from (31) that the introduction of the correction leaves X, Δk and Δn unaltered, and that if Y' is the value of Y obtained from the solution made in the usual way (that is, by ignoring the correction C_x), the true value, Y, is given by

$$Y=Y'+a.$$

As Y' is about $+17$ km./sec. in the usual system of equatorial co-ordinates, and X is very small, the effect of the correction is to move the right ascension of the antapex slightly nearer 90° than in the case of the uncorrected value (since $\tan A_0=Y/X$) and to increase slightly the solar speed or the parallactic motion 90° from the antapex.

The factor a is independent of the way the regions are delimited in declination. If we had used regions bounded by meridians 45° apart, the value of a would be about 0·4 km./sec., which represents a significant correction.

It is important to notice that the omission of the corrections C_x in the equations of condition does not lead to any error in the deduced values of Δk and Δn when the solution is made in equatorial co-ordinates.

7. *The Effect of* C_y.—(i) Consider the first part of the expression for C_y in (26), which we can write in the form

$$c_1=b(3\cos^2 D-2)\sec D.$$

With $\theta=10°$ the value of b is approximately $-\frac{1}{20}$ km./sec., and even with larger areas this part of the C_y correction is of little importance and its influence may be neglected.

(ii) Writing the second part of the correction C_y in (26) as c_2, we have, putting $A_0=90°$,

$$c_2=-d\sin A\sin D,$$

where

$$d=\frac{U}{6}(3\theta^2+\phi^2)\cos D_0.$$

With our values of U, θ, ϕ and D_0 we find that, approximately,

$$d=0\cdot4 \text{ km./sec.}$$

The equation of condition for the μ_δ components of proper motion is

$$-X\cos A\sin D-Y\sin A\sin D+Z\cos D+\frac{\kappa}{p}\Delta n\cos A=\bar{y}-d\sin A\sin D,$$

which can be written

$$-X\cos A\sin D-Y'\sin A\sin D+Z\cos D+\frac{\kappa}{p}\Delta n\cos A=\bar{y}, \qquad (32)$$

where

$$Y' = Y - d.$$

The solution of the equations of condition when the correction C_y is omitted gives the correct values of X, Z and Δn, but as Y' is the value obtained from the solution, the true value of the Y component of the parallactic motion is $Y' + d$.

8. *The Combined Effect of the C_x and C_y Corrections.*—The total effect of the C_x and C_y corrections in the solutions of Airy's equations in equatorial co-ordinates may be summed up as follows :—

(i) There is an increase in the Y component by about 0·5 km./sec., which will make the right ascension of the antapex approximate more closely to 90°, and which will also cause a decrease of nearly 1° in the numerical value of the declination, D_0, of the antapex. This latter result may be easily verified from Boss's results as follows. His solutions,* transformed into km./sec., and the signs of X, Y and Z being changed so as to agree with parallactic motion, are

$$X = -\frac{0{\cdot}03}{3{\cdot}85} \times 19{\cdot}5 = -0{\cdot}15 \text{ km./sec.},$$

$$Y = +\frac{3{\cdot}18}{3{\cdot}85} \times 19{\cdot}5 = +16{\cdot}1 \quad ,,$$

$$Z = -\frac{2{\cdot}17}{3{\cdot}85} \times 19{\cdot}5 = -1{\cdot}10 \quad ,,$$

from which as in his solution

$$D_0 \equiv \tan^{-1}\left(\frac{Z}{Y}\right) = -34^\circ{\cdot}3.$$

On increasing Y to 16·6 we obtain $D_0 = -33^\circ{\cdot}5$.

(ii) A further result is the increase of the equivalent solar speed $(X^2 + Y^2 + Z^2)^{\frac{1}{2}}$ from 19·5 to 19·9 km./sec., and an increase of Boss's M † from $3''{\cdot}85$ to $3''{\cdot}93$.

(iii) The applied corrections have no effect on the values of X, Z, Δk and Δn.

9. *The Effect of C_z.*—(i) Denoting the first part of the correction C_z, given by (28), by c_1, we write, putting $D_0 = -30°$,

$$c_1 = -\frac{U}{4}\theta^2 \sin D$$
$$\equiv -e \sin D.$$

The equation of condition is, from (4), and inserting the K term,

$$X \cos A \cos D + Y \sin A \cos D + Z \sin D + K = \bar{z} + c_1$$

or

$$X \cos A \cos D + Y \sin A \cos D + (Z + e) \sin D + K = \bar{z}.$$

---

* *A.J.*, **26**, 112, 1910.

† M is the centennial parallactic proper motion at an angular distance of 90° from the antapex.

Thus if Z' is the value of the Z component of the parallactic motion obtained from the solutions of the equations when the correction c_1 is omitted, the true value is $Z' - e$. With the usual values of U and θ, $e = 3/20$ km./sec. approximately. Since Z' is negative, the effect of the correction c_1 is to increase the numerical value of the declination, D_0, of the antapex by about 0°·3. Campbell's areas are on the whole about 30 per cent. greater than those assumed, so that due to this correction alone the increase in the numerical value of D_0 may be estimated to be $\frac{1}{2}°$. There will be also an increase in the solar motion of 0·1 km./sec. approximately.

(ii) The second part, c_2, of the correction C_z in (28) may be written

$$c_2 = f \sin A \cos D,$$

where

$$f = \frac{U}{6} \cos D_0 \{\phi^2 + \theta^2(3 - 2 \sec^2 D)\}.$$

With our values of ϕ and θ, f is positive if $D < 52°$. Hence for 5/7 of the areas we are considering, the effect of c_2 is to give a preponderatingly positive value of f. This is still further emphasised if we suppose the equations described in galactic co-ordinates as the weight attached to the equations of condition for low galactic latitudes will be several times greater than the weight in latitudes of $\pm$ 60° and over.

For $D = 0°$ the value of f is $+0·3$ km./sec., and for $D = 20°$, 40° and 60° the values are respectively $+\frac{1}{4}$, $+\frac{1}{7}$ and $-\frac{1}{5}$ km./sec. A rough system of weighting—weight 2 for $D = 0°$ and 20°, and weight 1 for $D = 40°$ and 60°—gives a mean value of f to be 0·2 km./sec.

The equation of condition is

$$X \cos A \cos D + (Y - f) \sin A \cos D + Z \sin D + K = \bar{z}, \qquad (33)$$

so that if Y' is the value of the Y component obtained by ignoring the correction c_2, the true value is $Y' + f$, and as an estimated result we can say that the true value is 0·2 km./sec. greater than that obtained in the usual way.

The combined results appear to indicate that, when the correction C_z is taken into account, the declination of the antapex should be increased numerically by about $\frac{1}{2}°$, and that the solar motion should be increased by about 0·2 or 0·3 km./sec.

10. *Practical Application.*—The previous sections show that, with the celestial sphere divided into regions of four or five hundred square degrees, the determination of the solar motion from proper motions or from radial velocities is not free from systematic errors. With the increase of observational material it might be thought desirable, or even essential, to divide the sphere into much smaller areas—say of 100 square degrees—for which the systematic errors would be of negligible amount. But this would mean the treatment of about 400 equations of condition, and with four unknowns as in each of (31), (32) and (33), the amount of labour required to achieve the solutions would be prodigious. It seems to me that, instead of diminishing the size of the regions, it would be more advantageous in every way to deal with considerably larger areas than are dealt with here—say with ϕ and θ each

equal to 15° or 20°, or even more—and to calculate the accurate values of C_x, C_y and C_z from the formulæ as given in sections 3, 4 and 5. These calculations can be done quite rapidly when the regions are bounded by parallels of declination (or of galactic latitude). For the corrections to be of the requisite accuracy it is only necessary that the stars in any given region should be fairly uniformly distributed over the area. *With this condition holding, the equation of condition formed for the centre of the region, with attached weight equal to the number of the stars in the region, is essentially the same, when the appropriate value of C_x or C_y or C_z is added, as if the equation of condition were formed for each star and the sum taken.*

In the following paper areas of 900 to 1200 square degrees are considered; the number of equations of condition is reduced to 34, thereby effecting a great saving of labour without appreciable injury, it is believed, to the precision of the results.

11. *Summary.*—(i) The systematic errors arising from the usual grouping of stars into areas of 400 or 500 square degrees, for the determination of the solar motion, are considered, and accurate and approximate formulæ are obtained.

(ii) Numerical estimates of the systematic errors are found when the proper motions and the radial velocities are used separately.

(iii) It is suggested that it is unnecessary to subdivide the sky into very small areas, and that it is quite adequate to deal with areas of considerable extent provided the necessary corrections, which can be quickly calculated, are applied to the usual equations of condition.

Observatory, Cambridge:
1936 *March* 6.

THE SOLAR MOTION AND GALACTIC ROTATION FROM RADIAL VELOCITIES.

W. M. Smart, M.A., D.Sc., and H. E. Green, M.A.

(Communicated by the Director, Cambridge Observatory)

1. *The Solar Motion.*—In a recent paper * by one of us, the radial velocities of nearly 3700 stars of spectral types B to M were used to ascertain if the distribution of radial velocities was in accordance with the two-streams theory. The material was arranged according to galactic latitude and according to spectral type, and was in a form suitable for an immediate determination of the solar motion. The values of the radial velocities were taken from Schlesinger's *Catalogue of Bright Stars* (1930), in which the limiting magnitude is $6^{m}\cdot5$; members of open clusters and the "high velocity stars" were omitted from the statistics. The areas into which the sky was divided are bounded by galactic "meridians," which we write as $G-\phi$ and

* W. M. Smart, *M.N.*, **96**, 165, 1936.

$G+\phi$, and by parallels of galactic latitude, $g-\theta$ and $g+\theta$, where (G, g) denote the galactic co-ordinates of the adopted centre of the region. The areas are much larger than those normally used in investigations of the solar motion. For example, the areas used by Campbell and Moore * are between 400 and 500 square degrees; those in the present investigation, excluding two polar areas, are between 900 and 1200 square degrees. Their centres are given in Table II of the first paper referred to. In the preceding communication † it is shown that, if the stars of an area are uniformly distributed over the area, the equation of condition formed for the centre of the region can be expressed in a manner that makes accurate allowance for the distribution of stars over the area. The number of equations of condition is thus considerably reduced, and theoretically there is no loss in precision in determining the constants of the solar motion.

2. In the subsequent numerical work we shall suppose that in any given area the stars are uniformly distributed over this area. Taking all spectral types together this condition is almost accurately fulfilled; for any given spectral class, however, the number of stars in the area is comparatively small, and this condition is, on the average, only approximately realised.

If $(-X, -Y, -Z)$ denote the components of the solar motion with respect to galactic axes and (l, m, n) are the direction-cosines of the adopted centre of the region, which we suppose contains N_1 stars, the equation of condition (with weight N_1) is

$$lX+mY+nZ+K=\frac{1}{N_1}\Sigma R+C_z, \tag{1}$$

where ΣR is the algebraic sum of the observed radial velocities of the N_1 stars and C_z is given ‡ accurately by

$$C_z=U\sin g_0\sin g(1-\cos\theta)+U\cos g_0\cos g\cos(G_0-G)\left\{1-\frac{\sin\phi}{\phi}\left(\frac{2\theta+\sin 2\theta\cos 2g}{4\sin\theta\cos^2 g}\right)\right\}. \tag{2}$$

In this last formula, (G, g) are the co-ordinates of the centre of the region, (G_0, g_0) are the co-ordinates of the solar antapex and U is the solar motion; also, the boundaries of the region are defined as indicated in section 1. The contribution of this area to the first of the normal equations is

$$N_1l^2X+N_1lmY+N_1lnZ+N_1lK=l\sum_{N_1}R+N_1lC_z. \tag{3}$$

Consider now the equal antipodal area, containing N_2 stars; the direction-cosines of its centre are $(-l, -m, -n)$, and C_z, by (2), changes sign. The equation of condition for this area is

$$-lX-mY-nZ+K=\frac{1}{N_2}\Sigma R-C_z,$$

---

* *Lick Publ.*, **16**, 1928. † *M.N.*, **96**, 461, 1936.
‡ *M.N.*, **96**, 467, 1936 (formula (27)).

and the contribution to the first normal equation is

$$N_2l^2X+N_2lmY+N_2lnZ-N_2lK=-l\sum_{N_2}R+N_2lC_z. \qquad (4)$$

Adding (3) and (4), we obtain the contribution of the two antipodal areas to the first normal equation. The contributions to the other normal equations are obtained in a similar manner. We write

$$\rho_1=\sum_{N_1}R+N_1C_z, \qquad (5)$$

$$\rho_2=\sum_{N_2}R-N_2C_z. \qquad (6)$$

The normal equations are then :

$$\begin{aligned}
X\Sigma(N_1+N_2)l^2+Y\Sigma(N_1+N_2)lm+Z\Sigma(N_1+N_2)ln+K\Sigma(N_1-N_2)l &= \Sigma l(\rho_1-\rho_2),\\
X\Sigma(N_1+N_2)lm+Y\Sigma(N_1+N_2)m^2+Z\Sigma(N_1+N_2)mn+K\Sigma(N_1-N_2)m &= \Sigma m(\rho_1-\rho_2),\\
X\Sigma(N_1+N_2)ln+Y\Sigma(N_1+N_2)mn+Z\Sigma(N_1+N_2)n^2+K\Sigma(N_1-N_2)n &= \Sigma n(\rho_1-\rho_2),\\
X\Sigma(N_1-N_2)l+Y\Sigma(N_1-N_2)m+Z\Sigma(N_1-N_2)n+K\Sigma(N_1+N_2) &= \Sigma(\rho_1+\rho_2), \qquad (7)
\end{aligned}$$

in which the summations are taken over all the pairs of antipodal regions.

The formulæ for l, m and n are :

$$l=\cos G\cos g\,; \qquad m=\sin G\cos g\,; \qquad n=\sin g. \qquad (8)$$

The values of l, m and n for the several regions are given later in Table VI.

3. Table I gives for each region the values of ΣR (the algebraic sum of the catalogue radial velocities) and the number, N, of stars in the region, antipodal areas being shown together ; thus, h and H are antipodal regions, and in the formulæ (5), (6), (7) and (8) N_1 refers to region h and N_2 to region H.

The first group, h to K, are centred on the galactic equator ; the second group, e to N, in galactic latitude $\pm 20°$; the third group, b to R, in galactic latitude $\pm 45°$; and the last two regions, a and A, are large polar areas.

Preliminary solutions were made separately for each spectral type, for all the spectral types B to M, and for all spectral types A to M, with the correction C_z omitted from the equations of condition. These preliminary solutions correspond to the usual procedure, except that our areas are from two to three times larger in extent than the average areas into which the celestial sphere is generally divided.

Table II shows the details of the preliminary solutions. From the third-last column it is seen that, in the galactic longitude of the antapex, there is a range of about 15° on either side of the value (204°·7) obtained for stars of all spectral types. A similar remark applies to the second-last column. The most noteworthy feature of the table is, however, the rather small value (18·84 km./sec.) for the solar motion, U, for stars of all spectral types, which may be regarded as the normal solar motion. The value usually obtained

TABLE I

Values of ΣR and N for the Regions, arranged according to Spectral Type

Region	B		A		F		G		K		M	
	ΣR	N	ΣR	N	ΣR	N	ΣR	N	ΣR	N	ΣR	N
h	+ 73	30	+ 15	11	− 55	7	+ 11	9	− 59	22	− 56	3
H	− 117	34	− 57	27	+ 64	24	− 52	8	−248	29	− 34	3
i	− 73	13	−278	16	−144	13	− 29	5	−358	27	+ 4	2
I	+ 667	38	+200	19	+ 89	8	+153	8	+330	24	+184	7
j	− 249	30	−491	29	−305	22	−126	13	−678	36	− 58	6
J	+1039	41	+ 74	11	+316	16	+ 54	13	+505	29	+101	3
k	− 506	43	−320	23	− 96	13	−122	9	−581	38	− 86	6
K	+1165	52	+119	16	+124	17	+106	10	+207	33	+ 49	4
e	+ 69	13	− 58	13	0	7	+ 8	9	+ 39	27	− 6	5
E	− 6	7	+ 23	24	+ 7	14	+ 45	15	− 50	37	−123	7
f	− 104	11	−200	18	− 30	10	−240	11	−454	27	− 24	3
F	+ 194	8	+229	17	+296	18	+ 79	21	+513	37	+ 11	7
g	− 205	21	−148	24	−235	25	− 94	12	−581	36	+ 19	4
G	+ 90	9	+ 58	12	+ 94	6	+104	9	+161	18	+ 87	3
l	+ 164	45	−158	16	− 90	8	− 67	8	−283	30	+ 36	5
L	+ 183	25	+254	27	+ 35	16	+ 91	15	+ 88	33	− 38	3
m	− 148	12	−566	36	−284	11	−126	6	−495	35	− 56	5
M	+1719	65	+272	21	+104	10	+239	12	+207	17	+ 80	4
n	− 261	16	−342	28	−342	25	− 96	17	−742	42	−110	7
N	+ 507	21	+307	17	+198	13	+153	7	+527	30	+137	5
b	+ 57	6	+ 51	13	− 15	11	+ 15	10	+320	23	+ 80	7
B	+ 35	4	+141	30	−130	22	−105	23	+109	47	+ 35	5
c	− 84	12	+ 8	18	− 75	13	− 92	13	− 45	30	+ 13	6
C	+ 100	5	+234	26	+ 86	14	+315	18	+549	41	+107	11
d	+ 14	11	− 68	17	+ 54	12	−182	13	−127	32	− 97	16
D	+ 63	7	+ 16	10	+ 28	14	+ 57	11	+109	27	− 37	5
p	− 66	7	−185	14	−103	11	−141	12	−164	32	+ 60	8
P	+ 134	13	+ 53	21	+155	28	−187	21	+160	35	+ 35	7
q	− 116	6	−406	30	−161	9	−205	16	−651	45	−176	11
Q	+ 211	14	+180	12	+ 86	8	+191	9	+326	20	+ 59	5
r	− 71	7	−324	35	−173	18	−380	19	−340	29	−160	8
R	+ 56	4	+111	9	+150	16	+ 72	5	+376	21	+138	7
a	+ 151	12	+268	28	+164	21	+ 73	21	+ 79	59	− 57	13
A	− 10	3	−333	74	−365	43	− 96	25	−395	70	−147	21

for U is about 19·5 km./sec. (see Table V below), and the deficiency just found in the preliminary solution is attributable to the neglect of C_z in the equations of condition.

TABLE II

Preliminary Solutions for the Solar Motion

Spectral Type	Number of Stars	X	Y	Z	K	G_0	g_0	U
		km./sec.				°	°	(km./sec.)
B	645	−17·28	− 9·97	−8·35	+4·77	210·0	−22·7	21·63
A	742	−14·03	− 3·34	−8·08	−0·02	193·4	−29·2	16·53
F	523	−14·20	− 3·74	−9·53	−0·60	194·7	−33·0	17·51
G	433	−14·24	− 6·71	−5·21	−0·98	205·2	−18·3	16·58
K	1118	−15·83	− 7·51	−7·21	−0·23	205·4	−22·4	18·95
M	222	−13·21	−11·23	−8·05	+0·77	220·4	−24·9	19·09
B to M	3683	−15·47	− 7·10	−8·07	+0·82	204·7	−25·4	18·84
A to M	3038	−14·68	− 6·00	−7·55	−0·21	202·2	−25·5	17·56

The relative values of U, in the last column, follow the general run of results for the different spectral types as found by Campbell and Moore (*loc. cit.*) from the radial velocities of 2149 stars.

The K term for the B stars has the value generally found in this kind of investigation.

4. With the values of G_0, g_0 and U, as given in Table II, the values of C_z were calculated for each region and for each spectral type. These values are shown in Table III.

TABLE III

Values of C_z

Region	B	A	F	G	K	M
h	+0·04	−0·07	−0·07	+0·03	+0·04	+0·17
i	−0·37	−0·36	−0·37	−0·31	−0·36	−0·25
j	−0·60	−0·44	−0·45	−0·48	−0·55	−0·52
k	−0·47	−0·26	−0·28	−0·36	−0·42	−0·48
e	+0·04	−0·17	−0·16	−0·03	−0·04	+0·17
f	−0·76	−0·63	−0·61	−0·65	−0·74	−0·59
g	−0·76	−0·46	−0·44	−0·58	−0·66	−0·73
l	−0·04	−0·23	−0·19	−0·07	−0·08	+0·09
m	−0·84	−0·69	−0·68	−0·71	−0·81	−0·67
n	−0·84	−0·53	−0·51	−0·65	−0·74	−0·80
b	+0·19	+0·10	+0·14	+0·08	+0·13	+0·27
c	−0·22	−0·13	−0·10	−0·22	−0·21	−0·13
d	−0·22	−0·03	−0·02	−0·18	−0·17	−0·21
p	−0·19	−0·30	−0·31	−0·15	−0·21	−0·11
q	−0·60	−0·53	−0·56	−0·45	−0·55	−0·52
r	−0·60	−0·43	−0·47	−0·41	−0·51	−0·59
a	−0·45	−0·35	−0·30	−0·45	−0·43	−0·31

The values of ρ_1 and ρ_2, given by (5) and (6), were then obtained for each region and for each spectral type. The normal equations (7) were then solved. The details of the solutions are shown in Table IV.

TABLE IV

Final Solutions for the Solar Motion

Spectral Type	X	Y	Z	K	G_0	g_0	U
	km./sec.				°	°	(km./sec.)
B	−17·97	−10·33	−8·58	+4·68	209·9	−22·5	22·43
A	−14·63	− 3·51	−8·18	+0·03	193·5	−28·5	17·13
F	−14·77	− 3·89	−9·68	−0·59	194·8	−32·4	18·08
G	−14·83	− 6·98	−5·25	−0·97	205·2	−17·8	17·21
K	−16·50	− 7·83	−7·30	−0·19	205·4	−21·8	19·67
M	−13·76	−11·65	−8·08	+0·04	220·2	−24·1	19·76
B to M	−16·09	− 7·37	−8·17	+0·84	204·6	−24·8	19·49
A to M	−15·29	− 6·25	−7·65	−0·18	202·2	−24·8	18·20

The effect of the C_z correction is now seen in the value of the normal solar motion (B to M stars). The value (19·5 km./sec.) now found is in good accordance with other determinations based on a large number of stars.

The position (α_0, δ_0) of the apex in equatorial co-ordinates is (267°·0, +32°·0). There is thus a significant increase of about 3° above the mean of previous determinations from radial-velocity measures. The first four lines of Table V are given * by Campbell and Moore (*loc. cit.*) and the fifth line gives our results.

TABLE V

Elements of the Solar Motion

	α_0	δ_0	U	No. of Stars and Data used
	°	°	(km./sec.)	
Charlier	269·3	+30·8	19·0	1986 rad. vel., 4182 p.m.'s and 646 parallaxes.
Strömberg	272·1	+29·5	20·6	1026 space velocities, spectral types A6 to M.
Wilson	270·8	+27·1	19·0	2748 rad. vel., 2305 p.m.'s.
Campbell and Moore	270·6	+29·2	19·65	2149 rad. vel., spectral types B to M.
Smart and Green	267·0	+32·0	19·5	3683 rad. vel., spectral types B to M.
Means	270·0	+29·7	19·55	

The results for each spectral class in Table IV are not quite comparable with the results of Campbell and Moore; our Class B consists of the subdivisions Bo to B9, whereas the B class of Campbell and Moore consists of Oe5 to B5; the respective subdivisions for the other classes are on similar principles.

5. *Probable Errors of the Elements of the Normal Solar Motion.*—We can obtain a fairly approximate idea of the probable errors of the solution for all the stars of Classes B to M as follows. From the normal equations, the weights of X, Y, Z and K are approximately proportional to

$$\sqrt{1350}, \quad \sqrt{1310}, \quad \sqrt{1050}, \quad \sqrt{3683}$$

* A more comprehensive résumé of results is given by Plaskett and Pearce, *M.N.*, **94**, 689, 1934.

respectively, which for simplicity we shall assume to be given by the proportions

$$1, \quad 1, \quad 1, \quad \sqrt{3}.$$

Campbell and Moore give the average residual radial velocity (regardless of sign) for stars of their different spectral classes. Taking the weighted mean, we find that the average residual radial velocity is 12·9 km./sec. The proportion of stars of different spectral types is hardly likely to differ appreciably from the proportion in our statistics, and ignoring the fact that their stars include a small proportion of Class Oe, we take 12·9 km./sec. as the average residual for our stars. As the residuals come theoretically from the independent equations of condition formed for each star separately, the probable error derived from the residual radial velocities is, numerically,

$$\frac{0{\cdot}84 \times 12{\cdot}9}{\sqrt{3683}} \quad \text{or} \quad 0{\cdot}18 \text{ km./sec.}$$

The probable error of either X or Y or Z is, numerically,

$$\sqrt{3} \times 0{\cdot}18 \quad \text{or} \quad 0{\cdot}31 \text{ km./sec.},$$

and the probable error of K is 0·18 km./sec.

We then derive the probable errors of G_0, g_0 and U; the respective values are

$$\pm 1^\circ{\cdot}01, \qquad \pm 0^\circ{\cdot}91 \quad \text{and} \quad \pm 0{\cdot}31 \text{ km./sec.}$$

The probable error of U may be estimated simply from the probable error given by Campbell and Moore, it being assumed that their normal equations are similar to our equations. We should expect our probable errors to be $\sqrt{\frac{2149}{3683}}$ times their value (as our solutions have been made in galactic co-ordinates, only the probable error of U can be found easily in this way). Their probable error for U is ± 0·31, and, applying the factor above, our probable error for U should be ± 0·23 km./sec.

6. *Solutions according to Galactic Latitude.*—Table VI gives the results of solving for the galactic zones 0°, ± 20°, ± 45° separately; the last

TABLE VI

Solutions for Galactic Zones, Types B to M

	Gal. Lat. 0°	Gal. Lat. 20°	Gal. Lat. 45°	Whole Sky
No. of Stars	900	1238	1155	3683
X	−16·21	−17·05	−15·51	−16·09
Y	− 7·68	− 7·69	− 6·49	− 7·37
$\sqrt{X^2+Y^2}$	17·94	18·70	16·81	
Z	...	− 8·39	− 6·01	− 8·17
K	+ 0·62	+ 1·05	+ 1·30	+ 0·84
G_0	205°·3	204°·0	202°·7	204°·6
g_0	...	−24°·2	−19°·7	−24°·8
U	...	20·50	17·85	19·49

column gives, for reference, the solutions for the whole sky already obtained.

So far as the entries in the table can be interpreted, there appears to be no general dependence of the results on galactic latitude, except that the comparatively small value of U for galactic latitude $\pm 45°$ is to be attributed to the small proportion of B stars in this zone ; the counts of B stars in the three zones are 281, 253 and 96 respectively.

7. *Galactic Rotation from the B-Type Stars.*—We now consider the B-type stars separately, inserting in the equations of condition the term depending on galactic rotation. This term is

$$\bar{r}A \sin 2(G - G_1) \cos^2 g,$$

where G_1 denotes the longitude of the centre of the galaxy, A is Oort's constant and $\bar{r}$ is the mean distance of the stars in parsecs. We have taken all the stars of subdivisions Bo to B9 together ; with more radial velocities at our disposal we should have made a subdivision in spectral types, say Bo to B4 and B5 to B9. Thus $\bar{r}$, in our results, applies to the whole range of Class B.

We write

$$\begin{aligned} u &= \bar{r}A \cos 2G_1, \\ v &= \bar{r}A \sin 2G_1, \end{aligned} \tag{9}$$

and

$$\begin{aligned} p &= \sin 2G \cos^2 g, \\ q &= -\cos 2G \cos^2 g. \end{aligned} \tag{10}$$

The equation of condition for a given region, with N_1 stars, is

$$lX + mY + nZ + K + pu + qv = \frac{1}{N_1}\rho_1,$$

its weight being N_1.

Similarly, the equation of condition for the antipodal region, with N_2 stars, is

$$-lX - mY - nZ + K + pu + qv = \frac{1}{N_2}\rho_2,$$

its weight being N_2. The values of ρ_1 and ρ_2 are given by (5) and (6).

The two regions combined contribute to the first normal equation :

$$X(N_1 + N_2)l^2 + Y(N_1 + N_2)lm + Z(N_1 + N_2)ln + K(N_1 - N_2)l + u(N_1 - N_2)lp + v(N_1 - N_2)lq = l(\rho_1 - \rho_2). \tag{11}$$

The contributions to the other normal equations are formed in a similar way, and finally the normal equations are obtained by summing for all the pairs of regions.

Table VII contains the values of the direction-cosines l, m and n for the various regions, and also the quantities p and q defined by (10). The remaining columns of the table refer to the statistics of the B stars in the several paired regions. The regions a, A (last line of the table) are not included in the discussion of the galactic rotation.

TABLE VII

	l	m	n	p	q	N_1+N_2	N_1-N_2	$\rho_1-\rho_2$	$\rho_1+\rho_2$
h	+0·383	−0·924	0	−0·707	+0·707	64	− 4	+ 193	− 44
i	+0·924	−0·383	0	−0·707	−0·707	51	−25	− 759	+ 603
j	+0·924	+0·383	0	+0·707	−0·707	71	−11	−1331	+ 797
k	+0·383	+0·924	0	+0·707	+0·707	95	− 9	−1716	+ 663
e	+0·470	−0·814	−0·342	−0·766	+0·442	20	+ 6	+ 76	+ 63
f	+0·940	0	−0·342	0	−0·884	19	+ 3	− 312	+ 87
g	+0·470	+0·814	−0·342	+0·766	+0·442	30	+12	− 318	− 124
l	+0·470	−0·814	+0·342	−0·766	+0·442	70	+20	− 22	+ 346
m	+0·940	0	+0·342	0	−0·884	77	−53	−1932	+1619
n	+0·470	+0·814	+0·342	+0·766	+0·442	37	− 5	− 799	+ 250
b	+0·365	−0·633	−0·682	−0·433	+0·25	10	+ 2	+ 24	+ 92
c	+0·731	0	−0·682	0	−0·5	17	+ 7	− 188	+ 14
d	+0·365	+0·633	−0·682	+0·433	+0·25	18	+ 4	− 53	+ 76
p	+0·365	−0·633	+0·682	−0·433	+0·25	20	− 6	− 204	+ 69
q	+0·731	0	+0·682	0	−0·5	20	− 8	− 339	+ 104
r	+0·365	+0·633	+0·682	+0·433	+0·25	11	+ 3	− 134	− 17
a	+0·358	0	−0·934	...	...	...	...	...	...

8. The solutions of the normal equations were made separately for the galactic zones 0° and 20° and for the whole sky (with the exception of the areas *a*, *A*). The detailed results are shown in Table VIII. In the last column are the results for the B stars, with rotation neglected, transcribed from Table IV for comparison.

TABLE VIII

Solutions for Solar Motion and Galactic Rotation

	Gal. Lat. 0°	Gal. Lat. 20°	Gal. Lat. 0° to 60°	Whole Sky (without rotation terms)
X	−16·39	−18·58	−17·65	−17·97
Y	−10·80	−10·80	−10·33	−10·33
Z	...	− 7·95	− 6·73	− 8·58
K	+ 4·91	+ 5·02	+ 4·82 (±0·20)	+ 4·68
G_0	213°·4	210°·2	210°·3 (±0°·8)	209°·9
g_0	...	−20°·3	−18°·2 (±1°·5)	−22°·5
U	19·63	22·91	21·53 (±0·34)	22·43
u	+ 2·91	− 1·24	+ 1·45 (±0·32)	...
v	− 3·18	− 2·31	− 2·50 (±0·31)	...
G_1	336°	301°	330° (±3°·0)	...
$\bar{r}A$	4·31	2·62	2·89 (±0·31)	...
$\bar{r}$ (parsecs)	253	154	170	...

The values of the longitude, G_1, of the galactic centre, it will be noticed, differ by 35° for the zones 0° and 20°, although the result for all the zones, namely 330°, is in good agreement with the usually quoted value. It will also be noticed that, for galactic zone 0°, the introduction of the rotational term reduces the amount of the solar motion to equality with that obtained in the normal solution.

Taking A to be 0·017 km./sec. per parsec—the mean of the values given by Oort,* and Plaskett and Pearce †—we obtain the mean distances of the

* *B.A.N.*, **4**, 82, 1927. † *M.N.*, **94**, 679, 1934.

B-type stars of Schlesinger's catalogue ; the results are given in the last line of Table VIII.

The K term remains practically unaltered by the introduction of the rotational term.

In the paper last referred to, Plaskett and Pearce gave as the reason, for the high value (5 km./sec.) of the K term for B-type stars, the inclusion in the statistics of 132 galactic stars between longitudes 210° and 330°. Kapteyn * had noticed, twenty years earlier, that these stars apparently formed an extensive cluster for which he found the convergent. Plaskett and Pearce, redetermining the convergent, place it at R.A. 84°, Dec. −23°, which is but 8° away from their adopted position of the solar antapex. It is not easy to see how a cluster of distant stars spread over 120° of galactic longitude could be maintained against the shearing effect of the galactic rotation. However, supposing that the stars have a common and parallel velocity, V_0, relative to the Sun, and rewriting their equation in the form

$$V_0 \cos \lambda + K = \overline{V}, \qquad (12)$$

where $\overline{V}$ is the mean radial velocity in a region and λ is the angular distance of the centre of the region from the convergent C, it is found from the solution of (1) that $K = 8{\cdot}3$ km./sec. and $V_0 = 15{\cdot}0$ km./sec. It would seem that, in this equation, K must be regarded as a systematic correction to the radial velocities of B-type stars, just as in the ordinary equation of condition for the solar motion. Later, Plaskett and Pearce remove the value (8·3) of K from the stars concerned, and in the subsequent general solution for all the stars round the galactic equator, the K term is found to be 1·1 km./sec., agreeing approximately with their estimate of the relativity correction for the B-type stars. However, this procedure appears to be erroneous.

The "cluster" stars are probably very nearly at rest, as a whole, with respect to the centroid of all the stars observed.

Observatory, Cambridge :
1936 *March* 7.

THE VARIABLE SPECTRUM OF π (52) AQUARII.

William J. S. Lockyer, M.A., Ph.D., Major (late R.A.F.).

The spectrum of the star π (52) Aquarii (H.D. 212571, R.A. $22^h\ 20^m{\cdot}2$, Dec. +0° 52′, 1900, Ptg. Mag. 4·42, Sp. Type B1emnη) has been photographed yearly at the Norman Lockyer Observatory since 1923 August, with the exception of the years 1925 to 1927. This star was included in a special investigation to re-photograph the spectra of the brighter stars of type Be, which P. W. Merrill had photographed in the years 1911 and 1912 with the 36-inch Lick refractor to record any possible changes.

The results obtained from the 1923 and 1924 observations have been previously published.†

* *Ap. J.*, **40**, 43, 1914. † *M.N.*, **84**, 421, 1924; **88**, 693, 1928.

Since 1924 eighty-four more photographs have been secured, and the present communication describes the results that have been obtained from this series.

The available months of observation during a year cover the months July to the following January, both months inclusive, and the programme set out was to secure at least one photograph each month.

All the photographs have been taken with the same instrument as before, namely, the Kensington Prismatic camera of 9-inch aperture and 120 inches focal length, with a 9-inch prism of 45° angle, giving a dispersion of 46·0 mm. between $H\beta$ and $H\delta$.

The chief characteristics of the spectrum of this star are as follows. The hydrogen lines consist of broad absorption bands. Sometimes double and sometimes single bright lines are superimposed on them, and again sometimes no bright lines are seen at all. The neutral helium lines are always strong and nebulous. The [K] line of ionised calcium is moderately strong and very sharp. The ionised magnesium absorption line at λ 4481 is always weak and nebulous. Other bright lines of the ionised metals, similar to those that appear in ϕ Persei or γ Cassiopeiæ, are visible in the best negatives. (See Plate 7.)

The present investigation is devoted entirely to the recorded changes in the appearances of the hydrogen lines, although variations in the intensities of other lines were also noted during the examination of the negatives. The method of determining the difference of intensity between the two bright components (when present) of each of the hydrogen lines was the same as adopted in previous investigations of this kind, namely, by eye estimate with a magnifying glass (× 2).* Thus it was estimated whether the violet component was *equal* to ($V = R$), a *little brighter* than ($V > R(L)$), *brighter* than ($V > R$), *much brighter* than ($V >> R$) and lastly *very much brighter* than ($V >>> R$), the red component. A similar procedure was adopted as regards the red component in relation to the violet, namely, ($R = V$), ($R > V(L)$), etc. In order to simplify the printing of the table figures were adopted to replace the letters, and the resulting notation was as follows :—

R alone	+14	V alone	−14
$R >>> V$	+11	$V >>> R$	−11
$R >> V$	+ 8	$V >> R$	− 8
$R > V$	+ 5	$V > R$	− 5
$R > V(L)$	+ 2	$V > R(L)$	− 2
$R = V$	0	$V = R$	0

In cases where the red (R) or violet (V) components appeared alone the figures (+14) or (−14) respectively were used.

When the bright components of the hydrogen lines were strong they could be observed as far down the spectrum as $H\eta$, but when they were weak they were restricted more or less to the lines $H\beta$, $H\gamma$ and $H\delta$. Estimates were therefore only made throughout on their appearance in those three lines. In the case of some of the negatives, when the bright lines were faint, the

* *M.N.*, **93**, 365, 1933.

estimates for $H\beta$ were not quite so good as those for $H\gamma$ because the sensitiveness of the plates fell off a little to the red side of $H\beta$. Further, the estimates for $H\delta$ were also less trustworthy than those for $H\gamma$, and more so than $H\beta$ under the same conditions because the bright components fell off greatly in intensity towards the violet. Thus the order of procedure in accuracy of the estimates may be stated to be (1) $H\gamma$, (2) $H\beta$ and (3) $H\delta$.

The following table (Table I) contains the estimates for each of the three hydrogen lines mentioned above. In column 1 is given the number of the Sidmouth negative, and in column 2 the year and day and month on which each photograph was taken. Columns 3, 5 and 7 contain the eye-estimate values, and columns 4, 6 and 8 their quality. In columns 3, 5 and 7 blank spaces indicate that the spectrum was not sufficiently dense at the wavelengths of those particular lines to warrant any deduction being made as to details in those lines, and the letters NBL mean that there were "no bright lines" to be seen at all. In columns 4, 6 and 8 blank spaces represent "good" estimates, (M) moderate and (P) poor estimates.

Column 9 is the estimated intensities of the general appearance of the bright lines *as a whole*, using the notation strong (S), weak (W), moderate (M) and very (V). Where the symbol (VW) appears this applies also to the instances when the bright lines are recorded as absent in all three hydrogen lines.

With reference to Table I it should be pointed out that there was no difficulty in determining the estimates of the intensities of the bright lines when they were strong, such as for the years 1923, 1924, 1928 to 1931. In the years 1932, 1933 and 1935 the bright lines were exceedingly faint or not visible at all. It was at first thought that satisfactory photographs of the spectrum in those years were not being secured. This, however, was not the case, for when these photographs were compared with those that contained strong bright lines, the intensity of the continuous spectrum in each case being selected as equal, they still displayed no bright lines. This showed conclusively that the bright lines had faded out.

While the bright lines were strong in the year 1934 it was very surprising to find that the first photographs taken in 1935 showed no bright lines at all. Several extra photographs were taken between July and November but none of them showed any trace of bright lines.

Thus it will be seen from Table I that the bright components of the hydrogen lines gradually diminished in intensity from 1928 to vanishing point in 1933, became prominent again in 1934 and disappeared again in 1935.

All the values given in Table I, with the exception of those for the years 1923 and 1924, are graphically shown in fig. 1. The filled-in circles represent the "good and moderate" estimates and the open circles "poor" estimates, each of them being the mean value derived from the negatives secured during any one month.

The scales on the left show the original method of making the eye estimates, and those on the right the corresponding figures adopted. The scale of years is given at the top and bottom, subdivided into months, and

each monthly mean value is plotted exactly underneath each subdivision, the vertical lines representing the month of January.

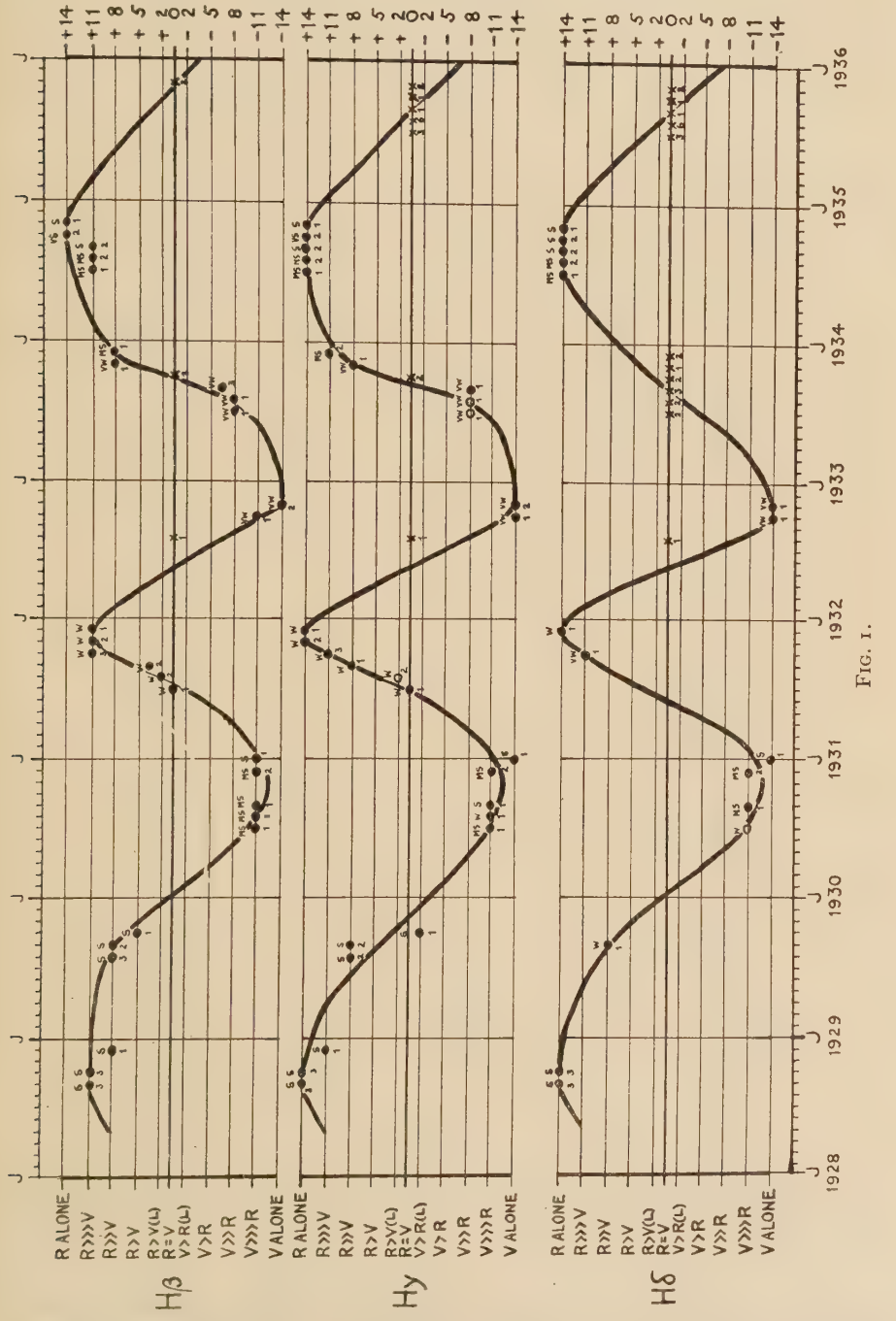

Fig. 1.

Each monthly mean has, printed above it, the mean intensity of the bright lines taken from column 9 in Table I and, below it, the number of estimates

TABLE I

Neg. No.	Year and Month	Hβ E	Hβ Q	Hγ E	Hγ Q	Hδ E	Hδ Q	Int. Br. L.
1	2	3	4	5	6	7	8	9
	1923							
323	Aug. 5	0		...		...		S
328	,, 7	0		− 2		− 2		S
367	Sept. 16	− 5		− 5		...		VS
	1924							
462	July 26	− 5	M	− 5		− 8	M	MS
467	Aug. 7	− 8	M	−11		−11		MS
481	,, 20	−11	P	...		...		MS
484	,, 25	−11	P	−11		− 8	P	MS
	1928							
1057	Sept. 4	+11		+14		+14		S
1064	,, 6	+11		+14		+14		S
1079	,, 20	+11		+14		+14		S
1090	Oct. 5	+11		+14		+14		S
1104	,, 21	+11		+14		+14		S
1106	,, 30	+11		+14		+14		S
1134	Dec. 14	+ 8		+11		...		S
	1929							
1236	Aug. 2	+ 8	P	+11	P	...		S
1237	,, 2	+ 8	M	+ 8	P	...		MS
1246	,, 25	+ 8	M	...		...		MS
1258	Sept. 2	+ 8		+ 8		+ 8		S
1266	,, 6	+ 8		+ 8		...		S
1313	Oct. 31	+ 5		+ 2		...		S
	1930							
1411	July 8	−11	M	−11	M	−11	M	MS
1438	Aug. 30	−11		−11	M	...		MS
1457	Sept. 27	−11		−11		−11		MS
1499	Dec. 8	−11		−11		−11		S
1505	,, 21	−11		−11		−11		MS
	1931							
1520	Jan. 9	−11		−14		−14		S
1636	July 9	0		0	M	...		W
1647	Aug. 16	+ 2	M	+ 2	P	...		W
1650	,, 17	+ 2	M	+ 2	P	...		W
1659	Sept. 5	+ 2	M	+ 8	M	...		W
1674	,, 11	+ 5	M	...		...		VW
1679	Oct. 7	+11		+11		+11	M	W
1683	,, 11	+11		+11		...		VW
1709	,, 30	+11		+14		...		W
1719	Nov. 12	+11		+14		...		W
1720	,, 14	+11		+14		+14		MW
1728	Dec. 7	+11		+14		+14		MW
	1932							
1827	Aug. 31	...		NBL		NBL		VW
1838	Oct. 1	...		NBL		NBL		VW
1841	,, 3	− 5		NBL		NBL		VW
1857	,, 31	−11		−14	M	−14	M	VW
1865	Nov. 21	...		−11	M	−11	M	VW

Neg. No.	Year and Month	*Hβ* E	*Hβ* Q	*Hγ* E	*Hγ* Q	*Hδ* E	*Hδ* Q	Int. Br. L.
1	2	3	4	5	6	7	8	9
	1932							
1866	Nov. 26	−14	P	−11	P	...		VW
1867	,, 28	−14		−14		−14		VW
	1933							
1993	July 22	− 8	M	− 8	M	...		VW
1994	,, 24	...		− 8	P	...		VW
1996	,, 26	...		NBL		NBL		VW
2002	Aug. 14	...		NBL		NBL		VW
2004	,, 16	− 8	M	− 8	P	NBL		VW
2001	,, 21	NBL		NBL		NBL		VW
2013	,, 23	...		NBL		NBL		VW
2017	,, 25	NBL		NBL		NBL		VW
2033	Sept. 9	− 8	M	− 8	M	NBL		VW
2035	,, 13	− 5	M	NBL		NBL		VW
2037	,, 14	− 5	M	NBL		NBL		VW
2043	,, 20	NBL		NBL		NBL		VW
2064	Oct. 8	...		NBL		...		VW
2076	,, 16	NBL		NBL		NBL		VW
2091	Nov. 12	+ 8		+ 8	M	...		VW
2098	,, 17	...		NBL		NBL		VW
2108	Dec. 9	...		+11	M	NBL		MS
2115	,, 14	+ 8		+11		NBL		MS
	1934							
2255	July 21	+11		+14		+14	M	MS
2263	Aug. 13	+11		+14		+14	P	MS
2265	,, 14	+11		+14	M	+14	P	MS
2273	Sept. 1	+11		+14		+14		MS
2274	,, 4	+11		+14		+14		S
2287	Oct. 3	+14		+14		...		VS
2289	,, 5	+14		+14		+14		S
2304	Nov. 1	+14		+14		+14		S
	1935							
2430	July 30	...		NBL		NBL		VW
2442	Aug. 9	...		NBL		NBL		VW
2448	,, 19	...		NBL		NBL		VW
2450	,, 20	...		NBL		NBL		VW
2458	Sept. 7	...		NBL		NBL		VW
2482	Oct. 29	...		NBL		NBL		VW
2488	Nov. 17	NBL		NBL		NBL		VW
2489	,, 18	NBL		NBL		NBL		VW

of which it is the mean. Where the photographs exhibited *no bright lines*, these are indicated by crosses placed on the horizontal line $V = R$, and below them the number of negatives used to form the mean. The reason why these crosses were placed in this $V = R$ line was because it seemed that they fell in place at the time when the bright components should be of about equal intensity.

For each of the three hydrogen lines smooth curves were drawn through

the mean estimate values to satisfy, as far as possible, the observations in each case. It will be seen that all the curves are of a very similar nature, having maxima towards the latter half of the years 1928, 1931 and 1934, and minima about the latter part of the years 1930 and 1932. It has been stated previously that the estimates for $H\gamma$ were considered to be more accurate than those for the other lines, so that the curve for this line would be the most appropriate for finding the epochs of maxima and minima for the determination of the period of variation.

Taking the dates of the maxima first those are, as near as can be determined, 1928 October 1, 1931 December 1 and 1934 September 15, which correspond to the Julian day numbers 2425521, 2426677 and 2427696 respectively. The intervals between the consecutive maxima are therefore 1156 and 1019 days, the mean being 1087·5 days. In the case of the two minima their dates are approximately 1930 November 15 and 1933 February 15, corresponding to the Julian day numbers 2426296 and 2427119 respectively. The interval between them is thus 823 days.

The last-mentioned interval from minimum to minimum is very much less than that between the maxima, indicating that the period of variation for these years is by no means regular.

While it is not necessary to refer here to the very early observations of this star, it may be of interest to draw attention to the bibliographical and observational record, from the date of its discovery as a bright-line star by Miss Maury in 1890 down to the year 1929, which has been published by Charles D. Higgs * in 1930.

The first statement regarding a period assigned to this star was given by R. H. Curtiss † in 1925 from observations made at Ann Arbor, who listed this star as a ϕ Persei variable with a period of 2000 days. Later on, in 1929, he revised ‡ this period to 2700 days. In both cases the variation was obtained from the changes in the relative intensity of the two bright components of the hydrogen lines.

In 1930 Higgs § made a study of some of the Lick Observatory negatives. These negatives were very few in number, amounting to only thirteen between the years 1915 to 1930. The conclusions he came to were that the attempts to correlate the separations of the bright components of the hydrogen lines or their radial velocity shifts, with the variations in relative intensity, or to establish a period for the latter, proved futile.

Higgs, however, drew attention to the fact that the type of variability of the relative intensity of the bright hydrogen components in the years 1928 and 1930 was very different from that in the years 1915 and 1919. This star had been under observation at Sidmouth during the years 1925, 1929 and 1930, and I pointed out ‖ that my observations corroborated those of Higgs for the years 1928 and 1930, but no data were available at Sidmouth for the previous years, with the exception of 1923 and 1924, to show that any radical changes had occurred.

Since the above observations were published three papers have appeared

* *Ap. J.*, **72**, 190, 1930. † *Pop. Ast.*, **33**, 537, 1925.
‡ *Pop. Ast.*, **37**, 579, 1929. § *Ap. J.*, **72**, 187, 1930. ‖ *Ap. J.*, **73**, 55, 1931.

by Dean B. McLaughlin * discussing observations made at Ann Arbor between 1924 and 1932. He states that the values for the relative intensities of the bright hydrogen components of $H\beta$ and $H\gamma$ "appeared to follow a curve with steep rise and gentle decline with a period of about 1900 days." It may be mentioned here that there is a gap in the observations extending from 1926 December to 1928 August. He mentions further that the plates taken in 1931 "showed that the period of 1900 days was not being followed at all."

In the third of the papers mentioned above he states: "Plates taken in 1932 gave still another surprise and forced the writer to conclude that probably π Aquarii is purely irregular in its variations." In his paper he publishes curves for the emission ratios of $H\beta$ and $H\gamma$ for the years 1925 to 1932. That portion of the curve for the years 1928 to 1932 agrees very closely with the Sidmouth curves.

The only prior Sidmouth observations relate to the years 1923 and 1924, which suggest a rapid decline in 1923 August and September to a minimum in 1924 August. If those were the only available observations made between 1923 and 1928, then they would indicate that possibly another maximum occurred in the latter part of 1925 followed by a minimum in 1927. Thus my curves for the years 1928 to 1935 could be extended backwards to the year 1923 with a period of about the same order of magnitude.

The observations made at Ann Arbor in 1925 and 1926 rule out, however, the suggested maximum in 1925 and possibly the suggested minimum in 1927.

It has been pointed out previously that the bright hydrogen components gradually diminished in intensity from 1928 to vanishing point in 1933, became prominent again in 1934 and disappeared again in 1935.

The disappearance of bright lines in Be-type stars has been noticed before, and Curtiss,† as long ago as 1923, showed that the evidence then available indicated that such stars eventually lose their emission lines and become normal stars of class B. The reappearance of emission in f^1 Cygni caused him ‡ to raise the question whether any of these stars permanently lose their emission.

McLaughlin § gives an interesting table of numerous Be-type stars showing the behaviour of the intensities of the bright hydrogen components before and after the year 1921. This indicates how the bright components wax or wane but not necessarily disappear. He is inclined to the view that "changes in total intensity of the emission lines are cyclic in character."

Merrill, Humason and Burwell ‖ raised the question "whether a B-type star can pass into the bright-line stage more than once." In the case of π Aquarii this question can be definitely answered in the affirmative.

Another Be-type star which has been, and still is, under observation at Sidmouth since the year 1923 is H.D. 20336.¶ This star has always been

* *Pub. Obs. Univ. Michigan*, **4**, 37, 1931; **4**, 190, 1932; *Ap. J.*, **77**, 221, 1932.
† *Pub. Obs. Univ. Michigan*, **3**, 2, 1923.
‡ *M.N.*, **88**, 205, 1928.
§ *Pub. Obs. Univ. Michigan*, **4**, 196, 1932.
‖ *Ap. J.*, **61**, 415, 1925.
¶ *M.N.*, **91**, 215, 1930.

noted for the great intensity of the bright hydrogen components, according to the Sidmouth observations dating from 1923. These lines have now become so reduced in intensity that at the present time (1935) they are scarcely visible.

Summary

(1) A discussion of 81 photographs of the spectrum of π Aquarii taken between 1928 September 4 and 1935 November 18.

(2) The variations between the relative intensities of the bright components of the hydrogen lines, *during this interval*, suggest a *mean* period of about 1087 days, but the period is not constant.

(3) There is evidence to indicate that this mean period was probably not in operation immediately prior to the year 1928.

(4) There are times when these bright hydrogen components disappear entirely.

(5) Brief references are made to the work of other observers.

DESCRIPTION OF PLATE 7

This plate illustrates the spectrum of π Aquarii when the bright components of the hydrogen lines were both absent and present.

No. 1. A comparison spectrum of γ Orionis.

No. 2. Negative No. 1079, 1928 September 20, showing the bright components in π Aquarii.

No. 3. Negative No. 2076, 1933 October 16, showing no bright components in π Aquarii.

The spectra have been enlarged twice and broadened with the clepsydra apparatus.

Norman Lockyer Observatory,
Sidmouth.

CENTRE TO LIMB VARIATION IN FRAUNHOFER LINE INTENSITY OVER THE DISC OF THE PRIMARY STAR OF U CEPHEI AND OF U SAGITTÆ.

R. O. Redman, M.A., Ph.D.

Summary

An attempt has been made by means of spectrographic observations during eclipse to detect changes of Fraunhofer line intensity from centre to limb of the primary component in each of the Algol systems, U Cephei and U Sagittæ. Corrections to the observed line intensities are required on account of the superposition of the secondary spectrum, and these corrections become rather large during the important phases near totality. However, the uncertainties thus introduced do not seem sufficiently great to affect the essential nature of the result that in the principal star

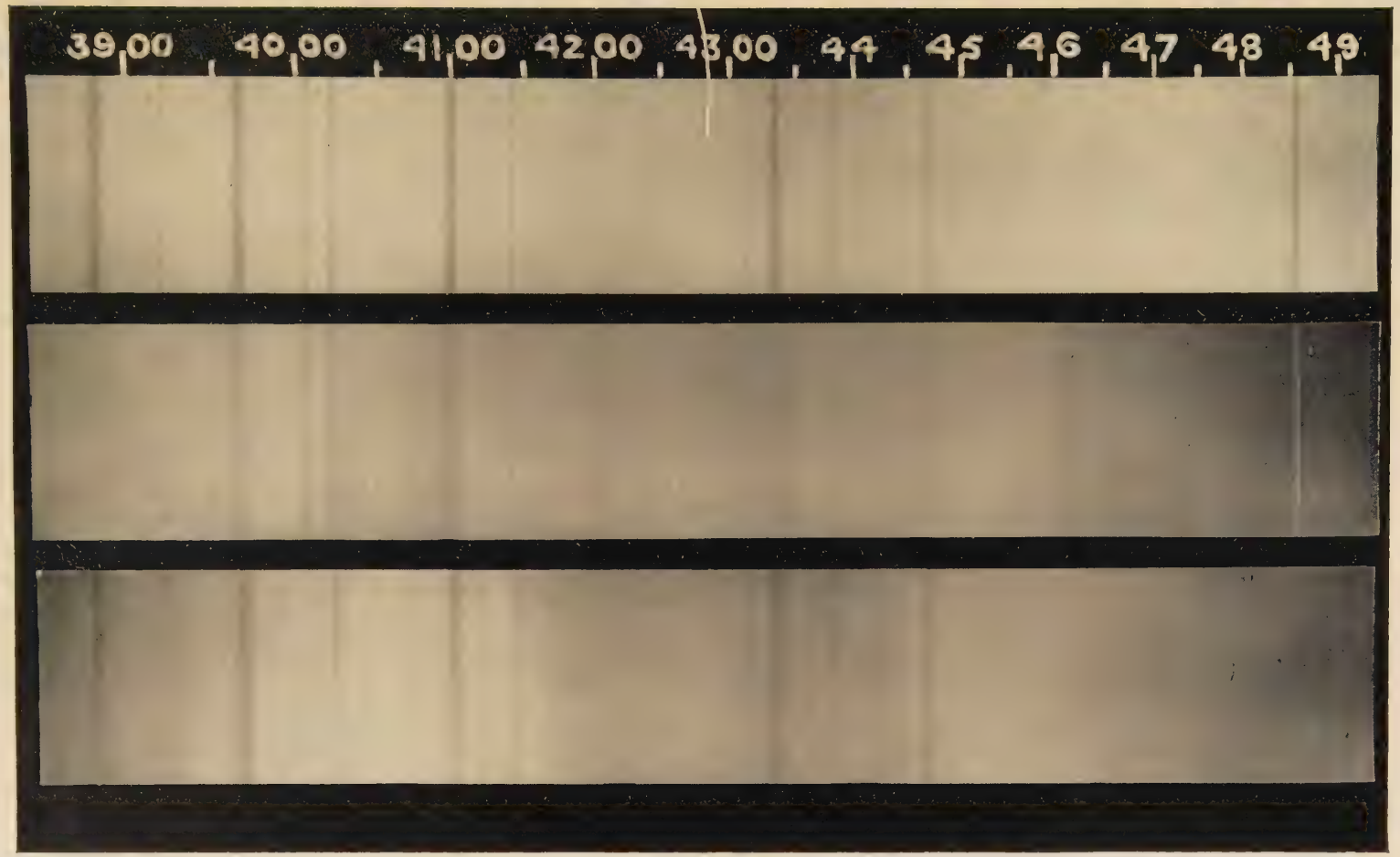

W. J. S. Lockyer The Variable Spectrum of π (52) Aquarii.

of U Cephei, spectral type Ao, the hydrogen Balmer lines behave as though they vanish at the limb, while in U Sagittæ, type B9, there is a definite fall in intensity from centre to limb. In the case of fainter lines, such as H (blended with $H\epsilon$) and K of ionized calcium, the measures were not sufficiently accurate to lead to any definite conclusion.

Introduction

Perhaps the most powerful observational test at present available for the theories of stellar atmospheres is that in which we study the variations of continuous or line spectrum when the star's surface is viewed at different angles. The angle between the line of sight and the normal to the surface is conventionally denoted by θ, and by observing, for instance, the disc of the Sun at points from centre to limb we may obtain the required data for all angles $\theta = 0°$ to $90°$. This type of observation is unfortunately only possible in the case of the Sun. We are unable to see any of the stars as discs in any existing telescope ; still less can we study the light from selected points of a star's disc by direct observation. Up to the present, therefore, we have been obliged to assume that results obtained from the Sun apply also to all stars.

Although the direct method is as yet impossible, it seems feasible to derive a certain amount of valuable information from measures of the spectrum changes shown by Algol variables during eclipse. These stars are close doubles in which, as viewed from the Earth, one component periodically eclipses the other. In most cases there is partial eclipse only, but in a relatively small number there is total eclipse. By careful observation of the light-curve it is possible to deduce the photometric orbit, which gives, *inter alia*, the size of each star in terms of their separation, the ratio of their surface brightnesses, and the eccentricity and inclination of their relative orbit. In the best conditions it is also possible to deduce whether the primary star is appreciably darkened to the limb. With this information in hand we can compute what part of the primary disc is visible at any phase of eclipse, and were we to know everything about the spectra of primary and secondary stars we could predict the exact appearance of the composite spectrum to be seen at any moment in terrestrial telescopes. To some extent it is possible to follow the reverse procedure, to disentangle primary and secondary spectra and deduce what would be seen in the ideal case when the secondary is perfectly non-luminous. Then, knowing the parts of the primary disc from which this spectrum has come, we can say something of the behaviour of the absorption lines between centre and limb.

In actual practice this method is not easy. We have selected for trial the two favourable cases U Cephei and U Sagittæ. These each consist of a relatively small primary star of high surface luminosity which is accompanied and from time to time totally eclipsed by a large secondary star of much lower surface brightness. The trouble arising from the presence of the secondary star's spectrum is then minimized, although by no means eliminated. The secondary spectrum, indeed, creates one of the two chief

difficulties of the work. The other is that each system, none too bright at maximum, fades in the course of a few hours of partial eclipse to something of the order of one-tenth of its original luminosity. At minimum both are fainter than 9th magnitude, while spectrograms have to be obtained with exposures not too long to blur the comparatively rapid changes which are taking place. In or near totality a small dispersion spectrograph has to be used which gives only comparatively low accuracy in the final results. Naturally it is quite impossible to measure the changing *profile* of the spectrum lines, as is done in solar work, and all we can hope for is information concerning the behaviour of the total intensity of the stronger lines of the spectrum between centre and limb of the primary star.

Before turning to the actual observations it may be well to mention briefly what kind of variation from centre to limb may be expected. From the theoretical standpoint there are two limiting cases :—

(*a*) The Fraunhofer line is formed by *pure scattering*, *i.e.* the atoms of the star's atmosphere emit every light quantum at the same frequency as that at which it is absorbed, atomic collisions are neglected, and there is no exchange between radiation energy and kinetic energy of atomic and electron translatory motion in the atmosphere. In this case the usual approximate solutions of the problem show that there is no change of line intensity between centre and limb.

(*b*) The line is formed by *pure absorption*, *i.e.* the atoms of the atmosphere absorb light quanta of frequencies in the neighbourhood of the line, and all the absorbed energy is converted into kinetic energy of translation by means of atomic collisions, being re-emitted subsequently anywhere in the continuous spectrum. In this case the approximate solutions show that absorption lines vanish entirely at the limb.

In the case of the Sun we have an intermediate state of affairs. Observations such as those of H. H. Plaskett show that both scattering and absorption are at work, and a model atmosphere in which both are taken into account predicts the actual variation of line profile from centre to limb better than either the pure scattering or the pure absorption model. The line profile is denied us in the stellar work under consideration and we must be content with the total line intensity. In the magnesium *b* lines of the solar spectrum Plaskett's measures * show an intensity variation, centre to limb, roughly one-half that given by the pure absorption model, and in default of other evidence we may look for a change of this order in the case of a star.

Observations

Thanks to the kindness of Dr. J. S. Plaskett, then Director of the Dominion Astrophysical Observatory, the writer was allowed to use the 72-inch reflector at Victoria during 1934 August and September, on 10 fine nights when U Cephei and U Sagittæ were at suitable phases. The first five nights were spent at the Newtonian focus with the slitless spectrograph recently designed by Dr. F. S. Hogg. This instrument has the great

* *M.N.*, **91**, 870, 1931.

advantage of very high speed ; indeed it is almost too fast for this work. Its chief disadvantage is that it has a very small dispersion, 136 A./mm. at $H\gamma$. Also, it needs some experience in manipulation if the best results are to be obtained, and a certain amount of time was spent in getting used to it. The best plates were obtained on the night of August 13, when Dr. Helen Hogg very kindly assisted. With her help a good series of spectrograms of U Cephei was obtained, running up to totality. The spectra were broadened by trailing the telescope in right ascension with the slow-motion buttons, the mechanical device designed for broadening being more suitable for fainter stars. Backed Eastman 33 or Eastman 40 plates were used, calibration and development being carried out as described below for the slit spectra.

After August 17 it was decided to use the Cassegrain slit spectrograph in its one-prism arrangement. The collimator is of 45 inches focal length and feeds a $2\frac{1}{2}$-inch prism, the beam from which may be photographed with any one of four interchangeable cameras. Of these, three were used, viz. IM, focal length 28 inches, dispersion 30·1 A./mm. at $H\gamma$; IS, $16\frac{1}{2}$ inches, 50·8 A./mm. ; ISS, 9 inches, 92·3 A./mm. Generally observations were started with the IM camera, with which very good strong spectrograms could be obtained in $1\frac{1}{2}$ to 2 hours (slit width 0·1 mm.) when either star was at or near maximum light. Then, with partial eclipse well in progress, a change was made to the ISS camera as rapidly as possible. The average time occupied from the conclusion of an exposure with the longer camera to the start of the next exposure with the short camera, including taking a focus plate with the latter, was 26 minutes, the operation being done single-handed on three out of five occasions. As the star became fainter the slit width was increased, up to a maximum of 0·2 mm. Backed Eastman 40 plates were used throughout. Totality in the case of U Cephei lasts about 2 hours and in the case of U Sagittæ about 100 minutes, which with a wide slit allowed fairly well-exposed photographs of both secondary spectra to be obtained entirely free of light from the primary. The wide slit, although it might be undesirable for radial velocity work, is unobjectionable when the plates are being used for determining line intensities. The lines may be widened, but their total intensities are unaffected.

Details of those of the plates which have been measured are to be found in Table I. Owing to its high declination and more favourable period, a much more complete set of observations was obtained for U Cephei than for U Sagittæ.

The plates on which both slit and slitless spectrograms were obtained were standardized for photometric purposes, using an auxiliary spectrograph with a neutral-tint glass wedge over its slit. The times of exposure in this spectrograph were arranged to be around 0·1 to 0·2 of the whole exposure time at the telescope. Development was carried out in M-Q, the plates being brushed throughout.

All the slit spectrograms and a selection of those taken on the slitless instrument were measured with the self-recording microphotometer at the Solar Physics Observatory, Cambridge, and total intensities were derived

for as many lines as possible, following the usual methods. In the plates of IM dispersion, where only the primary spectrum is visible, it was possible to measure the prominent hydrogen lines $H\beta$, $H\gamma$, $H\delta$, $H\epsilon$ and $H\zeta$, the helium lines $\lambda\lambda$ 4471 and 4026, the ionized magnesium line λ 4481, and the ionized calcium K line. Other lines, such as *Si*II $\lambda\lambda$ 4131 and 4128, *He* $\lambda\lambda$ 4922, 4388, were usually also visible but unsuitable for measurement. With the smaller dispersions conditions become much less favourable on account of plate grain, and with the ISS plates attention had to be confined to K and the hydrogen series. The H line and $H\epsilon$ are blended. Outside eclipse the hydrogen completely swamps the calcium line, while during totality the opposite is the case. With so many unfavourable factors, wide

TABLE I

Spectrographic Observations of U Cephei and U Sagittæ

U Cephei (Slit Spectrograph)

Plate No.	Julian Date	Phase of Star	Camera	Slit	Exposure Time
		d		mm.	minutes
23338	2427668·879	−0·105	ISS	·075	30
39	·910	−0·074	ISS	·100	50
40	·949	−0·035	ISS	·150	60
41	·987	+0·003	ISS	·150	46
62	673·733	−0·237	IM	·100	120
63	·804	−0·166	IM	·150	84
64	·860	−0·110	ISS	·075	30
65	·881	−0·089	ISS	·100	30
66	·905	−0·065	ISS	·150	36
67	·939	−0·031	ISS	·150	60
68	·984	+0·014	ISS	·150	54
69	678·717	−0·239	IM	·100	120
70	·792	−0·164	IM	·175	70
71	·844	−0·112	ISS	·075	30
72	·867	−0·089	ISS	·100	30
73	·896	−0·060	ISS	·150	50
74	·956	0·000	ISS	·150	120
415	693·740	−0·173	IM	·150	30
41	698·724	−0·175	IM	·100	120
42	·788	−0·111	ISS	·100	34
43	·813	−0·086	ISS	·100	40
44	·843	−0·056	ISS	·150	44
45	·901	+0·002	ISS	·200	120
46	·969	+0·070	ISS	·200	60
47	699·005	+0·106	ISS	·150	40
48	·029	+0·130	ISS	·100	26
76	704·800	+0·915	IS	·038	120
77	·857	+0·972	IS	·075	40
78	·881	+0·996	IS	·075	30
79	·899	+1·014	IS	·075	20
80	·936	+1·051	IS	·075	60

U Cephei (Slitless Spectrograph)

Plate No.	Julian Date	Phase of Star	Exposure Time *
		d	minutes
23287	2427663·811	−0·187	2
88	·821	−0·177	5
89	·828	−0·170	5
91	·851	−0·147	10
92	·860	−0·138	10
93	·872	−0·126	10
94	·883	−0·115	10
95	·894	−0·104	10
98	·927	−0·071	9
99	·938	−0·060	12
300	·949	−0·049	12
01	·963	−0·036	16
02	·979	−0·019	20

* The exposure times do not give a fair indication of the speed of the slitless spectrograph, since most of the spectra were made very broad.

U Sagittæ (Slit Spectrograph)

Plate No.	Julian Date	Phase of Star	Camera	Slit	Exposure Time
		d		mm.	minutes
23416	2427694·681	−0·178	IM	·100	90
17	·739	−0·120	ISS	·075	26
18	·763	−0·096	ISS	·100	40
19	·800	−0·059	ISS	·150	60
20	·860	+0·001	ISS	·200	100
73	704·659	−0·342	IS	·050	60
74	·701	−0·300	IS	·075	60
75	·737	−0·264	IS	·075	40

slit, small dispersion, coarse plate grain and a fuzzy primary spectrum, it was quite impossible ever to separate the two, and the blend was always measured as one line.

Errors of Measurement

A number of plates were measured twice, and the scatter between individual measures of the same plate showed an average error per line of about 10 per cent. Experience with the microphotometer in other work has shown it to be reliable to a much greater accuracy than this, so that most of the error must be attributed to variations in the position assigned to the continuous background and to uncertainties arising from irregular plate grain. The real errors of the individual measures are presumably greater than 10 per cent., especially near totality, while the weaker lines at all phases probably have greater errors than this. Indeed we shall see later that

observational errors made it impossible to derive any conclusion from the K line intensities, so that ultimately only $H\beta$, $H\gamma$ and $H\delta$ could be relied on.

Systematic errors are to be viewed with more concern than accidental errors. It seems safe to assume as negligible one particular source of systematic error, viz. a possibly erroneous calibration of the wedge. The writer took a small part in some of the earlier work of calibration, but the

TABLE II

Measured Line Intensities

The intensity unit is 1 A. complete absorption of the continuous spectrum

Exposures * lie outside eclipse
,, † lie within totality

U Cephei (Slit Spectrograph)

Phase	Camera		Intensities							
			$H\beta$	$H\gamma$	$H\delta$	$H\epsilon$+H	$H\zeta$	K	λ 4471	λ 4481
−0·239	IM	*	9·4	7·4	7·6	8·5		1·4	0·7	0·8
·237	IM	*	8·4	8·0	7·2	7·3	8·7	1·2	0·6	0·6
·175	IM		6·3	7·5	7·2	7·9	6·9	1·2	0·7	0·6
·173	IM		7·7	7·8	7·7				0·4	0·5
·166	IM		7·8	8·7	7·3	9·5	8·0	1·4	0·6	0·9
·164	IM		8·8	8·1	8·8	8·1		1·2	0·6	0·7
·112	ISS		6·0	6·3	6·6	13·2		2·0	0·6	0·4
·111	ISS		6·5	7·0	6·9		4·8		0·7	0·6
·110	ISS		7·8	6·2	6·3	8·6	7·6	2·0	0·4	0·7
·105	ISS		6·3	5·9	6·0	7·5	7·0	1·6	0·5	0·6
·089	ISS		5·5	6·3	5·7	8·2		3·8	0·2 :	0·6 :
·089	ISS		3·9	5·4	5·5	7·5	4·9	1·7	0·4 :	0·7 :
·086	ISS		4·6	4·4	3·4	6·9		2·4	0·6	0·7
·074	ISS		4·8	4·9	4·1	7·3		1·8	0·7 :	1·4 :
·065	ISS		1·9	4·0	2·7	9·5		6·6	0·7 :	0·3 :
·060	ISS		3·0	2·4	2·4	7·7		3·2		
·056	ISS		3·1	1·7	5·3				0·4 :	0·5 :
·035	ISS		2·3	2·0	1·8					
−0·031	ISS		4·3	3·0	1·6					
·000	ISS	†	2·4	2·4	1·9					
+0·002	ISS	†	2·7	1·9	1·8					
·003	ISS	†	2·3	1·9	1·6					
·014	ISS	†	2·7	2·6						
·070	ISS		5·8	5·9	5·8	8·7	7·9	2·2		
·106	ISS			7·7	9·9	7·5	7·8	0·9		
·130	ISS		8·8	7·1	6·2	9·9	8·7	1·3	0·7	0·5
·915	IS	*	7·1	8·2	7·8	10·1	7·5	1·4	0·4	0·8
·972	IS	*	6·9	7·6	8·9	8·5	8·1	1·3	0·7	0·9
·996	IS	*	5·7	8·3	8·2	9·1	9·1	1·1	0·5	0·9
1·014	IS	*	6·4	7·8	7·3	10·0		1·7	0·5	0·4
+1·051	IS	*	6·2	6·9	10·5	9·4	12·1	1·2	0·8	1·0

U Cephei (Slitless Spectrograph)

Phase		Intensities				
		Hγ	*Hδ*	*Hε* +H	*Hζ*	K
−0·187		6·9	7·2	8·7	6·0	1·5
·177		7·7	6·0	8·9	6·9	1·3
·170		6·0	6·6	8·0	7·0	1·6
·147		7·9	7·8	8·1	7·2	1·3
·138		7·8	6·7	7·6	6·8	1·3
·126		7·4	6·6	7·4	7·2	1·1
·115		6·5	7·2	7·2	5·5	1·4
·104		6·9	7·0	8·8		2·3
·071		1·9	3·0	6·1	3·0	4·9
·060				9·1		8·7
·049				10·0		13·7
·036				12·9		13·2
−0·019	†			10·3		13·1

U Sagittæ (Slit Spectrograph)

Phase	Camera		Intensities					
			Hβ	*Hγ*	*Hδ*	*Hε* +H	*Hζ*	K
−0·342	IS	*	11·1	8·9	9·9	9·3	7·9	0·8
·300	IS	*	9·5	8·2	9·0	9·4	10·0	1·3
·264	IS	*	8·5	8·7	9·8	10·0		0·6
·178	IM		10·1	8·7	8·1	10·0	9·3	0·9
·120	ISS		7·8	7·1	7·0	9·4	10·3	2·2
·096	ISS		9·5	9·5	7·3	9·2		3·2
−0·059	ISS		6·6	4·9	3·7	8·9		7·8
+0·001	ISS	†	5·2	3·0	3·2			

wedge constants here used depend practically entirely on measures made by Dr. C. S. Beals. The internal consistency of his measures show a high order of accuracy, and comparison of some of his observations based on this wedge with observations of other workers have failed to show any definite signs of systematic error. In the present work we are not aiming at a very high order of accuracy, so that we are justified in neglecting the calibration errors.

A more likely source of appreciable systematic error is to be sought in the changes from one dispersion to another. Owing to the limited time available for work at Victoria it was not possible to undertake observations to check this point. *A priori* one would not expect the error to be very big, and inspection of Table II, comparing measures taken at nearby phases

with IM and ISS cameras, suggests that any systematic error in the hydrogen lines does not exceed 10 per cent., a quantity which can be neglected in view of the final results. Another possibility is that some systematic error, as between strong lines, such as the hydrogen lines outside eclipse, and fairly weak lines, such as those of hydrogen at or near totality, may arise on account of plate grain. No check is available at this point, but the error would have to be very big to invalidate our results.

The stellar spectra are broadened by trailing the star image, giving intermittent exposure on the plate, while the standardizing exposures are continuous. It was for this reason that the total exposure time was made shorter on the standardizing spectrograph. In common with most workers in stellar spectrophotometry we have neglected any error which may arise from this variation in the character of the illumination of the plate. A few tests made at the Solar Physics Observatory suggest that the effect is small, and in any case it seems reasonable to suppose that were large errors caused by this method of procedure they would have been detected and commented on before now. Errors of the order of 1 per cent. or less need not concern us here.

Finally, there seems to be a systematic difference between slit and slitless measures, the latter giving smaller intensities (see fig. 1). This is what might be expected on account of the better definition obtained with a slit and perhaps on account of the very small dispersion of the slitless spectrograms. Although some error of this kind may be present, and not many slitless spectrograms have been employed in this paper, it must not be concluded that a slitless spectrograph is unsuitable for this kind of work. The experiments with the slitless instrument at Victoria were very encouraging, even though not very fruitful, and its great speed was undoubtedly a big advantage.

Physical Properties of U Cephei and U Sagittæ

For the reduction of the line intensities we need to know the dimensions, spectra, etc., of the individual components, so that this section is devoted to a summary of the relevant material, together with other information which should be borne in mind when the final results of the work are considered.

U Cephei.—The period is 2·49 days. There are photometric orbits by Dugan * and by Fetlaar,† and a spectroscopic orbit by Carpenter.‡ The system is abnormal in several respects :

(i) The period is slightly variable and is at present lengthening slowly.

(ii) There is a very serious discrepancy between the photometric and spectroscopic orbits ; in the former the orbital eccentricity is 0, in the latter it is 0·474.

(iii) There is a difference of some hours between the time of conjunction of the two stars as indicated by the spectroscopic work and that given by the light-curve.

* *Princeton Contributions*, 5, 1920. † *B.A.N.*, 3, 195, 1926.

‡ *Ap. J.*, 72, 205, 1930.

(iv) Principal minimum is not perfectly symmetrical, showing a steeper rise than fall. According to Dugan's work the components are flattened, there is a tidal lag and the different sides of the stars are of unequal brightness.

The light range is $6^{m}.85$ to $9^{m}.19$ and eclipse lasts approximately 10 hours, with about 2 hours of totality.

For our work we have neglected all complications and have assumed the following orbital elements, representing to some extent a compromise between Dugan's and Fetlaar's results :—

Time of principal minimum * J.D. 2424253·6622 + 2·492936 E.
Eccentricity of orbit 0.
Inclination „ „ 86°·4.
Radius of larger star 0·32.
„ „ smaller star 0·20.
Coefficient of darkening to limb (primary) $u = 2/3$.
Ratio of surface brightness of two stars (visual) 15.

The primary spectrum is of type A0, with extremely nebulous lines. Apart from the superposition of secondary spectrum, type K0, upon the primary, clearly visible during the more advanced stages of eclipse, nothing abnormal has been detected on the plates, although earlier observers have suggested slight peculiarities in the spectrum. The secondary spectrum seems to be that of a normal giant. The photographs taken at minimum suggest that the lines are not wider than would be caused by the wide slit, together with plate grain. (The geometrical image of slit on plate was 0·04 mm. wide, 3·7 A. at $H\gamma$.) Rotational broadening of the lines is certainly not greater in the secondary than in the primary.

An attempt was made to discover faint lines in the primary spectrum by means of microphotometer tracings taken with wide slit and high sensitivity, a method which has proved successful at the Solar Physics Observatory with nebulous lines in spectrograms of larger dispersion. It was thought at first that a number of new lines had been revealed, but suggested identifications gave one little faith in their reality. On one or two plates it was suspected that the K line was multiple, but this cannot be put at more than a suspicion and needs confirmation. A multiple K line during partial eclipse would not be surprising, as there may be a faint interstellar component and possibly one due to the primary star shining through the atmosphere of the secondary, as well as the normal primary and secondary components.

Some of the plates have been measured for radial velocity, but this work is not complete and the results are not needed here.

U Sagittæ.—This seems to be a more normal eclipsing variable than U Cephei and it is unfortunate that circumstances did not allow more extensive observations of it. The period is 3·38 days. There is a fairly recent photometric orbit by Fetlaar,† and Joy ‡ has determined the spectroscopic orbit. According to the latter, the primary spectrum is B9*n*, with helium lines weak, and the secondary spectrum is *g*G2. Joy mentions that

* Prager, *Katalog und Ephemeriden veränderlicher Sterne für 1935.*
† *B.A.N.*, 3, 195, 1926. ‡ *Ap. J.*, 71, 336, 1930.

the primary spectrum has poor lines, but it should be remarked that U Cephei is noticeably worse in this respect.

The total light range is $6^m.52$ to $9^m.40$. Eclipse lasts about 12·5 hours and totality about 100 minutes. There is evidence for a small variation in the period. For our work the following elements were used :—

Time of principal minimum * J.D. 2417130·4111 + 3·3806234 E.
Eccentricity of orbit 0.
Inclination „ „ 84°·5.
Radius of larger star 0·29.
„ „ smaller star 0·175.
Ratio of surface brightness (visual) 37.
No darkening to limb.

Reduction of Line Intensities

The observed values have to be corrected for the superposition of the secondary spectrum. It is clear that the uncertainties introduced by this correction, together with the actual observational errors, make it impossible for us to deduce any very accurate information concerning the variation from centre to limb of the primary star. We shall confine ourselves to determining which of the two limiting cases fits best the behaviour of the lines, viz. constant line intensity over the disc or complete fading of the line from centre to limb. Our observational data are sufficiently accurate, even for this limited purpose, only in the case of the hydrogen lines. The individual lines $H\beta$, $H\gamma$ and $H\delta$ are of very much the same intensity as each other at all phases, so that to obtain more reliable results the mean of the three has been taken after the corrections about to be described had been applied. Had any choice been possible, the hydrogen Balmer lines would have been avoided, since they are not the principal lines of the hydrogen atom, and strictly it is only to such lines that we can apply the classical theories of formation of Fraunhofer lines.

Let us consider a line at wave-length λ in the spectrum of the primary star at phase P. The observed intensity is affected by the superposition of the secondary star's spectrum. The latter is composed not only of a continuous spectrum but also of absorption lines, some of which will overlap the measured line of the primary spectrum. In what follows we consider (except in the special case of H and $H\epsilon$) only the effect of the same line in the secondary as we are measuring in the primary, *e.g.* when considering $H\gamma$ in the primary we consider the effect of the superposition of $H\gamma$ in the secondary. Other lines of the secondary are neglected, and it is assumed that the primary and secondary lines are always sufficiently blended for them to be measured together, a condition which seems to be always fulfilled in the spectrograms under consideration.

Let the uneclipsed part of the primary give rise to a continuous spectrum of intensity C_p in the neighbourhood of λ, and let the secondary give a corresponding intensity C_s. The line is measured relative to $C_p + C_s$, the total intensity being expressed as the equivalent of total absorption over so

* Prager, *loc. cit.*

many angstroms of continuous spectrum. If the real intensity of the line is x, the measured intensity, neglecting the secondary's absorption line, will be $z' = xC_p/(C_p + C_s)$.

The true intensity, y, of the absorption line in the secondary spectrum is measured on spectrograms obtained during totality. The presence of this line in the blended spectra outside totality adds to the measured intensity. y is expressed in terms of C_s, so that its apparent intensity in the measured spectrum during partial phases is $yC_s/(C_p + C_s)$. Hence the actual measured intensity is

$$z = \frac{xC_p}{C_p + C_s} + \frac{yC_s}{C_p + C_s}$$

and the required true intensity is

$$x = z\left(1 + \frac{C_s}{C_p}\right) - y\frac{C_s}{C_p}.$$

We have to evaluate C_s/C_p from the light-curve of the system, or, what amounts to the same thing, from the elements of the photometric orbit.

First we need the ratio of surface brightness of primary disc to secondary disc for all the wave-lengths of the lines to be reduced. For the moment we neglect darkening to the limb and consider the case of uniform discs (U Sagittæ). A ratio of surface brightness is given by the visual light-curve. It refers to light integrated over a certain range of wave-lengths, and its value would probably vary from one observer to another on account of differences of telescope transmission and of colour sensitivity of the eye. We assume that the values from visual observations, such as those given above, refer to a mean wave-length 5500 A., an estimate which cannot be very greatly in error. The ratios at other wave-lengths depend on the colour distribution in each spectrum. In the spectral region under consideration, stars appear to radiate very much like black bodies, and their colour distribution may be described sufficiently accurately by a single parameter, the temperature, or, better for our purpose, the "gradient." * Assuming black-body distribution, the following relation holds between the spectral intensities I_λ, I_λ' of two stars at wave-length λ :—

$$\frac{d}{d\left(\frac{1}{\lambda}\right)} \log_e \frac{I_\lambda}{I_\lambda'} = \phi' - \phi = \Delta\phi,$$

where $\phi = \frac{c_2}{T} \Big/ (1 - e^{-c_2/\lambda T})$ and c_2 is a constant $= 14320$ when the wave-length is measured in microns. ϕ differs from the "gradient" by a constant. Over the range of temperature found in ordinary stars, $\Delta\phi$ is very nearly a constant with respect to λ, so that for our two stars, having intensities in their continuous spectra $(I_p)_\lambda$ and $(I_s)_\lambda$,

$$\log_e \frac{(I_p)_\lambda}{(I_s)_\lambda} = \frac{\Delta\phi}{\lambda} + \text{constant}.$$

* Greenwich Publications, *Observations of Colour Temperatures of Stars*, 1932.

A value of $\Delta\phi$ is taken, consistent with the known spectral types of the two components. For U Cephei we have types Ao and Ko, and $\Delta\phi$ has been assumed to be 2·18; for U Sagittæ, types B9 and *g*G2, $\Delta\phi$ was taken to be 1·30. The final digit has little or no significance, and the actual figure could be as much as 10 per cent. from these values. Fortunately our results are quite insensitive to changes in $\Delta\phi$, as was shown by working through the corrections for U Cephei as though its secondary were a Go star. This involves a change in $\Delta\phi$ of over 40 per cent., but the final result was not greatly altered.

The constant in the equation just quoted is evaluated from the condition that I_p/I_s for $\lambda = 0{\cdot}55\ \mu$ coincides with the surface brightness ratio given by the visual light-curve. The value is $-1{\cdot}256$ for U Cephei and $+1{\cdot}247$ for U Sagittæ. Thus I_p/I_s was computed for the wave-lengths needed. In the case of U Sagittæ there is no observed darkening to the limb, so the computed values are sufficient as they stand. In the case of U Cephei, with darkening coefficient $\frac{2}{3}$, the brightness at any point of the disc is given by $\frac{1}{3}+\frac{2}{3}\cos\theta$, θ being defined as usual, and the brightness at the centre is $\frac{9}{7}$ the average value for the whole disc. On the Sun the darkening to the limb is accompanied by a certain amount of colour change, the limb being redder. There is probably a similar phenomenon on the disc of U Cephei but it must be neglected, for unfortunately there are no observations at present which can tell us anything on the point.

We have to deduce for different phases the amount of light coming from the uneclipsed part of the primary, and for this the following procedure was adopted. The primary disc was divided into zones by the circles corresponding to $\theta = 10°, 20°, 30°, 40°, 50°, 60°, 70°, 90°$, *i.e.* the circle radii were sin 10°, sin 20°, . . ., etc. of the whole disc radius, and the uneclipsed area of each zone was found graphically. In about half the whole number of cases the answer was checked by direct computation. The surface brightness was assumed constant in each zone, the average values in terms of the brightness at the disc centre being for the various zones $(\frac{1}{3}+\frac{2}{3}\cos 5°)$, $(\frac{1}{3}+\frac{2}{3}\cos 15°)$, . . ., etc. Hence, for U Cephei the uneclipsed part of the primary makes a total contribution to the continuous spectrum

$$C_p = \tfrac{9}{7} I_p \Sigma_\theta A_\theta (\tfrac{1}{3}+\tfrac{2}{3}\cos\bar{\theta}),$$

I_p being the mean brightness of the whole primary disc, A_θ the area of one of the zones, $\bar{\theta}$ the mean value of θ for that zone, and Σ_θ denoting summation over the uneclipsed parts of the zones.

Also

$$C_s = I_s A_s,$$

I_s being the mean brightness and A_s the total area of the secondary disc.

Hence

$$\frac{C_s}{C_p} = \frac{I_s}{I_p} A_s \frac{7}{9} \frac{1}{\Sigma A_\theta (\frac{1}{3}+\frac{2}{3}\cos\bar{\theta})},$$

and this can be evaluated for all necessary phases and wave-lengths.

For U Sagittæ there is no darkening and

$$\frac{C_s}{C_p} = \frac{I_s}{I_p} \frac{A_s}{\Sigma_\theta A_\theta}.$$

C_p was derived in this way rather than direct from the light-curve, because the zone areas are in any case required for computing the expected variation of line intensity.

We now have the necessary data for producing the corrected line intensities. In Table III the sign of the phase has been neglected and the spectral changes emerging from eclipse have been regarded as precisely equivalent to those going into eclipse. This would naturally be so if the two stars were as simply constructed as we have supposed. In the case of U Cephei, at least, there seem to be additional complications which show themselves in a certain asymmetry of the light-curve at principal minimum, where the rise is steeper than the descent. This asymmetry is borne out by the spectrograms, for the increase after totality of the primary spectrum relative to the secondary appears somewhat quicker than the corresponding decrease before totality. However, this effect has to be ignored in our reductions.

TABLE III

Corrected Intensities

U Cephei (Slit Spectrograph)

Phase	Intensities					
	Hβ	*Hγ*	*Hδ*	*Hε* + H	*Hζ*	K
0·056	4·6	1·0	9·1			
·060	3·8	2·6	2·8	5·6		−2·7
·065	1·2	5·2	3·2	8·8		+3·8
·070	8·6	7·8	7·3	7·9	9·4	−1·1
·074	6·5	6·1	4·8	6·3		−0·9
·086	5·5	4·9	3·7	6·2		+0·8
·089	6·7	7·3	6·4	6·9	5·2	+2·4
·089	4·5	6·2	6·2	7·7		0·0
·105	7·2	6·4	6·5	7·1	7·4	+0·5
·106		8·6	10·9	7·1	8·2	−0·2
·110	9·1	6·8	6·7	8·4	8·0	+1·0
·111	7·4	7·7	7·4		5·0	
·112	6·8	6·9	7·1	13·4		+1·1
·130	9·9	7·5	6·6	9·8	9·1	+0·5
·164	9·7	8·5	9·2	8·0		+0·7
·166	8·4	9·1	7·6	9·5	8·2	+0·9
·173	8·3	8·1	8·0	7·8		+0·7
·175	6·8	7·8	7·5		7·1	
Outside eclipse (5 plates)	7·5	8·1	8·4	8·9	9·3	+0·9

U Cephei (Slitless Spectrograph)

Phase	Intensities				
	Hγ	*Hδ*	*Hε* + H	*Hζ*	K
0·060			7·7		6·0
·071	1·7	3·5	4·6	3·3	2·6
·104	7·6	7·6	8·6		1·3
·115	7·0	7·7	6·9	5·8	0·4
·126	7·9	7·0	7·1	7·5	0·4
·138	8·3	7·1	7·4	7·0	0·6
·147	8·3	8·2	7·9	7·5	0·7
·170	6·2	6·8	7·9	7·2	1·2
·177	8·0	6·2	8·9	7·1	0·9
·187	7·2	7·5	8·7	6·1	1·1

U Sagittæ (Slit Spectrograph)

Phase	Intensities				
	Hβ	*Hγ*	*Hδ*	*Hε* + H*	K †
0·059	8·1	6·3	4·0	8·3	5·6
·096	10·5	10·5	7·9	9·1	2·2
·120	8·2	7·5	7·3	9·4	1·4
·178	10·4	8·9	8·4	10·0	0·5
Outside eclipse (3 plates)	9·9	8·8	9·8	9·6	0·5

* Reduced by assuming intensity = 10 within totality.
† „ „ „ „ = 12 „ „

Computation of Expected Intensity Variation

The corrected intensities of Table III are to be compared with those expected on the two hypotheses : (i) no change of intensity across the disc, (ii) complete fading of the lines from centre to limb.

(i) The tabulated corrected intensities give values as they would be observed if the secondary star were completely non-luminous, *i.e.* they are intensities averaged over certain fractions of the primary disc and measured relative to the continuous spectrum coming from the same disc area. Clearly, if there were no change of line intensity from centre to limb, the values of Table III should be constant.

(ii) In this case suppose the line intensity, becoming zero at the limb, obeys a cosine law, as does the general darkening in the continuous spectrum. The line intensity at any point of the disc, measured in terms of the con-

tinuous spectrum emitted from the same neighbourhood, is proportional to $\cos\theta$. We compute the expected result to be observed by again dividing the star disc into zones and supposing the surface characteristics of the star to be constant in each zone.

At any phase P let the uneclipsed area of one given zone be A_θ. The contribution of this zone to the continuous spectrum of the star in the neighbourhood of the absorption line considered is

$$kA_\theta(1-u+u\cos\theta),$$

where u is the darkening coefficient and k some constant. From this continuous spectrum a certain amount $I_0\cos\theta$ is lost by absorption in the line considered, where I_0 is the intensity of the line at $\theta=0$, measured in terms of the continuous spectrum at $\theta=0$.

Hence for this zone the total amount of energy lost in the absorption line is

$$kI_0A_\theta(1-u+u\cos\theta)\cos\theta.$$

The total amount of energy lost from the continuous spectrum of all the zones is

$$kI_0\Sigma A_\theta(1-u+u\cos\theta)\cos\theta$$

and the total continuous spectrum from all zones is

$$k\Sigma A_\theta(1-u+u\cos\theta),$$

so that the resultant intensity of the line, measured relative to the summed continuous spectrum, is

$$\frac{I_0\Sigma A_\theta(1-u+u\cos\theta)\cos\theta}{\Sigma A_\theta(1-u+u\cos\theta)},$$

where $u=\frac{2}{3}$ for U Cephei and 0 for U Sagittæ.

The scale of the predicted line variation is determined by I_0, which can be expressed in terms of $\bar{I}$, the mean intensity from the whole disc, which is the corrected observed intensity outside eclipse. For this, take A_θ to be the area of the zone θ to $\theta+d\theta$, *i.e.* $A_\theta=2\pi r^2\sin\theta\cos\theta d\theta$ and integrate

$$\bar{I}=\frac{I_0\int_0^{\frac{\pi}{2}}2\pi r^2\sin\theta\cos\theta(1-u+u\cos\theta)\cos\theta d\theta}{\int_0^{\frac{\pi}{2}}2\pi r^2\sin\theta\cos\theta(1-u+u\cos\theta)d\theta}$$

$$=I_0\frac{(4-u)}{(6-2u)}.$$

Hence

$$I_0=\tfrac{7}{5}\bar{I} \quad \text{for} \quad \text{U Cephei } (u=\tfrac{2}{3})$$

and

$$I_0=\tfrac{3}{2}\bar{I} \quad \text{for} \quad \text{U Sagittæ } (u=0).$$

A comparison of the observations with these two limiting cases is made in figs. 1 and 2. Of the two stars, U Cephei, with the greatest number of

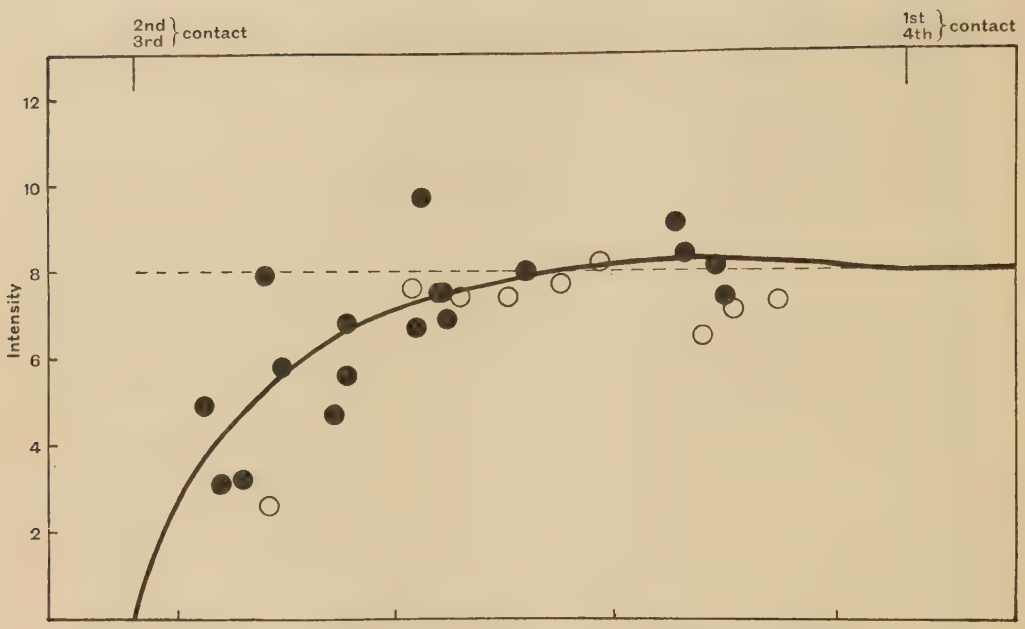

FIG. 1.—*Observations of the mean total line intensity of Hβ, Hγ and Hδ in the primary star of U Cephei during eclipse. Filled circles are from slit spectra, unfilled circles from slitless spectra. The continuous curve is computed on the hypothesis of complete vanishing of these lines at the limb. The dotted line is for uniform intensity over the disc.*

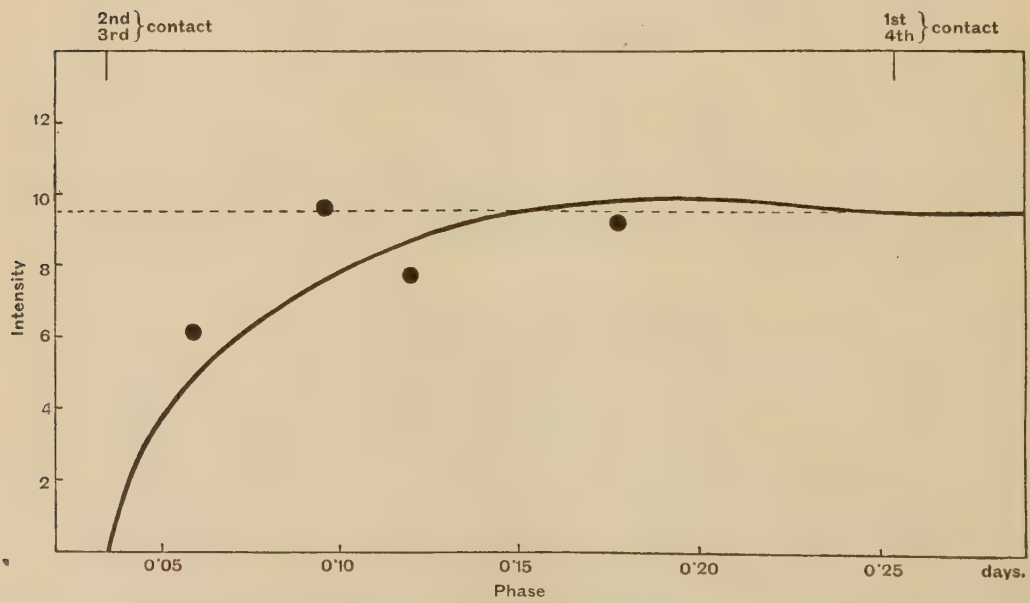

FIG. 2.—*Observations of mean total line intensity of Hβ, Hγ and Hδ in the primary star of U Sagittæ during eclipse. The continuous line is computed on the hypothesis of complete vanishing of these lines at the limb. The dotted line is for uniform intensity over the whole line.*

observations, gives the most striking result. The observed points are scattered about a great deal on account of accidental error, but on the whole they agree well with case (ii), *i.e.* with the supposition that the lines vanish to the limb. The general trend of the U Sagittæ plates is in the same direction but less marked, and suggests that the lines behave in some intermediate manner, as on the Sun. If one is justified in applying the classical theories of line formation to the Balmer series, then in U Cephei the lines behave as though formed by pure absorption, in U Sagittæ by simultaneous scattering and absorption.

Behaviour of the Calcium K Line

It would perhaps be of more fundamental interest from the theoretical worker's point of view if definite information concerning the K line could

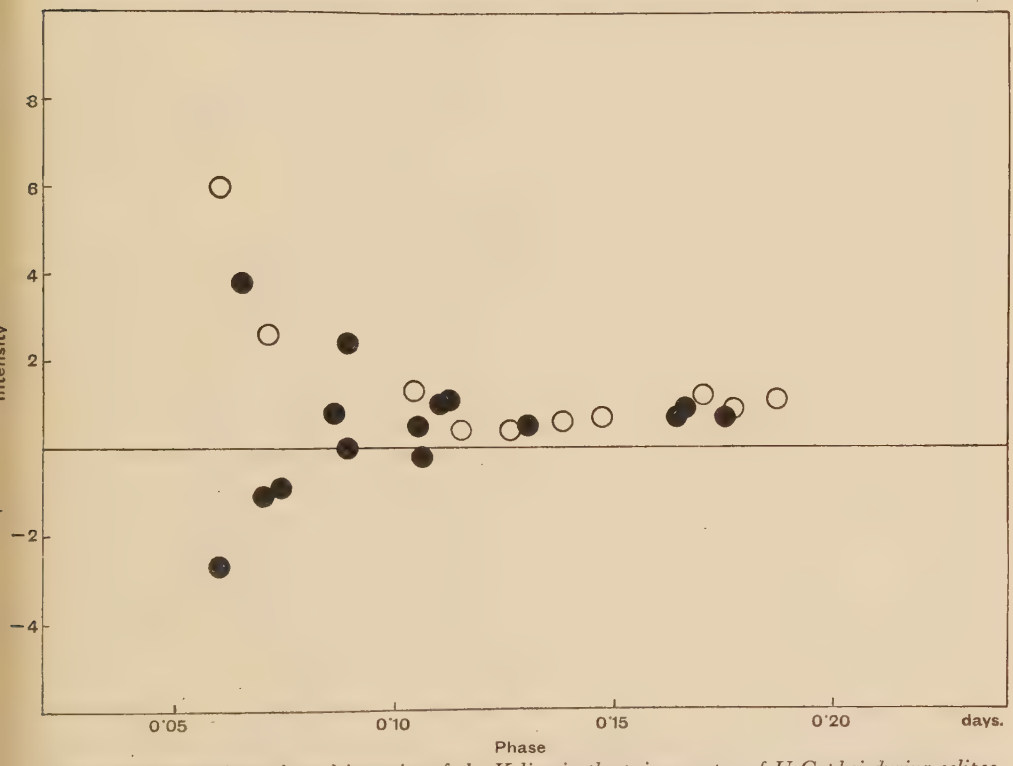

FIG. 3.—*Observations of total intensity of the K line in the primary star of U Cephei during eclipse. Filled circles are from slit spectra, unfilled from slitless spectra.*

be obtained from the measures. A plot of the line intensities for U Cephei, corrected by the same procedure as that outlined above, is given in fig. 3, but it will be seen that the results are quite inconclusive. At the phases nearest to totality the observational scatter becomes very great, and nothing definite can be deduced from the material. The trouble is purely observational. As is well known, the neighbourhood of the K line is more difficult to photograph than the λλ 4100 to 5000 region, particularly with a

glass spectrograph, and also the line itself in these two stars is much less intense in the primary spectrum than are the hydrogen lines. The secondary spectrum, on the other hand, has an extremely strong K line, which helps to complicate matters. The only favourable factor in this region is that, on account of the redness of the secondary compared with the primary, the value of C_s/C_p is small. An examination of individual plates suggests that the observations giving positive residuals near totality may be less unreliable than the others, and this is supported to some extent by U Sagittæ, where there are steadily increasing intensities towards totality. The latter, however, are affected by corrections based on an assumed K line intensity for the secondary spectrum, the necessary observations not being available. If the K line really does increase in intensity towards totality, even after correction, it must probably be attributed to what may be called the ζ Aurigæ effect, viz. the formation of an absorption line in light of the primary shining through the outer atmosphere of the secondary. It is true that neither secondary in this case is a super-giant, so that neither is likely to have the very extensive atmosphere of the secondary of ζ Aurigæ, but the effect must be present to some degree although the behaviour of the hydrogen lines indicates that it is not large. There may be a faint K line of interstellar origin in the spectra of both systems, but the expected intensity is so small that it will produce little complication here.

There seemed a chance that something might be made of the H line in U Cephei, the results to be combined with those from the K line. In the spectrum just outside eclipse we have a strong hydrogen $H\epsilon$ line blended with and entirely concealing the H line. As eclipse progresses the $H\epsilon$ line becomes relatively weaker, until during totality the secondary spectrum shows a very strong H line, blended with and entirely concealing a comparatively weak $H\epsilon$ line, just the reverse of the state of affairs outside eclipse. Now the intensity of $H\epsilon$ in the uneclipsed primary spectrum may be estimated fairly closely. $H\beta$, $H\gamma$, $H\delta$ and $H\zeta$ show a smooth progression of values, 7·5, 8·1, 8·4 and 9·3 respectively, so that we may interpolate and adopt 8·9 as the $H\epsilon$ value. Within total eclipse $H\beta$, $H\gamma$ and $H\delta$ have been measured but not $H\zeta$, as none of the plates obtained were sufficiently strongly exposed. The mean intensities for $H\beta$, $H\gamma$ and $H\delta$ within totality were respectively 2·5, 2·2 and 1·8, allowing us to assume $H\epsilon = 1{\cdot}5$ for the secondary. Then at intermediate phases the intensity of $H\epsilon$ in the combined spectrum may be predicted on the assumption that it vanishes at the limb of the primary, as $H\beta$, $H\gamma$ and $H\delta$ appear to do. With these data it is finally possible to correct the observed values of $H\epsilon$ + H, leaving residuals which are to be attributed to H alone. However, the errors are much too big and neither by themselves nor combined with the K line measures do the H values show any significant trend.

Discussion

The result of this work is quite a limited one, but it encourages us to believe that a similar procedure, carefully applied to a few selected eclipsing

binaries, would provide definite and valuable information which at the moment can be obtained in no other way. The study of the centre to limb variation, either in the continuous spectrum or in absorption lines, is undoubtedly one of the simplest and most reliable methods of investigating the processes which are at work in a stellar atmosphere, and as these need not necessarily be identical from star to star it is clearly desirable to devise some kind of observation, direct or indirect, of this type. The method is quite distinct from that lately used with great success by several observers, particularly at Berlin-Babelsberg and Mount Wilson, in the case of ζ Aurigæ, a bright eclipsing binary where it is possible to study absorption lines formed by a relatively very small primary star shining *through* a very extended atmosphere around the secondary.

With regard to the line intensities produced in the present work, it might be suspected that the rather large amount of correction it is necessary to apply makes the results of uncertain value. In the case of the H and K lines this may be admitted to be true, but the hydrogen measures rest on a much more certain footing. The corrections are in no sense arbitrary, but are given us, with little scope for variation, by other observations. They depend on (*a*) the relative intensities of the primary and secondary continuous spectra in the neighbourhood of the line considered, and (*b*) the intensity of the line in the secondary spectrum. (*a*) rests on, first, visual observations of the light-curve of the system, and, secondly, on the relative colours of the two stars. The visual observations in themselves are more accurate than we need ; the only doubt is as to what average wave-length they apply, but this cannot very well vary a great deal from the assumed value 5500 A. The corrections are not very sensitive to the size of the visual brightness ratio ; still less are they sensitive to the colours of the two stars, and these must in any case be given fairly accurately by the spectral types, since none is of a class likely to have an abnormal colour index. With regard to (*b*), fairly accurate observations are available from spectrograms taken during totality, and no troublesome uncertainty can very well arise here. The fact that the hydrogen lines are much weaker in the secondary than in the primary is a favourable factor.

It has been assumed in the work of applying corrections that the secondary line always lies within the profile of the corresponding primary line. Despite the fact that the primary star, particularly in U Cephei, is probably rotating quite rapidly, no separation or doubling of the lines was noticed. The explanation of this is that the dispersion used at the critical phases is very small, the slit was used very wide and plate grain was bad. Inspection of the U Cephei plates at phases 0·050 to 0·065 shows that either the blended line must have been measured, or the secondary only. We have proceeded on the supposition that the blended line was measured. There are two arguments against the alternative, viz. (i) If the measures included only the secondary line the corrected intensities should be zero. They never are in the case of the hydrogen lines. (ii) If the secondary line only was measured, the primary line should be visible alongside. It was never seen in this position.

We infer therefore that our corrections are substantially accurate. The fact that the two stars do not give the same result gives us confidence in the reality of the centre-limb variation. Spectroscopically U Cephei and U Sagittæ are similar systems and they have been observed by the same instrument and method, so that if the deduced centre-limb variation were merely due to systematic error (despite all evidence to the contrary) it should be the same for both stars.

Although Fraunhofer lines vanish at the limb when they are formed by pure absorption, it does not follow that the reverse is necessarily true, and we have always to remember that the classical stellar atmosphere models are simplified and idealized conceptions and are never more than approximations to the true state of affairs. As in most astronomical problems, more observations are urgently needed. If eclipsing variables are to be used as a source of information, not merely line intensities but accurate monochromatic light-curves are very much to be desired, even if obtained at only one or two wave-lengths. A suitable slitless spectrograph could probably be used for both this and the line-intensity work, although the same observations would probably not be sufficient simultaneously for both problems, and systematic errors would have to be watched carefully. Slit spectra are needed for U Cephei, where the discrepancy between spectroscopic and photometric orbits urgently needs investigation.

The writer wishes to express his gratitude to Dr. J. S. Plaskett for permission to use the instrumental equipment at the Dominion Astrophysical Observatory, and to the other members of the Victoria staff who gave assistance in the work, particularly Drs. Frank and Helen Hogg and Dr. C. S. Beals. Thanks are also due to Mr. E. Shirley, who has given help with the necessary computations.

Solar Physics Observatory,
Cambridge :
1936 *February* 26.

PHOTOMETRY OF FRAUNHOFER LINES IN THE REGION 5889–6271 A.

C. W. Allen, D.Sc. (*Hackett Research Student*).

Introduction.—At the meeting of the International Astronomical Union in Paris, 1935, it was decided that lines in the region of the Solar Spectrum 6200–6300 A. should be used for comparison of observations in Fraunhofer photometry. This region had already been investigated with a 3-prism spectrograph at Canberra,* but the central intensities are open to some doubt on account of the comparatively small dispersion of prisms in the red. Some observations of both equivalent breadth and central intensity in the red have therefore been repeated with the Rowland concave grating

* *Mem. C.S.O. Canberra*, No. 5, 1934. Later referred to as I.

of the Solar Physics Observatory at Cambridge. For central intensities the second order was used, as this gives considerably higher resolving power than the Canberra prism instrument, but it is thought that the resolution is still insufficient for completely reliable photometry of the fine solar lines. The region observed extends from 5889 A. to 6271 A.

A low dispersion monochromator, arranged by Mr. Moss, was used instead of a filter before the slit; it limited the region to about 500 A. Photographic photometry has been employed using backed Ilford Special Rapid Panchromatic plates. Each plate was standardised with a series of solar spectra whose intensities were varied by introducing neutral perforated absorption screens. These were calibrated with a vacuum thermo-element set up by Dr. Wormell. Some plates were developed with Metol-Hydroquinone, others with Hydroquinone, and all were brushed during development in order to minimise developer effect. All plates were measured with the Cambridge microphotometer and the intensities reduced in the usual way.

Equivalent Breadths.—The new values of equivalent breadth in this region are in substantial agreement with the earlier values. The remeasurement has been made merely as a check, and each observation in Table I represents only a single measurement of contour area. Values have been obtained in the first and second order, and in the first order one plate was taken in integrated sunlight instead of light from the centre of the disc which was used for all other investigations. The difference in equivalent breadth for integrated and central disc light is scarcely measureable. In the mean the new (Cambridge) values are 3 per cent. greater than the old.

Remeasurements have also been made in regions near 5300 A. and 5600 A. For the first region (15 lines) the new results are 12 per cent. greater than the old, and for the second region (45 lines) the new results are 15 per cent. greater. No definite reason can be given to account for this difference, but the new values are in better accord with the work of Righini * and Mulders † than the old.

Central Intensities.—In order to determine the instrumental contour for the grating lines Neon-tube spectra were photographed and photometered. An allowance was made for the fact that Neon lines have an isotopic component at a distance of 0·03 A. from the main line,‡ and a small correction was made for the thermal width of the lines. From this instrumental contour the observed central intensities were corrected by the method described in the earlier work (I). The effect of photographic scattering is automatically eliminated, and in this respect the method may have some advantage over the interferometer method of Shane.§ Only one detail in the earlier procedure was altered. It will be remembered that some form must be assumed for the shape of the uncorrected absorption contours, and for this purpose contours of both the forms e^{-ax^2} and $1/(x^2+a^2)$

* G. Righini, *O.M. Oss. As. Arcetri*, No. 51, 57, 1933.
† G. F. W. Mulders, *Zeit. f. Astrophys.*, **10**, 297, 1935.
‡ C. V. Jackson; *vide* R. O. Redman, *M.N.*, **95**, 742, 1935.
§ C. D. Shane, *L.O.B.*, No. 449, 1932.

TABLE I

Comparison of Equivalent Breadths at Canberra and Cambridge
(Milli-angstroms)

Wave-length	Canberra		Cambridge		
			First Order		Second Order
	From r_b	From Contour	Centre	Integrated	Centre
6213·443	79			70	83
6216·366	34			32	
6219·294	86	95		85	
6223·996	25		22	27	
6226·745	27		31	34	
6229·240	35	28	36	40	42
6230·111	18		16		17
6230·742	159		150	172	170
6232·655	81				87
6237·334	54		67	59	62
6238·396	40	47	43	43	
6240·659	51		40	44	48
6243·829	44		41	45	
6244·483	41		47	46	
6245·628	32		37	27	
6246·333	120	131	122	125	127
6247·569	56	58	50	49	60
6252·572	126	121	124	121	119
6255·966	14				15
6265·148	82	77	86	90	
6270·237	51			54	
6271·289	20			18	

were used, where a is a constant and x the distance from the centre of the line. For both of these forms corrections to the measured depth of the lines were worked out as a function of the measured breadth at half maximum depth. Faint lines are of the e^{-ax^2} type since they are broadened mainly by Doppler effect, and strong lines resemble the $1/(x^2+a^2)$ type. The two corrections are given by circles and crosses in fig. 1. The correction curve that was actually used lay between them, agreeing with e^{-ax^2} for faint lines and $1/(x^2+a^2)$ for strong ones.

Even with the high resolution of the second-order grating (theoretical resolving power 170,000) the corrections for instrumental broadening are very large. The narrowest observed Fraunhofer lines are not very much broader than the instrumental contour, and sometimes the corrected depth is as much as double the measured depth. Since the possibility of error in the resolving correction is so large, it is pointless to spend too much elaboration over the smaller corrections due to ghosts, scatter, and Eberhard effect. The total ghost intensity in this region is about 5 per cent., the

scatter about 3 per cent., and it has been assumed that the line depths have been increased by 4 per cent. by Eberhard effect. Test plates showed that this effect is just visible, and 4 per cent. should be an overcorrection if anything. In all 4 per cent. was added to the corrected line depth to allow for the minor corrections.

Fully corrected central intensities (r_c) for 60 lines between 5889 A. and 6271 A. are given in Table II. At least three measures were made for each

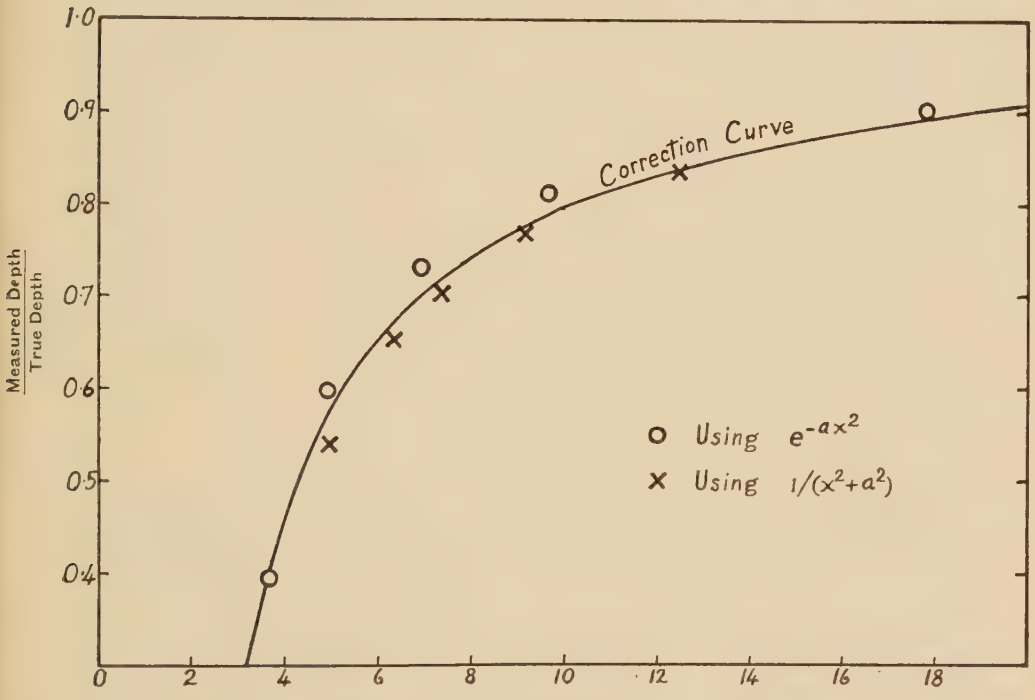

FIG. 1.—*Breadth at Half Maximum Depth (mm. on Trace).*

line. This table also contains uncorrected central intensities (r_m) for the Cambridge observations, and values of the line sharpness *d*. This has been defined (in I) as the ratio of the depth of the line to the depth of the normal solar line having the same equivalent breadth.

It must be admitted that there is a certain amount of ambiguity in applying the resolving correction, since it is difficult to be certain how much the spectroscopic breadth of the *Ne* lines has influenced the instrumental contour. The final result for the central intensity is very sensitive to any small change in the assumed instrumental contour. As it was my intention to make sure that full resolving correction was used, I made the magnitude of the correction as generous as possible by assuming that the true instrumental contour was very nearly as wide as the observed *Ne* lines. Nevertheless this should be fairly close to the truth. The result has been that the lines work out deeper than the observations made at Canberra (which suffer from the same ambiguity and are possibly undercorrected), and are now almost as deep as theory requires. Until further work is done

TABLE II

Observations of Observed Central Intensity r_m, Corrected Central Intensity r_c and Line Sharpness d made at Canberra and Cambridge. Central Intensities are expressed as a Percentage of the adjacent Continuous Spectrum

Wave-length	Excitation Potential	Canberra		Cambridge		
		r_c	d	r_m	r_c	d
5889·977	0·0	6	1·08	13	2	
5895·944	0·0	4	1·11	16	1	
5983·693	4·6	47		65	41	0·89
5984·830	4·7	42	0·86	55	29	0·96
5987·075	4·8	48		59	36	0·95
6003·027	3·9	40	0·97	56	29	0·95
6005·556	2·6	82		86	68	
6007·973	4·6	50		63	33	1·04
6008·572	3·9	39	0·95	54	28	0·94
6013·503	3·0	44	0·90	58	34	0·91
6016·653	3·0	36	0·97	53	30	0·89
6024·073	4·5	31		47	17	1·01
6065·499	2·6	24	1·08	45	13	1·00
6078·504	4·8	45		58	29	1·00
6079·021		59		71	48	0·94
6082·723	2·2	70		78	57	
6084·118		81		87	75	
6102·188	4·8	41	0·88	56	27	0·97
6102·733	1·9	22		38	7	1·05
6122·231	1·9	17	1·02	31	6	1·00
6126·230	1·1	81		86	75	
6127·918		59		69	45	0·97
6128·990	1·7	78		86	74	
6130·147	4·3	81		87	77	
6136·631	2·4	20	1·07	35	3	1·07
6137·709	2·6	23	1·01	36	4	1·08
6141·733	0·7	28		38	19	
6149·255	3·9	66		80	66	
6151·630	2·2	60		69	41	1·04
6157·739		52		61	30	1·07
6160·759	2·1	59		70	48	0·94
6162·185	1·9	18	1·00	26	4	0·99
6165·369		65		70	43	
6166·446	2·5	49	0·92	56	20	1·17
6169·570	2·5	29		43	12	1·04
6170·522	4·8	48		53	26	1·03
6173·348	2·2	49	0·92	56	21	1·16
6176·822	4·1	52		61	38	0·96
6180·216	2·7	58		63	36	1·07
6188·002	3·9	63		68	46	1·02
6191·192	1·7	48		54	21	1·10
6191·577	2·4	25	0·98	38	8	1·04
6200·327	2·6	48		56	28	1·00
6213·443	2·2	43		52	21	1·05
6216·366	0·3	75		80	68	

Wave-length	Excitation Potential	Canberra		Cambridge		
		r_c	d	r_m	r_c	d
6219·294	2·2	39	0·92	50	21	1·02
6223·996	4·1	78		83	65	
6226·745	3·9	76		81	66	
6229·240	2·8	70		75	57	
6230·111	4·1	84		87	78	
6230·742	2·5	22		38	14	0·95
6232·655	3·6	43		52	24	1·00
6237·334		58		68	51	0·81
6240·659	2·2	59		68	38	1·07
6246·333	3·6	30	0·94	44	18	0·96
6247·569	3·9	55	1·03	65	41	0·96
6251·845	0·3	89		91	84	
6252·572	2·4	28	1·02	40	9	
6255·966		88		86	70	
6259·598	4·1	88		88	80	
6261·112	1·4	63		65	39	1·12
6265·148	2·2	40	1·12	49	20	1·04
6270·237	2·8	59		63	31	1·16
6271·289	3·3	82		85	73	

spectroscopists might refrain from regarding it as proved that Fraunhofer lines are too shallow. The comparison with theory is given in the next section.

Comparison of Central Intensities with Theory.—It is possible to compute theoretical contours of Fraunhofer lines provided certain assumptions are made. In the present calculations Eddington's formula * has been used for the relation between the intensity r (at any part of the contour) and the absorption coefficient l_y. The broadening constants are (*a*) a damping constant $7{\cdot}0 \times 10^8$ sec.$^{-1}$ chosen to agree with the demands of multiplet intensities, and (*b*) the Doppler constant corresponding to a temperature of 6000° K and an atomic weight of 56. These data are reasonable but chosen with the view to making the agreement between experiment and theory as close as possible.

The most convenient way to study the problem is to plot central intensity against equivalent breadth for both experiment and theory. This was done in my earlier work for the wave-lengths 4500 A. and 6000 A., and for the first of these regions the agreement was fairly close. For the second region the new observations are shown in fig. 2, where it is seen that the difference between theory and observation is not very great—it may not be real. The six observations of Shane † at 5600 A. are included. Since his lines are to the violet of 6000 A. they should be deeper instead of less deep than mine.

There are several ways of accounting for the difference between observation and theory if it is real. Redistribution of frequency may be partly

* A. S. Eddington, *M.N.*, **89**, 620, 1929. † C. D. Shane, *loc. cit.*

responsible. It is very probable that turbulent motion in the reversing layer produces shifts in the lines sufficient to produce an extra broadening. This suggestion could not be accepted to explain the discrepancy in the older observations at Canberra since there appeared to be such a difference

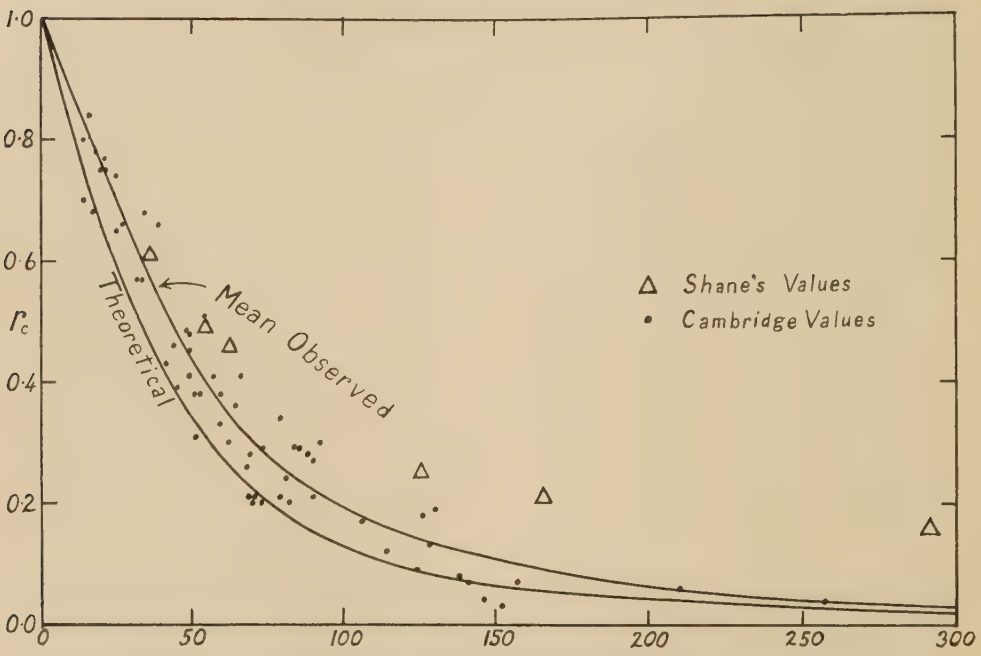

FIG. 2.—*Equivalent breadth in milli-angstroms.*

between the effect at 4500 A. and 6000 A.; but now that we find the difference between theory and observation is practically the same at the two wave-lengths the explanation becomes available again. Provided the turbulence was on a fairly large scale compared with the depth of the

TABLE III

Excitation potential in volts .	1 – 2	2 – 3	3 – 4	4 – 5
Mean sharpness d . . .	1·05	1·05	0·96	0·98
No. of observations . .	*5*	*18*	*8*	*9*

reversing layer it should not affect the equivalent breadth of the lines; thus it is not surprising that the Doppler broadening required to explain the development curve (*i.e.* curves of fig. 8 in I) agrees with the motion due to a thermal temperature of 6000° K and not the larger motion found by adding turbulence. The shallowing influence of cyclical transitions and electron captures probably affects only the strongest lines and does not need consideration here.

If the new central intensities are used for a redetermination of the *F*-curve (see I, p. 48) for 6000 A. the curve becomes steeper and practically

parallel to the original curve for 4300 A. This represents an improved agreement with theory.

From the measures of central intensity it is possible to make a new estimate of the line sharpness d (see I). These correlate sufficiently well with the earlier observations, and give as before a decreasing line sharpness with increasing excitation potential. The results are given in Table III.

The above work has been carried out with the assistance of a Hackett Research Studentship granted by the University of Western Australia.

Solar Physics Observatory,
Cambridge :
1936 *March.*

THE BALMER DECREMENT IN THE SPECTRA OF PROMINENCES.

R. v. d. R. Woolley, Ph.D.

It will probably be generally admitted that all questions relating to the theoretical intensities of lines either in emission or absorption spectra can only be disposed of satisfactorily when all the atomic transitions linked with the line in question are taken into account, unless it can be demonstrated that their effect is negligible. Thus in 1929 Eddington urged, as an objection to the theory of the formation of an absorption line which he was describing at the time, that a complete theory should consider all the transitions interlocked with the line in question ; but nobody has been able to work out a satisfactory treatment of the formation of a large number of interlocked lines. One avenue of approach is the treatment of small sets of interlocked lines which are considered to be the most important out of the array of possible transitions : we can judge the usefulness of such a procedure by the success with which it accounts for observational facts, and in particular by its greater success than that of a treatment which deals with one line at a time. The present writer made an attempt to account for the observed central intensities of the Balmer lines in the Fraunhofer spectrum by considering four transitions at a time, following the methods of Rosseland and Pannekoek : in the present note, the same theory will be brought to bear on the Balmer decrement in the spectra of prominences. The present work differs substantially from previous work on the Balmer decrement in emission spectra—specifically, that of Cillié—as attention will here be paid to the composite nature of the Balmer series, the influence of Lyman radiation and the metastability of the $2S$ state. The relation between the present work and that of Cillié will be discussed in a later section.

Relative intensities of various lines in the Balmer series in the spectra emitted by prominences have been measured from time to time by a number of observers. The first was Schwarzschild, at the eclipse of 1905, who

measured relative intensities in the series from $H\beta$ to $H\zeta$, and also the Ca^+ lines H and K, in four prominences which appeared at that eclipse. Twenty years later Davidson and Stratton measured the relative intensities of a large number of lines in the ultra-violet. In 1927 Pannekoek and Doorn measured the decrement from $H\alpha$ to $H\epsilon$ at the eclipse of that year.

More recently the Balmer decrement in the spectra of prominences seen without eclipse has been measured at Pulkowa by a photographic method, from $H\beta$ to $H\epsilon$, and at Greenwich by a visual method, from $H\alpha$ to $H\beta$.

Schwarzschild adopted as a unit of relative intensity the energy contained in 1 A. of the solar spectrum in the neighbourhood of the line. The mean values observed on various occasions are given below, together with some constants which are of use in making computations of this sort. It is here assumed that the colour temperature of the centre of the Sun is 7000° between $H\alpha$ and $H\delta$. This assumption enters into the values here given for Pannekoek's results, the other observers having expressed their observations directly in the Schwarzschild unit.

TABLE I

Observations of the Balmer Decrement in Prominences in Schwarzschild's Units

Observer	$H\alpha$	$H\beta$	$H\gamma$	$H\delta$
Schwarzschild *	...	1·00	0·35	0·10
Pannekoek †	7·8	1·00	0·33	0·29
Perepelkin ‡	...	1·00	0·39	0·15
Newton § (1)	5·2	1·00	...	...
(2)	4·5	1·00	...	...
No. of ergs in 1 A. of a black-body spectrum at 7000°.	0·68	1·00	1·06	1·07
Intensity of the lines in thermodynamical equilibrium at 6000° in ergs.	7·78	1·00	0·29	0·12
Ditto, in Schwarzschild's units	11·4	1·00	0·28	0·12

The entry, Newton (1), is computed as follows. The Greenwich measures of intensity were made in the wave-length of maximum illumination of the prominence for each line, and the ratio of the total energy in $H\alpha$ and $H\beta$ has been computed with the assumption that the widths of the lines in angstroms are proportional to their wave-lengths. A large number of measurements are included in this result. Later, Mr. Newton measured one prominence in several wave-lengths in both $H\alpha$ and $H\beta$ so that contours could be drawn for each emission line. This observation gives the result (2), which has not been published. Pannekoek's result for $H\alpha$ is not considered by its author to have great weight.

Schwarzschild had no theoretical intensities of the hydrogen lines with which to compare his observations, but Davidson and Stratton were able to

* *Ast. Mitt. Göttingen*, **13**, 69, 1906.
† *Verh. K. Akad. Wet. Amsterdam*, **14**, 21, 1930.
‡ *Poulkova Obs. Circular* No. 13, 1935.
§ *M.N.*, **96**, 5, 1935.

compare their observed intensities with those predicted by a formula due to Schrödinger and Pauli. This formula gives the same results for each line as a whole as the detailed work of Sugiura and Slack does when the components of the various lines are added together. But to compare any theory of line intensities with observed emissions, it is necessary to decide how the atoms are distributed among the stationary states. The simplest assumption to make is the assumption that the distribution is given by Boltzmann's formula, which is supposed to be true when the gas which emits the lines is in thermodynamical equilibrium. When this is assumed, it is found that the temperature of the thermodynamical equilibrium which gives the same Balmer decrement as one observes in the prominences is absurdly high for a prominence, from which we conclude—willingly enough—that the prominence is not in thermodynamical equilibrium.

The hypothesis that the distribution of atoms among the stationary states is governed by a temperature characteristic of the prominence would presumably be correct if collisions between atoms governed the distribution : the prominence would then be in Milne's local thermodynamical equilibrium. But one does not expect to find that collisions are important in anything so rarified as a prominence, and one expects to find the distribution of atoms among the stationary states governed by the radiation field, and that the prominence is in radiative equilibrium ; not Milne's monochromatic radiative equilibrium, but in a polychromatic radiative equilibrium.

Suppose there are m stationary states, including the state of ionisation. Let A_{hk} be the probability of a transition from state h to state k in a given radiation field, and let n_h be the number of atoms per c.c. in state h, so that $n_h A_{hk}$ is the number of transitions from state h to state k per c.c. per second. Further, let

$$A_{kk} = -\sum_{h=1}^{m} A_{kh} \quad (h \neq k).$$

The condition of polychromatic radiative equilibrium is that the number of atoms leaving each state is equal to the number arriving at that state, or, for state k,

$$\sum_{h=1}^{m} n_h A_{hk} = 0. \qquad (1)$$

There are m simultaneous equations of type (1) and $(m-1)$ unknowns. The determinant formed out of the A's must vanish, and the number of atoms in the states n_h are proportional to the minors of any row of the determinant. This equation has been used by Rosseland,* McCrea,** Pannekoek † and the present writer,‡ and a modification of it was used by Cillié.§ A notation introduced by Pannekoek is helpful in dealing with (1). Let n_h^0 be the number of atoms in state h at some temperature T, which is most conveniently taken equal to the colour temperature of the radiation. Write $n_h/n_h^0 = t_h$ and $n_h^0 A_{hk} = (hk)$. Equations (1) become

* *Ap. J.*, **63**, 218, 1926. † *B.A.N.*, **7**, 151, 1933 ; *M.N.*, **95**, 725, 1935.
‡ *M.N.*, **94**, 631, 1934. § *M.N.*, **92**, 820, 1932.
** *Camb. Phil. Soc. Proc.*, **24**, 506, 1928.

$$\sum_{h=1}^{m}(hk)t_h = 0. \tag{2}$$

If the radiation field is a temperature field so that an elementary volume of gas is exposed to full radiation corresponding to the same temperature on all sides, then $(hk) = (kh)$ and the solution is $t_h = 1$ for all h, the atoms arranging themselves in the equilibrium distribution for the temperature. We deal commonly with dilute radiation. If the elementary volume of gas is exposed to temperature radiation on one side only, the dilution factor W is one-half. In the case of an elementary volume of gas just outside the Sun, as in a prominence, additional dilution is caused by Fraunhofer lines. If $k > h$ we have

$$(hk) = Wr(kh), \tag{3}$$

where r is the central intensity of the Fraunhofer line corresponding to the transition hk.

To reduce the determinants to manageable proportions, and also because some of the coefficients which we would require in an exhaustive analysis are lacking, we consider only four states at a time.* For the Balmer lines the sets of four terms considered separately are: $1S$, $2P$, ND, O; $1S$, $2P$, NS, O; $1S$, $2S$, NP, O. State O is the ionised state (denoted by 5 in earlier papers). Evaluating the minors, we find for the cycles NS and ND,

$$\frac{t_N}{t_1} = \frac{12.2N.ON + 12.2O.ON + 12.O1.2N + 12.O2.2N + 10.ON.21}{21.N2.ON + 21.2O.NO + 21.O1.N2 + 21.O2.N2 + O1.NO.21 + 1O.ON.2N + 1O.ON.2O + 1O.O2.2N + O1.NO.2N + O1.NO.2O + O1.2O.N2}, \tag{4}$$

and for the cycle with NP,

$$\frac{t_N}{t_1} = \frac{1N.2N.ON + 1N.2O.ON + 1N.O2.2N + 1N.O1.2N + 1N.O1.2O}{N1.2N.ON + N1.2O.ON + N1.O2.2N + N1.O1.2N + N1.O1.2O + 1O.2N.ON + 1O.2O.ON + 1O.O2.2N + O1.2N.NO + O1.2O.NO + O1.2O.N2}. \tag{5}$$

Pannekoek gives a table of values of (hk) up to $N = 4$. Beyond this, values of (NO) could not be constructed as the oscillator strengths required had not been calculated numerically. To compute $(5O)$ for $H\gamma$ one has to calculate f values for transitions from states $5S$, $5P$, $5D$ to the ionised state, *i.e.* for the continuous spectra at the head of the Brackett series. The asymptotic formulæ for the f values at the head of this series, computed for the purposes of this paper from Sugiura's formulæ,† are as follows:—

$5S - nP$	$5P - nS$	$5P - nD$	$5D - nF$
$9{\cdot}3n^{-3}$	$0{\cdot}6n^{-3}$	$9{\cdot}1n^{-3}$	$8{\cdot}6n^{-3}$

The weak series $5D - nP$ may be neglected. Oscillator strengths for the continuous spectrum at the head of each series may be deduced from the continuity at the head of the series.‡

We get in this way for the three series

* This work is described in detail in *M.N.*, **94**, 631–635, 1934; and **95**, 725–727, 1935.

† *Sci. Papers Inst. Tokio*, **11**, 1, 1929. ‡ *M.N.*, **95**, 107, 1934.

$5S-O$	$5P-O$	$5D-O$
·093	·097	·086

The condition of continuity is not satisfied in detail by Sugiura's values for the earlier series : this probably indicates some flaw in the underlying theory. The above values for the Brackett series are, however, in good agreement with Kramers' formula when one makes allowance for the $5F$ and $5G$ series. (Kramers' formula gives values for the Brackett series as a whole without respect to degeneracy, and Gaunt's calculations do the same.)

We can now extend Pannekoek's table * as follows :—

TABLE II

Number of Transitions $n-m$

	f	$\log(nm)-5$
$1S-5P$	·0139	2·096
$2S-5P$	·042	1·255
$2P-5S$	·0012	0·179
$2P-5D$	·044	1·753
$5S-O$	·09	$\bar{1}$·66
$5P-O$	·10	0·18
$5D-O$	·09	0·36

Table II gives values of (nm), where $n > m$ (it being supposed here in this convention that O is greater than any other symbol). The upward transitions (mn) are calculated from $(mn) = Wr(nm)$, where $W = \frac{1}{2}$ and r is the central intensity of the Fraunhofer line corresponding to the transition nm. We take $r = 1$ for all continuous spectra, and following Thackeray † and Allen ‡ we take $r = 0{\cdot}15$ for $H\alpha$, $H\beta$ and $H\gamma$. It is not so easy to estimate r for the Lyman series. Presumably the Lyman Fraunhofer lines have low central intensities, but the prominence might be optically thick enough to blanket the Lyman radiation without affecting the Balmer radiation. We approach the matter by leaving the central intensity of the relevant lines in the Lyman lines represented by the symbol r. Using Pannekoek's table and Table II, we computed t_N/t_1 from (4) and (5) for the S, P and D terms, with $N = 3$, 4 and 5. The emission of an atom in any line is then

$$\sum_{S,P,D} t_N q_N A_{N2},$$

where $q_N = 1$, 3, 5 for the S, P and D terms. Numerical values are shown in Table III.

TABLE III

Population of States and Emission

Line	N	t_N/t_1			Emission in the Line
		ND	NP	NS	
$H\alpha$	3	$·003+·037r$	$·007+0{\cdot}5r$	$·09+·037r$	$·0054+·116r$
$H\beta$	4	$·015+·037r$	$·017+0{\cdot}5r$	$·23+·037r$	$·0156+·135r$
$H\gamma$	5	$·017+·037r$	$·017+0{\cdot}5r$	$·14+·037r$	$·0192+·148r$

* *M.N.*, **95**, 726, 1935. † *M.N.*, **95**, 296, 1935.

‡ *Memoirs of the Commonwealth Solar Observatory*, **5**, 2, 1934.

For all physical values of r ($0 < r < 1$) state 3 is depopulated more than state 4, etc., so that $H\alpha$ is weakened relative to $H\beta$, etc., as compared with thermodynamical equilibrium. Hence the apparent high temperature deduced from the ratio $H\beta/H\alpha$. Relative populations for various values of the intensity of the Lyman lines r are shown in Table IV.

TABLE IV

Relative Populations

State	$r=0$	$r=\cdot01$	$r=\cdot1$	$r=1$
3	0·34	0·39	0·58	0·81
4	1·00	1·00	1·00	1·00
5	1·24	1·23	1·16	1·11

Multiplying the relative populations in Table IV by the emission in thermodynamical equilibrium shown in Table I, we get the emission from the prominence, supposing it to be insufficiently thick to give self-absorption in the Balmer lines. Table V shows the result for $r=\cdot01$ and $r=1$ with some comparisons.

TABLE V

*The Balmer Decrement in Prominences, etc.**

	$H\alpha$	$H\beta$	$H\gamma$
Prominences			
Mean observed value	5·0	1·00	0·35
Thermodynamical equilibrium	11·4	1·00	0·28
Polychromatic radiative equilibrium, with $r=\cdot01$.	4·4	1·00	0·34
Polychromatic radiative equilibrium, with $r=1$.	9·3	1·00	0·30
Cillié, electron capture	4·1	1·00	0·44
Planetary nebulæ (Plaskett) †			
N.G.C. 1976	5·9	1·00	0·45
N.G.C. 7027	8·5	1·00	0·32

The observed decrement in prominences agrees well with the approximate (four state) calculations on the theory of polychromatic radiative equilibrium with a small value of r. Cillié's theory and the observations of the decrement in planetary nebulæ will be discussed later.

The Balmer Series Beyond Hγ.—The lines $H\delta$, etc., cannot be dealt with unless special computations of oscillator strengths are undertaken. The behaviour of the Balmer decrement near the head of the series can, however, be determined without such calculations. Consider the set of terms having a common principal quantum number N. The combined oscillator strength is given by Kramers' formula ‡

* The units are the "Schwarzschild's units" of Table I.

† *H.C.O. Circular*, 335, 1928.

‡ See *M.N.*, 95, 106, 1934, Table II. (There is a misprint of n for π.) In the above we suppose $\bar{g}=1$.

$$\Sigma qf/N = \frac{8}{3\sqrt{3} \cdot \pi},$$

while $\Sigma q = N^2$. The average f value for the continuous spectrum from an S, P or D term is therefore proportional to N^{-1}, *i.e.* $(ON) \sim N^{-1}$ for large N. But $(1N)$ and $(2N) \sim N^{-3}$ for large N, and these terms may be neglected in comparison with (ON), $(O1)$ or $(O2)$. In both (4) and (5) no terms in N are left except (ON) and (NO), which cancel out top and bottom since $(NO) = W \cdot (ON)$, so that t_N/t_1 tends to a limit as N assumes large values. The Balmer decrement at the head of the series is accordingly equal to the equilibrium value for the colour temperature of the radiation field—averaged over all wave-lengths down to the Lyman series.

Cillié's Calculations and the Decrement in Planetary Nebulæ.—Cillié calculates the Balmer decrement in planetary nebulæ by a method which is essentially similar to ours, although there appear to be great differences at first sight. He calculates the probability of an atom in a given state capturing an electron, but this is of course equivalent to calculating the emission or absorption coefficient at the head of a series. Appealing to physical intuition he assumes, following Zanstra, that an electron captured in a high state cascades downwards, emitting various line quanta, and that the reverse processes can be omitted, and Cillié calculates the proportions in which the quanta of $H\alpha$, $H\beta$ and $H\gamma$ will be emitted, the distribution of atoms among the states being determined by an equation analogous to (1). His equation is, in fact, a special case of (1), in which $r = 0$ for all line transitions. The numerical result which he finds is not very different from our result with $r = 0$, but his intensity for $H\gamma$ is greater than ours because he pays no attention to azimuthal quantisation. In the detailed theory states $5G$ and $5F$ cannot contribute to $H\gamma$ as the transitions $5G$ or $5F \rightarrow 2P$ or $2S$ are forbidden. His inclusion of the states up to $N = 7$ has an advantage over our treatment, and it appears from his work that the extra states do not make much difference to the decrement. Cillié finds hardly any dependence of the decrement upon temperature, a result with which we agree, for with $r = 0$ and W small (as in a nebula) the principal term in t_N/t_1 is $W \cdot (ON)/(N2)$, which varies approximately with $exp(-\chi_N/RT)$. Now χ_N is 0·5 volt for $N = 3$ and is smaller for larger values of N, so that doubling the temperature from 10,000° to 20,000° will only alter the ratio $H\beta/H\alpha$ by 10 per cent. Cillié is accordingly unable to account for variations in the decrement from one nebula to another.

From our point of view it is not at all clear that $r = 0$ for the Lyman lines, especially if Zanstra can speak of the Lyman radiation pressure causing the expansion of the nebula. Plaskett's result for the decrement in N.G.C. 7027 fits $r = 1$ better than $r = 0$. The difference between N.G.C. 7027 and N.G.C. 1976 may be attributed to the difference in r, the effective intensity of the Lyman lines, or it may be due to self-absorption of the Balmer lines. If there is a great pressure of Lyman radiation there will be atoms in states $2S$ and $2P$, especially the metastable $2S$, and the nebula is not transparent to Balmer radiation.

According to measurements (see page 425 of this issue) by Greaves and

Martin, the Balmer decrement from $H\alpha$ to $H\beta$ showed well-marked changes in the spectrum of Nova Herculis from 1934 December to 1935 March. Generally speaking, in the early stages when the lines had absorption components the ratio $H\beta/H\alpha$ was much larger than that found in nebulæ or prominences ; here self-absorption is suggested very strongly by the presence of the absorption components to the lines. Afterwards the decrement approached the normal nebular value with $r=0$, such as one would expect if the central star showed heavy Lyman lines and the surrounding shell was too weak to entrap the Lyman radiation.

Royal Observatory, Greenwich :
1936 *March* 7.

ABSORPTION LINES AND THE INTEGRAL EQUATION OF RADIATIVE EQUILIBRIUM.

Eberhard Hopf.

(Communicated by S. Chandrasekhar)

1. *Introduction.*—For grey material in radiative equilibrium we have Milne's well-known integral equation

$$B(\tau)=\tfrac{1}{2}\int_0^\infty E(|\,\tau-t\,|)B(t)dt,$$

where $B(\tau)$ is the integrated black-body radiation for the temperature at the optical depth τ. The solution of the problem is known to be of the form

$$B(\tau)=\tfrac{3}{4}F(\tau+q(\tau)),$$

where πF denotes the constant net flux and where $q(\tau)$ increases between the values

$$q(0)=\frac{1}{\sqrt{3}}, \qquad q(\infty)=0{\cdot}71.$$

The surface temperature is thus determined by the relation *

$$B(0)=\frac{\sqrt{3}}{4}F.$$

Although Milne's standard model of a stellar atmosphere fits the observational results in the case of the Sun fairly well, a more refined model was required in order to explain certain marked discordances between theory and observation. Thus the centre-limb contrast of the Sun's radiation is lower than on the standard model. Milne and Lindblad have explained this fact by taking into account the blanketing effect of the reversing layer. In order to obtain a satisfactory theory it was, however, necessary to introduce the

* See the author's Cambridge Tract, *Mathematical Problems of Radiative Equilibrium*, Cambridge University Press, 1934.

formation of the absorption lines in the reversing layer in a much more direct way. This was done by Woolley and, on essentially more general lines, by Chandrasekhar. Thus Chandrasekhar found it possible to account for H. H. Plaskett's high value of the colour temperature at the centre of the Sun's disc.* An important feature of Chandrasekhar's model of the outer layers is the uniform distribution of the absorption lines over the entire spectral range. This is, of course, but a crude approximation to the observed distribution of the Fraunhofer lines. Its significance rests, however, in the fact that, after the integration through the spectrum, the equations remain linear in the integrated black-body radiation B.

The purpose of the present paper is to give a rigorous discussion of Chandrasekhar's model. It is found that the mathematical methods developed in the author's Tract are still applicable to the present problem. The equations are transformed into a system of linear integral equations which is shown to have a unique solution lying between certain limits. At great optical depth τ we find, as in Milne's standard case, that

$$B(\tau) \sim \tfrac{3}{4}F\tau,$$

provided that τ is measured in terms of Rosseland's mean absorption coefficient. In the special case of pure local thermodynamical equilibrium, moreover, the precise value of $B(0)$, *i.e.* of the boundary temperature, will be derived.

2. *The Fundamental Equations.*—Within the continuous spectrum the usual equation of transfer holds,

$$\cos\theta\frac{dI_\nu}{\rho dx} = \kappa_\nu I_\nu - \kappa_\nu B_\nu,\dagger \tag{1}$$

where $I_\nu(x, \theta)$, $B_\nu(x)$, $\kappa_\nu(x)$ denote respectively specific intensity, black-body intensity and absorption coefficient at the depth x and for the frequency ν.

Within an absorption line, however, the equation of transfer becomes

$$\cos\theta\frac{dI_\nu}{\rho dx} = (\kappa_\nu + \alpha_\nu)I_\nu - (1-\epsilon_\nu)\alpha_\nu \mathfrak{J}_\nu - (\kappa_\nu + \epsilon_\nu\alpha_\nu)B_\nu, \tag{2}$$

where

$$\mathfrak{J}_\nu = \frac{1}{4\pi}\int I_\nu d\omega, \tag{3}$$

integrated through all directions. $\alpha_\nu(x)$ is the mean coefficient of scattering in the line, and $\epsilon_\nu(x)$ denotes the relative amount of ν-radiation lost by photo-electric ionizations or by collisions of the second kind, $0 \leqq \epsilon_\nu \leqq 1$.‡

Following Chandrasekhar we shall assume that the coefficient κ_ν of

* S. Chandrasekhar, "The Radiative Equilibrium of the Outer Layers of a Star with Special Reference to the Blanketing Effect of the Reversing Layer," *M.N.*, **96**, 21, 1935. Reference to former work is found in this paper.

† Since, as in the author's Tract, θ is counted from the outward normal of the layers, the signs on the right-hand side, and also the sign of the net flux πF_ν, differ from those in Chandrasekhar's paper.

‡ Chandrasekhar, *loc. cit.*

continuous absorption is independent of ν, and that the same holds for α_ν, ϵ_ν in the different absorption lines. As, formally, (1) is but a special case of (2), $\alpha_\nu = 0$, we are thus dealing, again purely formally, with a division of the spectrum into two parts, each of which is characterized by a set of three constants (with respect to ν) κ, α, ϵ. The mathematical analysis will considerably gain in clearness if, generally, the spectrum be divided into N parts such that throughout the ith part equation (2) holds with κ_ν, α_ν, ϵ_ν independent of ν within this part,

$$\kappa_i(x), \quad \alpha_i(x), \quad \epsilon_i(x); \qquad i = 1, \ldots, N.$$

Again following Chandrasekhar we suppose that the absorption lines are uniformly distributed in the spectral range, more generally, that each of those N parts is uniformly distributed in $0 < \nu < \infty$. Let the constant a_i denote the relative density of the ith part throughout the spectrum. We have, of course,

$$\Sigma a_i = 1. \tag{4}$$

On integrating (2) through the ith part we obtain

$$\cos\theta \frac{dI_i}{\rho dx} = (\kappa_i + \alpha_i) I_i - (1 - \epsilon_i)\alpha_i \mathfrak{J}_i - a_i(\kappa_i + \epsilon_i \alpha_i) B,^* \tag{5}$$

where I_i is the integrated intensity in the ith part of the spectrum and where

$$\mathfrak{J}_i = \frac{1}{4\pi}\int I_i d\omega. \tag{6}$$

B is, of course, the total black-body radiation at the depth x. Notice that, in (5), B obtains the density factor a_i. In the actual case, one of the N parts represents the continuous spectrum ($\alpha_i = 0$), whereas the other parts represent different kinds of absorption lines.†

By equating the total amount absorbed by the volume element to the amount emitted and by applying Kirchhoff's law we obtain the equation of radiative equilibrium,

$$B\Sigma a_i(\kappa_i + \epsilon_i \alpha_i) = \Sigma(\kappa_i + \epsilon_i \alpha_i)\mathfrak{J}_i. \tag{7}$$

From (5), (6) and (7) the constancy of the total net flux is derived in the usual way. On setting

$$\pi F_i = \int I_i \cos\theta d\omega,$$

we find

$$F(x) = \Sigma F_i(x) = \text{constant}. \tag{8}$$

Similarly, the quantities

$$K_i = \frac{1}{4\pi}\int I_i \cos^2\theta d\omega \ ‡ \tag{9}$$

---

* The appearance of the i in κ_i is, of course, a purely mathematical invention.

† The two extreme cases $\epsilon_i = 0$ and $\epsilon_i = 1$ signify pure scattering and pure local thermodynamical equilibrium respectively.

‡ K is defined as by Chandrasekhar and equals, therefore, $\frac{1}{4}$ of the K of my Tract.

are shown to satisfy the equation

$$\sum \frac{1}{\rho(\kappa_i+\alpha_i)}\frac{dK_i}{dx}=\tfrac{1}{4}\sum F_i=\tfrac{1}{4}F. \tag{10}$$

3. *Formulation of the Problem. The Integral Equations.*—We suppose that at great depth, $x\to\infty$, the ratios

$$\frac{\kappa_i(x)+\alpha_i(x)}{\kappa_j(x)+\alpha_j(x)} \qquad (\kappa_i=\kappa)$$

have definite limits. For the sake of greater clearness we shall, moreover, assume that those ratios are actually constant sufficiently far below the surface. In the astrophysical case the common limit will equal one $\left(\frac{\alpha_i}{\kappa}\to 0\right)$.

For Chandrasekhar's model, the Rosseland coefficient of absorption is given by

$$\frac{1}{\bar\kappa}=\sum\frac{a_i}{\kappa_i+\alpha_i}. \tag{11}$$

On introducing the new quantities $\mu_i(x)$, $\lambda_i(x)$ by

$$\mu_i=\frac{\kappa_i+\alpha_i}{\bar\kappa}, \qquad \lambda_i=\frac{\kappa_i+\epsilon_i\alpha_i}{\bar\kappa}, \qquad \mu_i\geqq\lambda_i, \tag{12}$$

our hypothesis asserts the constancy of the μ_i at great depth ($\mu_i=1$ in the astrophysical case). (11) and (12) imply

$$\sum\frac{a_i}{\mu_i}=1. \tag{13}$$

We now introduce the optical depth τ by

$$d\tau=\rho\bar\kappa dx$$

and suppose the total depth infinitely large. The fundamental equations (5) and (7) are, now,

$$\cos\theta\frac{dI_i}{d\tau}=\mu_iI_i-(\mu_i-\lambda_i)\mathfrak{J}_i-a_i\lambda_iB \tag{14}$$

and

$$B\Sigma a_i\lambda_i=\Sigma\lambda_i\mathfrak{J}_i, \tag{15}$$

$i=1,\ \ldots,\ N$. They imply (8) and (10), *i.e.* the relations

$$F=\Sigma F_i=\text{constant} \tag{16}$$

and

$$\sum\frac{1}{\mu_i}\frac{dK_i}{d\tau}=\tfrac{1}{4}F. \tag{17}$$

As the μ_i are constant at great depth, we obtain from (17)

$$\sum \frac{I}{\mu_i} K_i = \tfrac{1}{4} F\tau + \text{constant}, \tag{18}$$

for τ large.

Problem.—Given a set of numbers $a_i > 0$ satisfying (4) and a set of functions $\lambda_i > 0$, $\mu_i \geqslant \lambda_i$ satisfying (13), the μ_i being constant for large τ. (14) and (15) are to be solved for $I_i \geqq 0$ if the radiation incident on the surface vanishes,

$$I(0, \theta) = 0, \qquad \theta < \frac{\pi}{2}, \tag{19}$$

for a given net flux πF.

Solving (14) for I_i we obtain

$$I_i = \begin{cases} \sec\theta \int_\tau^\infty e^{-\int_\tau^t \mu_i ds \sec\theta} [(\mu_i - \lambda_i)\mathfrak{J}_i + a_i\lambda_i B]dt \\ |\sec\theta| \int_0^\tau e^{-\int_t^\tau \mu_i ds |\sec\theta|} [(\mu_i - \lambda_i)\mathfrak{J}_i + a_i\lambda_i B]dt \end{cases} \tag{20}$$

in the two cases $\theta < \frac{\pi}{2}$ and $\theta > \frac{\pi}{2}$ respectively. In the first case (19) is used, while in the second case no boundary condition is required.*

Hence, on inserting in (6),

$$\mathfrak{J}_i(\tau) = \tfrac{1}{2} \int_0^\infty E\left(\left| \int_t^\tau \mu_i ds \right| \right) [(\mu_i - \lambda_i)\mathfrak{J}_i(t) + a_i\lambda_i B(t)]dt, \tag{21}$$

$E = E_1$ being the first of the well-known functions E_n.† (21), taken in conjunction with (15), is the required system of integral equations for the functions .

4. *Construction of a Solution.*—It is convenient to introduce the notation

$$L_i(f_i, F) \equiv \tfrac{1}{2} \int_0^\infty E\left(\left| \int_t^\tau \mu_i ds \right| \right) [(\mu_i - \lambda_i)f_i + a_i\lambda_i F]dt \tag{22}$$

for the linear integral operator on the right-hand side of (21). The system of integral equations in question is, then,

$$f_i = L_i(f_i, \phi), \qquad \phi = \frac{\Sigma\lambda_i f_i}{\Sigma\lambda_i a_i}. \ddagger \tag{23}$$

An important property of the operators L_i is their positivity. The inequalities

$$f_i(\tau) \leqq g_i(\tau), \qquad 0 < \tau < \infty,$$

for all i evidently imply the inequalities

---

* This is easily seen by an argument similar to the one employed in proving Theorem 1 of the author's Tract.

† See p. 21 of my Tract.

‡ We must, in the sequel, bear in mind that the second argument ϕ in $L_i(f_i, \phi)$ is always connected to the f_i's by means of the second equation (23).

$$L_i(f_i, \phi) \leqq L_i(g_i, \psi),$$

$$\phi = \frac{\Sigma \lambda_i f_i}{\Sigma \lambda_i a_i}, \qquad \psi = \frac{\Sigma \lambda_i g_i}{\Sigma \lambda_i a_i},$$

for all τ and all i. The positivity will enable us to argue similarly as in the simpler cases treated in my Tract.

We now prove

Theorem 1.—The equations (23) have a positive solution of the form

$$f_i(\tau) = a_i(\tau + q_i(\tau)), \qquad |\, q_i(\tau)\,| < C, \tag{24}$$

where the constant C depends only on the μ_i and not on the a_i or λ_i.

Proof.—We begin with the remark that in the case

$$f_i = a_i f, \qquad \phi = \frac{\Sigma \lambda_i f_i}{\Sigma \lambda_i a_i} = f$$

necessarily

$$(\mu_i - \lambda_i) f_i + a_i \lambda_i \phi = a_i \mu_i f.$$

On integrating by parts and using the function E_2 we obtain, still in that case, the formula

$$L_i(a_i f, f) = a_i f(\tau) - \frac{a_i}{2} E_2\left(\int_0^\tau \mu_i ds\right) f(0) + \frac{a_i}{2}\int_\tau^\infty E_2\left(\int_\tau^t \mu_i ds\right) df(t) - \frac{a_i}{2}\int_0^\tau E_2\left(\int_t^\tau \mu_i ds\right) df(t). \tag{25}$$

We shall apply this formula to two important special cases, the first being the case $f = c =$ constant. We thus obtain

$$L_i(a_i c, c) = a_i c - \frac{a_i c}{2} E_2\left(\int_0^\tau \mu_i ds\right), \tag{26}$$

which implies the important inequalities

$$L_i(a_i c, c) < a_i c, \qquad (c > 0), \tag{27}$$

for all values of τ. In the second case in question, namely, $f = \tau$, we find

$$L_i(a_i t, t) = a_i \tau + \frac{a_i}{2}\left[\int_\tau^\infty E_2\left(\int_\tau^t \mu_i ds\right) dt - \int_0^\tau E_2\left(\int_t^\tau \mu_i ds\right) dt\right]. \tag{28}$$

As, now, the $\mu_i(t)$ are constant for t sufficiently large, say for $t > b$, the first term within the square bracket will equal, for $\tau > b$,

$$\int_\tau^\infty E_2(\mu_i(t - \tau)) dt = \frac{1}{\mu_i} E_3(0). \tag{29}$$

The second term can, again for $\tau > b$, be written

$$-\int_0^b E_2\left(\int_t^\tau \mu_i ds\right) dt - \frac{1}{\mu_i} E_3(0) + \frac{1}{\mu_i} E_3(\mu_i(\tau - b)), \tag{30}$$

the first part of which is evidently of the form

$$-\int_0^b E_2(\rho+(\tau-b)\mu_i)dt = -bE_2(\rho^*+(\tau-b)\mu_i),$$

where ρ and ρ^* remain bounded.

Hence the sum of (29) and (30), *i.e.* the square bracket on the right of (28), equals, for $\tau > b$,

$$[\,.\,.\,.] = \frac{1}{\mu_i}E_3(\mu_i\tau-\mu_i b) - bE_2(\mu_i\tau+\rho^*-\mu_i b).$$

Since, now, the quotients

$$\frac{E_3(x)}{E_2(x)}, \qquad \frac{E_2(x+A)}{E_2(x)}, \qquad A = \text{constant},$$

lie between positive limits,* we infer that, for $\tau > b$,

$$|\,[\,.\,.\,.]\,| < \text{constant } E_2(\mu_i\tau).$$

A suitable choice of the constant will render this true also for $\tau < b$. Notice that the constant depends only on the behaviour of the functions μ_i. As the E_2-term in (26) will obey a similar inequality, we obviously obtain inequalities of the form

$$a_i\tau - \frac{a_iC}{2}E_2\left(\int_0^\tau \mu_i ds\right) < L_i(a_it,\, t) < a_i\tau + \frac{a_iC}{2}E_2\left(\int_0^\tau \mu_i ds\right), \tag{31}$$

for any $\tau \geqq 0$. The constant C depends on the μ_i's only.

The principal consequence of (26) and (31) are the two sets of inequalities

$$L_i\{a_i(t+C),\, t+C\} < a_i(\tau+C) \tag{32}$$

and

$$L_i\{a_i(t-C),\, t-C\} > a_i(\tau-C), \tag{33}$$

holding for all values of τ. They represent a generalization of the two key-inequalities † established in Milne's standard case. Similarly as in this case (32) and (33) imply the existence of a solution of (23) between the limits

$$a_i(\tau-C) < f_i < a_i(\tau+C).$$

This time, however, it is preferable to start with the upper functions as initial functions

$$f_i^{(1)} = a_i(\tau+C),$$

$$f_i^{(n+1)} = L_i(f_i^{(n)},\, \phi^{(n)}), \qquad \phi^{(n)} = \frac{\Sigma\lambda_i f_i^{(n)}}{\Sigma\lambda_i a_i}.$$

The positivity argument then shows that, for any i,

$$f_i^{(1)}(\tau) > f_i^{(2)}(\tau) > \ldots > a_i(\tau-C).$$

---

* § 8 of the author's Tract. † (89) and (90) in the author's Tract.

The limit functions

$$f_i(\tau) = \lim_{n=\infty} f_i^{(n)}(\tau), \qquad \phi(\tau) = \lim_{n=\infty} \phi^{(n)}(\tau),$$

are as usual seen to satisfy (23). This arrangement is preferred because $f_i^{(1)}$ and therefore, according to the positivity of the operators, all functions $f_i^{(n)}$ automatically become positive. The limit functions are thus immediately shown to be positive,* which completes the proof of Theorem 1.

5. *The Net Flux. Uniqueness.*—To obtain the solution of our general problem we have to multiply our solution of (23) by a constant factor and determine its relation to the given total net flux πF. This results in the

Theorem 2.—The solution of the problem formulated above is given by

$$\mathfrak{J}_i(\tau) = \tfrac{3}{4}Fa_i f_i(\tau), \qquad B(\tau) = \tfrac{3}{4}F\phi(\tau),$$

where f_i and ϕ are the functions of Theorem 1.

Proof.—Notice that thus

$$B(\tau) \sim \tfrac{3}{4}F\tau, \qquad \mathfrak{J}_i(\tau) \sim a_i B(\tau),$$

for τ large. We must remember, here, that τ is measured in terms of the Rosseland coefficient of absorption.

For our purpose we need two more equations. They are obtained on inserting the expressions (20) for the intensities into F_i and K_i. Hence

$$\begin{aligned} F_i = 2\int_\tau^\infty E_2\left(\int_\tau^t \mu_i ds\right)[(\mu_i - \lambda_i)\mathfrak{J}_i + a_i\lambda_i B]dt \\ - 2\int_0^\tau E_2\left(\int_t^\tau \mu_i ds\right)[(\mu_i - \lambda_i)\mathfrak{J}_i + a_i\lambda_i B]dt \end{aligned} \tag{34}$$

and

$$K_i = \tfrac{1}{2}\int_0^\infty E_3\left(\left|\int_t^\tau \mu_i ds\right|\right)[(\mu_i - \lambda_i)\mathfrak{J}_i + a_i\lambda_i B]dt. \tag{35}$$

On settling, tentatively,

$$\mathfrak{J}_i = ca_i f_i, \qquad B = c\phi,$$

we find that the square bracket in (35) is of the form

$$\mu_i\mathfrak{J}_i + o(1) = \frac{ca_i}{\mu_i(\infty)}\mu_i(t)\int_0^t \mu_i ds + O(1),$$

thus yielding

$$\frac{\mu_i(\infty)}{ca_i}K_i = \tfrac{1}{2}\int_0^\infty E_3(\,|\,x-y\,|\,)y\,dy = \tfrac{1}{3}x + O(1),$$

where

$$x = \int_0^\tau \mu_i ds = \mu_i(\infty)\tau + O(1).$$

Hence

$$K_i = \frac{ca_i}{3}\tau + O(1).$$

* At least non-negative. The positivity is, then, readily inferred from the integral equations (23).

If this be inserted in (18) the relation

$$\frac{c}{3}\sum\frac{a_i}{\mu_i}=\frac{F}{4}$$

follows which, according to (13), proves our theorem.

It is necessary to complete our investigation by the

Theorem 3.—Every positive solution of the integral equations (23) is necessarily a constant multiple of the solution of Theorem 1.

Proof.—We can argue in a similar way as in Milne's standard case. Suppose g_i, ψ to be a non-negative solution of (23),

$$g_i(\tau)\geqq 0, \qquad \psi(\tau)\geqq 0. \tag{36}$$

We prove that

$$g_i = cf_i, \qquad \psi = c\phi.$$

For this purpose let

$$b = \text{greatest lower bound of } \psi(\tau)/\phi(\tau).$$

The functions

$$\mathfrak{f}_i = g_i - bf_i, \qquad B = \psi - b\phi, \tag{37}$$

represent a solution of the equations (23) with the properties

$$B\geqq 0, \qquad \text{gr. l. b. of } B/\phi = 0. \tag{38}$$

An additional complication, as compared with the standard case, arises, however, from the fact that the inequalities

$$\mathfrak{f}_i\geqq 0 \tag{39}$$

are not in evidence. Their proof may be postponed to the end of the section.

Our aim is to show that $\mathfrak{f}_i\equiv B\equiv 0$. Two cases are again possible. Either the greatest lower bound in (38) is attained for a finite $\tau=\tau_0$ or not. In the first case we need only to observe that, for $\tau=\tau_0$, $B=0$ and, in virtue of (39) and of

$$B=\frac{\Sigma\lambda_\nu\mathfrak{f}_\nu}{\Sigma\lambda_\nu a}, \tag{40}$$

$\mathfrak{f}_i=0$. The left-hand sides of (23) therefore vanish for $\tau=\tau_0$, whence $\mathfrak{f}_i\equiv B\equiv 0$. In the second case, however, it follows that

$$\lim_{\tau\to\infty}\frac{B(\tau)}{\tau}=0. \tag{41}$$

Observe here that $\phi\sim\tau$ for τ large. Hence, in virtue of (39) and (40),

$$\lim_{\tau\to\infty}\frac{\mathfrak{f}_i(\tau)}{\tau}=0. \tag{42}$$

From (21) and (35) and from $E_3<E_1$,

$$K_i<\mathfrak{f}_i$$

and, therefore,

$$\lim_{\tau\to\infty}\frac{K_i(\tau)}{\tau}\leqq\lim_{\tau\to\infty}\frac{\mathcal{J}_i(\tau)}{\tau}.$$

If this be combined with (18) and (42) we obtain $F\leqq 0$ for the net flux. This gives if (34), $\tau=0$, be taken into account

$$0\geqq F=\Sigma F_i=2\Sigma\int_0^\infty E_2\left(\int_0^t\mu_i ds\right)[(\mu_i-\lambda_i)\mathcal{J}_i+a_i\lambda_i B]dt,$$

whence, in virtue of (38) and (39), $\mathcal{J}_i\equiv B\equiv 0$.

The proof of (39) will now be outlined. Dropping the affix i in (21) we may write this equation

$$\mathcal{J}(\tau)=\wedge(\mathcal{J})+P(\tau), \tag{43}$$

where, according to $B\geqq 0$,

$$P(\tau)\geqq 0, \tag{44}$$

and where the operator $\wedge$ is defined by

$$\wedge(f)=\tfrac{1}{2}\int_0^\infty E\left(\left|\int_t^\tau\mu ds\right|\right)(\mu-\lambda)f dt. \tag{45}$$

Notice that λ has a positive lower bound and that, therefore, for all values of t,

$$0\leqq\mu-\lambda\leqq\vartheta\mu\,;\qquad 0<\vartheta<1,$$

ϑ being a constant. Applying $\wedge$ to the particular function

$$1+\int_0^\tau\mu ds=x$$

we find after some simple integrations that

$$\wedge\left(1+\int_0^t\mu ds\right)\leqq\vartheta(1+x+\tfrac{1}{2}E_3(x)-\tfrac{1}{2}E_2(x))\,; \tag{46}$$

whence, in virtue of $E_3<E_2$,

$$\wedge\left(1+\int_0^t\mu ds\right)<\vartheta\left(1+\int_0^\tau\mu ds\right). \tag{47}$$

(24), (36) and (37) show, now, that the quantity

$$\beta=\text{greatest lower bound of }\frac{\mathcal{J}(\tau)}{1+\int_0^\tau\mu ds}$$

cannot be minus infinity. We thus obtain

$$\mathcal{J}(\tau)\geqq\beta\left(1+\int_0^\tau\mu ds\right),$$

and, according to (43) and (44),

$$\mathcal{J}(\tau)\geqq\wedge(\mathcal{J})\geqq\beta\wedge\left(1+\int_0^t\mu ds\right). \tag{48}$$

We are to prove that $\beta \geqq 0$. If, on the contrary, $\beta < 0$, we should infer from (47) and (48) that

$$\mathfrak{J}(\tau) > \vartheta\beta\left(1 + \int_0^\tau \mu ds\right).$$

Hence $\beta \geqq \vartheta\beta$ or $\beta(1-\vartheta) \geqq 0$, in contradiction to the assumption $\beta < 0$. The proof of our theorem is thus completed.

6. *A Special Case. The Boundary Temperature.*—We now consider the special case of pure local thermodynamical equilibrium, $\epsilon_i = 1$, *i.e.*

$$\lambda_i = \mu_i,$$

and suppose that, for every i separately,

$$\mu_i = \text{constant}.$$

In this case, the fundamental equations (22), (23) go over into a single integral equation for ϕ,

$$\phi(\tau) = \int_0^\infty H(|\tau - t|)\phi(t)dt, \tag{49}$$

where

$$H(u) = \tfrac{1}{2}\frac{\Sigma a_i \mu_i^2 E(\mu_i u)}{\Sigma a_i \mu_i}. \tag{50}$$

(49) is just the type of equation studied in my Tract.*

Our present Theorem 1 asserts the existence of a solution of (49) having the form

$$\phi(\tau) \sim \tau$$

for τ large. Theorem X of the Tract gives, then, the precise value of $\phi(0)$,

$$\phi(0) = \sqrt{2H_4(0)},$$

where

$$H_1 = H, \qquad H_{n+1} = \int_u^\infty H_n du.$$

This evaluates to

$$\phi(0) = \sqrt{E_4(0)\Sigma\frac{a_i}{\mu_i}\Big/\Sigma a_i\mu_i}, \qquad E_4(0) = \tfrac{1}{3}.$$

Taking into account the present Theorem 2 and (13) we finally obtain the relation

$$B_0 = \frac{\sqrt{3}}{4\sqrt{\Sigma a_i \mu_i}} F, \tag{51}$$

which is to be taken in conjunction with (13). From Cauchy's inequality,

$$1 = \left(\Sigma\sqrt{\frac{a_i}{\mu_i}}\sqrt{a_i\mu_i}\right)^2 < \Sigma\frac{a_i}{\mu_i}\Sigma a_i\mu_i = \Sigma a_i\mu_i$$

---

* Equations (110) and (118). All the hypotheses, namely, the relations (116), (117) and (119), are readily seen to be fulfilled in the present case.

unless $\mu_1=\mu_2=\ldots=1$. *Hence the boundary temperature proves to be lower than in Milne's standard case.* This was already stated by Dr. Chandrasekhar on the base of his approximate calculations. We are also able to confirm his second statement, namely, that the temperature gradient is higher than in the case of grey material. We know from our Theorem 2 that, for τ large,

$$B(\tau)\sim\tfrac{3}{4}F\tau,$$

where τ is the Rosseland depth

$$\tau=\int_{-\infty}^{x}\bar{\kappa}\rho dx.$$

Now

$$\bar{\kappa}=\frac{1}{\sum\frac{a_i}{\kappa+\alpha_i}}>\frac{\kappa}{\Sigma a_i}=\kappa,$$

unless $\alpha_i\equiv 0$.

Another property of the solution of (49) is that in

$$\phi(\tau)=\tau+q(\tau)$$

the remainder function $q(\tau)$ increases. For the proof the reader is referred to § 16 of my Tract. On closer inspection it will be noticed that the general proof given there makes only use of the inequalities

$$H_n^2<H_{n-1}H_{n+1}. \tag{52}$$

These inequalities are well known to be satisfied by the functions E_n. In the case (50) we find

$$H_n(u)=\frac{\Sigma a_i\mu_i^{3-n}E_n(\mu_i u)}{\Sigma a_i\mu_i},$$

and, on using $E_n^2<E_{n-1}E_{n+1}$,

$$H_n(u)\sum a_i\mu_i<\sum_i\sqrt{a_i\mu_i^{3-(n-1)}E_{n-1}(\mu_i u)}\sqrt{a_i\mu_i^{3-(n+1)}E_{n+1}(\mu_i u)},$$

whence, by the Cauchy inequality, (25) follows.

Limits for $q(\infty)$ could also be derived in the present case. The application of Chapter IV of my Tract leads to rigorous but exceedingly complex expressions.

Department of Mathematics,
The Massachusetts Institute of Technology,
Cambridge, Mass.:
1936 *February* 18.

THE RELATION BETWEEN THE PERIOD AND THE ECCENTRICITY IN THE ORBITS OF THE BINARY STARS.

H. Horrocks, M.A.

1. *Introduction and Summary.*—The various physical factors that have been considered in attempts to explain the well-known relation between the eccentricity and period in the orbits of binary stars have not been found adequate. Russell * examined the effect of tidal action, and found that the increase in the dimensions of the orbit is quite inadequate for the present purpose. Jeans † has examined the effect of a secular decrease in the masses of the stars, and found that the eccentricity remains constant and that the semi-major axis of the orbit varies inversely as the total mass. With the range of observed stellar masses this does not allow a sufficiently great increase in the orbital dimensions. Walters ‡ has examined the average effect of encounters in the case of close spectroscopic binaries, and found that after a sufficiently long interval the eccentricity would be increased appreciably but that the change in the semi-major axis would be insignificant.

In the present paper the effect of the propagation of gravity with finite velocity is examined. We find that the eccentricity and the period will be increased, and that the resulting relation between them agrees satisfactorily with the observed statistical relation. The effect of varying mass is also included in our equations. The motion of a binary system in space is also examined, and appears to be not inconsistent with available observational evidence.

The time scale for the development of the orbits of binary stars under these circumstances is also examined. It is proportional to the velocity of propagation of gravity, and need not exceed the time scale derived from the theory of stellar evolution by the loss of mass by radiation in order that a sufficiently large value may be assigned to that velocity to satisfy other necessary conditions. The eccentricity is found to increase rapidly when small.

2. *Forces and Accelerations.*—We adopt the fundamental equation given by Jeans for the motion of a star when losing mass by radiation, viz.

$$\text{mass} \times \text{force} = \text{acceleration},$$

the underlying assumption being that when matter in motion is being transformed into radiation, the radiant energy carries away the same nett momentum as the matter "annihilated" had before transformation.

* *Ap. J.*, **31**, 185, 1910.
† *M.N.*, **85**, 2, 1924.
‡ *M.N.*, **92**, 786, 1932 ; **93**, 28, 1932.

We consider two masses m_1, m_2, and write $M = m_1 + m_2$. Introduce two quantities p and q defined by

$$Mp = m_1 - m_2, \quad \text{and} \quad M^2q = 2m_1m_2 = \tfrac{1}{2}M^2(1 - p^2). \tag{1}$$

Let (x_1, y_1, z_1), (u_1, v_1, w_1), (a_1, b_1, c_1) be the co-ordinates, velocity components, and components of acceleration of mass m_1, and similarly for mass m_2. Define $(\bar{x}, \bar{y}, \bar{z})$, $(\bar{u}, \bar{v}, \bar{w})$, $(\bar{a}, \bar{b}, \bar{c})$ as follows :—

$$M\bar{x} = m_1x_1 + m_2x_2, \qquad M\bar{u} = m_1u_1 + m_2u_2, \qquad M\bar{a} = m_1a_1 + m_2a_2, \text{ etc.} \tag{2}$$

It is to be noted that when masses m_1, m_2 in motion have varying mass, the velocities and accelerations of the centre of mass are given by the equations

$$\bar{u} = \dot{\bar{x}} + \tfrac{1}{2}\dot{p}(x_2 - x_1), \text{ etc.}, \quad \text{and} \quad \bar{a} = \dot{\bar{u}} + \tfrac{1}{2}\dot{p}(u_2 - u_1), \text{ etc.} \tag{3}$$

We have the further relations

$$u_1 + u_2 = 2\bar{u} + p(u_2 - u_1), \text{ etc.}, \tag{4}$$

$$m_1u_1 - m_2u_2 = M[p\bar{u} - q(u_2 - u_1)], \text{ etc.} \tag{5}$$

We may suitably call $(\bar{u}, \bar{v}, \bar{w})$ and $(\bar{a}, \bar{b}, \bar{c})$ the mass velocity and mass acceleration of the system.

In considering the mutual gravitational attractions of two stars when the action of gravity is propagated with finite velocity, we shall assume that each star can be treated as if its whole mass were concentrated at its centre. For close binary stars, such as eclipsing variables, this approximation will cease to give a close representation of the forces under consideration, for not only are the components deformed by tidal action, but also the time for gravitational action to be propagated through either star is then comparable with the time for propagation between the centres.

Retaining only terms of the first order of small quantities, we thus assume that the star m_1 is attracted at time t towards the point

$$([x_2 - \kappa ru_2], [y_2 - \kappa rv_2], [z_2 - \kappa rw_2])$$

as if m_2 occupied that position. Here r is the distance between the centres of the two stars at time t, and κ is the reciprocal of the velocity of propagation of gravity. Putting G for the constant of gravitation, the components of force on m_1 are (X_1, Y_1, Z_1) where

$$X_1 = Gm_1m_2r^{-4}[x_2 - x_1 - \kappa ru_2][r + 3\kappa\{(x_2 - x_1)u_2 + (y_2 - y_1)v_2 + (z_2 - z_1)w_2\}], \quad \text{etc.} \tag{6}$$

3. *Equations of Motion.*—From the equations

$$m_1a_1 = X_1, \qquad m_2a_2 = X_2, \text{ etc.},$$

we can now derive the six equations of motion in the form

$$a_2 - a_1 + GMr^{-3}(x_2 - x_1) = Gr^{-4}\left[\begin{array}{l} 3\kappa(x_2 - x_1)\sum_{xyz}(x_2 - x_1)(m_1u_1 - m_2u_2) \\ -\kappa r^2(m_1u_1 - m_2u_2) \end{array}\right], \text{ etc.}, \tag{7}$$

$$\dot{\bar{u}} + \tfrac{1}{2}\dot{p}(u_2 - u_1) = \tfrac{1}{2}GMqr^{-4}\left[\begin{array}{l} 3\kappa(x_2 - x_1)\sum_{xyz}(x_2 - x_1)(u_1 + u_2) \\ -\kappa r^2(u_1 + u_2) \end{array}\right], \text{ etc.} \tag{8}$$

If both stars are passing through the x-axis at the instant under consideration the equations take the form

$$a_2 - a_1 + GMr^{-3}(x_2 - x_1) = 2\kappa GMr^{-2}[p\bar{u} - q(u_2 - u_1)], \tag{9}$$

$$b_2 - b_1 = -\kappa GMr^{-2}[p\bar{v} - q(v_2 - v_1)], \text{ etc.,} \tag{10}$$

$$\dot{\bar{u}} + \tfrac{1}{2}\dot{p}(u_2 - u_1) = \kappa qGMr^{-2}[2\bar{u} + p(u_2 - u_1)], \tag{11}$$

$$\dot{\bar{v}} + \tfrac{1}{2}\dot{p}(v_2 - v_1) = -\tfrac{1}{2}\kappa qGMr^{-2}[2\bar{v} + p(v_2 - v_1)], \text{ etc.,} \tag{12}$$

the remaining two equations being similar in form to equations (10) and (12).

4. *Transformation to Rotating Axes.*—Now consider a set of rotating axes $O(x, y, z)$ with the origin at the centre of m_1, with Ox passing through the centre of m_2 making $x_2 = r$, and with Oy in the plane of the velocity of m_2 relative to m_1 in the direction which makes the y-component of that velocity positive. Write (U, V, W) for the components of the mass velocity of the system at any time parallel to the directions of these axes. For the angular velocities of the axes write

$$\omega_x = \dot{\psi}, \qquad \omega_y = 0, \qquad \omega_z = \dot{\theta}.$$

The equations of motion must now be written in the form

$$\ddot{r} - r\dot{\theta}^2 + GMr^{-2} = 2\kappa GMr^{-2}[pU - q\dot{r}], \tag{13}$$

$$\frac{1}{r}\frac{d}{dt}(r^2\dot{\theta}) = -\kappa GMr^{-2}[pV - qr\dot{\theta}], \tag{14}$$

$$r\dot{\theta}\dot{\psi} = -\kappa GMr^{-2}[pW], \tag{15}$$

$$\dot{U} - V\dot{\theta} = \kappa qGMr^{-2}[2U + p\dot{r}] - \tfrac{1}{2}\dot{p}\dot{r}, \tag{16}$$

$$\dot{V} + U\dot{\theta} - W\dot{\psi} = -\tfrac{1}{2}\kappa qGMr^{-2}[2V + pr\dot{\theta}] - \tfrac{1}{2}\dot{p}r\dot{\theta}, \tag{17}$$

$$\dot{W} + V\dot{\psi} = -\tfrac{1}{2}\kappa qGMr^{-2}[2W]. \tag{18}$$

5. *Secular Variations of the Orbit.*—Introducing $v = \theta - \omega$, the well-known solution for unperturbed motion (*i.e.* for instantaneous propagation of gravitational attraction and constant mass) is

$$\left.\begin{aligned} r^{-1} &= F + E\cos v, \qquad r^2\dot{\theta} = h, \qquad h^2F = GM, \\ U &= U_0\cos v + V_0\sin v, \qquad V = V_0\cos v - U_0\sin v, \end{aligned}\right\} \tag{19}$$

in which ω, h, E, U_0, V_0 are all constants, and also W is constant and $\dot{\psi}$ is zero. Letting these quantities vary when the mass is not constant and κ is not zero, and retaining quantities of the first order in $\dot{M}$ and κ, we obtain after some reduction

$$\dot{r} = hE\sin v,$$

$$\begin{aligned} \frac{dE}{d\theta} + \frac{\dot{M}}{M}\frac{F}{h}r^2\cos v &= 2\kappa qhF^2\cos v - 3\kappa qhFE\sin^2 v \\ &\quad + \kappa pF[3U_0\sin v\cos v + V_0(3\sin^2 v - 1)] \\ &\quad + \kappa pFr[E - F\cos v][V_0\cos v - U_0\sin v], \end{aligned} \tag{20}$$

$$\begin{aligned} E\frac{d\omega}{d\theta} + \frac{\dot{M}}{M}\frac{F}{h}r^2\sin v &= 2\kappa qhF^2\sin v + 3\kappa qhFE\sin v\cos v \\ &\quad + \kappa pF[U_0(1 - 3\cos^2 v) - 3V_0\sin v\cos v] \\ &\quad - \kappa pF^2r\sin v[V_0\cos v - U_0\sin v], \end{aligned} \tag{21}$$

$$\frac{1}{h}\frac{dh}{d\theta} = \kappa qhF - \kappa pFr[V_0 \cos v - U_0 \sin v], \tag{22}$$

$$\begin{aligned}\frac{dU_0}{d\theta} - V_0\frac{d\omega}{d\theta} &= \tfrac{1}{2}\dot{p}Fr^2 \sin v + \kappa pFrW^2 \sin v \\ &\quad + \tfrac{1}{2}\kappa pqh^2F[F \sin v + 3E \sin v \cos v] \\ &\quad + \kappa qhF[U_0(3\cos^2 v - 1) + 3V_0 \sin v \cos v],\end{aligned} \tag{23}$$

$$\begin{aligned}\frac{dV_0}{d\theta} + U_0\frac{d\omega}{d\theta} &= -\tfrac{1}{2}\dot{p}r^2[F \cos v + E] - \kappa pFrW^2 \cos v \\ &\quad - \tfrac{1}{2}\kappa pqh^2F[F \cos v + E(1 - 3\sin^2 v)] \\ &\quad + \kappa qhF[3U_0 \sin v \cos v + V_0(3\sin^2 v - 1)],\end{aligned} \tag{24}$$

$$\frac{dW}{d\theta} = -\kappa qhFW + \kappa pFWr[V_0 \cos v - U_0 \sin v], \tag{25}$$

$$\frac{d\psi}{d\theta} = -\kappa pFWr. \tag{26}$$

It is clear that in the above equations (20) to (26) differentiation with respect to v can be substituted for differentiation with respect to θ since the approximation is to the first order. To determine the secular variations of the orbital elements we integrate these equations between v and $v + 2\pi$, thus obtaining the increments ΔE, etc., in a revolution relative to the apse. Neglecting quantities of the first order, and introducing the usual angle ϕ defined by $e = \sin\phi$, where e is the eccentricity of the orbit, we have

$$\int_v^{v+2\pi} r dv = 2\pi F^{-1} \sec\phi, \qquad \int_v^{v+2\pi} r \cos v dv = -2\pi F^{-1} \tan\frac{\phi}{2} \sec\phi,$$

$$\int_v^{v+2\pi} r^2 dv = 2\pi F^{-2} \sec^3\phi, \qquad \int_v^{v+2\pi} r^2 \cos v dv = -2\pi F^{-2} \sin\phi \sec^3\phi,$$

$$\int_v^{v+2\pi} r \cos^2 v dv = \pi F^{-1} \sec^2\frac{\phi}{2} \sec\phi.$$

Also we have

$$P = 2\pi h^{-1} F^{-2} \sec^3\phi, \tag{27}$$

hence

$$\Delta E + \frac{M}{M}\frac{F}{h}\int_v^{v+2\pi} r^2 \cos v dv = \Delta E - E\frac{\Delta M}{M} = E\left[\frac{\Delta e}{e} - 2\frac{\Delta h}{h}\right],$$

where P is the orbital period. After some reduction we thus obtain

$$\frac{1}{e}\Delta e = \pi\kappa GMq\frac{1}{h} + \tfrac{1}{2}\pi\kappa pV_0 \tan\frac{\phi}{2}\sec^2\frac{\phi}{2}, \tag{28}$$

$$\frac{1}{h}\Delta h = 2\pi\kappa GMq\frac{1}{h} + 2\pi\kappa pV_0 \tan\frac{\phi}{2}\sec\phi, \tag{29}$$

$$\Delta\omega = \tfrac{1}{2}\pi\kappa pU_0 \tan\frac{\phi}{2}\sec^2\frac{\phi}{2}, \tag{30}$$

$$\Delta U_0 - V_0\Delta\omega = \pi\kappa GMq\frac{1}{h}U_0, \tag{31}$$

$$\Delta V_0 + U_0\Delta\omega = \pi\kappa GMq\frac{1}{h}V_0 + 2\pi\kappa pW^2\tan\frac{\phi}{2}\sec\phi + \tfrac{1}{2}\pi\kappa G^2M^2pq\frac{\sin\phi}{h^2}, \tag{32}$$

$$\Delta W = -2\pi\kappa GMq\frac{1}{h}W - 2\pi\kappa pV_0W\tan\frac{\phi}{2}\sec\phi, \tag{33}$$

$$\Delta\psi = -2\pi\kappa pW\sec\phi. \tag{34}$$

6. *Case of Double Stars with Components of Equal Mass.*—Among the double stars whose orbital elements are known and for which the mass or $m\sin^3 i$ has been determined for each component, very few have a mass ratio less than $\frac{2}{3}$. When the components are of equal mass we have $p=0$ and $q=\frac{1}{2}$. When the mass ratio is as small as $\frac{2}{3}$ we have $p=0{\cdot}2$ (20 per cent. of its maximum value) and $q=0{\cdot}48$. In view of the fact that in equations (28) to (34) p always occurs multiplied by e when other terms are present in the expressions for the secular variations, the assumption of equal mass is to be expected to give a good approximation to the motion in the great majority of cases for which observational data are available. Putting ν for the circular component of the velocity in the relative orbital motion, we then have

$$\left.\begin{aligned}&\Delta\omega = \Delta\psi = 0,\\ &\Delta\log e = \tfrac{1}{2}\Delta\log h = \Delta\log U_0 = \Delta\log V_0 = -\tfrac{1}{2}\Delta\log W = \tfrac{1}{2}\pi\kappa\nu.\end{aligned}\right\} \tag{35}$$

From equations (35) and (27) we have at once

$$h = Ce^2, \qquad f = PM^2e^{-6}(1-e^2)^{\frac{3}{2}} = 2\pi C^3G^{-2} = \text{const.} \tag{36}$$

In this case we can at once derive also an expression for the time that a binary star orbit takes to develop from eccentricity e_1 to eccentricity e_2. Using equation (27) for the period ($=\Delta t$) and equations (35) and (36) for Δe and h, we find at once

$$\frac{\Delta t}{\Delta e} = \frac{4C^4e^7}{\kappa G^3M^3(1-e^2)^{\frac{3}{2}}}. \tag{37}$$

7. *Orbital Plane and Motion in Space.*—It is to be noted that (34) does not give the rotation of the orbital plane in space. Let us take axes $O(\xi, \eta)$ fixed as regards orientation and coinciding at a particular instant with the negative direction of Oy and the positive direction of Ox respectively. If (ξ, η) are the projections of the pole of the orbital plane at any time during the course of the next revolution, we have to our degree of approximation

$$\dot\xi = \dot\psi\cos\theta, \qquad \frac{d\xi}{d\theta} = -\kappa pFWr\cos(\omega+v), \tag{38}$$

$$\dot\eta = \dot\psi\sin\theta, \qquad \frac{d\eta}{d\theta} = -\kappa pFWr\sin(\omega+v). \tag{39}$$

For the change in the course of a revolution we have

$$\Delta\xi = 2\pi\kappa pW \cos\omega \tan\frac{\phi}{2}\sec\phi, \tag{40}$$

$$\Delta\eta = 2\pi\kappa pW \sin\omega \tan\frac{\phi}{2}\sec\phi. \tag{41}$$

Thus in all cases the orbital plane rotates about the line of apsides, the side towards which the smaller mass moves at periastron tilting towards the component of mass velocity normal to the orbital plane, the amount of the tilt being proportional to pW and approximately proportional to e. For binaries with equal components the orbital plane has no rotation either secular or periodic as appears in equation (15).

As regards the mass velocity of the system, when the components are of equal mass equations (35) give at once U_0 and V_0 proportional to each other and to the eccentricity, and W inversely proportional to the square of the eccentricity. The motion of the system is thus expected to be such that the normal component of mass velocity will tend to vanish rapidly, but the component in the plane of the orbit will tend to increase more slowly whilst retaining a constant inclination to the line of apsides. On the whole there should be a tendency for the resultant mass velocities of binary systems to be increased when the eccentricities have been doubled or trebled, but the dispersion of the velocities is to be expected to be considerable. A test of the theory on this ground is therefore hardly to be expected to be satisfactory. Moreover, the question of the choice of frame of reference arises. If we assume that the action of gravity is propagated in a medium which is at rest relative to the average of matter in a large volume of space, we may be concerned with the peculiar motions of the stars. The mean peculiar radial velocities of the stars in sections two and three of the table are given. These are seen to be slightly greater for visual than for spectroscopic binaries. The evidence cannot be regarded as sufficient either to favour or to condemn the theory.

The results of numerous investigations seeking any possible systematic distribution of the poles of the orbital planes of binary stars are in conflict. It appears that the available observational material is insufficient to establish any systematic grouping of the poles, and also that, even if such a tendency exists, the dispersion about the mean distribution is very great. This negative result is at least in conformity with our theory, for we have seen that for systems with nearly equal components any rotation of the orbital planes would be small and would decrease through the reduction of the normal component of the mass velocity.

8. *Comparison with Observed Eccentricities and Periods.*—A relation of the form given in (36) should hold statistically, the degree of accordance of the various groups taken depending on the dispersion in the initial conditions of the orbital motion of binary systems as specified by C. In his recent edition of his book *The Binary Stars* Aitken gives a list of orbits for 116 visual and 326 spectroscopic binaries. We have computed $\log [Pe^{-6}(1-e^2)^{\frac{3}{2}}]$ from the mean values of P and e given for various ranges of period. The results are

TABLE

$\log f = \log PM^2 e^{-6}(1-e^2)^{\frac{3}{2}}$ and $\log (f/M^2)$ (*Period in Days*)

	Range of P	No.	Mean Values of		$\log\left(\frac{f}{M^2}\right)$	Systems of Total Mass $< 3{\cdot}5\odot$						Systems of Total Mass $> 3{\cdot}5\odot$						No.	Mean Pec. Rad. Vel.
						No.	Mean Values of				$\log f$	No.	Mean Values of				$\log f$		
			P	e			$\frac{m_2}{m_1}$	$\log P$	$\log M$	e			$\frac{m_2}{m_1}$	$\log P$	$\log M$	e			km. sec.
Ecl. var.	0^d–5	21	$1^d{\cdot}86$	·026	9·78														
Spectroscopic binaries	0^d–5	119	$2^d{\cdot}74$	·053	8·09	13	·89	·284	·34	·040	9·36	28	·87	·433	·98	·039	10·84	40	12
	5^d–10	53	$7^d{\cdot}42$	·155	5·72	5	·83	·796	·33	·033	10·33	8	·91	·867	·96	·158	7·58	12	17
	10^d–20	48	$13^d{\cdot}6$	·222	5·02	9	·84	1·110	·25	·382	4·02	7	·90	1·135	1·18	·195	7·74	16	15
	20^d–50	29	$29^d{\cdot}8$	·358	4·06							4	·90	1·426	·69	·403	5·06		
	50^d–100	13	$69^d{\cdot}8$	·234	5·59	4	·86	1·827	·42	·432	4·71							8	19
	100^d–500	36	$229^d{\cdot}$	·279	5·63														
	$> 500^d$	26	$5^y{\cdot}81$	·286	6·54														
Visual binaries	0^y–50	47	$27^y{\cdot}9$	·444	5·98	19	·92	3·961	·20	·405	6·60	8	·95	3·996	·90	·458	7·67	20	16
	50^y–100	23	$72^y{\cdot}4$	·546	5·77	11	·88	4·408	·17	·526	6·21	3	·85	4·399	·59	·76	5·74	14	21
	100^y–150	22	$120^y{\cdot}$	·530	6·08	8	·86	4·661	·36	·501	6·99	6	·86	4·613	·79	·610	7·17	12	15
	$> 150^y$	24	$249^y{\cdot}$	·615	5·92	13	·88	4·880	·15	·609	6·17	6	·84	4·992	·66	·639	7·14	14	16
Statistical eccentricities		500	$2000^y{\cdot}$	·61	6·85														
		800	$5000^y{\cdot}$	·76	6·41														
Spectroscopic binaries with periods greater than 5^d						18	·84	1·18	·31		5·93	19	·90	1·08	·98		7·11		
Visual binaries						51	·89	4·40	·21		6·46	23	·89	4·47	·77		7·15		

given in the first section of the table. The results are also given for 21 eclipsing binaries with periods less than five days for which Shapley * gives

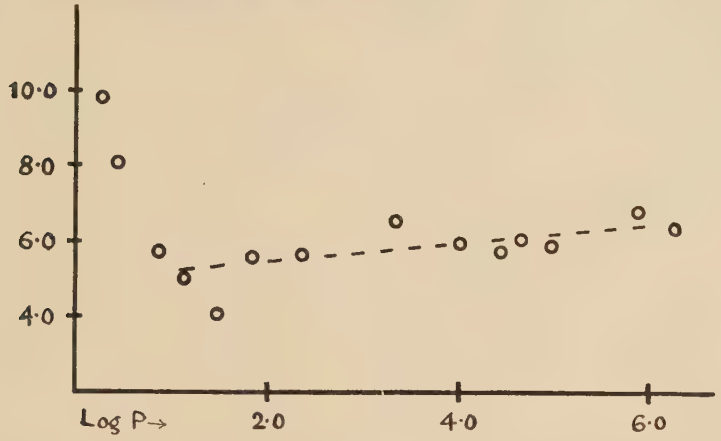

FIG. 1.—*Values of log* $[Pe^{-6}(1-e^2)^{\frac{3}{2}}]$, *based on mean values of P and e for groups of eclipsing binaries, spectroscopic binaries, visual binaries and binaries for which statistical eccentricities are available, are plotted as ordinates against the logarithm of the period in days as abscissæ.*

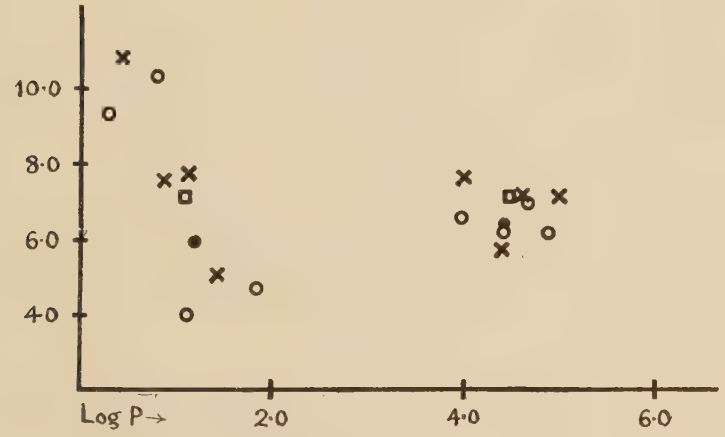

FIG. 2.—*Values of log* $[PM^2e^{-6}(1-e^2)^{\frac{3}{2}}]$, *based on mean values for groups of spectroscopic and visual binaries with known mass ratios greater than* $\frac{1}{3}$, *are plotted as ordinates against the logarithm of the period in days as abscissæ.*

Systems of total mass less than $3{\cdot}5\odot$ *: circles. The dots represent means for all visual and all spectroscopic binaries with periods greater than five days. Systems of total mass greater than* $3{\cdot}5\odot$ *: crosses. The squares represent means for all visual and all spectroscopic binaries with periods greater than five days.*

first-grade orbits and for which a mean value of *e* can be derived. The mean values of the eccentricity for orbits of very long period derived by Russell have also been used. This expression should be constant if there is not a systematic variation in the mean masses of the groups and if our assumptions are reasonably near the truth. It is seen that, except for systems

* *Princeton Univ. Obs. Contributions*, No. 3, 1915.

with periods less than five days, the deviations of this function from a constant value are not excessive, especially if we note that the large eccentricity for the group of spectroscopic binaries with periods from 20 to 50 days is due to a few exceptional stars.

For 102 of the spectroscopic systems given by Aitken $m \sin^3 i$ is available for each component. In only 24 of these does the mass ratio not exceed $\frac{2}{3}$. For 89 of the visual systems masses are given, and to these we may add 9 for which masses are given by Pitman.* Using the mass ratios obtainable from Pitman's determinations of the masses of the components and those given by Huffer,† and supplying the mass ratios by similar methods to Pitman's in a few remaining cases where the total masses are given by Aitken, we have 74 systems in which the mass ratio exceeds $\frac{2}{3}$. These and the 78 spectroscopic systems whose mass ratio exceeds $\frac{2}{3}$ have been examined in greater detail with the aid of the function of the period mass and eccentricity given in (36). The results are given in the second and third sections of the table.

We have taken $\frac{3}{2}(m_1+m_2)\sin^3 i$ as an estimate of the mass of a spectroscopic system, and all the material has been divided into two groups, those with total mass less than $3{\cdot}5\odot$ and those with greater mass. Considering the small amount of material available for this detailed examination, the deviations from constancy of the expression (36) may be regarded as not excessive. The dispersion in the results for spectroscopic binaries with periods greater than five days is undoubtedly due in no small measure to the fact that the groups are too small for the effect of the unknown inclination to be the same in each. These results are summarised by grouping all spectroscopic binaries with periods greater than five days in each mass group, and the visual binaries similarly. In neither group is an increase of the period by the factor 2000 accompanied by an increase in the expression (36) by a factor as large as 4. Comparison of the two groups according to mass, however, shows a difference due almost entirely to the factor M^2. It may be not unreasonable to suppose that there is a systematic difference between the initial circumstances of the orbital motion for the more massive and the less massive systems.

A closer examination shows that for both groups of spectroscopic binaries according to mass $\log(fM^{-\frac{3}{2}})$ is very closely equal to 5·55, and that its value is very nearly 6·1 for both groups of visual binaries according to mass. This result suggests that, apart from other sources of intrinsic differences of the constant C from one system to another due to the circumstances attending their formation, C tends to be larger for systems of greater mass in such a way that $\log(CM^{-\frac{1}{2}})$ is statistically more nearly constant than is $\log C$ itself.

It must be remarked that considerations of this kind must be viewed with considerable caution, since M is the *present* mass of a binary star, and the ratio of the masses of two unequal systems does not remain constant throughout their evolutionary development. Bearing this in mind, we may say that if an empirical relation of this nature between C and the present masses of binary systems for which orbits have been determined

* *A.J.*, **39**, 57, 1929. † *Ap. J.*, **80**, 269, 1934.

is roughly true, then the value of the expression $\log [Pe^{-6}(1-e^2)^{\frac{3}{2}}]$ as a means of testing the theory is enhanced. In that case, besides smoothing the intrinsic differences between different binary systems by the use of a larger number of orbits, this expression has the advantages that there is a tendency for the real differences of C from one system to another to be cancelled by those of M in the factor C^3M^{-2}, and that for spectroscopic systems it is free from the effect of the unknown inclination of the orbital plane.

One further feature calls for comment. We have found above that $\log (fM^{-\frac{2}{3}})$ for systems of known mass is greater for visual binaries than for spectroscopic binaries, the gradient with respect to $\log P$ being $\frac{1}{6}$. It is of interest to examine the results in the first section of the table to obtain some indication as to whether this difference is real or accidental. Excluding the relatively close binaries of period less than five days, $\log (fM^{-2})$, derived from the mean values for all orbits, can be well represented as a linear function of $\log P$ with gradient $\frac{1}{4}$, the only group with a considerable discordance being that to which we have already referred as containing a few exceptional stars. Now $\log (fM^{-2})$ might be expected to be larger for groups of longer period due to their containing a relatively larger number of small masses than do the groups of shorter period, though this effect should not be large if average values of $\log C$ and $\log M$ are related as indicated above. No great degree of certainty is attached to the agreement of the relation between these two gradients with what might be expected, but it does at least suggest that though the theory may perhaps account for by far the larger part of the variation of the eccentricity with period, there is a possibility that a small residual variation remains to be accounted for.

9. *Time Scale.*—Taking the semi-major axis of the Earth's orbit, the year, and the Sun's mass as units, our observational data give

$$\log [4C^4G^{-3}M^{-3}] = 3{\cdot}3 \text{ for small mass ; } = 2{\cdot}5 \text{ for large mass.}$$

It will be sufficient for our purpose to write equation (37) in the form

$$\frac{\Delta t}{\Delta e} = \frac{2}{3}\frac{10^8}{\kappa\gamma}\frac{e^7}{(1-e^2)^{\frac{3}{2}}}$$

for all binary systems with equal components, γ being the velocity of light.

If $T(0{\cdot}01)$ is the time in years for the eccentricity to increase by 0·01, we find the rate of development at various eccentricities to be as follows :—

e	0·2	0·3	0·4	0·5	0·6	0·7
P	32^d	380^d	$6^y{\cdot}6$	30^y	120^y	420^y
$\kappa\gamma T(0{\cdot}01)$	9	170	14.10^2	8.10^3	4.10^4	15.10^4

The corresponding period is given, assuming an average value of $\log M$.

The rapidity of the development of the orbit when the eccentricity is small is remarkable. It must be observed that these figures give the *present* rate of development of a *typical* system (in the sense that $\log C$ and $\log M$ have average values) for any of the tabulated values of the orbital eccentricity. If we trace the history of an individual system backwards, allowance must be made for the fact that the mass was larger at an earlier stage of development if it is admitted that appreciable mass is lost in the course of stellar

evolution. In this case, then, the development of the eccentricity in the early stages was even more rapid relative to its subsequent development than the above figures indicate, and the period was relatively shorter.

Hepperger * has discussed in some detail the problem of two bodies when gravity is propagated with finite velocity for the case when the mass ratio is small and the mass is constant. He concluded that one second is the upper limit to the time in which gravity must be propagated from the Sun to the Earth if the effect on the longitudes of the planets is not to be too great to be compatible with observation. In deriving this result he used a small value for the velocity of the solar system and permitted a considerable influence on the motion of the Moon. Using 20 km./sec. for the solar motion in his calculations we find that the effect on the longitude of Mercury amounts to 200″ in 100 years if the above velocity is assumed for the propagation of gravity. He points out that, in the case of the Moon, terms due to orbital motion have a considerable effect on the longitude, and in the same interval this amounts to 3500″. The latter will be kept smaller than 3″·5 and the former smaller than 0″·2 if the velocity of propagation of gravity is at least 1000 times as great as the above. This leads to the conclusion that the velocity of propagation must be assumed to be greater than 5×10^5 times the velocity of light.

The total time for a "typical" binary system to develop an eccentricity of 0·6 is found from the results given above to be not greater than $25 \times 10^4/(\kappa\gamma)$ years. Using the minimum value for the velocity of propagation of gravity derived above, we find that about 10^{11} years will be required, an interval which is intermediate between estimates of the age of the Earth's crust and the time scale given by the theory of the loss of mass by radiation. By comparison with the latter there is reasonable scope for an increase in the assumed velocity of propagation of gravity and a consequent reduction of its effects on motions in the solar system well below observable magnitudes.

NEW METHODS FOR COMPUTING METEOR HEIGHTS.

Balfour S. Whitney.

(Communicated by Charles P. Olivier)

Meteor heights deduced from ordinary visual observations from two stations are subject to large errors because of the great difficulty in observing and plotting the path of the meteor accurately. In the first section of this paper formulæ are developed by means of which the recorded directions from the two stations of corresponding points on the observed paths of a meteor, say the beginning points, are adjusted through equal angles, these adjustments being the smallest possible which will refer the recorded directions to a common point. In the second part, a least squares solution

* *Sitzungsberichte der Wiener Akademie*, **97**, 337, 1888.

is given for the case of observations from n stations, which may be useful for computing heights of multiply-observed meteors or fireballs.

I. Let the co-ordinates of the two stations S_1 and S_2, referred to axes having the centre of the Earth as origin, X-axis toward the vernal equinox, Y-axis toward the point $\alpha = 90°$, $\delta = 0°$, and Z-axis toward the north pole, be (X_1, Y_1, Z_1) and (X_2, Y_2, Z_2) respectively, where, in the usual notation,

$$X_i = R_i \cos \phi_i' \cos \theta_i, \qquad Y_i = R_i \cos \phi_i' \sin \theta_i, \qquad Z_i = R_i \sin \phi_i' \qquad (i = 1, 2).$$

Let (α_1, δ_1) and (α_2, δ_2) be the co-ordinates of corresponding points on the paths of the meteor as observed from S_1 and S_2 respectively, and let P_1 and P_2 be the feet of the common perpendicular to the two lines determined by S_1, (α_1, δ_1) and S_2, (α_2, δ_2). If the observations were accurate, these two lines would intersect, and P_1 and P_2 would coincide. The direction-cosines of S_1P_1 and S_2P_2 are :

$$\begin{aligned} \lambda_1 &= \cos \delta_1 \cos \alpha_1, & \mu_1 &= \cos \delta_1 \sin \alpha_1, & \nu_1 &= \sin \delta_1 ; \\ \lambda_2 &= \cos \delta_2 \cos \alpha_2, & \mu_2 &= \cos \delta_2 \sin \alpha_2, & \nu_2 &= \sin \delta_2. \end{aligned}$$

The angle Θ between S_1P_1 and S_2P_2 and the direction-cosines (λ, μ, ν) of P_1P_2 are given by the equations :

$$\cos \Theta = \lambda_1\lambda_2 + \mu_1\mu_2 + \nu_1\nu_2,$$
$$\lambda = k(\mu_1\nu_2 - \mu_2\nu_1), \qquad \mu = k(\nu_1\lambda_2 - \nu_2\lambda_1), \qquad \nu = k(\lambda_1\mu_2 - \lambda_2\mu_1), \qquad (1)$$

where

$$k = \pm \operatorname{cosec} \Theta.$$

Let

$$P_1P_2 = d, \qquad S_1P_1 = d_1, \qquad S_2P_2 = d_2.$$

Then

$$d = \lambda(X_2 - X_1) + \mu(Y_2 - Y_1) + \nu(Z_2 - Z_1).$$

To derive expressions for d_1 and d_2 we may proceed as follows. The equations of S_1P_1, S_2P_2 and P_1P_2 in parametric form are

$$S_1P_1 : \begin{cases} x = X_1 + d'\lambda_1, \\ y = Y_1 + d'\mu_1, \\ z = Z_1 + d'\nu_1 ; \end{cases} \qquad S_2P_2 : \begin{cases} x = X_2 + d''\lambda_2, \\ y = Y_2 + d''\mu_2, \\ z = Z_2 + d''\nu_2 ; \end{cases} \qquad P_1P_2 : \begin{cases} x = \xi + \rho\lambda, \\ y = \eta + \rho\mu, \\ z = \zeta + \rho\nu. \end{cases}$$

Since P_1P_2 intersects S_1P_1, it is possible to determine ρ and d' in such a way that

$$X_1 + d'\lambda_1 = \xi + \rho\lambda, \qquad Y_1 + d'\mu_1 = \eta + \rho\mu, \qquad Z_1 + d'\nu_1 = \zeta + \rho\nu.$$

The condition that these three equations in d' and ρ be compatible is that

$$\begin{vmatrix} \xi - X_1, & \lambda_1, & \lambda \\ \eta - Y_1, & \mu_1, & \mu \\ \zeta - Z_1, & \nu_1, & \nu \end{vmatrix} = 0.$$

Expanding this determinant :

$$(\xi - X_1)(\mu_1\nu - \mu\nu_1) + (\eta - Y_1)(\nu_1\lambda - \nu\lambda_1) + (\zeta - Z_1)(\lambda_1\mu - \lambda\mu_1) = 0.$$

Similarly, for P_1P_2 and S_2P_2:

$$(\xi - X_2)(\mu_2\nu - \mu\nu_2) + (\eta - Y_2)(\nu_2\lambda - \nu\lambda_2) + (\zeta - Z_2)(\lambda_2\mu - \lambda\mu_2) = 0. \qquad (2)$$

These two equations define the common perpendicular. Substituting the co-ordinates of P_1, $(X_1 + d_1\lambda_1,\ Y_1 + d_1\mu_1,\ Z_1 + d_1\nu_1)$, in (2), solving for d_1, and then eliminating λ, μ, ν by means of (1), we get, after a reduction in which the relations $\lambda_1^2 + \mu_1^2 + \nu_1^2 = 1$ and

$$\sin^2\Theta = (\mu_1\nu_2 - \mu_2\nu_1)^2 + (\nu_1\lambda_2 - \nu_2\lambda_1)^2 + (\lambda_1\mu_2 - \lambda_2\mu_1)^2$$

are used,

$$d_1 \sin^2\Theta = (X_2 - X_1)[\lambda_1(1 - \lambda_2^2) - \lambda_2(\mu_1\mu_2 + \nu_1\nu_2)]$$
$$+ (Y_2 - Y_1)[\mu_1(1 - \mu_2^2) - \mu_2(\nu_1\nu_2 + \lambda_1\lambda_2)] + (Z_2 - Z_1)[\nu_1(1 - \nu_2^2) - \nu_2(\lambda_1\lambda_2 + \mu_1\mu_2)]$$

Similarly,

$$d_2 \sin^2\Theta = (X_2 - X_1)[\lambda_1(\mu_1\mu_2 + \nu_1\nu_2) - \lambda_2(1 - \lambda_1^2)]$$
$$+ (Y_2 - Y_1)[\mu_1(\nu_1\nu_2 + \lambda_1\lambda_2) - \mu_2(1 - \mu_1^2)] + (Z_2 - Z_1)[\nu_1(\lambda_1\lambda_2 + \mu_1\mu_2) - \nu_2(1 - \nu_1^2)]$$

The co-ordinates of P_1 and P_2 are then:

$$P_1:\ \xi_1 = X_1 + d_1\lambda_1, \qquad \eta_1 = Y_1 + d_1\mu_1, \qquad \zeta_1 = Z_1 + d_1\nu_1;$$
$$P_2:\ \xi_2 = X_2 + d_2\lambda_2, \qquad \eta_2 = Y_2 + d_2\mu_2, \qquad \zeta_2 = Z_2 + d_2\nu_2.$$

If P is a point on P_1P_2 such that $\angle P_1S_1P = \angle P_2S_2P = \gamma$, then, letting $\overline{P_1P} = Kd$,

$$\tan\gamma = \frac{Kd}{d_1} = \frac{(1 - K)d}{d_2}; \qquad K = \frac{d_1}{d_1 + d_2}.$$

The co-ordinates of P are thence:

$$x = (1 - K)\xi_1 + K\xi_2, \qquad y = (1 - K)\eta_1 + K\eta_2, \qquad z = (1 - K)\zeta_1 + K\zeta_2.$$

The altitude of P above the Earth's surface is given with sufficient accuracy by

$$h = \sqrt{x^2 + y^2 + z^2} - R,$$

R being the radius of the Earth at the latitude of P.

The value of γ may be taken as a measure of the agreement of the observations, as it is the smallest angle by which they must be corrected to refer them to the same point. Obviously this method for computing heights can be used very conveniently for discussing the errors in meteor observations. Beginning and end heights of three meteors have been computed by this method and the results have been compared with those found by other methods.

No space is given here to methods for determining whether or not two observations refer to the same meteor, as this question has been discussed in well-known publications.

II. For the case of observations from n stations, let the direction-cosines of the direction of observation from the station $S_i(X_i,\ Y_i,\ Z_i)$ be

$$(\lambda_i,\ \mu_i,\ \nu_i), \qquad (i = 1, \ldots, n).$$

We shall find the co-ordinates of a point $P(x, y, z)$ such that the sum of the squares of the distances, Δ_i, from P to the n lines of observation will be a minimum. These distances are given by the formula

$$\Delta_i^2 = (x - X_i)^2 + (y - Y_i)^2 + (z - Z_i)^2 - [\lambda_i(x - X_i) + \mu_i(y - Y_i) + \nu_i(z - Z_i)]^2.$$

Summing over i:

$$\Sigma\Delta_i^2 = \Sigma(x - X_i)^2 + \Sigma(y - Y_i)^2 + \Sigma(z - Z_i)^2 - \Sigma[\lambda_i(x - X_i) + \mu_i(y - Y_i) + \nu_i(z - Z_i)]^2.$$

A necessary condition for a minimum is that the partial derivatives of $\Sigma\Delta_i^2$ with respect to x, y and z vanish. Differentiating and rearranging the terms:

$$\begin{aligned}
x(\Sigma\lambda_i^2 - n) + y\Sigma\lambda_i\mu_i + z\Sigma\lambda_i\nu_i &= \Sigma(\lambda_i^2 - 1)X_i + \Sigma\lambda_i\mu_i Y_i + \Sigma\lambda_i\nu_i Z_i, \\
x\Sigma\lambda_i\mu_i + y(\Sigma\mu_i^2 - n) + z\Sigma\mu_i\nu_i &= \Sigma\lambda_i\mu_i X_i + \Sigma(\mu_i^2 - 1)Y_i + \Sigma\mu_i\nu_i Z_i, \\
x\Sigma\lambda_i\nu_i + y\Sigma\mu_i\nu_i + z(\Sigma\nu_i^2 - n) &= \Sigma\lambda_i\nu_i X_i + \Sigma\mu_i\nu_i Y_i + \Sigma(\nu_i^2 - 1)Z_i.
\end{aligned}$$

These equations determine the co-ordinates of P, from which h may be computed as in Section I. Three of the six heights found by Method I have also been computed by Method II.

It may be noted that the above method does not adjust the observations in such a way as to make the sum of the squares of the actual residuals of the observations a minimum, *i.e.* the angles $PS_i(\alpha_i, \delta_i)$. Formulæ can easily be set up by means of which this could be done, from the equations for Δ_i^2; but they lead to equations of the second degree in the co-ordinates of P, and consequently would involve a much more laborious solution. The procedure followed above has the defect of implicitly assigning greater weights to the observations from the stations farther from the meteor or fireball. If the importance of the fireball warrants it, and if the computer has the necessary time and patience, a new solution may be carried out with each observation weighted inversely as $\overline{SP}$; but the slight gain in accuracy would seldom justify the additional labour.

Summary

1. Formulæ are developed for computing the heights of meteors by means of which the observed directions from two stations are adjusted through equal angles, and which furnish minimum values for the errors of observation.

2. A least squares solution is developed for determining heights of meteors or fireballs from observations made at two or more stations.

Flower Observatory of the University of Pennsylvania, Upper Darby, Pa.:
1936 *January* 20.

FURTHER NOTE ON THE EQUATORIAL CURRENT OF JUPITER.

A. Stanley Williams.

This note, which relates exclusively to the *South* Equatorial Current, is supplementary to the one published in the *Monthly Notices*, **95**, 723, 1934. It was stated therein that the work of getting better or additional values of the rotation period was still in progress. It has in fact met with unhoped-for success. The previous note had given particulars of five additional or better determinations of rotation period, whilst the present one adds six more to the number. So that we now have a practically complete set of first-class observations for the 30 years 1880 to 1910. Below are short particulars of the recent determinations.

Opposition of 1880–81

The material for this opposition consisted of 163 central meridian transit observations and micrometrically determined positions,* and about 420 positions derived from drawings of the planet, of which there are some very fine series relating to this opposition. Of these 420 observations 90 were derived from the drawings of O. Boeddicker, made with the Rosse six-foot reflector, 191 from those of Niesten, 86 from those of E. E. Barnard and 44 from those of J. Kortazzi, and there were a few others. These observations, although derived from drawings, have been of the utmost value for making sure the correct indentification of the different spots and in increasing the number of those available for determining the rotation period. The mean rotation period from 43 spots is $9^h\ 50^m\ 28^s{\cdot}1$, wt. 3. The spots were so numerous, so well observed and over such long intervals of time that there can be no hesitation in giving this result weight 3. The remarkable Denning or runaway spot or spots, for there were two similar spots close together, are included in the mean. The rotation period of these two spots was $9^h\ 50^m\ 04^s{\cdot}0$, no less than 24^s shorter than that now found for the whole current.

Opposition of 1883–84

There were 19 C.M. transits observed by Denning, 20 by Terby, 1 by Niesten and 27 by the writer; altogether 67 in number. Also 163 rough positions were derived from the drawings of Boeddicker, Lohse, Niesten, Noble, De-Ball, Terby and Denning. The mean rotation period from 22 spots is $9^h\ 50^m\ 24^s{\cdot}0$, wt. 3. The spots were distributed pretty regularly all round the planet. The Denning spot is still a runaway spot, but the

* Most of these were included in a paper by the writer published in *M.N.*, **71**, 145, 1910. Some of the conclusions therein are superseded by the more recent work, but it is interesting to see that the present much longer rotation period now found for the current had already been foreshadowed by the inadequate observations then available.

difference is less than it was formerly, $10^s.2$ only, whilst the line of demarcation between it and the other spots is not so sharply marked.

Opposition of 1884–85

There were 39 C.M. transits only available, namely, 2 observed by Barnard, 2 by Denning, 24 by Terby and 11 by the writer. But 139 rough positions were also derived from the drawings of several observers, in particular 36 from those of Terby, 32 from those of Boeddicker, 13 from those of Niesten and 49 from those of Lohse. From these 178 observations a rotation period of $9^h\ 50^m\ 23^s.5$, wt. 3, was derived from 24 spots. The Denning spot seems to have lost its runaway character, or to have disappeared, as its identification is uncertain. Both Denning and Hough seem to have lost sight of the principal spot about this time, and there is no spot amongst those under consideration having a rotation period markedly shorter than the average. The individual observations by Hough unfortunately do not seem to have been published, and of Denning's no more than two for this opposition.

Opposition of 1891

There were 350 C.M. transits observed by Williams and 1 by Terby. Also 9 accurate positions by Hough from his micrometer measures. Sixty-seven additional rough positions were also derived from various drawings of the period, so that the total observations numbered 427. The mean rotation period from 33 spots is $9^h\ 50^m\ 27^s.4$, wt. 3. Hough from 5 of his measures of a single spot found a period of $9^h\ 50^m\ 26^s.4$, which is very near to the mean value stated above, notwithstanding that one of his 5 observations refers to a different spot.

Opposition of 1893–94

There were 85 C.M. transits observed by the writer and 3 accurate positions from measures of a Lick photograph. About 222 rough positions were also derived from drawings by Antoniadi, G. T. Davis, Lohse, H. McEwen, Niesten and the observers of the Jupiter Section of the B.A.A. A good determination of the rotation period was made from these, namely, $9^h\ 50^m\ 30^s.9$, wt. 3, from 34 spots.

Opposition of 1895–96

Excepting for 17 observations by A. A. Nijland at Utrecht and 4 by the writer there are no C.M. transits of spots. On the other hand, there are a great many excellent drawings of the planet, and from these no less than 438 rough positions were derived, chiefly from the drawings of Antoniadi, Brenner, Lohse, Niesten, Nijland and the B.A.A. observers. The mean rotation period from 40 well-observed spots is $9^h\ 50^m\ 30^s.5$, wt. 3. Although this result is based nearly entirely upon rough positions derived from drawings, yet the observations are so numerous, so accordant and extend over such long intervals of time, six months or more, that there

can be no hesitation in giving it weight 3. The 40 spots were arranged pretty uniformly all round the planet, and show that the motion of the current was nearly uniform throughout its extent.

Since this will probably bring to an end the writer's work on the variable velocity of the South Equatorial Current, he would wish to state a few final results and conclusions. In the following table are included all the yearly observations of rotation period having weight 3 with the corresponding velocities. They are 26 in number, and form a nearly complete record for the 30 years 1880 to 1910. This table should be considered as supplementing and not as superseding Table I of the chief paper.*

Observed Velocities of the S. Equatorial Current

Date	Rotation Period	Velocity km./hr.	Date	Rotation Period	Velocity km./hr.
	h m s			h m s	
1880·8	9 50 28·1	+ 2·8	1898·3	9 50 24·0	+ 7·0
1881·9	24·9	+ 6·1	1899·4	24·5	+ 6·6
1883·0	19·9	+12·1	1900·5	23·0	+ 8·4
1884·1	24·0	+ 7·0	1901·6	30·0	0·0
1885·2	23·5	+ 7·8	1902·7	26·3	+ 4·4
1887·3	22·4	+ 9·1	1903·8	26·0	+ 4·8
1888·4	27·8	+ 2·6	1904·9	29·4	+ 0·7
1889·5	30·3	− 0·4	1906·0	31·4	− 1·7
1890·6	28·0	+ 2·2	1907·0	28·3	+ 2·0
1891·7	27·4	+ 3·1	1908·1	32·5	− 3·0
1892·8	25·3	+ 5·6	1909·2	26·5	+ 4·2
1893·9	30·9	− 1·8	1910·3	27·4	+ 3·1
1896·1	30·5	− 0·6	[1916]	[36·1]	[− 7·3]
1897·2	34·6	− 5·5	[1924]	[43·6]	[−16·3]

The first column of the table gives the date, stated now to the nearest tenth of a year, and the second the observed rotation period. The third column requires a little explanation. The mean rotation period of the current from the observations included in the table is $9^h\ 50^m\ 28^s{\cdot}09$. This is very near to the rotation period which has for many years past been used for computing "System I" of the Jupiter ephemerides, namely, $9^h\ 50^m\ 30^s{\cdot}0$.† The latter has therefore been adopted as a convenient standard datum to which should be referred the observed velocity of the current in the various years. That is, a velocity corresponding to the rotation period $9^h\ 50^m\ 30^s{\cdot}0$ has been assumed to be the datum for velocity, there not being any fixed point on the planet to which the velocities could be directly referred. The velocities with reference to this assumed datum are given in the third column of the table, and are stated in kilometres per hour.

This table is represented in diagram form in the adjoining figure, which must be considered as superseding fig. 1 of the chief paper. Comparing it with the latter, it will be seen that the preceding part of the velocity

* Published in *M.N.*, **94**, 243, 1934.

† This period was first adopted by Albert Marth in his ephemeris for 1889, and was based on the observations of two spots only, observed by the writer in 1888 (see *M.N.*, **49**, 88, 1888). Observers of the planets and satellites owe a deep debt of gratitude to Marth for his invaluable ephemerides.

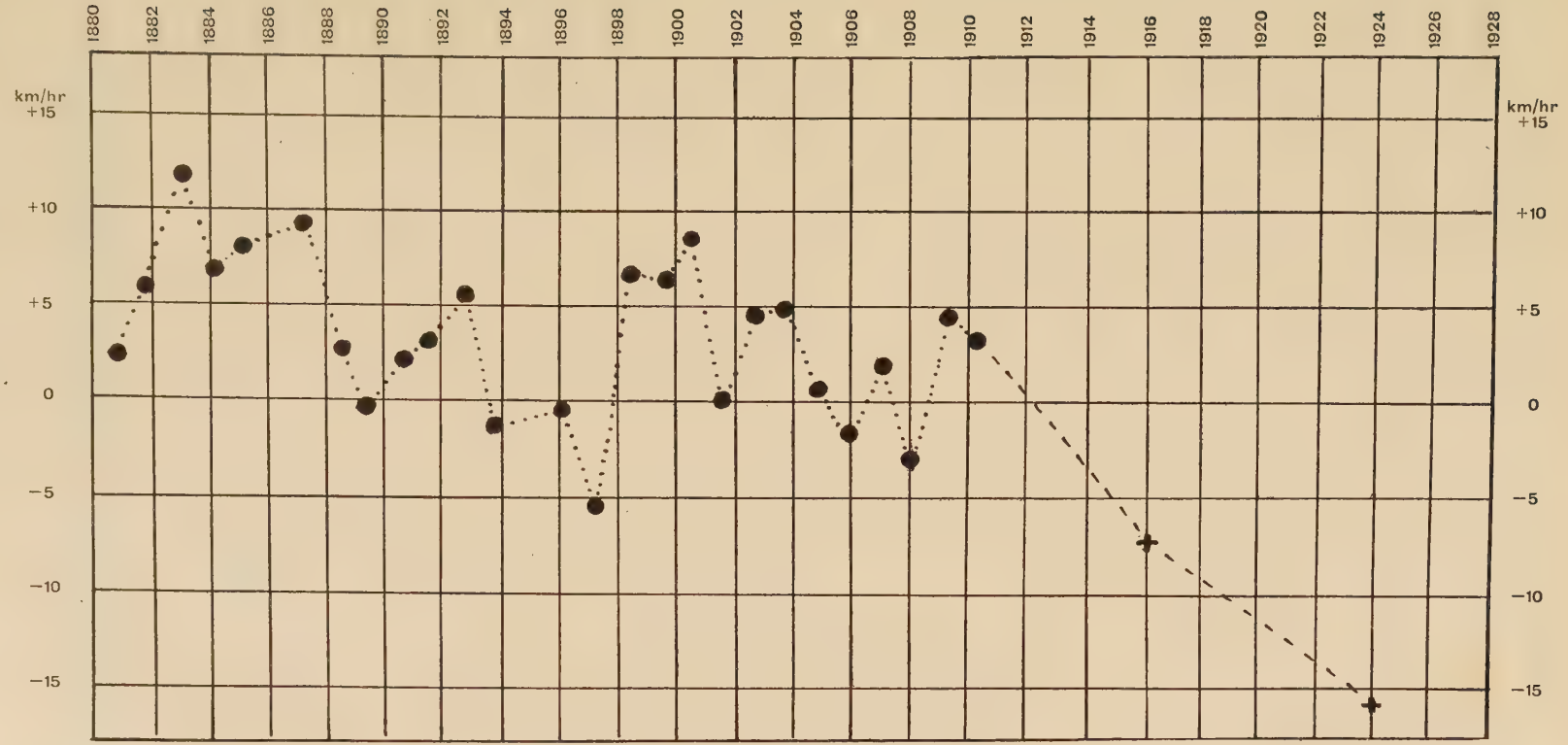

Revised Velocity Curve of South Equatorial Current.
Zero Velocity corresponds to Rotation Period $9^{h}\ 50^{m}\ 30^{s}\cdot0$.

"curve" has been much changed by the more accurate and additional observations now available, and for the better; but that, on the other hand, the last two observations have been rendered more divergent. The latter, marked by a + in the diagram, are each the mean of 7 years' observations. The separate results for these are given in Table I of the chief paper. Having regard to the widely discordant values of these separate results, it may be doubted what, if any, weight should be attributed to these means for our present purposes. Under the circumstances it seems safest to disregard them and to rely upon the more accurate observations of the 30 years 1880 to 1910 alone. It is a matter for gratification that we should now possess a practically complete record of reliable observations for the period in question.

Some Final Conclusions

(1) With regard to the interesting subject of periodicities, it is significant that the revised velocity curve still fails to give any definite indication of either the 11-year sunspot period or the 12-year period of the planet's revolution round the Sun, nor in fact of any long-period periodicity whatsoever, excepting perhaps a doubtful one of about 9 years. Shortly it may be said that the solar influence does not appear to be reflected in the variable velocity of the South Equatorial Current.

(2) The apparent existence of a shorter periodicity of about $2\frac{1}{2}$, or better 3, years was referred to in the chief paper. This may have some connection with the possible 9-year periodicity above mentioned. The task of separating so short a periodicity as 3 years from the other minor fluctuations of velocity is not insuperable, and it is to be hoped that some younger and abler man than the writer may be persuaded to undertake the task.

(3) But perhaps the most important and significant result is the very definite continual decrease, apart from minor fluctuations, in the velocity of the current during the 30 years 1880 to 1910. In this period the velocity decreased from +7 km./hr. to zero velocity. This continual decrease is quite certain, and indeed conspicuous, though a change of only 7 km./hr. in 30 years is small in comparison with the planetary velocity of the current. This latter velocity is about 350 km./hr. more rapid than that of the (visible) surface material to the south of the current. It is possible that this slow secular decrease may ultimately prove to be part of some long-period periodicity, but if so the period must be a very long one. The two observations of 1916 and 1924 seem to show that the decreasing velocity had continued to about the year 1927.

(4) The abnormal behaviour of the runaway spots in the years 1880 to 1884 * is deserving of particular notice.

(5) The mean rotation period of the South Equatorial Current, based on nearly 10,000 observations of a great many spots, is $9^h\ 50^m\ 28^s.09$.

Polvarth, St. Mawes:
1936 *February* 11.

* And probably also in 1879, in which year Lohse observed a white spot with the short period of $9^h\ 49^m\ 59^s$. It was probably identical with one of the two principal spots of 1880.

ELEMENTS OF VARIATION OF YZ ANDROMEDÆ.

A. Stanley Williams.

In his variable star ephemerides for 1935 Prager gave December 2 as the date of maximum for this variable ($0^h\ 19^m\ 37^s$, $+30°\ 05'{\cdot}4$, 1855). A good series of observations made here gives December 8 as the date from observation, only 6 days later than the predicted date, which was based on a period of 207·2 days. However, a slightly longer period would suit still better all the observations now available, and I have therefore made a re-determination of the elements of variation, as under :

$$\text{Maximum} = \text{J.D. } 2424410 + 207^d{\cdot}5\ \text{E.}$$

The residuals O − C are satisfactorily small, as will be seen from the comparison below.

E.	Obs. Max.	Comp. Max.	O − C
0	J.D. 2424404	4410·0	−6·0
2	4825	4825·0	0·0
4	5240*	5240·0	0·0
5	5445 ±	5447·5	−2·5
7	5858	5862·5	−4·5
18	8145*	8145·0	0·0

Only the two observations marked with * were well observed during both the increasing and decreasing light. The above elements also satisfy the earlier photographic observations referred to in the *M.N.*, 87, 502, 1927, and those of Barrett published in the *A.N.*, 5558, 1928, and those of Ross in the *Astronomical Journal*, 882, 1927.

Polvarth, St. Mawes :
1936 *February* 17.

OBSERVATIONS OF OCCULTATIONS MADE AT TEDDINGTON DURING 1935.

John L. Haughton, D.Sc.

The observations were made as described in *M.N.*, 95, 495, 1935. The position of the observatory, measured from a 6-inch O.S. map, is

$$\phi = 51°\ 25'\ 15''\ \text{N.}$$
$$\lambda = 0°\ 19'\ 20''{\cdot}5\ \text{W.}$$

The probable errors given previously were obtained by adding together all the maximum probable errors of the individual observations, *e.g.* clock rate, starting of stop-watch, observation of occultation, etc. I am indebted

to Dr. Comrie for pointing out to me that it is more correct to take the square root of the sum of the squares of these errors, and I have done so in the table given below.

An effort was made to estimate the lag between the time of disappearance or reappearance and the time of pressing the stop-watch, and a correction for this has been applied in Column 6. The amounts subtracted are : 0·3 sec. for Nos. 54, 57, 69, 71 and 75 ; 0·5 sec. for Nos. 63, 64, 67, 69 and 83 ; 1 sec. for Nos. 58 and 59.

No.	Date	Star	Mag.	Phase	U.T.	Prob. Error	Remarks
	1935				h m s	s	
54	Jan. 14	17 Tauri	3·8	D	16 49 55·7	± 0·3	
57	14	η Tauri	3·0	D	18 16 00·0	0·3	
58	16	125 Tauri	5·0	D	18 48 11·3	0·7	Difficult
59	Mar. 12	WZC 414	7·0	D	18 33 19·1	0·5	Difficult
63	July 18	ρ Aquarii	5·4	R	22 37 21·9	0·6	
64	19	170 B Aquarii	6·1	R	00 41 14·8	0·4	
65	24	B.D. +19° 432	7·0	R	01 20 42·0	?	Doubtful
67	25	B.D. +23° 563	6·1	R	01 24 42·6	0·5	
69	Aug. 21	WZC 207	6·7	R	02 01 50·2	0·4	
71	Sept. 7	λ Sagitarii	2·9	D	19 29 07·6	0·3	
75	21	44 Geminorum	5·9	R	00 45 13·7	0·4	
79	Nov. 6	22 B Piscium	6·5	D	18 36 51·0	0·5	
81	Dec. 1	18 Aquarii	5·5	D	18 40 14·5	0·5	
83	31	19 Piscium	5·3	D	18 07 45·9	0·4	

OCCULTATIONS OF STARS BY THE MOON, OBSERVED AT ENGELHARDT OBSERVATORY, KASAN, DURING THE YEAR 1934.

(Communicated by the Secretaries)

The reductions were made by I. W. Belkowitsch.

No.	Date	U.T.	Star	Mag.	Phase	Instrument and Power	Observer
	1934	h m s					
1	Apr. 16	17 39 10·5	16 Tauri	5·4	D	H 132	B
2	16	17 40 15·0	17 Tauri	3·8	D	H 132	B
3	16	18 7 43·7	20 Tauri	4·1	D	H 132	B
4	16	18 9 8·9	q Tauri	4·3	D	H 132	B
5	23	19 4 46·1	18 Leonis	5·8	D	H 132	B
6	23	19 56 47·5	19 Leonis	6·4	D	H 132	B
7	23	19 56 46·7	,,	,,	D	A 110	N
8	Dec. 18	12 29 2·6	η Tauri	2·9	D	H 132	B
9	18	12 28 59·3	,,	,,	D	A 80	T
10	18	12 50 27·5	B.D. +23° 557	4·0	D	H 132	B

No.	Date	U.T.	Star	Mag.	Phase	Instrument and Power	Observer
	1934	h m s					
11	Dec. 18	12 50 27·4	B.D. +23° 557	4·0	D	*r* 58	D
12	18	12 50 28·5	,,	,,	D	M 56	M
13	18	12 58 37·2	B.D. +23° 558	6·2	D	A 80	T
14	18	12 58 34·9	,,	,,	D	H 132	B
15	18	12 58 37·6	,,	,,	D	M 56	M
16	23	19 44 38·9	θ Cancri	5·5	D	A 119	A

The time-corrections of the chronometer were found from the Rugby wireless signals.

Observers :
D = I. A. Dukov.
M = D. J. Martinoff.
T = N. I. Tchudowitchew.
N = Miss S. V. Nekrasova.
A = Mrs. L. D. Agafonova.
B = I. W. Belkowitsch.

Instruments used :
A = Astrograph (110 mm.).
H = Heliometer (106 mm.).
r = Refractor (finder) (135 mm.).
M = Refractor (150 mm.).

Engelhardt Observatory :
1935 *December.*

OCCULTATIONS OF STARS BY THE MOON, OBSERVED AT TOMSK UNIVERSITY OBSERVATORY DURING THE YEAR 1935.

N. Goryatscheff.

(Communicated by the Secretaries)

($\phi = 56° 28' 06''·3$; $l = 5^h 39^m 47^s·16$ east of Greenwich)

Date (U.T.)	Local Sidereal Time	Star	Mag.	Phase
	h m s			
Feb. 7·523230	3 20 02·7	B.D. +8° 80	8·4	D
7·622209	5 42 58·0	136 B Piscium	6.5	D
9·672259	7 03 07·3	26 Arietis	6·1	D
10·813538	10 31 03·7	B.D. +22° 504	7·4	D
10·814268	10 32 07·0	B.D. +22° 505	8·0	D
Apr. 7·659966	10 30 05·8	B.D. +24° 674	6·3	D
8·648403	10 17 20·6	B.D. +25° 878	8·5	D
8·703985	11 37 36·1	B.D. +25° 901	8·7	D
8·725786	12 09 04·8	B.D. +25° 910	8·5	D
8·777888	13 24 18·7	B.D. +25° 941	6·8	D
11·665145	10 53 20·7	B.D. +19° 1963	7·6	D
May 6·655689	12 18 15·4	5 Geminorum	5·9	D
6·687568	13 04 17·2	B.D. +24° 1165	8·2	D
9·753646	14 51 31·7	54 Cancri	6·3	D
July 24·794023	20 49 28·2	B.D. +22° 510	8·5	R
24·839512	21 55 09·2	B.D. +22° 518	7·0	R

Apparent Places of Occulted Stars

Star	α	δ	Authority
	h m s	° ′ ″	
B.D. +8° 80	0 33 03·01	+ 8 31 06·8	Tou. ph. +9° 028·94
136 B Piscium	0 37 50·71	+ 9 00 08·4	Am. Eph.
26 Arietis	2 27 00·48	+19 34 14·8	Am. Eph.
B.D. +22° 504	3 29 35·51	+23 09 11·6	Abbadia 1561
B.D. +22° 505	3 29 38·43	+23 10 09·3	Abbadia 1562
B.D. +24° 674	4 35 26·17	+25 05 35·2	Gr_{1910} 1996
B.D. +25° 878	5 32 28·99	+25 32 58·6	Gr_{1910} 2448
B.D. +25° 901	5 35 32·66	+25 16 45·2	Gr_{1910} 2478
B.D. +25° 910	5 36 47·71	+25 13 59·1	Gr_{1910} 2498
B.D. +25° 941	5 39 39·57	+25 24 45·1	Gr_{1910} 2541
B.D. +19° 1963	8 12 16·40	+18 53 35·5	Abbadia 4878
5 Geminorum	6 07 34·48	+24 26 14·4	Am. Eph.
B.D. +24° 1165	6 07 42·34	+24 41 40·6	Gr_{1910} 2944
54 Cancri	8 47 26·42	+15 35 29·2	Am. Eph.
B.D. +22° 510	3 30 43·92	+22 32 44·3	Abbadia 1573
B.D. +22° 518	3 33 10·92	+22 59 59·9	Abbadia 1596

Observer : Prof. N. Goryatscheff.

Instruments : Zeiss telescope, 90-mm. aperture, magnifying power 90 ; chronometer, Ericsson.

Tomsk, Siberia, U.S.S.R.,
University Astronomical Observatory :
1936 *February* 5.

OCCULTATIONS OF STARS BY THE MOON, OBSERVED AT THE ASTRONOMICAL OBSERVATORY, KIEW, IN THE YEAR 1935.

S. D. Tscherny.

(Communicated by the Secretaries)

No.	Date 1935	U.T. h m s	Star	Mag.	Phase
1	Apr. 8	17 0 44·79	125 Tauri	5·0	D
2	May 11	19 29 29·57	155 B Leonis	6·5	D
3	Sept. 11	18 48 31·64	ζ Aquarii	5·4	D
4	Oct. 7	17 37 26·46	94 B Capricorni	6·0	D
5	8	17 58 53·98	96 B Aquarii	6·5	D
6	Nov. 13	19 31 48·50	8 Geminorum	6·1	D
7	13	19 50 18·46	9 Geminorum	6·3	D
8	Dec. 8	19 45 39·89	104 B Tauri	5·5	D

Instrument used : Merz-Repsold refractor, 243 mm., power 120.
All the observations were made by S. D. Tscherny.

Notes

Nos. 2, 5 : instantaneous.
Nos. 1, 3, 4, 7 : good.
No. 6 : satisfactory.
No. 8 : through clouds and fog.

Astronomical Observatory, Kiew :
1936 *January* 29.